Development of Heterogeneous Catalysts for Bleaching in Automatic Dishwashing

Naomi Markham

December 2020

Thesis submitted in accordance with the requirements of Cardiff University for the degree of Doctor of Philosophy

Acknowledgments

I would like to thank the catalysis CDT and the EPSRC for the opportunity and the funding of this project alongside Reckitt Benckiser. To Prof. Graham Hutchings, Prof. Stuart Taylor and Dr Mark Douthwaite for their expertise, support and guidance throughout my project. To Dr Alias Al-Bayati, Dr Torsten Roth, Claudia Schmaelzle and the whole innovation team at Reckitt Benckiser for their input and support for the project. Finally, to my family and friends who have supported me for the past four years and kept me on track.

Abstract

Bleaching in automatic dishwashing products currently uses sodium percarbonate and tetraacetylethylenediamine (TAED) to form peracetic acid, which is the primary bleaching agent. Premium products utilise a homogeneous catalyst, MnTACN, to enhance the bleaching performance through oxygen transfer to the stain. The formation of peracetic acid was investigated over a range of reagent concentrations and conditions to ascertain if a catalyst was required to increase the formation of peracetic acid or aid oxidation of the stain. Peracetic acid was facile under a range of reagent concentrations; however, at low temperatures and neutral or acidic pH, peracetic acid formation was reduced or not observed. Under these conditions a catalyst could be used to increase the formation of peracetic acid and improve bleaching; however, these conditions were not relevant to the automatic dishwashing application.

The amount of peracetic acid formed was linked to the performance in both tea stain bleaching tests and morin oxidation, increasing peracetic acid amount in solution increases tea stain bleaching and morin oxidation. MnTACN was tested for tea stain oxidation and was found to be highly active. For morin oxidation it was demonstrated that MnTACN can bleach morin with peracetic acid, hydrogen peroxide and O_2 as the oxidant. Demonstrating the highly active nature of MnTACN for automatic dishwashing.

Manganese, copper, iron and zinc supported on ZrO_2 were tested for tea stain bleaching and copper and zinc were active for heterogeneous stain removal. Copper catalysts were investigated and an acid treatment with HNO_3 removed large copper

oxide particles, improving the tea stain bleaching activity of the copper catalysts. Characterisation using X-ray diffraction (XRD) and X-ray photon spectroscopy (XPS) showed that, after the acid treatment, ZrO_2 under went a phase change to intimately mixed $CuZrO_3$ and the presence of copper hydroxide species on the surface. Copper catalysts were tested for morin oxidation and the rate of morin oxidation increased over time, indicating an induction phase for the catalyst, which was further investigated with a radical scavenger, mannitol. Addition of mannitol to the morin oxidation reaction in the presence of copper catalysts reduced the conversion of morin over time, showing that copper catalysts generate radicals. Overall, a heterogeneous catalyst has been found to be active for heterogeneous stain bleaching.

Table of Contents

Chapter 1: Introduction

Bleaching is defined as degradation of a stain via oxidation, which the process either a) removes the stain entirely from the surface by improving aqueous solubility, or b) oxidises the chromophore centres of the stain sufficiently, such that it is no longer coloured.[1] Bleaching agents are contained in detergent formulations, which are multicomponent mixtures in which surfactants are not the sole active agent. Alongside surfactants and bleaches, builders, enzymes and other auxiliaries are also present, each with a unique action for a more complete visual clean for the consumer in the dishwasher.[2]

In automatic dishwashing, the most commonly used bleaching system is based on hydrogen peroxide (H_2O_2) and such systems are termed as active oxygen detergents, owing to the presence of peroxyl species. This represents a superior alternative to chlorine-based bleaching systems such as hypochlorate, due to the environmental impact of the formed chlorine-based by-products. Hydrogen peroxide based bleaching systems exhibit limited performance below 50 °C and, due to this, there has been significant research into oxidation catalysts for such processes.[3] Catalysts are used in reactions to increase kinetic rates, this is achieved by lowering the activation energy of the reaction, as the catalyst offers a lower energy alternative pathway to transform the reactants to the products.[4] The thermodynamics of the reaction are not changed by a catalyst as the initial energy of the reactants and final energy of the products is not changed.

1.1 *Introduction to Catalysis*

1.1.1 *History of Catalysis*

Catalysis has been used throughout human history prior to the term first being coined in 1835. In ancient Egypt, Mesopotamia, Georgia and Iran, beer and wine were brewed using yeast. Yeast is an enzyme that acts as a biocatalyst to ferment sugars and form alcohol.[5] As early as 1746, industrial processes were developed using catalysts.[6] John Roebuck produced concentrated sulfuric acid in lead-lined chambers by burning sulfur containing ores in air. The addition of nitrous oxide (N_2O) dramatically increased the yield of sulfuric acid, acting as the catalyst in this reaction.[7]

In the 1800s, publications and patents using catalysts began to emerge; however, knowledge of how these materials worked was limited. The contact process for the oxidation of sulfur dioxide (SO_2) to form sulfuric acid was commercialised in 1831, which utilized platinum as the catalyst.[6] Ammonia decomposition was also studied in the early 1800s; Thenard used hot metals to catalyse this reaction and was the first to publish catalytic activity trends, showing that iron was more active than copper, silver, gold and platinum.[8] Davy and Faraday used platinum wire for the first reported catalytic oxidation reaction,[9] which combined air and coal-gas, a mixture of carbon monoxide (CO) and hydrogen (H_2), with the platinum catalyst. It was this discovery that provided the foundation for the Davy lamp, which found use in coal mines, alerting miners to toxic atmospheres. In 1820, the importance of surface area was first reported, when the process was improved through the application of finely divided platinum.[9] The technique for increasing platinum surface area was subsequently employed in 1823 by Dobreiner, for alcohol oxidation.

After this early work was completed, Berzelius presented an overview of the field to the Stockholm Academy of Sciences in 1835.[10] Coining the term catalysis, derived from the Greek word meaning to loosen. Berzelius' proposed that enhanced activity was due to the adsorption of reactants onto the surface of the catalyst, which was observed by Faraday the year before while working on electrolysis. Development of industrial catalysts continued with the commercialisation of the Deacon process, which is the formation of Cl_2 from HCl *via* oxidation over copper chloride, in 1875, [11] large scale ammonia synthesis by BASF in 1910 and Fischer-Tropsch fuel synthesis in 1930.[12] This cemented catalysis as an important field in chemical synthesis and for large scale industrial processes.

1.1.2 *Types of Catalysis*

Catalysts are classified by the phase of the catalyst with regards to the phase of the reactants.[4] For example; catalysts that exist in a different phase to the reactants are known as heterogeneous catalysts. Most commonly, such catalysts exist as solids and the reactants exist as either liquids or gases. Sub classes of heterogeneous catalysts are electro- and photo-catalysis. Homogeneous catalysts are the name given to a catalyst when it exists in the same phase as the reactants. The field of biocatalysis covers the use of enzymes in biochemical reactions. In such reactions a microorganism, isolated enzyme or an enzyme immobilised onto a support are used as the catalyst. Each catalyst type has different general properties and advantages which are compared in Table *1*

Table 1: Comparison of general properties of different types of catalysts.

Type of Catalyst	Selectivity	Thermal Stability	Separation	Active Site	Example
Heterogeneous	Low	High	Facile	Multiple different surface sites	Ammonia Synthesis
Homogeneous	High	Low	Difficult	Well defined	Hydroformylation
Bio	High	Low	Improved when immobilised	Well defined	Glucose to fructose for soft drinks

1.1.3 *Role of Catalyst in a Reaction*

The classical definition of a catalyst was given by Ostwald in 1902, which stated that a catalyst is a substance that changes the rate but not the thermodynamics of a chemical reaction. To understand how a catalyst enables an increase in the rate of reaction, it is important to consider the fundamental steps of a reaction.[13] For a reaction A + B = C + D, A and B need to go through a transition state, which decomposes to the products C and D. This requires an activation energy, curve (a) E_{a1}, as shown in Figure 1. In the case of reversible reactions, C and D can react to reform A and B *via* activation energy E_{a1} plus E_{a2}.

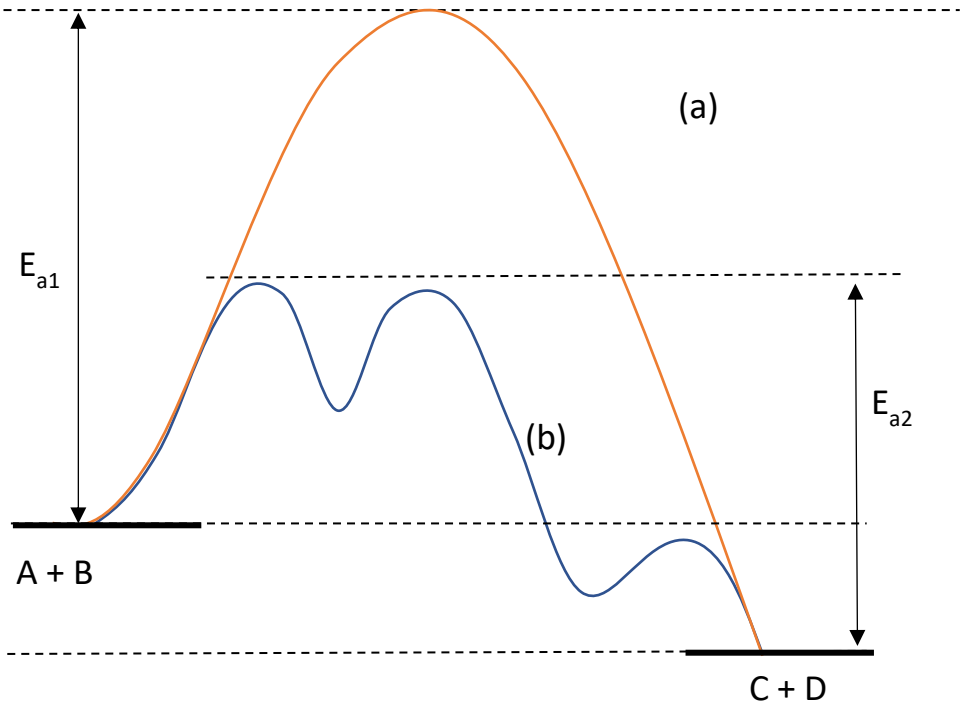

***Figure 1**: Energy diagram for A + B = C + D, with and without a catalyst present. Where (a) = energy profile of a reaction with no catalyst present and the activation energy E_{a1} and (b) = energy profile of a reaction with a catalyst present and the activation energy E_{a2}.*

The addition of a heterogeneous catalyst into the reaction opens a new pathway where A and B adsorb onto the catalyst surface to form the intermediate shown by curve (b). Absorption of A and B onto the catalyst surface still requires an activation energy (E_{a2}), however, this is lower than when a catalyst is not present. Curve (b) represents a reaction where the absorption of the reactants is an exothermic process as it releases energy. Figure 1 shows a simplified energy diagram for a reaction. There can be many other reaction steps to a reaction that can be represented on an energy diagram, such as bond breaking/formation and surface diffusion.

1.2 *Overview of Bleaching Chemistry*

Bleaching with hydrogen peroxide is used in a domestic setting to clean clothes, dishes and surfaces. The same chemistry is also applied in an industrial setting, to bleach pulp and raw cotton.[14] Household detergent market in the EU is worth €29.1 billion in 2018, with automatic dishwashing products worth €2.7 billion in 2018.[15]

1.2.1 *Bleaching with H_2O_2 and solid H_2O_2 Sources*

Predating the use of modern detergents in the home was the use of soap. The invention of soap was recorded in 2800 BC in Babylonia.[16] Soap is typically composed of fatty acid salts that can be generated using the saponification reaction. The process was fully commercialised in the 1850s. Hard soaps contain the sodium salt of a long chain carboxylic acid. Colgate, Lever brothers, Palmolive and Proctor & Gamble made soap widely available through application of the ammonia process, which was used to generate inexpensive sodium carbonate needed to form the hard soaps.

The first detergent was launched for the laundry market in 1878 by Henkel, which is known as “Bleich Soda”;[17] however this does not align with the modern definition of a detergent, as the formulation only contained sodium carbonate and sodium silicate, not any active oxygen species. Henkel subsequently launched the first active oxygen containing detergent in 1907, which contained sodium perborate, a persalt of hydrogen peroxide.

In the coming decades, competitors followed suit with their own detergents for washing machines and then for dishwashers, as these appliances became more common in the household. Modern detergents also contain soaps, builders, enzymes and fragrances in addition to the bleaching system.[3] In the current market *ca.*

750,000 t of bleaching systems are produced annually, of which 85 % contain peroxide derivatives.[18] In the EU market, bleaching has always been carried out using peroxide detergents. In the US, hypochlorite is predominantly used as higher water volumes are present in the dishwasher, and therefore a stronger bleaching agent is needed. The use of hypochlorite is decreasing as peroxide based bleaches are cheaper and more environmentally benign[19]

H_2O_2 is highly unstable when exposed to heat or other chemicals; at low levels of decomposition there is a discernible pressure build-up in sealed containers from the generation of O_2, which can be explosive.[20] Therefore companies use a solid source of H_2O_2, to enable its safe transportation and enhance the shelf life of the product.

1.2.1.1 *Sodium Perborate*

Sodium perborate was used in Henkel's first detergent in 1907 and was commonly used in the industry until the 1990s, when concerns were raised about perborate ecotoxicity. Since 2012, EU regulations have been in place to remove phosphates and borates from consumer products and improve the biodegradability of the overall formulation.[21]

Sodium perborate is a persalt, which means that there are peroxycarbonate bonds present and H_2O_2 is released when the compound comes into contact with water. The general formula is $NaBO_3.nH_2O$ where n = 1 (monohydrate) or 4 (tetrahydrate). From the crystal structure it has been shown that the monohydrate form is the anhydrous salt of disodium 1,4 – diboratetetroxane dianion, as shown in Figure 2, and the tetrahydrate being the hexahydrated form of the perborate.[22]

Initially the tetrahydrate form was used in formulations, but this was replaced by monohydrate due to the higher active oxygen content; 15 wt% compared to 10 wt% for the tetrahydrate.[23] This lead to an increase in bleaching performance without the need to increase the weight of the formula.

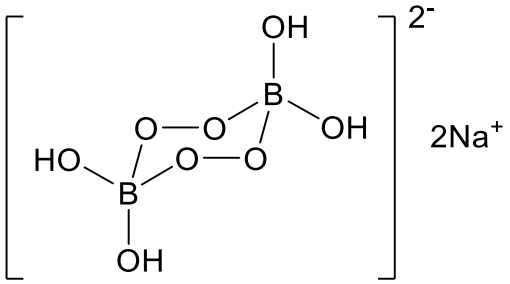

***Figure 2**: Structure of sodium perborate "monohydrate".*

1.2.1.2 *Sodium Percarbonate*

Sodium percarbonate began to replace sodium perborate in such formulations in the 1990s as a more environmentally benign H_2O_2 source.[23] Sodium percarbonate is now standard in detergent formulations in the EU. The structure is an adduct of sodium carbonate and H_2O_2, meaning there are no peroxycarbonate bonds present as in sodium perborate,[24] which makes percarbonate less stable than perborate. Therefore, it requires the addition of sodium silicate or sulfate coatings in granular form to improve the shelf-life of the product.[25] Even with the addition of these coatings, sodium percarbonate releases H_2O_2 at the same rate as perborate[19] and has an active oxygen content of 13 wt% that is comparable to the monohydrate of sodium perborate.[23]

1.2.2 *H_2O_2 Bleaching Mechanism and Limitations*

It was assumed that the active bleaching species formed from H_2O_2 would be a radical species, such as $OH^{\bullet}$, or singlet O_2.[26] After a series of studies by Spiro and co-workers,[27] it was demonstrated that radical species were not responsible for bleaching and the perhydroxyl anion (OOH^-) was the active species.[28] Radical species and singlet O_2 were found to be inactive in the bleaching of phenolphthalein. Oxidation and epoxidation of the dye proceeded *via* reaction with the perhydroxyl anion rather than the hydroxyl anion, as the perhydroxyl anion is a stronger nucleophile. The widely accepted mechanism, Scheme 1, is nucleophilic attack by the perhydroxyl anion on an alkene group in the chromophore.[2]

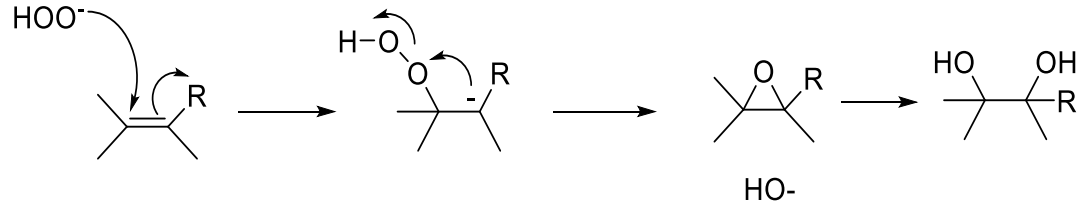

***Scheme 1**: Nucleophilic attack of perhydroxyl anion on electrophilic centre of chromophore.*

Traditionally in the home, handwashes and early machines used water at the boil. Since the 1970s there has been a consumer drive to lower wash temperatures to improve energy efficiency and decrease the degradation of synthetic fibres in the wash.[19] Standard temperatures for both washing machines and dishwashers are 40 – 80 °C, which limits the bleaching efficiency of H_2O_2 as higher temperatures are required to bleach stains. K.Dithmar *et al.* demonstrated the effect of temperature

on bleach performance with sodium perborate.[29] At a temperature of 60 °C, the remaining peroxide concentration after two hours was double that compared to at 85 °C. The higher amount of H_2O_2 left in solution correlated to lower bleaching performance; suggesting that a higher temperature is required to form the perhydroxyl anion required for bleaching. Similarly, bleach performance with H_2O_2 was severely limited at lower temperatures.

As the bleaching reaction, i.e. the oxidation of the stain, is first order with respect to H_2O_2 and the stain concentration, at lower temperatures bleaching could also be improved by increasing the amount of H_2O_2 in the formulation,[2] but this would increase formulation size and increase the costs for consumers. Bleach activators have therefore been developed to improve bleaching at lower temperatures.

1.2.3 *Addition of Bleaching Activators to H_2O_2 Sources*

Bleach activators can be defined as acylating agents, which react with H_2O_2 in the wash to form peracids. Effective bleach activators exhibit fast rates of perhydrolysis, resulting in the formation of the corresponding peracid; a stronger nucleophile, and therefore, a more effective bleaching agent than H_2O_2. In addition to this, the bleach activator needs to be relatively inexpensive and fully biodegradable.

The first bleaching activator was patented in 1927 and used a fatty acid, such as caprylic acid, to generate organic peracids to aid bleaching.[30] In the 1950s a range of aliphatic carboxylic acid amides (RCONR'R'') were patented to improve bleaching at temperatures below 100 °C.[29] Tetraacetylglycoluril (TAGU) was commercialised in the 1970s by Henkel.[31] TAGU is expensive and non-biodegradable and, therefore, it is no longer used in formulations. Bleach activators must be relatively inexpensive

and biodegradable, due to regulations, to be successfully commercialised. Only tetraacetylethylene diamine (TAED) and nonanoyloxybenzenesulfonate sodium (NOBS), Figure 3, have been commercialised in Europe and the US markets.[18]

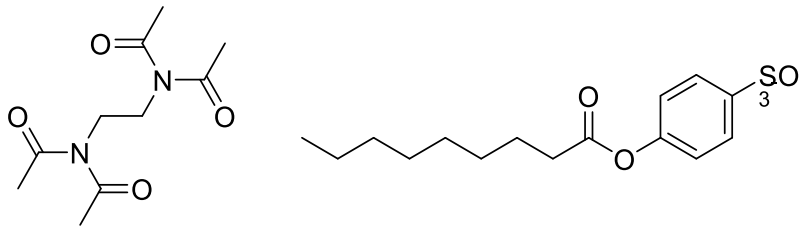

(a) (b)

Figure 3*: Structure of (a) TAED and (b) NOBS.*

1.2.3.1 *Tetraacetylethylene diamine (TAED)*

TAED, Figure 3, was first launched by Unilever in 1978 and has become ubiquitous in laundry and dishwasher formulations in the EU.[32] H_2O_2 reacts with TAED to form peracetic acid, the bleaching agent in the process. TAED reacts to form triacetacetylethylenediamine (TriAED) to release 1 mole of peracetic acid, then TriAED reacts further to form diacetylethylenediamine (DAED) and release 1 mole of peracetic acid, Scheme 2.[33] This reaction is known as perhydrolysis. TAED, TriAED and DAED are all biodegradable.[34]

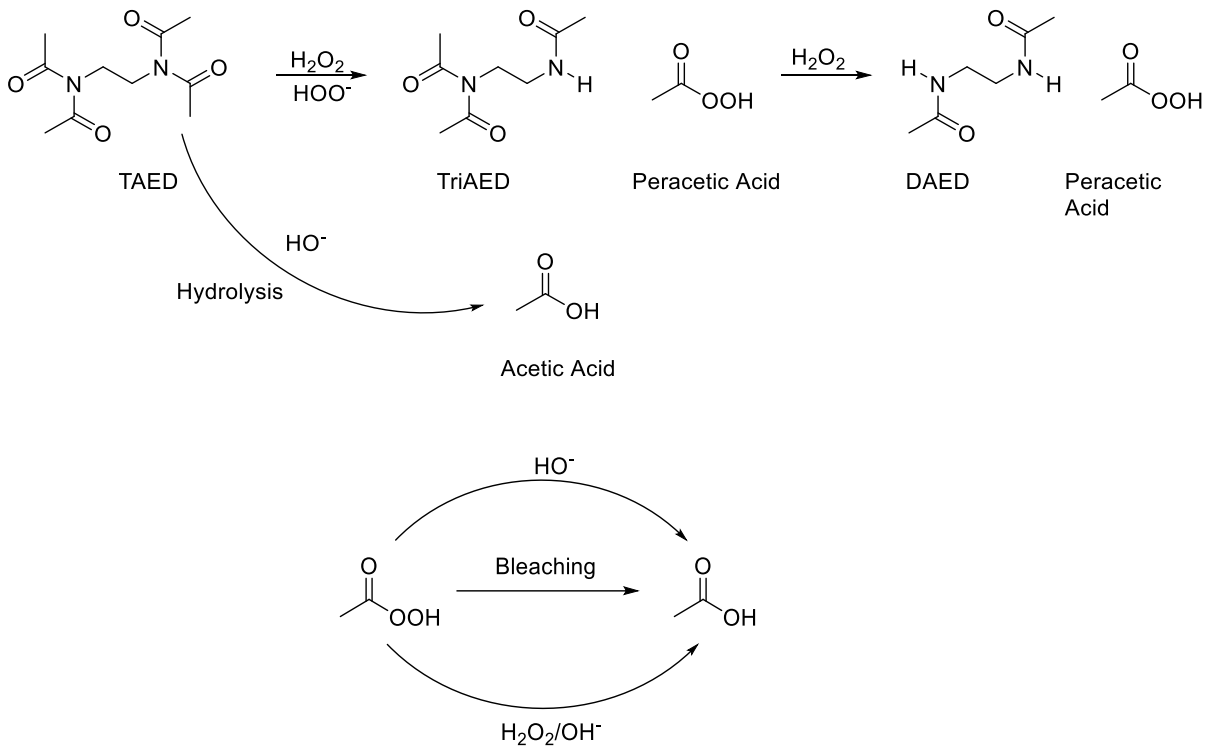

***Scheme 2**: Reaction scheme of TAED with H2O2 to form 2 moles of peracetic acid.*

Theoretically, 4 moles of peracetic acid could be released by TAED, instead of 2 moles; however, DAED does not undergo further perhydrolysis as the amide bond is stabilised *via* resonance.[33] Perhydrolysis of TAED is facile, as it is temperature independent and has been shown to proceed at near neutral pH.[25,35,36] TAED perhydrolysis also does not yield exactly 2 moles of peracetic acid, due to the competing base catalysed hydrolysis reaction forming acetic acid.[33] Acetic acid is also formed after bleaching with peracetic acid or from the decomposition of peracetic acid with hydroxy ions. The sodium percarbonate/TAED system has also been demonstrated to be effective as a disinfectant and kills bacteria in the wash.[37]

Many studies have demonstrated the benefits of adding TAED to sodium percarbonate on bleaching performance. A mixture of sodium percarbonate and

TAED is more active than preformed peracetic acid at temperatures > 60 °C, as an excess of H_2O_2 boosts performance at high temperatures.[23] In addition, peracetic acid is thermally unstable and has a high rate of decomposition at these high temperatures.[31]

1.2.3.2 *Nonanoyloxybenzenesulfonate Sodium (NOBS)*

SNOBS, Figure 3, was developed in 1983 by Proctor and Gamble and launched in 1988 as a component in the product Tide.[38] This activator was designed to bleach hydrophobic greasy stains that build up on fabrics.[39] SNOBS reacts with H_2O_2 *via* perhydrolysis to form peroxynonanoic acid, which is the active bleaching species as shown in Scheme 3(a). Proctor and Gamble claim that an optimal chain length of C6 – C10 is required to deliver the active species close to the stain, as these percarboxylic acids are surface active. One mole of peracid is released for every mole of SNOB. By comparison, TAED releases two moles of peracid per mole and therefore SNOBS is less volume efficient. Despite this, SNOBS have been shown to have a higher bleaching performance under the more dilute wash conditions used in the US and Japan.[19]

In contrast to TAED, the peracid formed from the SNOBS can react with an additional molecule of SNOBS to form a diacyl peroxide (DAP), ***Scheme 3***(b). In the example given in ***Scheme 3*** with a C9 molecule, this would yield dinonanoyl peroxide.[25,2] DAP is a less powerful bleaching agent than peroxynonanoic acid; however, DAP is active on a wider range of stains as it is hydrophobic. As DAP exhibits some bleaching activity and increases the type of stains that can be bleached with the system, a small amount of DAP present in the wash is beneficial. To ensure low formation rates of

DAP during the wash, and therefore ensuring peracetic acid oxidises the stains rather than forming DAP, a high persalt to SNOBS ratio and high pH are required.[40]

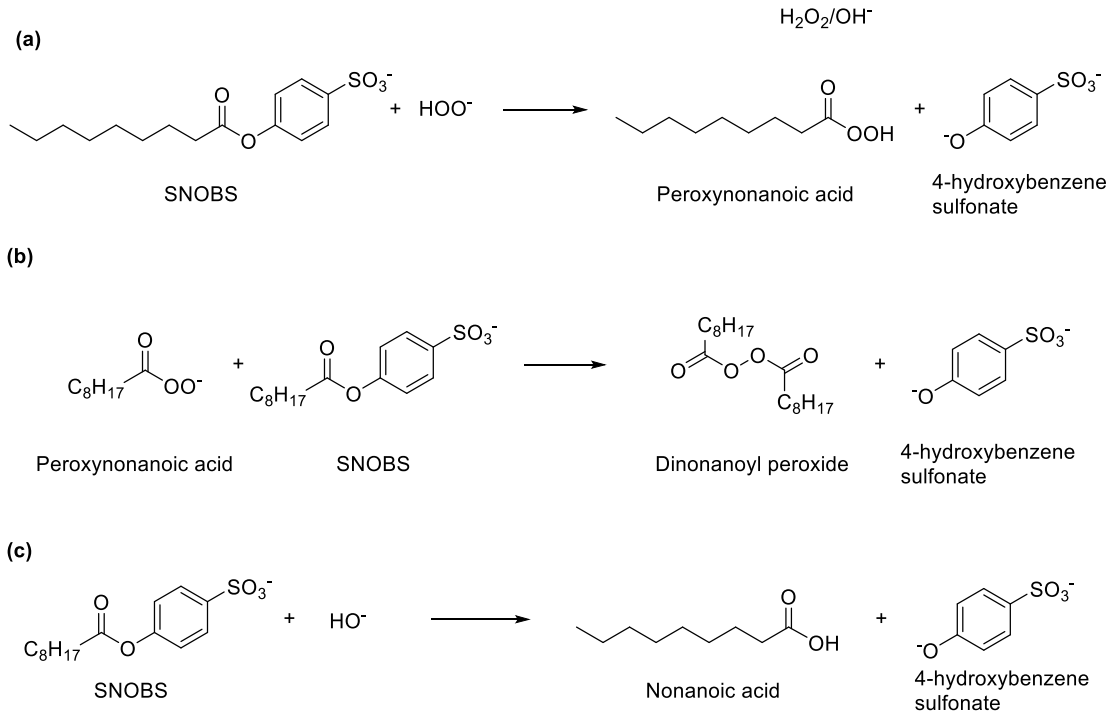

***Scheme 3**: (a) = Reaction scheme of SNOBS with HOO- to form peroxynonanoic acid. (b) = Reaction scheme of peroxynonanoic with SNOBS to form dinonanoyl. peroxide, (c) = Hydrolysis of SNOBS to form nonanoic acid.*

Generally, peracid bleaching performance can be increased by the addition of electronegative groups, which increases the oxidation potential of the peracid.[33] To achieve this with SNOBS, aromatic groups can be added to the ester. SNOBS, in addition to perhydrolysis, also undergoes hydrolysis to form a corresponding carboxylic acid; nonanoic acid in the example in ***Scheme 3***. The presence of surfactants and differing substituents on the ring can decrease hydrolysis to maximise the formation of the peracid.[41]

1.2.3.3 *Other Bleach Activators on the Market*

TAED and NOBS are generally used in UK, EU and US markets. In Japan, two other activators have also been commercialised, sodium lauroyloxybenzene (LOBS) and 4-decanolyoxybenzoic acid (DOBA), as given in Figure 4. LOBS and DOBA are both based on SNOBS.[18]

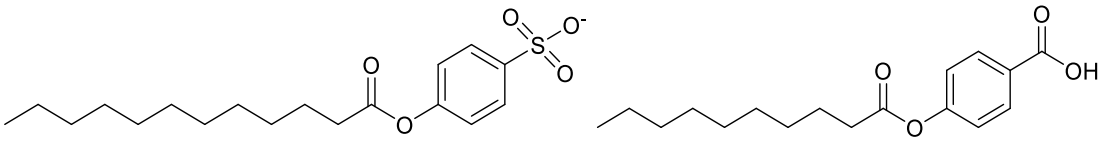

(a) (b)

***Figure 4**: Structure of bleach activators (a) LOBS and (b) DOBA*

LOBS was initially published in the same Proctor and Gamble patent as NOBS[38]. LOBS is often less water soluble than NOBS, as they typically consist of longer saturated carbon chains.[23] LOBS is the most commonly used bleach activator in Japan and is found in powder tablets and liquid products.[42] The perhydrolysis of LOBS with the perhydroxyl anion forms peroxydodecanoic acid. Due to the highly hydrophobic nature of the peracid, LOBS can remove lipophilic stains effectively.[23] In comparison to TAED, the antibacterial effect of LOBS is higher at lower concentrations of the bleach system, which may increase the commercial appeal of this activator as wash conditions change.[43]

DOBA has a hydroxybenzoic acid leaving group similar to SNOBS. One benefit of DOBA is that, under an acidic or neutral pH, it is insoluble in water; therefore, DOBA can easily be stored in liquids as a dispersion.[23] The perhydrolysis of DOBA results in

the release of peroxydecanoic acid, which is also hydrophobic and so exhibits high bleaching activity on oily stains. Similar to LOBS, DOBA has greater antibacterial effects when compared to TAED. DOBA is also biodegradable and can be combined with TAED to increase the range of stains bleached by the formulation.[44]

Overall, a successful bleach activator needs to release a high quantity of peracid per gram of material, to exhibit an enhancement in bleaching compared to H_2O_2. Furthermore, it needs to be fully biodegradable and non-toxic as it comes into contact with consumers' laundry and dishes. For laundry applications, fabric and dye damage needs to be limited to ensure consumer satisfaction. Finally, to ensure commercialisation, the bleach activator needs to be inexpensive to keep the formulation affordable for the consumer. These requirements have limited the number of commercialised bleach activators, even with the large number of publications of potential activators in the literature.

1.2.4 *Use of Preformed Peracids*

Peracids have a greater bleaching activity than H_2O_2 alone, and therefore, to reduce formula size and cost, it could be beneficial to use formulations containing preformed peracids. The use of preformed peracids would remove the need for the presence of both H_2O_2 and a bleach activator in the formula. The use of preformed peracids avoids the use of activators, and therefore minimises the mass of the formulation. Use of low molecular weight peracids, such as peracetic acid, must be avoided, as these are thermodynamically unstable and may lead to pressure build-up causing an explosion during product transportation and storage.[23]

Peroxycarboxylic acids were initially investigated, including acyl peroxides, mono/di peracids[45] and peroxybenzoic acid.[46] These peroxycarboxylic acids were all found to be active for bleaching, are water soluble, and can exhibit antibacterial properties. These compounds typically have an active oxygen content of 0.05 – 10 wt%, which is structure dependent. In an alkaline environment these compounds are unstable, even when isolated. As a result, products containing these preformed peroxycarboxylic acids have a short shelf-life and are therefore are not commercially viable. Efforts were made by Unilever and P&G to improve the stability of peroxycarboxylic acids under alkaline conditions, as alkalinity is required for bleaching of stains. This was achieved principally through ring substitution[46] or through the addition of urea to the formulation[45], but these strategies resulted in only a minor improvement in stability.

To increase the stability of peroxy acids, amido linkages can be incorporated. This was successfully demonstrated with 6-(phthalimido)peroxyhexanoic acid (PAP), shown in Figure 5.[47] Hydrogen bonding between the molecules form chains, increasing stability in the solid state, which decreases decomposition. Bleaching performance with these compounds is optimum at pH 7 - 10 and 20 – 50 °C, aligning with standard wash conditions. PAP solubility also increases with pH, and therefore, stable suspensions can be produced in acidic media for a stable commercial formula. There is continuing interest in the PAP, despite its limited commercialisation.[48,49]

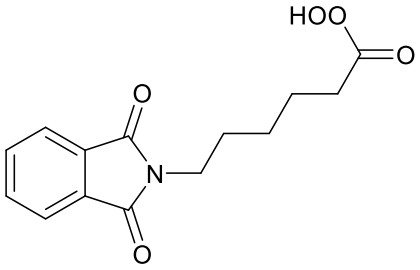

***Figure 5**: Structure of preformed peroxyacid – PAP*

1.2.5 *Aerial Bleaching*

Bleaching with H_2O_2 and peracids is atom inefficient as only oxygen is required to remove the chromophores from stains *via* oxidation. Persalts account for 20 wt% of the average formulation and the removal of the persalt/activator system would reduce formula size.[2] Aerial bleaching, defined as bleaching using atmospheric oxygen, has been reported in the patent literature since 2000.[18] Unilever published a patent containing a catalyst that uses O_2 from a solid source rather than from the atmosphere.[50] In 2001, Unilever patented a range of transition metal complexes as catalysts for aerial bleaching that used atmospheric O_2 and did not rely on a solid source of O_2.[51] Unilever and Clariant have published other patents showing catalyst bleaching with atmospheric O_2.[52,53] Despite the clear advantages of this approach, and the continued interest, no products involving aerial bleaching have been commercialised to date.

To summarise the preceding section, there are many factors that can affect the commercialisation of a bleaching system, which include: the cost, the stability of the formulation, and its atom efficiency. The focus of this work is concerned with the use of a sodium percarbonate and TAED system, which generates peracetic acid *in situ*.

The sodium percarbonate/TAED bleaching system is of most interest as the majority of the formulations sold in the UK and EU use this as the bleaching system.

1.3 *Use of Catalysts in Bleaching*

At temperatures below 50 °C, the bleaching performance of sodium percarbonate and TAED is limited.[3] This presents a challenge, as consumers wish to operate at lower temperatures or shorter cycles to reduce costs and help the environment. One way to improve the bleaching performance of the H_2O_2/activator formulation would be to incorporate the use of a catalyst. Investigations have focused on the use of homogeneous transition metal catalysts to oxidise the polyphenolic chromophores in stains.[54] Manganese based catalysts have been at the forefront of many of these studies, as they are non-toxic and commonly found in nature. The most well-known example of a bleach catalyst is manganese 1,4,7-trimethyl-1,4,7-triazacyclononane (Mn(Me_3-TACN)),[55] which was first launched by Unilever as a component in Persil Power in 1994.

Selectivity is a key issue with bleach catalysis, especially for laundry applications, as dyes have similar structures to the chromophores in stains. Eventually Mn(Me_3-TACN) was removed from the market for laundry application due to unacceptable fibre damage[56], but it is still used in automatic dishwashing. Despite the wide range of bleach catalysts reported in the literature, few have been commercialised, which is due to high costs, fabric damage, or stability in the formulation.

1.3.1 *Manganese Homogeneous Catalysts*

1.3.1.1 *Manganese Salts*

Since the 1980s studies have shown that manganese salts can activate H_2O_2 by removing a proton and forming OOH^-; Unilever's early patent, for example, demonstrated the potential of using $MnSO_4$ as a catalyst.[57] J. Oakes, who authored

the patent, showed that addition of manganese salts in the presence of carbonate ions improves bleaching at 40°C in comparison to H_2O_2 and bleach activator systems. It was concluded that the transition metal ion must have carbonate present to effectively activate H_2O_2 to aid bleaching. Burgess and co-workers[58] published similar findings for $MnSO_4$ in 2002, for a range of alkene epoxidations, using H_2O_2 or $^tBuO_2H$ as the oxidant. EPR investigations into the mechanism showed that the reaction proceeded *via* a peroxymonocarbonate intermediate. It was therefore postulated that the catalytic performance of $MnSO_4$ was attributed to an oxygen transfer *via* a Mn-peroxycarbonate species containing Mn^{4+}.

Manganese salts are often unstable under wash conditions and, as a result, Mn precipitates out of solution as MnO_2. In laundry applications, MnO_2 can stick to the fabrics, resulting in damage. The fabric damage can be a result of the catalysts being unselective and removing the chromophores from dyes, as well as from the stains. Additionally, Mn species bound to the dye can damage fabric over time. To limit damage to the fabric, sequestering agents can be added, such as EDTA and heptonic acids.[59] Manganese and other transition metals bound to organic ligands can lead to improved stability, which have been reported in the patent literature.[60,61] Such compounds are, however, not currently used in formulations.

1.3.1.2 *Mn(Me$_3$-TACN)*

The use of Mn(Me_3-TACN) as a catalyst in bleach systems was patented by Unilever in 1991,[62] and was the first commercialised bleach catalyst, launched in Persil Power products. The catalyst was first published in 1988 as a model enzyme catalyst.[63] The original Unilever patent showed that the catalyst was highly effective at bleaching

tea stains at 40 °C, with an optimal performance observed at pH 9 - 11. In the presence of hydrogen peroxide or sodium perborate/TAED system, the addition of Mn(Me_3-TACN) improved bleaching over a range of conditions. Initially this catalyst was commercialised for laundry applications; however, the catalyst had to be removed from the market due to high levels of fabric damage.[56] Mn(Me_3-TACN) is still used in some commercial detergents for automatic dishwashing, to improve the removal of harsh coloured stains.

As Mn(Me_3-TACN) is one of only a few commercialised bleach catalysts, there have been a range of papers published that investigate the bleaching mechanism. Electron paramagnetic resonance spectroscopy (EPR) was used to identify possible catalytic intermediates that form in studies from Unilever and Gilbert *et al.*[55,64,65] It was suggested that the first step of the reaction, ***Scheme 4***(a), involves a one electron transfer from a phenolate ion, transforming the Mn^{IV}-Mn^{IV} species into Mn^{III}-Mn^{IV}, which is active in EPR. This di-nuclear species cannot undergo hydrolysis and therefore an oxidation is required to form the mono-nuclear Mn^{IV} species, which was also identified through EPR and electron mass spectrometry (ES-MS), shown in Scheme 4(b).[66] The second step, in Scheme 4(c), is the oxidation of Mn^{III} and Mn^{IV} to Mn^{IV} and Mn^{V}, either in the di-nuclear or mono-nuclear form. Hage and co-workers[55] compared the activity of the Mn(Me_3-TACN) catalyst with a manganese catalyst that had a stable Mn^{III}-Mn^{IV} bond. At pH < 9.5, the Mn(Me_3-TACN) had the higher bleaching performance, suggesting both mono and di-nuclear species are active for bleaching. At pH 10, the two catalysts exhibited similar activities, indicating that the di-nuclear species is needed for bleaching at pH 9.5 and above. A similar mechanism,

with the formation of mono-nuclear Mn^{V}=O species was proposed by Gilbert *et al*[67] for the oxidation of azo dyes. Using EPR and electrospray ionisation mass spectrometry (ESI-MS), there was no evidence of a radical mechanism found, though ESI-MS showed the reaction of the dye with $Mn^{IV}L(OH)_3$ species formed from perhydrolysis of the di-nuclear manganese species with HO_2^-.

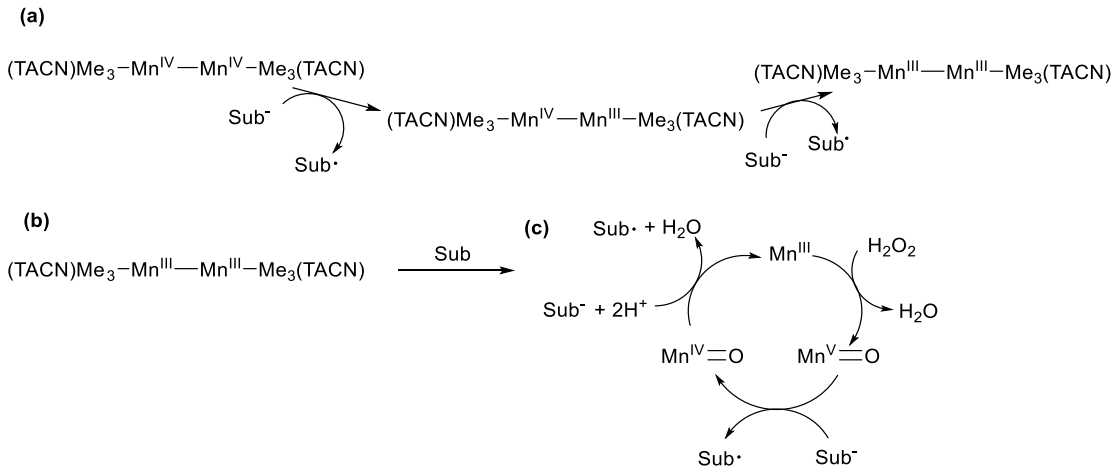

***Scheme 4**: Mn(Me$_3$-TACN) postulated reaction mechanism for the oxidation of organics proposed by Gilbert et al.*[66]

Sorokin *et al*[68] published a study on metallophthalocyanines as potential bleach catalysts for the perborate and percarbonate with TAED system. Mn(Me$_3$-TACN) was used for comparison to assess whether the new materials were comparable to the current industry standard. In this study, mannitol and ethanol were used to trap OH radicals that may be formed during the oxidation of catechol, a model stain compound. It was concluded that Mn(Me$_3$-TACN) forms radicals to oxidise catechol; however, in the presence of perborate or percarbonate only with Mn(Me$_3$-TACN), there was no reduction in the conversion of catechol with mannitol or ethanol. There is no data for percarbonate/TAED oxidation, but for perborate/TAED with Mn(Me$_3$-

TACN), the initial rate of conversion is reduced in the presence of ethanol. After 10 minutes, the catechol conversion reached 92 %, whereas the conversion reached 100 % in the absence of ethanol. Due to the small difference in overall conversion of catechol in the presence of radical scavengers, and no further mechanistic investigation, it is difficult to conclude whether the bleaching is predominately facilitated by a radical mechanism from the results of this paper alone.

Mn(Me_3-TACN) has been investigated for a wide range of oxidation reactions beyond bleach catalysis. The catalyst is active for styrene and 4-vinylbenzoic acid oxidation and, using oxygen labelling experiments, it was shown that the mechanism proceeds *via* oxygen transfer rather than radical generation.[55,69] In a mixture of H_2O_2 and acetone, Mn(Me_3-TACN) epoxidizes cinnamic acid *via* the same Mn^V=O intermediate suggested for bleaching.[70] Epoxidation in non-aqueous media has also been reported, which are considered to follow similar mechanisms to those previously reported for Mn(Me_3-TACN).[71]

1.3.1.3 *Manganese Schiff-Base Complexes*

Schiff base ligands, a sub class of imines, were first discovered in 1864 by Hugo Schiff and have the general structure R_2C=NR'.[72] The metal is coordinated *via* the nitrogen in the imine group and another group attached to the ligand, most commonly an aldehyde. Clariant[73] and Henkel[74] have patented the use of Schiff-Base catalysts for bleaching, mainly with Mn in the oxidation state of +3, as shown in Figure 6. Clariant claim that these compounds are highly effective oxidation catalysts for laundry, cleaning and textile bleaching. Henkel focus on the use of the catalyst for hard surface bleaching, such as dishwashing. Both companies report an improvement in

bleaching performance when compared to the sodium percarbonate/TAED system. It is not clear whether any of these catalysts have yet been commercialised.

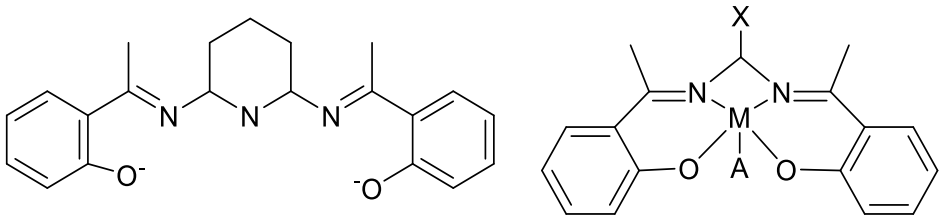

(a) (b)

***Figure 6**: Schiff base ligands patented by (a) Clariant and (b) Henkel.*[73,74]

The mechanism has not been studied for bleaching under alkaline aqueous conditions. For the epoxidation of alkenes and oxidation of sulphides, the formation of a high valent Mn^{V}=O species is again suggested to be important. The high valency Mn intermediate then bonds to the substrate, which then undergoes oxidation.[75] Pietikainen[76] studied the epoxidation of alkenes with peroxycarboxylic acids generated *in situ*. It was shown that these catalysts were efficient for the oxidation of alkenes using the peroxycarboxylic acid, again, postulating that the reaction proceeds through a high valent Mn^{v}=O intermediate species.

1.3.1.4 *Manganese Cross Bridged Macrocyclic Complexes*

Proctor and Gamble have patented a range of cross bridged macrocyclic based complexes, an example is given in Figure 7[77,78] It is claimed in these patents that the reported catalysts are active with and without H_2O_2 in the formulation, however, it is difficult to draw conclusions from these patents as no data has been published on stain bleaching. Busch *et al*[79] tested Mn(II) and Fe(II) cross bridged macrocycles for oxygen transfer and hydrogen abstraction in the epoxidation of cyclohexadiene.

Mn^{4+} was found to be an active intermediate, with a higher activity for hydrogen abstraction over oxygen transfer mechanism.

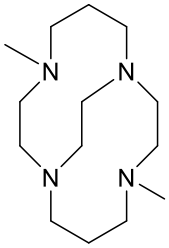

***Figure 7**: Biscyclam ligand*

1.3.1.5 *Manganese Complexes with Terpyridine*

Manganese complexes with terpyridine ligands have been patented by Ciba, as shown in Figure 8. These catalysts are reported to be more efficient at bleaching than the sodium percarbonate/TAED system.[80,81] As with many of the other bleach catalysts, these were found to be active for epoxidation. In addition to improving bleaching activity in comparison to the sodium percarbonate/TAED system, Ciba patented a catalyst with a modified terpyridine ligand that catalyses oxidation reaction with atmospheric O_2.[82]

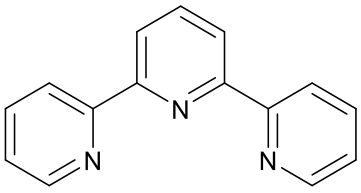

***Figure 8**: Example of terpyridine ligand structure - 2,2':6',2'' terpyridine ligand.*

Wieprecht *et al*[83] investigated the possible mechanism of terpyridine based catalysts for the oxidation of morin and trolox, and compared the oxidation activity to

Mn(Me_3-TACN). For morin oxidation, the terpyridine catalyst out performed Mn(Me_3-TACN). It was found that substitution of electron donating groups on the 4' position of the pyridine ring had the biggest impact on the activity of the catalytic oxidation. Hydroxo and amino groups yielded the highest performing catalysts; however, terpyridine catalysts were not active for the oxidation of Trolox, which Mn(Me_3-TACN) is still highly active for. Trolox oxidation pathway is *via* a series of one electron transfers. The lack of activity for terpyridine complexes suggests that this catalyst does not facilitate this oxidation pathway, whereas Mn(Me_3-TACN) can perform one electron transfers. A reaction mechanism is not proposed. In earlier work by Limburg *et al*[84,85] investigating the oxidation of water with manganese terpyridine catalysts, a high valent intermediate species was postulated to be responsible for O-O bond activation.

1.3.1.6 *Manganese Complexes with Polypyridineamine Ligands*

Henkel[86] and Clariant[87] have also patented catalysts consisting of polypyridineamine ligands, shown in Figure 9. Henkel patented a manganese catalyst with tris(2-pyridylmethyl) amine (TPA) ligand, which was demonstrated to be highly active for morin oxidation but no data on stain removal was published. Clariant patented tetrakis(2-pyridinylmethyl)-1,2-ethanediamine (TPEN) for bleaching in detergents and found that it effectively bleached a range of stains, including tea and curry, in combination with hydrogen peroxide. Elf-Atochem have patented a manganese catalyst with an N,N′-bis(2-pyridylmethyl)-ethylenediamine (bispicen) ligand for pulp bleaching; however, pulp bleaching is conducted at acidic pH and high catalyst dose.[88] As with previous bleach catalysts, a study in 2000 by Brinksma *et al*[89] showed

that bispicen is active for the epoxidation of alkenes in the presence of hydrogen peroxide, but no mechanism was postulated.

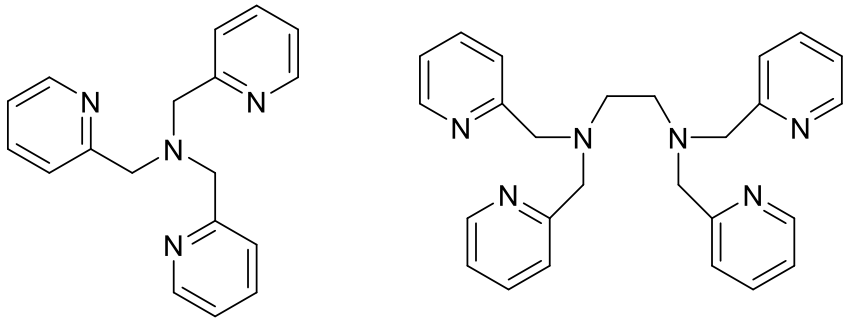

(a) (b)

***Figure 9**: Polypyridineamine ligands patented by (a) Henkel and (b) Clariant.*[86,87]

1.3.2 *Iron Bleaching Catalysts*

Other transition metal complexes have also been studied for bleaching. The majority of patents cited for manganese as bleach catalysts also confirm that iron, cobalt, copper, zinc, and chromium are also active catalysts for many of the ligands discussed. Iron and cobalt complexes have been developed for the removal of stains.

1.3.2.1 *Iron Complexes with tris(pyridine-2ylmethyl) amine (TPA)*

Iron complexes with TPA were patented by the University of Minnesota in 1997.[90] The patent confirms that these complexes are active for the oxidation of alkenes, as well as the removal of acid red 88 dye in solution. In combination with H_2O_2, and no bleach activator present, there was a modest improvement in stain removal.

The oxidation mechanism which occurs in these complexes has not been investigated in aqueous media; however, Chen *et al*[91] studied the mechanism of an iron TPA complex in acetonitrile for olefin epoxidation. The presence of Fe^{III}-OOH catalytic

intermediate was identified using ESI-MS and was postulated to be required for epoxidation. When tBuOOH was used as the oxidant instead of H_2O_2, a radical mechanism was involved that proceeds *via* another high valent iron species, $Fe^{V}=O$.[92] Kaizer *et al*[92] trapped and observed the intermediate, which was characterised by infrared spectrometry, (Scheme 5).

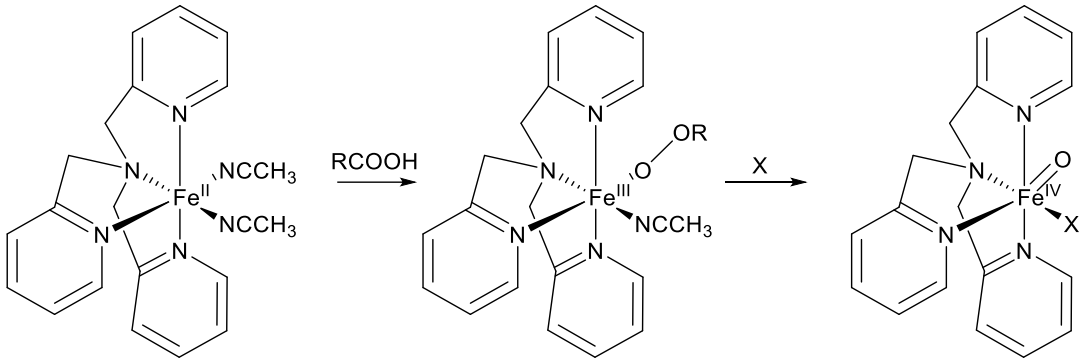

***Scheme 5**: Proposed formation of $Fe^{IV}=O$ high valent species.*[92]

1.3.2.2 *Iron Complexes with Pentadentate Nitrogen Donor Ligands*

A wide variety of pentadentate ligands have also been patented as bleach catalysts, the first of which was patented by Unilever in 1995.[93] The most active ligand described in the patent is N,N-bis(pyridine-2-yl-methyl)-bis(pyridine-2-yl)methylamine, which was given the abbreviation N_4Py, (***Figure 10***). $Fe(N_4Py)$ exhibited a high activity for stain removal in the presence of sodium percarbonate and TAED at alkaline pH. The oxidation activity was further demonstrated for the bleaching of acid red 88 dye from solution and for the oxidation of cyclohexene. Unilever further increased the activity of this ligand in 1999 by replacing methylamine groups with aminoethane, known as MeN_4Py.[94]

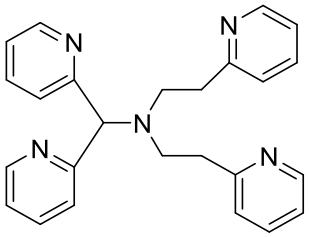

N_4Py

***Figure 10**: N_4Py ligand*

Further patents were filed using the ligands MeN_4Py and N_4Py for aerial bleaching.[95,96] These catalysts were efficient at removing curry and tomato stains under an alkaline pH, which extends the stain profile for aerial bleaching beyond hydrophilic stains, such as tea, as had previously been reported.[95] Unilever also patented a large group of other similar ligands, which have a wide stain bleaching profile.[97]

EPR, ES-MS and UV-Vis have been used to study the mechanism of reaction of N_4Py ligands.[98] For this, $[(N_4Py)Fe^{III}OOH]^{2+}$ was isolated and characterised after exposure to H_2O_2. The low spin iron (III) complex was demonstrated to be active for the hydroxylation of cyclohexane, suggesting that high valent iron species are viable intermediates in oxidation reactions. Roelfes et al[99] also proposed that the same intermediate is formed, which then forms hydroxyl radicals and $[(N_4Py)Fe^{IV}O]^{2+}$, and both are active for oxidation.

The reactivity of these complexes is mainly based on radical species and therefore they have a different mechanism of stain bleaching compared to MnTACN. The non-radical mechanism of MnTACN catalysts may explain the increased efficiency of

MnTACN for oily stain removal over these iron complexes.[100] Under general alkaline wash conditions, pH 10, FeN_4Py forms the less active adduct $Fe^{III}O_2$, which limits the bleach activity of the catalyst.[14] FeN_4Py catalysts may still be active at alkaline pH as the phenolic stains are easier to oxidise at high pH. There was no indication of a radical mechanism under these conditions.

1.3.2.3 *Iron Complexes with Macrocyclic Tetraamidate Ligands*

In 1996 Collins patented macrocyclic tetraamide iron complexes for solution bleaching in wastewater streams and dye transfer in laundry, in the presence of peroxy acids.[101] The mechanism under these conditions has not been studied; however, the authors published mechanistic details for the reaction when tBuOOH was used as the oxidant.[102] It was found that the catalysts lose activity over time after the addition of fresh oxidant and substrate *via* a deactivation mechanism with a Fe^{IV}=O intermediate. Substituting ethyl for methyl groups on the ligand side chains improved catalyst lifetime.

In 2003, the Collins group published mechanistic insights into the mononuclear Fe^{III} tetraamidato complexes for oxidation catalysis.[103] It was found that, in the presence of O_2, the complex yields an oxo-bridged Fe^{IV} dinuclear complex that is active for the oxidation of benzyl alcohols and methyl orange dye. There was no evidence of a radical mechanism and a two-electron transfer mechanism was postulated for the oxidation of alcohols.

1.3.3 *Cobalt Bleach Catalysts*

Cobalt pentaamine complexes were first patented by Solvay Interox in 1988[104] and later by Proctor and Gamble in 1996.[105] Proctor and Gamble claimed that the further

addition of a carboxylic acid ligand improves the bleaching activity. This catalyst was specifically developed for use in automatic dishwashing. Thompson *et al*[106] investigated a range of transition metal catalysts for phenolphthalein oxidation with H_2O_2, and $[Co(NH_3)_5Cl]^{2+}$ was the most active catalyst. H_2O_2 activation removed chlorine from the complex, forming the active catalyst $[Co(NH_3)_5(OOH)]^{2+}$, but no further mechanistic details were investigated.

A range of cobalt catalysts with TPA, trispicen and N_4Py ligands have also been patented by Degussa, mainly for use in pulp bleaching.[107] A peroxocobalt (III) species was suggested to be an intermediate in the bleaching process; however, there is no other literature that supports this claim.

1.3.4 *Heterogeneous Catalysis*

Overall, research into bleach catalysis has been dominated by homogeneous catalysis, as these catalysts are highly active and selective towards the chromophore centres in stains. Heterogeneous catalysts are, however, well known to be active for both oxidation reactions and the disproportionation of H_2O_2.[1] Investigation of new heterogeneous catalysts for bleaching is more common as these materials are generally more cost effective and open up the possibility of reusable bleach catalysts.

1.3.4.1 *Heterogenization of Known Homogeneous Bleach Catalysts*

There has been recent interest in immobilising well known highly active homogeneous bleach catalysts with the aim of increasing activity and generating a reusable catalyst. In 2008, Veghini *et al*.[108] supported Mn(Me_3-TACN) on heteropolyacids (HPA), such as $H_4[SiW_2O_{40}]$. The addition of Mn(Me_3-TACN) to the HPA formed an insoluble orange powder. Oxidation activity of the generated

heterogeneous catalyst was quantified for the oxidation of alcohols, alkanes and alkenes. In comparison to Mn(Me_3-TACN), the heterogeneous version had lower activity but higher selectivity towards the oxidation product. The advantage of this method is that the active site of the original homogeneous catalyst remains intact.

Similarly, the Nakagaki group investigated the immobilisation of Manganese porphyrins on silica coated magnetite and clay nanotubes.[109] Bleaching activity was assessed by the removal of Brilliant Green (BG) dye from solution. Complexes formed with silica coated magnetite were easily separated from the reaction using a magnet and were more active for dye removal on the first reuse. The clay nanotube complexes lost bleaching activity on reuse but were easily separated by filtration. Overall both complexes had high bleaching activity; however, the timescale of the reaction was over hours not minutes, which is much longer than standard household wash cycles.

Salen ligand complexes are well known in bleach and oxidation catalysis. These have been encapsulated in NaY zeolite, using the impregnation and "ship-in-a-bottle" method, for pulp bleaching with H_2O_2 and peracetic acid.[110] Immobilisation of copper(II) salen complexes using the "ship-in-a-bottle" method enhances the selectivity and activity of the homogeneous Cu(II) complex. UV-Vis and Fourier transform infrared spectroscopy (FTIR) attributed the activity of the catalyst to the formation of copper-hydroperoxide species.

1.3.4.2 *Polyoxometalates*

Polyoxometalates (POMs) are anions with transition metal oxo-bridged structures; depending on the anion used these can be classified as homogeneous or

heterogeneous catalysts. In the current literature, the focus is on the use of POMs for pulp bleaching.[111,112] Vanadium POMs were tested with molecular oxygen for wood pulp bleaching in the production of paper; however, the cellulose damage was too high for commercialisation.[111] Gaspar *et al*[112] tested manganese (III) POMs also for aerial pulp bleaching, with the general formula $[XW_{11}Mn^{III}(H_2O)O_{39}]^{n-}$ where X = boron, silicon or phosphorus. It was found that the silicon-containing POM had the highest activity, due to the higher redox potential in comparison to tungsten-based POMs. Again, these catalysts are not suitable for commercialisation as the rate of delignification, which is required for effective bleaching, is slow.

Unilever and Henkel have patented POMs for the use in laundry and automatic dishwasher bleaching.[113,114] Unilever patented the use of Keggin-type POMs with zinc, cobalt, nickel, copper and manganese for aerial stain bleaching. It was shown that the catalysts were active for tea and strawberry stain removal from fabric. Henkel recently patented manganese and molybdenum POMs for bleaching with H_2O_2 or molecular oxygen, specifically for use in automatic dishwashing detergents; however, limited stain data is included in the patent to draw conclusions on the activity of the catalysts.

1.3.4.3 *Metal Oxides*

Heterogeneous transition metal oxide catalysts have been tested for bleaching and oxidation of organics with H_2O_2. Investigation into the potential bleach activity of these catalysts is typically conducted using a solution-phase model stain compound, and not the stain itself. MnO_x nanoparticles suspended on polyelectrolyte brushes were investigated by Polzer *et al.*[115] for the oxidation of morin. Morin is a brown

compound found in tea leaves that can be used as a model compound for stain removal. It was found that the rate limiting step of the reaction was the absorption of both H_2O_2 and morin onto the surface of the catalyst. A reaction mechanism *via* a singlet oxygen active species was postulated. Therefore, the mechanism of bleaching with heterogeneous nanoparticles may be radical in nature and different from what has been observed for homogeneous catalysts, especially Mn(MeTACN). Mn(MeTACN) oxidation goes *via* high valent mono-nuclear intermediate species that oxidise the substrate through oxygen transfer.

Copper was also investigated for benzyl alcohol oxidation[116] and for the degradation of methyl orange[117]. For benzyl alcohol oxidation, copper (II) complexes, copper and copper oxide nanoparticles supported on SBA-15 conversions were compared. Copper oxide supported on SBA-15 exhibited low conversion of 20 % and high selectivity to the benzaldehyde product of 73 %. In comparison, copper (II) complexes exhibited higher conversions of 73 % after 30 min. For methyl orange oxidation, copper species were incorporated into the framework of MgAlO. Cu(II) and Cu (I) species were present in the catalyst and the postulated mechanism suggested a redox reaction between Cu(II) and Cu(I) with H_2O_2 to form radical species. Conversion of methyl orange was 99 %, showing the potential of copper catalysts for oxidation of coloured complexes.

Fe_3O_4 catalysts were investigated for the oxidation of catechol by Gogoi and co-workers[118]. Fe_3O_4 supported on CeO_2 showed Fenton like chemistry and exhibited 89 % catechol degradation, with H_2O_2 as an oxidant, after 1 hour. It was found that increasing surface area and decreasing particle size improved the catalyst

performance, which could be modified by the amount of Fe_3O_4 supported on CeO_2; however, acidic conditions were used for the oxidation of catechol, pH 2 – 4, indicating that under alkaline conditions Fenton chemistry may not be suitable.

Photocatalysis has also been studied for the removal of dyes with metal oxides. Chen *et al.*[119] prepared ZnO catalysts *via* the sol-gel method for the degradation of methyl orange under UV light with H_2O_2 as the oxidant. ZnO is active for methyl orange degradation between pH 2 – 10, although acidic pH is favoured. Investigation into the mechanism with radical scavengers indicates that superoxide ions are the active species for the reaction. Overall, metal oxide catalysts show potential for removal of organics and coloured species in solution.

1.4 *Chemistry in a Dishwasher*

The number of dishwashers in households has been increasing steadily since the first electric dishwasher was launched in the 1950's.[120] Over the following decades, dishwashers have become more energy and water efficient.[3] However, there is a push from consumers for a shorter wash cycle and lower temperatures. The addition of a catalyst into dishwashing formulas may help achieve this. The complex mixture in the formula and the set conditions of the wash increase the complexity of the challenge.

1.4.1 *History of Dishwashing*

The first dishwasher was hand powered and invented in 1850,[121] but it was not reliable and difficult to use. Josephine Cochrane patented the first reliable hand powered dishwasher in 1887.[122] It was said she was annoyed at her servants for always breaking and scuffing the plates when they washed the dishes. The first electric dishwasher was invented in 1929 by Miele;[123] however, dishwashers were not a commercial success until the 1950s.

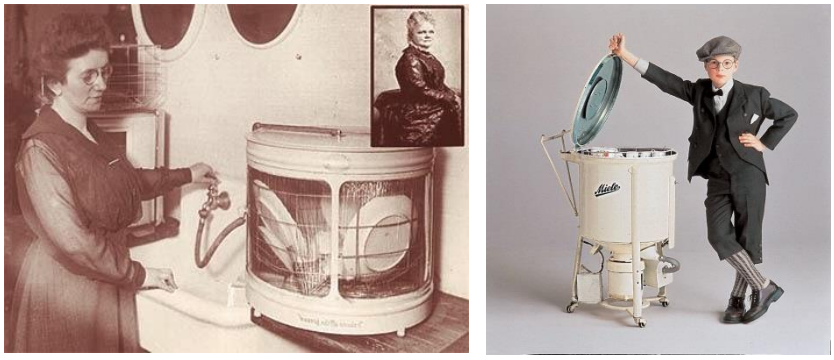

***Image 1**: Images of Josephine Cochrane's dishwasher and the first electric dishwasher by Miele.*[124,123]

In the UK, since the mid-1990s dishwasher ownership has almost doubled.[120] Over time dishwasher technology has improved to the point that use of a dishwasher is more energy and water efficient than hand washing.

Components of a Tablet Formulation

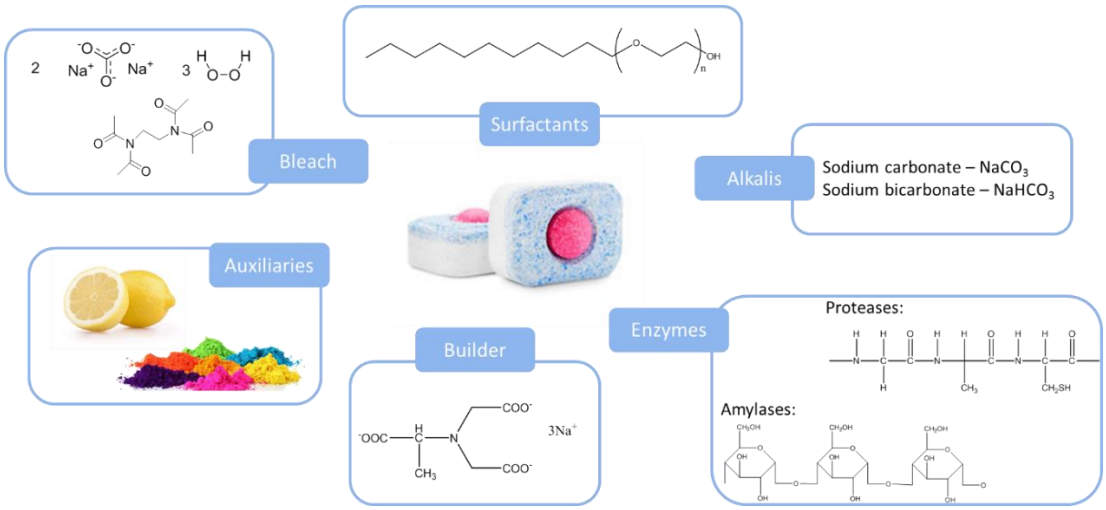

***Figure 11**: Overview of formulation for dishwasher tablets.*[125]

There are many different stains to tackle during a dishwasher run. Formulations not only have a bleaching system but also enzymes, builders and fragrances, the different parts of a formulation are shown in Figure 11 The bleaching system is mainly comprised of sodium percarbonate, a source of H_2O_2, and TAED. TAED is a bleach activator that reacts with H_2O_2 to form peracetic acid. A builder is also added to remove metal ions from the wash liquor. Calcium and transition metals can degrade peracetic acid before it reaches the stain, and therefore removing these from the solution improves the bleaching performance of the tablet.

Stains formed by proteins and fats cannot be eliminated by bleaching and need enzymes to be removed from the dishware. A mixture of lipases and amylases are

added to the full formulation. The enzymes added must be active at the high pH and temperatures of a typical wash. It is also important that any prospective catalyst does not denature these enzymes.

As the product is for consumers, the look and fragrance of the tablet play an important role in consumer satisfaction, which is an important indicator for commercial viability. Generally, white or bright dyes are added to the formula to make the tablet look appealing. The use of black, brown, or grey coloured compounds can dissuade consumers from using the tablet. Consumers associate white formulas with bleaching performance whilst a tablet containing black particulates is typically associated with poor performance by the consumer, regardless of actual results. Similarly, the smell of the dishwasher after the wash is important to consumers. The remaining smell of food stuffs after the wash is associated by consumers with poor cleaning, and therefore fragrances also play an important part in the formulation.

1.4.2 *Standard Dishwashing Conditions*

Conditions for the wash have been optimised so each compound is active and can contribute to cleaning. Bleaching is most active at a pH above 10; however, above this pH the surface of glassware is corroded making them appear cloudy over multiple washes. [2]

Figure 12 shows the temperature profile of a standard dishwasher program. The tablet is released at the start of the main wash as the temperature is increasing up to the set wash temperature. The time of the main wash varies from program to program, but for standard industry testing, the main wash is 8 mins.[126] Therefore, all

the active ingredients must dissolve and be fast action to remove stains and dirt in a short time. New active ingredients for use in dishwasher formulations must be able to improve cleaning at alkaline pH, in a temperature range of 30 – 80 °C and have an acceptable dissolution time.

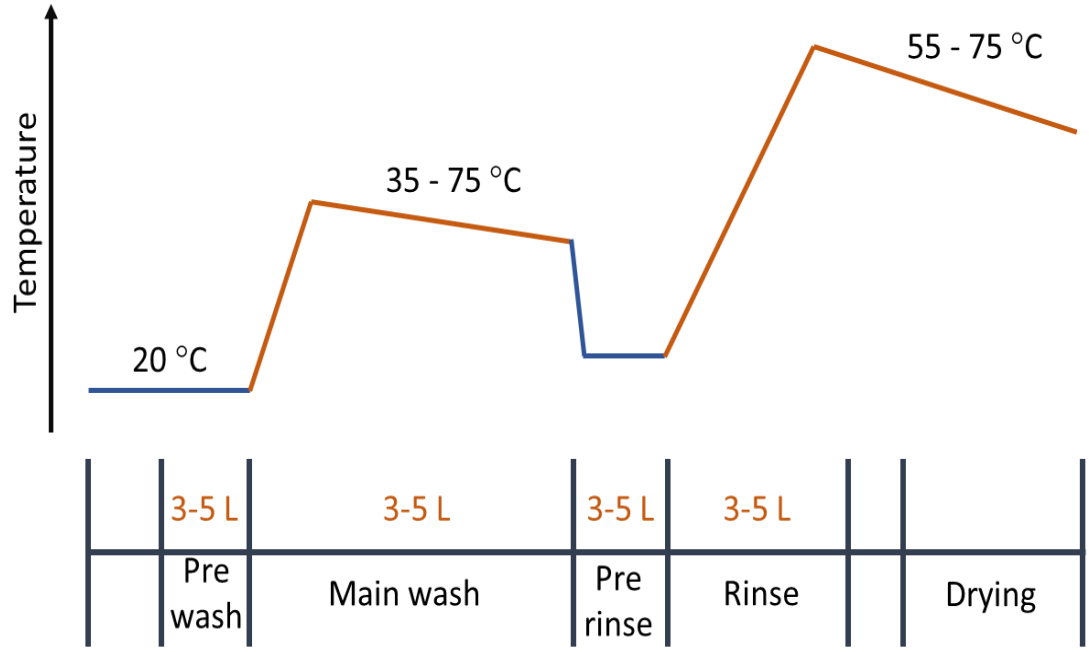

***Figure 12**: Temperature profile of standard dishwasher program.*[125]

1.5 *Model Stains for Formulation Development*

Development of new formulas requires testing in a dishwasher using consumer relevant conditions with model stains. The preparation of these stains and the methods to test them are industry wide for comparison between brands.[126] Tea, milk, tomato, pasta, egg and meat stains are all used to test how effective each part of the formula is at removing these stains from the dishes. These model stains are all prepared onto plates, bowls, and glassware, which are loaded into the dishwasher. In addition to these stains, a soil is added to simulate the food waste that is present in most household dishwasher runs. This also has a range of food types present to try to accurately simulate the different compounds present in the wash liquor during the run.

Ketchup, mustard, starches, animal fats and eggs are all added to the soil mixture. It is imperative that every part of the formula can still be effective in hard water and in solution with the various soil components. All applicative testing must also be run under these conditions otherwise the tablet may not be effective in real world conditions.

1.5.1 *Tea Stain Model*

Harsh coloured stains are required for testing the bleaching system of dishwasher tablets. Tea is the industry standard, which contains a mixture of theaflavins and thearubigins, structure shown in Figure 13, that gives strains their distinctive dark brown colour.[127] Tea stain composition depends on the hardness of the water used to brew the tea, the tannin content of the tea and the age of the stain.[128] Each of these factors affect how easily the stain can be removed.[129]

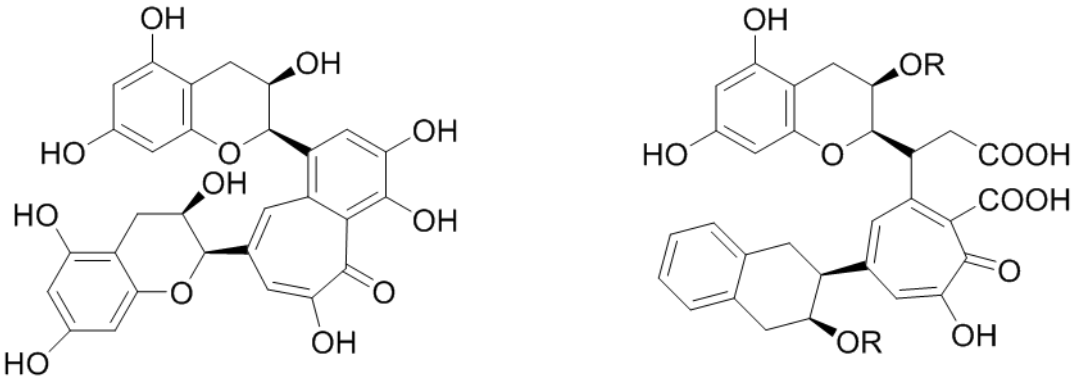

***Figure 13**: Structure of theaflavin and thearubigin which are responsible for the brown colour of tea and tea stains.*

Hard water is defined by the concentration of $CaCO_3$ dissolved in the water. Increasing calcium content increases the harshness of the stain, as calcium bridges form between polyphenol molecules, and also between the polyphenols and the surface of the cup.[129] Hard water can also cause the formation of "tea scum". This forms on the liquid surface and is caused by calcium bridging between polyphenols in solution.[130] As the stain is left exposed to air, oxidation reactions occur between the polyphenols, increasing the harshness of the stain making it harder to remove.

Tannin content of the tea affects the harshness of the stain. Green tea, which does not contain flavonoids, does not leave a stain on the cup surface. During the oxidation of green tea to form black tea these flavonoids are formed. [131] Thearubigins are responsible for the characteristic brown colour. Different tea leaves and blends have varying amounts of these polyphenols present.[132] Brewing a tea extracts polyphenols from the leaves, which are absorbed onto the cup surface. Calcium

bridging and oxidations reactions also occur at the liquid/gas interface on the cup surface, making the stain harder to remove.

Formation of tea stains can be lessened by addition of other compounds into the tea brew. A slice of lemon adds citric acid into the water. The citric acid acts as a binder and removes calcium from the water.[133] This decreases calcium bridging between the polyphenols, leading to a stain that is easier to remove. Addition of milk to tea also hinders stain formation.

1.5.2 *Model Compounds for Bleaching*

The chemical structure of tea stains is difficult to define and can be affected by a wide range of parameters. For investigation of potential bleach catalysts, model compounds are used to quantify catalytic activity and investigate possible bleach mechanisms. As stains are comprised of phenolic compounds, model compounds such as phenol,[134] gallic acid[135], catechol[68] and morin[136] have all been reported for bleach or oxidation of organics, (Figure 14).

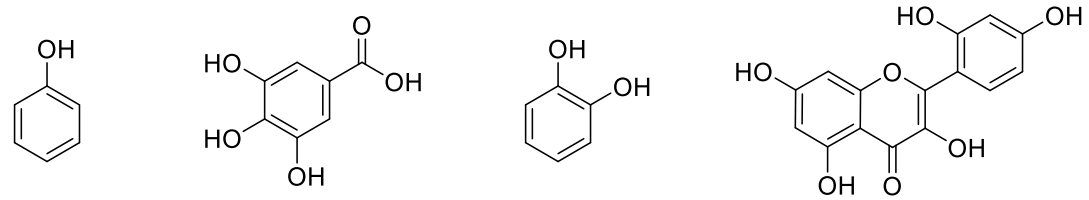

***Figure 14**: Possible bleaching model compounds*

Sorokin *et al.*[68] investigated the oxidation of catechol with H_2O_2, perborate, perborate/TAED and percarbonate with metallophthalocyanine catalysts. Fe, Mn and Co catalysts were active, and the results indicated the best activity was observed with

sodium percarbonate, which suggests that catechol may be a suitable model compound for sodium percarbonate/TAED bleaching formulations. Warmoeskerken and co-workers[136] investigated morin as a model compound for bleaching cotton fibres with Mn(MeTACN). The results showed that the catalyst is highly effective for bleaching with and without H_2O_2 present. Morin has also been used as a model compound to investigate dendrimer encapsulated Pd, Pt and Au oxidation catalysts.[137,138] Co_3O_4 nanoparticles have been studied as a potential heterogeneous catalyst for bleaching in the oxidation of morin with H_2O_2 as the oxidant.[139] Overall, morin has been shown to be a useful model compound for bleaching.

1.6 *Aims of the Project*

This project is focused on the improvement of bleaching systems in automatic dishwashing with the addition of a heterogeneous catalyst into the wash. Current technology is based on homogeneous catalysts that are active for bleaching; however, these are expensive and lost at the end of each wash cycle. Development of a heterogeneous catalyst has the potential to improve bleaching while lowering the cost of the formulation. With further development of dishwasher technology, heterogeneous catalysts could be reused between washes and incorporate photoinduced bleaching technology and aerial bleaching formulas.

The objectives of this project are:

- To identify new heterogeneous catalytic materials that are simple to synthesise and are comparable in activity to the current industry standard, MnTACN

- Investigate the current bleach reaction with sodium percarbonate/TAED and how the current catalysts improve bleaching
- Understand key properties of developed heterogeneous bleach catalysts *via* a bleach model reaction and characterisation
- Applicative testing of active bleach catalysts in a dishwasher to assess the suitability of new catalytic materials for product formulations

References

1 J. J. Dannacher, *J. Mol. Catal. A Chem.*, 2006, **251**, 159–176.

2 G. O. Bianchetti, C. L. Devlin and K. R. Seddon, *RSC Adv.*, 2015, **5**, 65365–65384.

3 G. Reinhardt, C. Miranda, M. Martin and K. Bleach, 2013, **8**, 11–12.

4 O. Deutschmann, H. Knözinger, K. Kochloefl and T. Turek, in *Weinheim: Wiley-VCH*, 2009.

5 J. R. H. Ross, *Heterogeneous catalysis : fundamentals and applications*, Elsevier, 2012.

6 J. N. Armor, *Catal. Today*, 2011, **163**, 3–9.

7 E. M. Jones, *Ind. Eng. Chem.*, 1950, **42**, 2208–2210.

8 J. L. Gay-Lussac, in *A History of Chemistry*, Macmillan Education UK, London, 1964, pp. 77–98.

9 L. B. Hunt, *Platin. Met. Rev*, 1979, **23**, 29–31.

10 J. E. (Johan E. Jorpes, *Jac. Berzelius: his life and work,* University of California Press, 1970.

11 R. L. Burwell, *ACS Symp. Ser. ACS*, 1983, 3–12.

12 J. L. Casci, C. M. Lok and M. D. Shannon, *Catal. Today*, 2009, **145**, 38–44.

13 S. Glasstone, K. J. Laidler and H. Eyring, *The Theory of Rate Processes: The Kinetics of Chemical Reactions*, McGraw-Hill Book Company, New York, 1941.

14 R. Hage and A. Lienke, *Angew. Chemie - Int. Ed.*, 2005, **45**, 206–222.

15 A.I.S.E, Market and economic data - AISE, https://www.aise.eu/our-industry/market-and-economic-data-2292.aspx, (accessed 18 May 2019).

16 J. Toedt, D. Koza and K. V. Cleef-Toedt, *Chemical composition of everyday products*, Greenwood Press, 2005.

17 Henkel, Henkel.com, https://www.henkel.com/company/milestones-and-achievements/history, (accessed 29 January 2019).

18 G. Reinhardt, *J. Mol. Catal. A Chem.*, 2006, **251**, 177–184.

19 N. J. Milne, *J. Surfactants Deterg.*, 1998, **1**, 253–261.

20 C. W. Jones, *Applications of hydrogen peroxide and derivatives*, Royal Society of Chemistry, 1999.

21 REGULATION (EU) No 259/2012, *Off. J. Eur. Union*, 2012, 16–21.

22 A. McKillop and W. R. Sanderson, *Tetrahedron*, 1995, **51**, 6145–6166.

23 U. Zoller, *Handbook Of Detergents, Part E: Applications*, M. Dekker, 2008.

24 R. G. Pritchard and E. Islam, *Acta Crystallogr. Sect. B Struct. Sci.*, 2003, **59**, 596–605.

25 U. Tsoler, *Handbook of detergents. Part C, Analysis*, M. Dekker, 2005.

26 S. H. Zeronian and M. K. Inglesby, *Cellulose*, 1995, **2**, 265–272.

27 K. M. Thompson, W. P. Griffith and M. Spiro, *J. Chem. Soc. Chem. Commun.*, 1992, 1600–1601.

28 K. M. Thompson, W. P. Griffith and M. Spiro, *Faraday Trans*, 1993, **89**, 4035–4043.

29 United States Patent Office, 2,898,181, 1959.

30 United States Patent Office, 1,697,805, 1928.

31 G. Broze, *Handbook of Detergents. Part A: Properties*, Marcel Dekker, 1999.

32 G. Reuss, W. Disteldorf, A. O. Gamer and A. Hilt, *Ullmann's Encyclopedia of Industrial Chemistry*, 2000.

33 D. M. Davies and M. E. Deary, *J. Chem. Soc. Perkin Trans. 2*, 1991, 1549.

34 A. S. Freddy Adams, Stephen J. Blunden, Rudy van Cleuvenbergen, C.J. Evans, Lawrence Fishbein, Urs-Josef Rickenbacher, Christian Schlatter, *Volume 3 of The Handbook of Environmental Chemistry Anthropogenic Compounds*, Springer-Verlag, 1990.

35 C. Xu, X. Long, J. Du and S. Fu, *Carbohydr. Polym.*, 2013, **92**, 249–253.

36 X. Long, C. Xu, J. Du and S. Fu, *Carbohydr. Polym.*, 2013, **95**, 107–113.

37 E. Stepan, C. Neamtu, C. Enãscuta, V. Ordeanu, M. Necsulescu, A. A. Andries and A. Irimia, *Revisita Chim.*, 2008, **59**, 3–8.

38 United States Patent Office, 4,412,934, 1983.

39 A. Cahn, *Proceedings of the 3rd World Conference on Detergents*, AOCS Press, 1994.

40 E. Kissa, J. M. Dohner, W. R. Gibson and D. Strickman, *J. Am. Oil Chem. Soc.*, 1991, **68**, 532–538.

41 T. C. Bruice, J. K. Katzhendler and L. R. Fedor, *J. Am. Chem. Soc.*, 1968, **90**, 1333–1348.

42 M. Tsumadori, *J. Oleo Sci.*, 2001, **50**, 367–372.

43 M. Tsumadori, *Changing Marketplace in Asia - Developed Markets in Japan, Korea and Taiwan*, AOCS Press, 2003.

44 G. Reinhardt, L. Cuypers, A. Ince and N. Jeckel, *SOFW*, 2006, **132**, 36–43.

45 United Kingdom Intellectual Patent Office, GB847702A, 1958.

46 United States Patent Office, US3075921, 1963.

47 World Intellectual Property Organization, WO1990007501A1, 1990.

48 World Intellectual Property Organization, WO 2011/005905 Al, 2011.

49 World Intellectual Property Organization, WO 2013/064811 A1, 2013.

50 World Intellectual Property Organization, WO 99/65905, 1999.

51 World Intellectual Property Organization, WO 02/48301 A1, 2001.

52 World Intellectual Property Organization, WO 2013/092051 A1, 2013.

53 European Patent Office, EP 1 557 457 B1, 2005.

54 T. J. Collins, *Acc. Chem. Res.*, 1994, **27**, 279–285.

55 R. Hage, J. E. Iburg, J. Kerschner, J. H. Koek, E. L. M. Lempers, R. J. Martens, U. S. Racherla, S. W. Russell, T. Swarthoff, R. P. van Vliet, J. B. Warnaar, L. Van Der Wolf and B. Krijnen, *Lett. to Nat.*, 1994, **369**, 637–639.

56 M. Verrall, *Nature*, 1995, **373**, 181.

57 European Patent Office, 0 082563 B1, 1982.

58 B. S. Lane, M. Vogt, V. J. DeRose and K. Burgess, *J. Am. Chem. Soc.*, 2002, **124**, 11946–11954.

59 European Patent Office, 0 124 341 B1, 1984.

60 European Patent Office, 0 327 11 B1, 1993.

61 European Patent Office, 0 408 131 B1, 1991.

62 European Patent Office, EP 0 458 397 B1, 1991.

63 J. Bonvoisin, M. Corbella, S. E. Vitols, J. J. Girerd, K. Wieghardt, U. Bossek, B. Nuber and J. Weiss, *J. Am. Chem. Soc.*, 1988, **110**, 7398–7411.

64 B. C. Gilbert, N. W. J. Kamp, J. R. Lindsay Smith and J. Oakes, *J. Chem. Soc. Perkin Trans. 2*, 1997, 2161–2166.

65 B. C. Gilbert, N. W. J. Kamp, J. R. L. Smith and J. Oakes, *J. Chem. Soc. Perkin Trans. 2*, 1998, 1841–1844.

66 B. C. Gilbert, J. R. L. Smith, A. Mairata i Payeras and J. Oakes, *Org. Biomol. Chem.*, 2004, **2**, 1176–1180.

67 B. C. Gilbert, J. R. L. Smith, M. S. Newton, J. Oakes and R. P. Prats, *Org. Biomol. Chem.*, 2003, **1**, 1568–1577.

68 A. Sorokin, L. Fraisse, A. Rabion and B. Meunier, *J. Mol. Catal. A Chem.*, 1997, **117**, 103–114.

69 R. Hage and J. Kerschner, *Trends Inorg. Chem.*, 1998, **35**, 6461.

70 B. C. Gilbert, J. R. Lindsay Smith, A. Mairata I Payeras, J. Oakes and R. Pons I Prats, *J. Mol. Catal. A Chem.*, 2004, **219**, 265–272.

71 D. E. De Vos, J. L. Meinershagen and T. Bein, *Angew. Chemie (International Ed. English)*, 1996, **35**, 2211–2213.

72 P. Giorgio Cozzi, *Chem. Soc. Rev.*, 2004, **33**, 410–421.

73 European Patent Office, EP 0 869 171 B1, 2004, 99, 1–10.

74 World Intellectual Property Organization, WO 97/07191, 1997.

75 T. Katsuki, *Coord. Chem. Rev.*, 1995, **140**, 189–214.

76 P. Pietikäinen, *J. Mol. Catal. A Chem.*, 2001, **165**, 73–79.

77 World Intellectual Property Organization, WO 98/39098, 1998.

78 World Intellectual Property Organization, WO 00/29537, 2000.

79 T. J. Hubin, J. M. McCormick, S. R. Collinson, M. Buchalova, C. M. Perkins, N. W. Alcock, P. K. Kahol, A. Raghunathan and D. H. Busch, *J. Am. Chem. Soc.*, 2000, **122**, 2512–2522.

80 World Intellectual Property Organization, WO 02/088289 A2, 2001.

81 World Intellectual Property Organization, WO 2004/007657 A1, 2004.

82 World Intellectual Property Organization, WO 2004/039933 A1, 2004.

83 T. Wieprecht, J. Xia, U. Heinz, J. Dannacher and G. Schlingloff, *J. Mol. Catal. A Chem.*, 2003, **203**, 113–128.

84 J. Limburg, J. S. Vrettos, M.-N. Collomb, L. M. Liable-Sands, A. L. Rheingold, R. H. Crabtree and G. W. Brudvig, *Science (80-.).*, 1999, **283**, INOR-495.

85 J. Limburg, J. S. Vrettos, H. Chen, J. C. De Paula, R. H. Crabtree and G. W. Brudvig, *J. Am. Chem. Soc.*, 2001, **123**, 423–430.

86 World Intellectual Property Organization, WO 97/30144, 1997.

87 European Patent Office, EP 0 783 035 B1, 1996.

88 World Intellectual Property Organization, WO 94/00234, 1993.

89 J. Brinksma, R. Hage, J. Kerschner and B. L. Feringa, *Chem. Commun.*, 2000, **2**, 537–538.

90 World Intellectual Property Organization, WO 97/48710, 1997.

91 K. Chen, M. Costas, J. Kim, A. K. Tipton and L. Que, *J. Am. Chem. Soc.*, 2002, **124**, 3026–3035.

92 J. Kaizer, M. Costas and L. Que, *Angew. Chemie - Int. Ed.*, 2003, **42**, 3671–3673.

93 European Patent Office, EP 0 765 381 B1, 1995.

94 European Patent Office, EP 0 909 809 B1, 1999.

95 World Intellectual Property Organization, WO 00/12808, 2000.

96 World Intellectual Property Organization, WO 02/50229 A1, 2002.

97 United States Patent Office, US 2003/0230736 A1, 2003.

98 M. Lubben, A. Meetsma, E. C. Wilkinson, B. Feringa and L. Que, *Angew. Chemie Int. Ed. English*, 1995, **34**, 1512–1514.

99 G. Roelfes, M. Lubben, R. Hage, L. Que and B. L. Feringa, 2000, 2152–2159.

100 World Intellectual Property Organization, WO 02/072746 A1, 2002.

101 World Intellectual Property Organization, WO 98/03625, 1998.

102 C. P. Horwitz, D. R. Fooksman, L. D. Vuocolo, S. W. Gordon-Wylie, N. J. Cox and T. J. Collins, *J. Am. Chem. Soc.*, 1998, **120**, 4867–4868.

103 A. Ghosh, A. D. Ryabov, S. M. Mayer, D. C. Horner, D. E. Prasuhn, S. Sen Gupta, L. Vuocolo, C. Culver, M. P. Hendrich, C. E. F. Rickard, R. E. Norman, C. P. Horwitz and T. J. Collins, *J. Am. Chem. Soc.*, 2003, **125**, 12378–12379.

104 European Patent Office, EP 0 272 030 A2, 1988.

105 World Intellectual Property Organization, WO 96/23859, 1996.

106 K. M. Thompson, W. P. Griffith and M. Spiro, *J. Chem. Soc. Faraday Trans*, 1994, **186**, 69–77.

107 European Patent Office, EP 1 199 402 A2, 2001.

108 D. Veghini, M. Bosch, F. Fischer and C. Falco, *Catal. Commun.*, 2008, **10**, 347–350.

109 G. M. Ucoski, G. S. Machado, G. D. F. Silva, F. S. Nunes, F. Wypych and S. Nakagaki, *J. Mol. Catal. A Chem.*, 2015, **408**, 123–131.

110 N. Zhang and X. F. Zhou, *J. Mol. Catal. A Chem.*, 2012, **365**, 66–72.

111 I. A. Weinstock, R. H. Atalla, R. S. Reiner, M. A. Moen, K. E. Hammel, C. J. Houtman, C. L. Hill and M. K. Harrup, *J. Mol. Catal. A Chem.*, 1997, **116**, 59–84.

112 A. Gaspar, D. V. Evtuguin and C. Pascoal Neto, *Appl. Catal. A Gen.*, 2003, **239**, 157–168.

113 US Patent Office, US 6,074,437, 2000.

114 European Patent Office, EP 3 415 593 A1, 2018.

115 F. Polzer, S. Wunder, Y. Lu and M. Ballauff, *J. Catal.*, 2012, **289**, 80–87.

116 P. Cruz, Y. Pérez, I. Del Hierro and M. Fajardo, *Microporous Mesoporous Mater.*, 2016, **220**, 136–147.

117 J. Han, H. Zeng, S. Xu, C. Chen and X. Liu, *"Applied Catal. A, Gen.*, 2016, **527**, 72–80.

118 A. Gogoi, M. Navgire, K. C. Sarma and P. Gogoi, *Chem. Eng. J.*, 2017, **311**, 153–162.

119 X. Chen, Z. Wu, D. Liu and Z. Gao, *Nanoscale Res. Lett.*, 2017, **12**, 143.

120 UK households: ownership of dishwashers 1994-2014 | Survey, https://www.statista.com/statistics/289151/household-dishwashing-in-the-uk/, (accessed 12 June 2017).

121 United States Patent Office, 7365, 1850.

122 United States Patent Office, US731341, 1903.

123 Miele, Miele, https://www.miele.com/en/com/history-2089.htm, (accessed 16 May 2020).

124 Universal and Appliance Dishwasher Centre, How the Dishwasher Has Changed Our World | Universal Appliance and Kitchen Center, https://uakc.net/blog/dishwasher-changed-world/, (accessed 16 May 2020).

125 Chemistry in your cupboard: Finish- Learn Chemistry, http://www.rsc.org/learn-chemistry/resource/res00000009/finish?cmpid=CMP00000011, (accessed 12 November 2018).

126 IKW, *sofw Journal, Home Pers. Care Ingredients Formul.*, 2016, 37–38.

127 S. Li, C.-Y. Lo, M.-H. Pan, C.-S. Lai and C.-T. Ho, *Food Funct.*, 2013, **4**, 10–8.

128 Y. Tanizawa, T. Abe and K. Yamada, *Food Chem.*, 2007, **103**, 1–7.

129 K. Yamada, T. Abe and Y. Tanizawa, *Food Chem.*, 2007, **103**, 8–14.

130 M. Spiro and Y. Y. Chong, *Food Chem.*, 1997, **59**, 247–252.

131 H. Savolainen, *J. Appl. Toxicol.*, 1992, **12**, 191–192.

132 J. J. Dalluge and B. C. Nelson, *J. Chromatogr. A*, 2000, **881**, 411–424.

133 M. Spiro, Y. Y. Chong and D. Jaganyi, *Food Chem.*, 1996, **57**, 295–298.

134 K. Fajerwerg and H. Debellefontaine, *Appl. Catal. B Environ.*, 1996, **10**, 229–235.

135 D. Mantzavinos, *Process Saf. Environ. Prot.*, 2003, **81**, 99–106.

136 T. Topalovic, V. A. Nierstrasz and M. M. C. G. Warmoeskerken, *Fibers Polym.*, 2010, **11**, 72–78.

137 M. Nemanashi and R. Meijboom, *Langmuir*, 2015, **31**, 9041–9053.

138 P. Ncube, T. Hlabathe and R. Meijboom, *Appl. Surf. Sci.*, 2015, **357**, 1141–1149.

139 M. S. Xaba and R. Meijboom, *Appl. Surf. Sci.*, 2017, **423**, 53–62.

2 Chapter 2 Experimental

2.1 *Source and Purity of Chemicals Used*

All chemicals used are given below with approximate purity and the supplier.

Copper nitrate, > 99 %, **Sigma Aldrich**

Zirconia nitrate, > 99 %, **Sigma Aldrich**

Iron nitrate, > 99 %, **Sigma Aldrich**

Manganese nitrate, > 99 %, **Sigma Aldrich**

Zinc nitrate, > 99 %, **Sigma Aldrich**

Oxalic acid, anhydrous > 99%, **Sigma Aldrich**

Ethanol, denatured, **Sigma Aldrich**

Nitric acid, 70% > 99 %, **Sigma Aldrich**

Sodium percarbonate **provided by Reckitt Benckiser**

TAED **provided by Reckitt Benckiser**

MGDA **provided by Reckitt Benckiser**

Peracetic acid solution, 35 wt% **Fischer Scientific**

Manganese oxide, > 99 %, **Sigma Aldrich**

Sulfuric acid, > 99%, **Sigma Aldrich**

Catechol, > 99 %, **Sigma Aldrich**

Sodium carbonate, anhydrous > 99 %, **Sigma Aldrich**

Morin hydrate, > 99 %, **Sigma Aldrich**

Ferroin indicator, 0.1 wt% in water, **Sigma Aldrich**

Cerium (IV) sulfate, > 99 %, **Sigma Aldrich**

Potassium iodide, > 99 %, **Sigma Aldrich**

Ammonium molybdate, > 99 %, **Sigma Aldrich**

Sodium Thiosulfate, > 99 %, **Sigma Aldrich**

2.2 *Definitions*

Conversion of TAED, H_2O_2 and catechol was calculated as a percentage based on the moles of reagent quantified in the reaction, using the following equation:

$$Conversion\ (\%) = \left(1 - \left(\frac{Final\ moles}{Initial\ moles}\right)\right) x\ 100$$

Peracetic acid and DAED yield was calculated as a percentage based on the theoretical maximum number of moles of product that could be formed during the reaction, using the following equation:

$$Yield\ (\%) = \left(\frac{Final\ mole}{Theoretical\ max.moles}\right) x\ 100$$

For morin reactions, the conversion was expressed as a ratio between the concentration measured at a certain time and the initial concentration at the start of the reaction. The following equation was used:

$$\frac{C}{C_0} = \frac{Concentration\ (M)}{Initial\ Concentration\ (M)}$$

2.3 *Catalyst Preparation*

2.3.1 *Oxalate Gel Method*

Catalysts were prepared using an oxalate gel method, where metal precursors are co-precipitated in solution using the addition of excess oxalic acid. Oxalate gel method was used to synthesise various mixed metal oxide catalysts at differing molar ratios. Cu, Zn, Fe and Mn were all synthesised with ZrO_2, following the method described by Deng and co-workers.[1,2]

An exemplary experimental procedure for the preparation of Cu:Zr (50:50 molar ratio) is outlined below. Copper nitrate (0.01 mol) and $ZrO(NO_3)_2$ hydrate (0.01 mol) were dissolved separately in absolute ethanol (100 mL) at room temperature in air. After dissolution in an ultrasonic bath at 30 °C for 30 minutes, the two solutions were combined and stirred at room temperature, in air, for 2 h. Oxalic acid dihydrate (0.024 mol) was subsequently added to this solution at once, resulting in the immediate precipitation of the metal oxalates. The solution was left to age for an additional 2 h at room temperature, in air. The oxalate gel was then collected *via* filtration and dried at 110 ° C in a static air oven for 16 h. After drying, the remaining solid was crushed into a fine powder using a pestle and mortar.

To prepare the oxide catalyst, the mixed metal oxalate precursor was calcined. The oxalate was added to a Coors high alumina combustion boat and calcined in a Carbolite tube furnace. The tube furnace was heated to 150 - 550 °C at a heating rate of 10 °C/min. Once at the desired temperature, it was maintained for an additional 2 h. During the calcination, air was flowed over the catalyst at a rate of 50 mL/min.

The same procedure described above was used to synthesise a range of catalysts. The molar ratio was differed by changing the amount of copper nitrate and zirconia nitrate used in the preparation, whist keeping total metal moles at 0.02. In some cases; iron, manganese and zinc nitrates were used in place of copper to synthesise different composition catalysts.

2.3.2 *Acid Treatment Post Calcination*

In some cases, removal of surface metal was achieved through washing the materials with concentrated HNO_3 (70.1 %). For this, the metal oxide (0.2 g) was stirred in HNO_3

(70 wt%, 200 mL) for 2 h at room temperature. The catalyst was collected and separated from the acid by centrifugation (50 mL portions, 3500 rpm, 5 mins). Deionised water was then added and the catalyst resuspended by agitation. Once again, the mixture was centrifuged to separate the catalyst from the acidic washing, which was then decanted off. This process was repeated until the post centrifugation washing had a pH of 7. Typically, the catalyst was washed three times. The washed catalyst was then dried in a static air furnace at 110 °C for 16 h.

2.4 *Investigation into the Bleaching Process*

To further understand the current bleaching process with sodium percarbonate as a solid source of H_2O_2 and TAED as the bleach activator, two types of experiments were devised:

1) The formation of peracetic acid was investigated through the addition of different ratios of sodium percarbonate and TAED, at different temperatures, and at different pH.
2) Investigating the decomposition of peracetic acid using a standardised peracetic acid solution, under different temperatures and at different pH

These reactions were analysed *via* the use of (i) a cerium sulfate titration to quantify H_2O_2 concentrations, and (ii) an iodometric titration to quantify the concentration of peracetic acid, as described in Section 1.6. High performance liquid chromatography (HPLC) was also used to quantify the concentrations of TAED and the products of per hydrolysis and hydrolysis of TAED.

2.4.1 *Peracetic Acid Formation Reactions*

Sodium percarbonate (0.37 mM - 5.3 mM) and TAED (0.05 – 1.1 mM) were added to water (90 mL) and stirred for 30 s at varying temperatures (15 – 70 °C) and varying pH (6 – 11). After 30 s, two samples (2 x 5 mL) were taken for immediate analysis v*ia* cerium sulfate and iodometric titration. Another sample (1 mL), was withdrawn and quenched with MnO_2 (10 mg) and H_2SO_4 (1 M, 1 drop) on ice. This sample was analysed *via* HPLC.

2.4.2 *Peracetic Acid Decomposition Reactions*

Peracetic acid solution (35 wt.% solution diluted to 2.2 mM) was added to water (90 mL). This was stirred for 16 mins under varying temperatures (30 – 70 °C) and varying pH (6 – 10). In addition, one reaction was run with each MGDA (0.41 mM), H_2O_2 (5.3 mM), and MnTACN (3 mg). Titration samples (2 x 5 mL) were taken at 0, 4, 8, 16 mins for analysis *via* cerium sulfate and iodometric titration.

2.4.3 *Decomposition of Hydrogen Peroxide*

Sodium percarbonate (5.3 mM) was dissolved in distilled water (180 mL) at 50 °C. Three initial samples (5 mL) were taken for analysis *via* cerium sulfate titration to quantify H_2O_2 present in the solution. TAED (1.1 mM), and a catalyst (10 mg) was added to the solution and stirred for 8 mins at 50 °C. At the end of the reaction, three samples were taken for analysis by cerium sulfate titration. The amount of H_2O_2 quantified from samples taken at 0 and 8 mins were used to calculate H_2O_2 conversion during the reaction.

2.5 *Assessment of Bleaching Performance*

Different methods were used to qualify and quantify the bleaching performance of different bleaching reagents and catalysts. In industry, standard assessment of bleaching performance is carried out using tea stains on tea cups, and a visual evaluation used to assess the applicative performance of a formulation. Alongside this, catechol and morin oxidation reactions were trialled to provide a more accurate measure of quantifying bleaching performance and influence of the catalyst.

2.5.1 *Catechol Oxidation with HPLC Analysis*

Catechol (8 mM) was added to water (90 mL) at 50 °C. After full dissolution was achieved (*ca.* 10 min), the reaction was commenced by the instant addition of sodium percarbonate (5.3 mM) and TAED (1.1 mM). Typically, reactions were run for 8 min during which the reaction temperature was maintained at 50 °C. 8 min reactions were chosen as this is a typical wash length in a dishwasher cycle. For reactions completed at different pH, a stock solution of sodium carbonate (1 M) was added dropwise until the desired pH was reached. A sample (5 mL) of the reaction was taken for analysis *via* HPLC. The sample was cooled in ice and neutralised with H_2SO_4 (0.5 M) to halt the reaction before analysis; different methods were trialled to stop the reaction, which is further discussed in Chapter 3, Figure 20.

The conversion of catechol was quantified through use of HPLC equipped with a diode array detector (DAD); a wavelength of 210 nm was used to monitor the Catechol concentration. An external calibration was conducted, whereby, a series of aqueous catechol solutions were prepared (1.8 mM – 8 mM) and evaluated using the same analytical procedure. The corresponding calibration is shown in **Figure 15**.

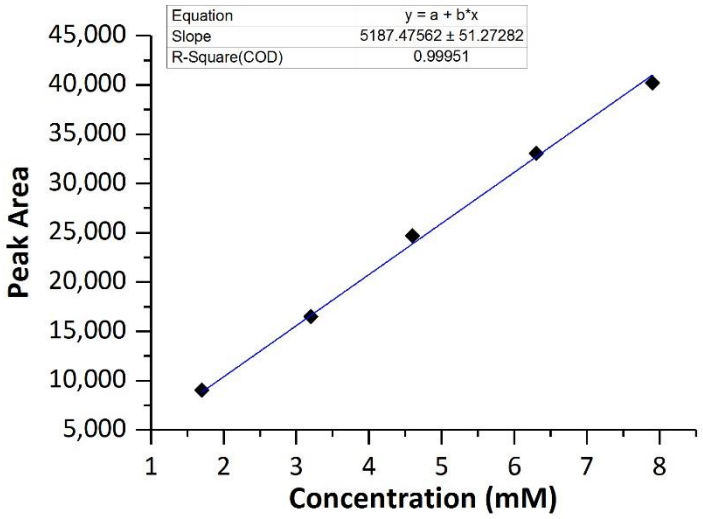

***Figure 15**: Calibration of catechol for HPLC at 210 nm.*

2.5.2 *Morin Oxidation with UV-Vis Analysis*

The conversion of Morin was monitored and quantified using UV-Vis at the maximum absorption of morin, 414 nm. A stock solution of morin (0.9 mM, 100 mL) was prepared for each series of experiments. Sodium carbonate (50 mM) was added to adjust the pH of the stock solution to 10 to ensure morin fully dissolved in the water.[3]

For the experiments, an aliquot of the morin stock solution (10 mL) was added to water (80 mL) at 50 °C, yielding an overall morin concentration of 0.1 mM. Sodium percarbonate (5.3 mM), TAED (1.1 mM), and the catalyst (homogeneous 0.01 mg, heterogeneous 0.1 mg) were added, and the solution was stirred at 50 °C for 30 mins. Samples were analysed at 0, 2, 4, 6, 8, 10, 15- and 30-minute intervals, recording the max absorption at 414 nm.

Calibration of morin concentration and UV-Vis absorbance was achieved using an external calibration method. For this, a series of morin solutions in the range of 0.01 mM to 0.1 mM were prepared and analysed by UV-Vis, **Figure 16**.

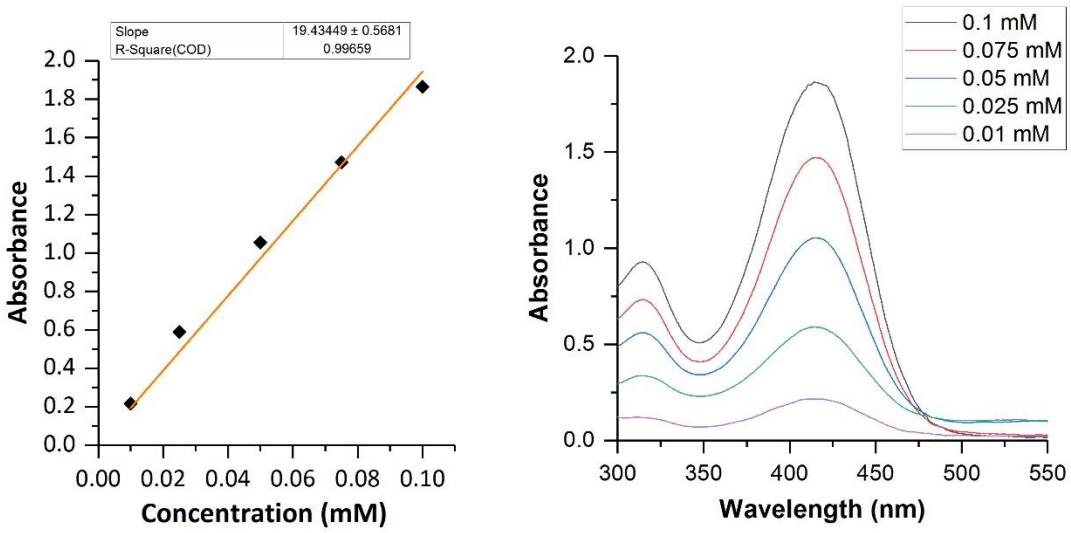

***Figure 16**: Calibration of Morin in UV-Vis.*

To ensure that the morin conversion observed was due to oxidation and not an interaction with the sodium percarbonate and TAED, morin was stirred with the reagents at room temperature for 30 minutes. **Figure 17** shows the interaction between morin with sodium percarbonate and TAED. There is no change in the maximum absorbance of morin for either sodium percarbonate or TAED, as the peak does not shift during the reaction. Therefore, any conversion observed during a morin reaction can be attributed to oxidation or degradation of morin and not a separate interaction with the reagents.

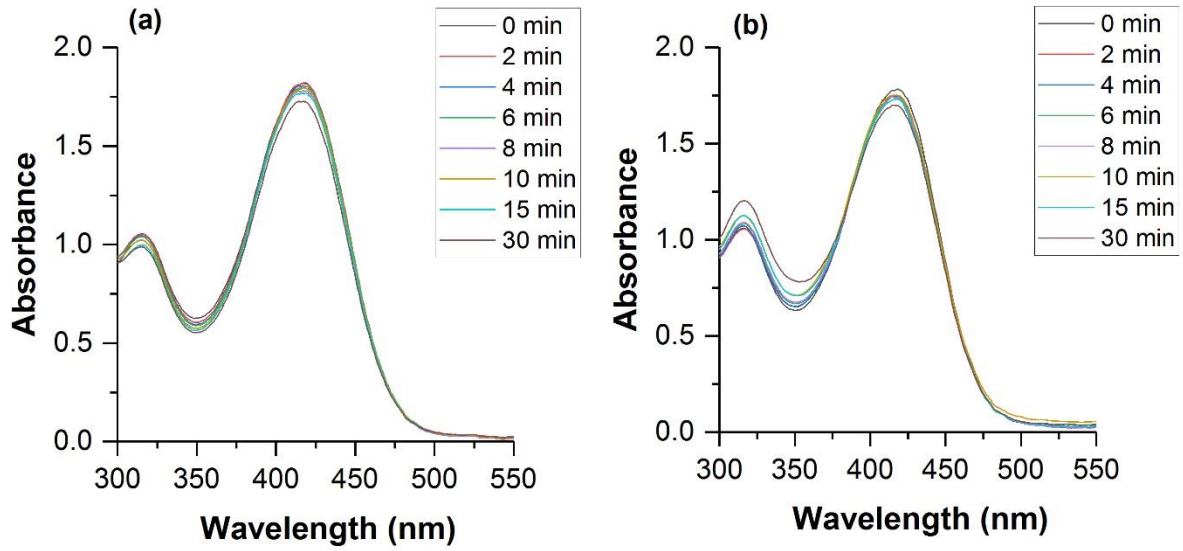

***Figure 17**: Interaction of morin with (a) sodium percarbonate and (b) TAED. Water (90 mL), morin (0.1 mM), sodium carbonate (50 mM), sodium percarbonate (5.3 mM), TAED (1.1 mM), pH = 10.5, 30 mins.*

2.5.3 *Tea Stain Bleaching*

Reckitt Benckiser prepared tea stains on cup surfaces for assessment of bleaching performance of various wash systems following the IKW procedure.[4] Tea cups (Baucher article no. 6215/18) were filled with a tea solution (100 mL, black Assam tea - 30 g in 2 L , 3 mmol Ca + Mg, ferric sulfate) at 85 °C. Every 5 mins, 20 mL of the tea solution was removed to yield clear rings on the side of each cup. This process was repeated with fresh tea solution. All the tea cups used in testing were stained using this procedure at Reckitt Benckiser. Stained tea cups are then left to age for 4 weeks before bleaching to ensure consistency across batches.

2.5.3.1 *Tea Cup in a Beaker (TC)*

Sodium percarbonate (1.5 g, 5.3 mM), TAED (0.45 g, 1.1 mM) and MGDA (0.2 g) were added to tap water (1.8 L, 5 °dH, 89 ppm $CaCO_3$) at 50 °C under vigorous stirring. A pre-stained tea cup is half submerged in the wash solution and the catalyst (3 mg) was added, set-up shown in **Figure 18**.After 8 mins the cup was removed from the beaker and rinsed three times in fresh tap water to remove any solution residue and to stop bleaching continuing on the cup surface after the experiment was completed. The bleaching performance was visually evaluated using a 1 – 10 scale, with 1 being no visible bleaching activity and 10 being a completely bleached surface. This protocol is followed across the fast moving consumer goods industry and is used to compare performance between competitors.[4] To ensure there is no biased in the scoring, the tea cups were scored blind without knowing which cup was used in which test, to ensure accurate scoring.

***Figure 18**: Photograph of the experimental set up of the tea cup in a beaker bleaching performance test*

2.5.3.2 *Automatic Dishwasher Testing*

The following method is an industry standard procedure carried out by all testing labs in every company developing dishwashing formulations.[4] Before running the dishwasher, a standard soil must be prepared, which consists of a range of ingredients. The different ingredients are combined, which includes: protein, fat, starch and highly coloured stains, for example ketchup. Ballast plates and cups are placed in the dishwasher to simulate a real wash and maintain a constant heating rate between runs.

The dishwasher is pre-conditioned in the absence of soil and tablet, at 45 °C, with a 8 min wash cycle. In testing cycles, four stained tea cups are loaded onto the top rack,

and the cleanliness of these cups is assessed by the same scale as the tea cup bleaching protocol, outlined above. Three testing runs are then completed with soil (50 g), tablet (16 – 20 g, finish quantum max), and catalyst (10 mg) included at 45 °C and for 8 mins. To ensure reproducibility between runs is achieved, the tablet is placed into the bottom of the dishwasher after the dosing chamber has opened, the catalyst is also added at this point. Two cleaning wash cycles are then completed, firstly with Neodisher (30 mL) 65 °C for 30 min, secondly citric acid (30 mL) 45 °C for 8 min.

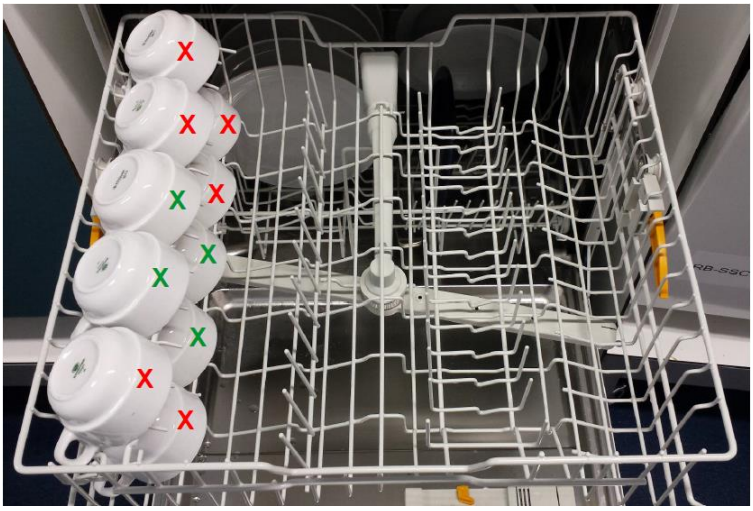

***Figure 19**: Photograph of the placement of the tea cups being assessed for bleaching in the dishwasher test. X = Cups which are evaluated for bleaching performance, X = Clean cups which remain in the dishwasher to ensure even heating*

2.6 *Quantification of Active Oxygen Species and Bleaching Reagents*

A method to simultaneously quantify both H_2O_2 and peracetic acid was required to understand the effect of bleaching reagents on the formation and decomposition of peracetic acid. Cavallini *et al.*[5] compared different combinations of cerium (IV) sulfate, iodometry and permanganate titrations with or without the addition of catalase or diethyl phenylenediamine (DPD), which react with H_2O_2 and peracetic acid respectively. The study concluded that using a cerium sulfate titration followed by iodometric titration was highly accurate for a wide range of sample concentrations. This method was trialled and adapted for simultaneous determination of H_2O_2 and peracetic acid, under wash conditions comparable to those used in automatic dishwashing.

A titration can be used to calculate the concentration of a species in a solution by reacting a solution of known concentration with the sample, which has a known volume.[6] In the following titrations, the titrant, i.e. solution in the burette, is the standard solution with a known concentration. The sample taken from the reaction, the titrate, has an unknown concentration with a known volume. Indicators are used to identify the end point of the reaction, to ensure accurate calculation of the unknown concentration.

2.6.1 *Cerium Sulfate Titration Using Ferroin Indicator*

The use of cerium (IV) compounds for titrations was proposed in the 1860s and further investigated in the 1920s.[7] The reduction of Ce^{4+} to Ce^{3+} happens readily in acidic media and can be used for redox titrations. An indicator is required to observe

the end point of the reaction. Ferroin (tris(1,10-phenanthroline) iron (II) complex), which is red in colour, is added to the titrate and turns pale blue when oxidised, indicating the end point of the reaction.

Hurdis and Romeyn developed a titration method to quantify H_2O_2 using cerium (IV) sulfate with ferroin indicator in 1954.[8] Cerium (IV) reacts with H_2O_2 in the following reaction:

$$2Ce^{4+} + H_2O_2 \rightarrow 2Ce^{3+} + O_2 + 2H^+$$

An advantage of this titration method is that other peroxides and peracetic acid do not react, therefore allowing the quantification of H_2O_2 only.[5]

To quantify H_2O_2, a titration with cerium (IV) sulfate is used. A titration sample (5 g), was added to H_2SO_4 (99 %, 4 drops) and ferroin indicator (4 drops). The aqueous solution was then titrated against an aqueous solution of cerium (IV) sulfate (0.0085 M) and the volume needed to change the colour of solution from red to pale blue was recorded. The moles of H_2O_2 present in the sample was calculated using the following equation:

$$moles\ of\ H_2O_2 = \frac{\left({}^{V_T}/_{Sa}\right)\ x\ S\ x\ C_T}{2000}$$

Where V_T = volume of titre, Sa = mass of sample, S = mass of solvent in reaction, C_T = concentration of titrant, i.e. cerium (IV) sulfate.

2.6.2 *Iodometric Titration*

Iodometric titrations can be used to quantify a wide variety of compounds in solution. Potassium iodide solution is added to the titrate and sodium thiosulfate is used as the titrant, which reduces the iodide.[9] The following reaction occurs:

$$2Na_2S_2O_3 + I_2 = 2NaI + Na_2S_4O_6,$$

which can also be described as:

$$2S_2O_3^{2-} \rightarrow S_4O_6^{2-} + 2e^-$$

$$I_2 + 2e^- \rightarrow 2I^-$$

Therefore, 2 equivalents of sodium thiosulfate are needed to reduce iodine ions to iodide. Often starch is used as an indicator to clearly identify the end point of the titration; starch forms a complex with iodine and, when thiosulfate is in slight excess, it reacts with the iodine bound to the starch, turning the solution from navy blue to colourless.

To quantify the concentration of peracetic acid in a reaction, an iodometric titration was used in combination with the cerium (IV) sulfate titration. For this, a reaction sample (5 g), was added to H_2SO_4 (10 mL, 0.5 M), KI (10 mL, 10 wt%) and ammonium molybdate (4.6 M). The solution was titrated against sodium thiosulfate (0.01 M). The volume required to reduce the iodide fully is recorded, which is evidenced by the solution changing colour from brown to colourless. The total oxidant moles present in the sample was calculated using the following equation:

$$Total\ moles\ of\ active\ oxygen = \frac{\left({}^{V_T}/_{Sa}\right)\ x\ S\ x\ C_T}{2000}$$

Where V_T = volume of titre, *Sa* = mass of sample, *S* = mass of solvent in reaction, C_T = concentration of titrant, i.e. sodium thiosulfate.

To calculate the moles of peracetic acid in solution, the moles of H_2O_2, calculated from the cerium sulfate titration, was subtracted from the moles of active oxygen species, calculated from the iodometric titration.

2.6.3 *Development of Method to Quantify Active Oxygen Species*

To develop the titration method to quantify both H_2O_2 and peracetic acid simultaneously, standard solutions were tested to ensure the titrations were accurate. This was followed by testing samples titrated with both titration methods sequentially and with separate samples for each titration method.

***Table 2**: Determination of H_2O_2 and peracetic acid concentrations from known stock solutions using ceria and iodometric titrations.*

Standard Solution of H_2O_2 (mM)	Concentration Calculated from Ceria Titration (mM)	Standard Solution of Peracetic Acid (mM)	Concentration Calculated from Iodometric Titration (mM)
8	8.4	2.2	6.9
4	4.2	1.1	3.3
2	2.8	1.6	3.4

Table 2 shows that the cerium (IV) sulfate titration for quantifying H_2O_2 is accurate and a reliable method; however, the iodometric titration overestimates the concentration of the peracetic acid stock solution. At low concentrations of peracetic acid, It was found that the addition of a starch indicator increased the titration

volume which increased inaccuracy in the final calculated concentration of peracetic acid. The peracetic acid titrations were repeated without the starch indicator, as shown in **Table 3**. As the titrations were more accurate at the desired concentrations without indicator, the indicatorwas removed from the titration method.

Table 3*: Determination of peracetic acid concentration from a known stock solution using iodometric titration with no starch indicator.*

Standard Solution of Peracetic Acid (mM)	Concentration Calculated from Iodometric Titration (mM)
2.4	2.7
2.9	3.0
3.2	3.4

2.6.4 *Error Analysis of Developed Titration Method*

To calculate the error of the titration method, a standard reaction with sodium percarbonate and TAED was repeated five times and three samples taken for each titration at 0 and 30 s. Therefore, the error in the analysis and the error in the reaction was considered. Error between samples of the same reaction were calculated using the following equation:

$$\%\ error\ of\ samples = \left(\frac{Range/_2}{Average}\right) x\ 100$$

To calculate the error between repeats of the reaction, an average of the sample repeats was taken (**Figure 20**), and these values were used for the equation stated above. The range was divided by 2 to give the error above and below the average, therefore, an error of 5 % is representative of 5 % deviation above and below the

average value. To combine the error of analysis and the error between reactions the following equation was used:

$$Error\ of\ Titration\ method = \sqrt{sample\ error^2 + \ reaction\ error^2}$$

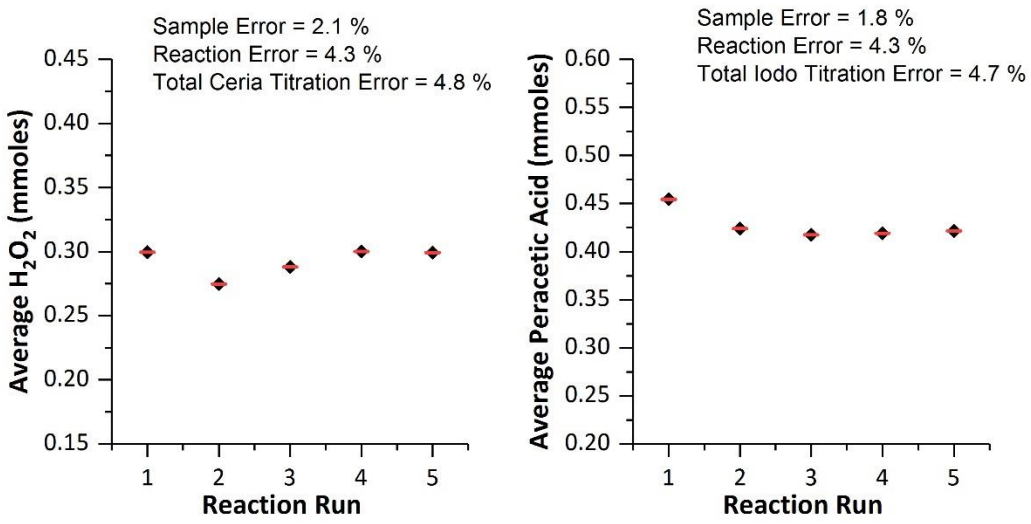

***Figure 20**: Error analysis of the titration method, five repeats of standard bleaching reaction. Water (90 mL), sodium percarbonate (5.3 mM), TAED (1.1 mM), 50 C, 30 s. Samples titration after 30 s.*

Total combined error for the ceria and iodometric titration methods, calculated using the square root of the sum of the squared error values shown in **Figure 20**, is 6.7 %, indicating that the error for titration is acceptable.

2.6.5 *Modified Titration Method*

After considering the error and the accuracy of the titration method, the following procedure was used to quantify H_2O_2 and peracetic acid in reactions.

A sample of the reaction (5 mL), was added to H_2SO_4 (0.5 M, 4 drops) and ferroin indicator (4 drops), which had been cooled in ice. This solution was titrated against

cerium (IV) sulfate (100 mL, 0.0085 M) until the solution turned from red to pale blue. The titration volume was recorded. Another sample of the reaction (5 mL) was added to H_2SO_4 (0.5 M, 10 mL), KI (10 mL of 10 wt% solution) and ammonium molybdate (2 drops, 0.73 M) at room temperature. This was titrated against an aqueous solution of sodium thiosulfate (0.01 M) until the solution turned from yellow to colourless.

2.6.6 *High Performance Liquid Chromatography (HPLC)*

HPLC was used to quantify TAED and the perhydrolysis and hydrolysis products of TAED. TAED undergoes perhydrolysis to form peracetic acid and DAED *via* TriAED. Simultaneously, TAED can undergo hydrolysis to form acetic acid, which can also be formed from the decomposition of peracetic acid, shown in **Figure 21**. HPLC methods were developed to quantify TAED, DAED and acetic acid under varying conditions.

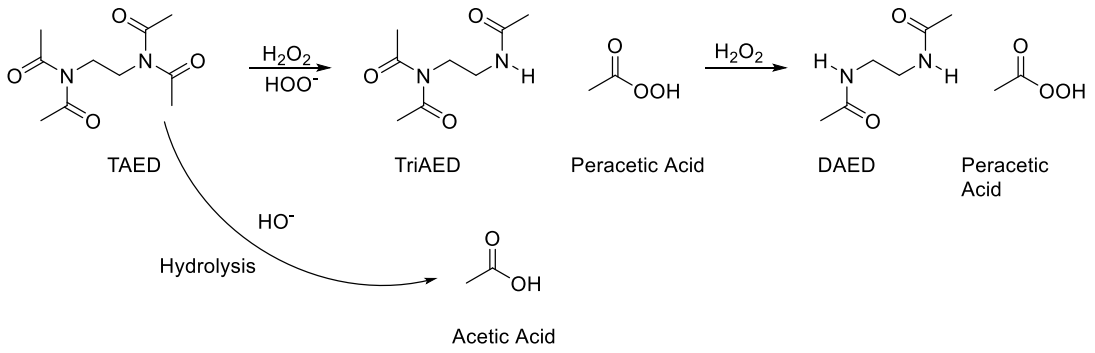

***Figure 21**: Reaction scheme of TAED with H_2O_2 to form 2 moles of peracetic acid.*

Liquid chromatography is the separation of molecules in a liquid over a solid stationary phase, with the stationary phase encapsulated into a column packed with solid spheres.[10] Different species are separated while travelling through the column, and the time it takes for a certain molecule to travel through the column depends on

its interaction with both the stationary phase and mobile phase. The time taken for the molecule to elute is known as the retention time. The retention time is used to identify the separate components of a liquid solution.

There are four types of columns used in HPLC: normal phase, reverse phase, ion exchange and size exclusion. With normal phase columns, the stationary phase is more polar than the mobile phase and the molecules are separated based on polarity. Generally, silica columns are used for such applications. Reverse phase columns are less polar than the mobile phase, generally hydrocarbons are used in these columns. Ion exchange separates molecules based on ionic forces with the stationary phase; for this, an acidic or basic column is used. Finally, size exclusion uses a porous stationary phase to separate molecules based on size. Size exclusion columns typically use a mixture of polymers to create pores.

In a typical HPLC set up, the mobile phase reservoir is situated on top of the instrument. The choice of mobile phase depends on the column and the solution being analysed. The flow and make-up of the mobile phase, which consists of either one solvent (isocratic) or a mixture of solvents at changeable ratios (gradient), is controlled by a pump. The mobile phase reaches a 6-way Rheodyne valve where a small amount of the sample (typically 1-80 μL) is injected into the mobile phase. This then travels to the column. After the column, where the various compounds are separated, is the detector, which generates a response that is dependent on a given property of the chemical within.

There are many types of a detector that can be used in conjunction with HPLC; more than one is often used to accurately quantify given mixtures due to the specific

requirements of the detector. Most commonly, UV/Vis detectors are used either at fixed or variable wavelengths, a diode array detector (DAD) simultaneously quantifies multiple wavelengths of light. Refractive index detector (RID) can also be used to identify and quantify the eluted molecules by measuring the difference in refraction of the effluent relative to the mobile phase. HPLC can also be used in conjunction with mass spectrometry to identify the molecules as they are eluted.

DAD detectors use a deuterium lamp and emit a large range of wavelengths of light, the light is passed through an achromatic lens into the sample cell. The sample is exposed to all wavelengths of light. The light that has passed through the sample hits a holographic grating, which disperses the light so that it hits the detector, which in turn generates the chromatogram. The response is generated by comparing the absorption of a cell containing the mobile phase and a cell containing the sample. The difference in absorption between the sample and the mobile phase generates the response, and therefore the signal may not be proportional to the concentration as it depends on the compounds absorption. DAD can only be used for compounds that absorb light and is therefore not suitable for the quantification of all analytes.

RID measures how much the sample deflects the light in comparison with the mobile phase as quantified in a separate reference cell. The refractive index of the mobile phase and the sample is measured by passing over a beam of light. RID is considered a universal detector as all liquids will refract light; however, sensitivity can be too low if the difference in refractive index between the mobile phase and sample is low. Therefore, RID is used in combination with other detectors to identify the compounds present in the sample. Generally, as the intensity of the peaks measured

is proportional to the concentration, a calibration can be used to calculate concentrations in solutions as well as identify the different components of a solution.

For the quantification of TAED and DAED in bleaching solutions, the following HPLC method was used.

An Agilent 1260 Infinity series HPLC was used with a C18 column. Mobile phase of 0.1 % H_3PO_4 in H_2O and acetonitrile with gradient elution was used, the ratio of H_2O to acetonitrile (ACN) is given in **Table 4**. The total run time of the method was 24 mins with a flow rate of 0.5 mL/min and a sample injection volume of 5 μL. A DAD detector was used with peaks monitored at 254 nm.

***Table 4**: Gradient elution of mobile phase for HPLC analysis of TAED and DAED.*

Time (min)	H_2O (%)	ACN (%)
0	60	40
2	50	50
6	40	60
8	30	70
10	20	80
20	60	40

2.6.7 *Bleaching Score of Tea Stains*

The visual evaluation of tea stains was carried out by assessing the amount of stain removal on the bottom of the cup and the visibility of the lines on the side of the cup. The scale runs from a score of 1 to 10, with 1 being a cup that has not been washed and 10 a completely clean cup as if it was new.

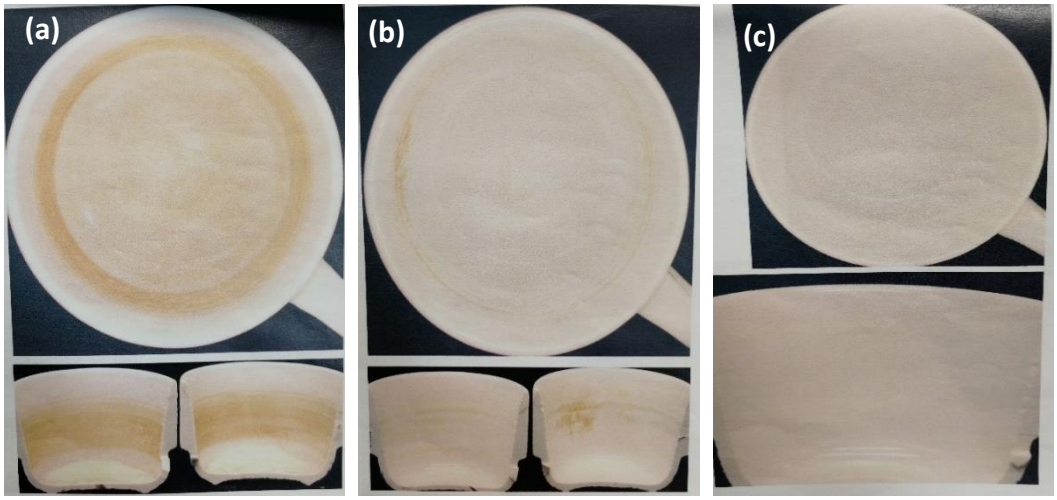

***Figure 22**: Examples of the tea staining for each level of scoring system for bleach performance evaluation. (a) = 1-4, (b) = 5-7, (c) = 8-10.*

As shown in **Figure 22**, the scoring system is grouped into three primary categories; a large difference in stain removal is observable between each category. A score of 1 – 4 indicates that the bottom of the cup still possesses stains and the lines on the side of the cup are still visible. As the score increases from 1 to 4, less of the stain is left on the bottom of the cup and the lines are still defined but become less visible. From 5 – 7 the bottom of the cup is completely clean and the bottom lines on the side are removed. As the score increases to 7, the upper lines become less visible and less well defined. At scores of 8 – 10 there are only areas of the stain left and these areas are faint. These areas of stain become smaller and less visible until a score of 10 is reached, where there is no stain left on the cup surface.

As there are larger differences between the three groups of scores than between individual scores, the difference between a score of 3 and 5 is more significant than between 3 and 4.

2.7 *Catalyst Characterisation*

2.7.1 *Brunauer-Emmett-Teller (BET) Surface Area Analysis*

BET surface area measurements use an absorbate to calculate the surface area of a material. When an inert adsorbate, such as N_2, comes into contact with a surface, molecules physisorb. Physisorption is when molecules become weakly bound to a surface, i.e. there are no covalent or ionic bonds present. At a certain pressure, the adsorbate will form a monolayer on the surface of the material, which is when the adsorbate completely covers the surface but is only at a depth of one molecule. The surface area of a material is related to the number of molecules in a monolayer and the cross-sectional area of the adsorbate.

Nitrogen is dosed to a measured amount of catalyst until an equilibrium is reached between the free nitrogen and the nitrogen bound to the surface. The pressure of nitrogen, the equilibrium between the free and bound nitrogen, and the volume of nitrogen is recorded. Using a modified version of the Langmuir adsorption model, an isotherm can be plotted as v vs P/P_o. The BET approximation is used in the area where the isotherm is linear.

$$\frac{1}{v\left(\left(\frac{p_0}{P}\right)-1\right)} = \frac{c-1}{v_m c}\left(\frac{P_0}{P}\right) + \frac{1}{v_m c}$$

Where v = absorbed gas volume, v_m = monolayer gas volume, p = equilibrium pressure, p_0 = saturation pressure, c = BET constant. The BET constant is given as $c = \exp\left(\frac{E_1 - E_L}{RT}\right)$. Where E_1 = heat of adsorption of one monolayer and E_L = heat of liquefaction.

A catalyst sample (*ca.* 0.25 g) was degassed under vacuum at 110 °C for 2 h to remove any residual physisorbed molecules from the sample. The weight was recorded after degassing and the sample placed into the Quantachrome Nova 2200. A 5-point BET was run to calculate the surface area of a material. At each point, a different amount of N_2 was added to the sample tube below the vapour pressure of N_2. The pressure in the tube was recorded at each point.

2.7.2 *Diffuse Reflectance Infrared Fourier Transform Spectroscopy (DRIFTS)*

DRIFTS is based on infrared spectroscopy. Infrared light (IR) is shone onto a sample, the typical spectrometer uses wavenumbers from 14,000 – 10 cm^{-1}. Infrared radiation is absorbed by the sample, causing the molecules to vibrate. If this vibration results in a change of dipole moment in the molecule then the molecule is IR active and can be detected.[11] The measured intensity is proportional to the change in the dipole moment and is plotted against the wavenumber at which this occurs.

DRIFTS is mainly used to characterise uneven surfaces and powders. Instead of measuring the single reflectance of the incidence beam, the diffusely scattered light over the surface of the sample is measured.[12] As this internal reflectance is measured; the sample preparation is important to improve the refractive index of the sample. Therefore, the sample is finely ground and diluted in equally finely ground potassium bromide, mixed well and packed into the sample cell.

A Bruker Tensor 27 spectrometer was used for DRIFTS analysis. The sample was ground and mixed with potassium bromide and loaded into the in-situ cell, which

was a Praying Mantis high temperature (HVC-DRP-4). N_2 was flowed over the sample and measurements taken at 1 min intervals.[13]

2.7.3 *Copper Surface Area Analysis*

A BET technique was also used to quantify the surface area of copper in the catalysts. Copper metal reacts with N_2O to form N_2 and copper oxide. Therefore, a sample with copper metal can be titrated with N_2O and the amount of N_2 generated is measured to calculate the surface area of copper.

$$Cu\ surface\ area = \frac{N_2\ volume\ x\ N_a x\ 2}{C_m x\ 24000\ x\ S_{dCu}}$$

Where N_a = Avogadros number and S_{dCu} = surface density of copper. This assumes that the N_2 emitted results in half a monolayer of oxygen on the surface of the catalyst, and the surface density of Cu is 1.47 x10^{19} atoms/m^2. The factor of 24000 represents the conversion factor, from volume to moles of N_2, using the ideal gas equation in the units of the data obtained by the temperature programmed analyser. As 2 moles of Cu react with 1 mole of O, the moles of N_2 need to be multiplied by 2 to correctly calculate the number of Cu moles.

Catalyst (*ca.* 100 mg) was inserted into a quartz tube and plugged with quartz wool. The sample was then purged with He to remove any impurities from the sample for 5 minutes. As copper metal is required for this experiment (and not copper oxide), the sample was first reduced. 10% H_2/Ar (30 mL/min) was flowed over the catalyst at 140 °C (10 °C/min), then heated to 225 °C (1 °C/min), and held for 20 minutes. The lower ramp rate is used to ensure sintering of the sample does not occur, as the

reduction of Cu oxides is a highly exothermic process.[14] Sample was flushed with He for 10 minutes at 220 °C.

The sample was then cooled in helium at 80 mL/min to 65 °C for the titration. N_2O (113 μL) was subsequently pulsed over the sample 12 times, with a stabilisation time of 5 minutes between each pulse. The programme finishes with 3 pulses of N_2, which are used for calibration. Unreacted N_2O was trapped by a molecular sieve. A thermal conductivity detector (TCD) was used to quantify the N_2 produced.

2.7.4 *X-Ray Diffraction (XRD)*

X-ray diffraction can be used to identify the composition of a powdered material, the crystal structure and the crystallite size. X-rays are generated by heating a tungsten filament, which serves as a cathode; the resultant electrons emitted are accelerated towards a target material, the anode. This target material is frequently made from copper. When the electrons hit the target material, energy is lost and X-rays are emitted, which are targeting towards the sample.

Braggs law relates the interplanar spacing in a unit cell to the wavelength of the x-rays used. Braggs law is defined as:

$$2dsin\theta = n\lambda$$

Where d = interplanar spacing, θ = Bragg angle, n = order of reflection (always an integer) and λ = wavelength of x-ray source.

A peak is only observed when the angle obeys Bragg's law; as the angle of reflectance is the same for multiple unit cells, constructive interference occurs, and therefore a peak is recorded at that angle. These angles are different for each place within a unit

cell, as in e.g. a BCC unit cell the 110 and 200 planes will have different Bragg angles. Only when that angle is correct will a peak be observed. If the angle is not the Bragg angle, destructive interference between X-rays reflecting off the sample occurs and no diffraction pattern is detected (**Figure 23**).

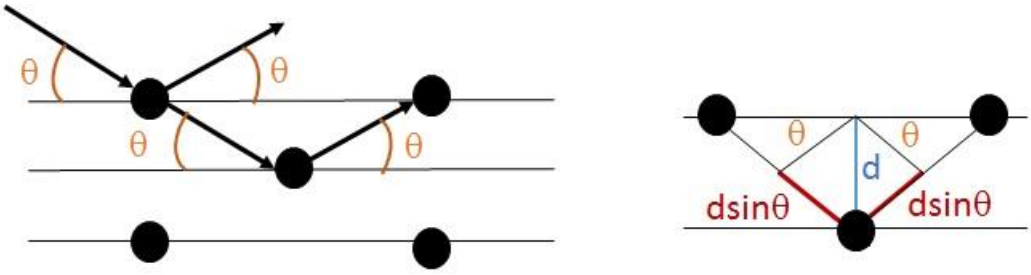

***Figure 23**: Diagram of the interplanar spacing in a unit cell between atoms and the Bragg angle.*

To perform the measurement, a powder sample is placed on a stationary stage. Both the X-ray source and the detector are placed on the circumference of a circle around the sample stage. These rotate around the sample to change the angle of the X-ray beam. The angle between the sample surface and the X-ray source is θ, the angle between the X-ray source and the detector is 2θ. The X-ray source and detector rotate and measure the spectrum at different values of 2θ. When the angle satisfies Bragg's law, a peak is observed. This peak can be used to identify the material, the phase of the material, and the crystallinity.

A PANalytical X'Pert Pro system was used to collect powder X-ray diffraction spectra,[15] equipped with a Cu Kα X-ray source that operated at 40 kV and 40 mA. Data was collected from 2θ 10° to 80° for 30 minutes using an X'Celerator detector.

2.7.5 *X-Ray Photoelectron Spectroscopy (XPS)*

XPS can be used to identify the species on the surface of the catalyst. The technique relies on the photoelectric effect; when x-ray energy is absorbed by a bound electron in an atom the electron is removed from the atom. In XPS, X-rays are used to displace electrons from the atom and the energy of these electrons is measured.

The energy recorded is the binding energy of the electron, which is calculated from the kinetic energy of the electron and the photon energy of the X-ray source.

$$BE = h\nu - KE$$

Where *BE* = binding energy of an electron, *hν* = X-ray photon energy and *KE* = kinetic energy of the released electron.

Given that the electrons removed from the atoms have discreet energies, which depend on the atomic orbitals of an atom, the BE can be used to identify the element present. The BE can also be influenced by the oxidation state, chemical environment and the lattice structure; the influence these parameters have on the BE can further help identify the element and the surface species present on the catalyst surface.

XPS is a surface technique and can only gain information about a sample up to 10 atoms deep.[16] This is because electrons ejected from deeper in the sample will interact with other electrons present in the sample; therefore, loss of energy occurs and the electrons will not be detected.

Generally, an aluminium X-ray source is used and filtered by a monochromator crystal to ensure the desired wavelength of X-rays is used. The X-rays hit the sample and the ejected electrons are filtered according to their energy before hitting a

detector. The loss of electrons leads to a progressively more positively charged sample surface, resulting in an increase in binding energy. A flood gun emits low energy electrons to counteract this effect by neutralising charge build-up on the sample surface.

Thermo-Fisher Scientific K-Alpha X-ray photoelectron spectrometer was used to acquire the data. The X-ray source is aluminium Kα, which was operated at 72 W. To minimise charge, argon ions and low energy electrons were used giving a C(1s) binding energy of 284.2 eV.

2.7.6 *Scanning Electron Microscopy (SEM)*

Scanning electron microscopy uses a source of electrons to image the surface of a material. Electrons are generated and fired at the sample in a narrow beam that travels over the surface of the material. Different experimental parameters may be changed to improve the quality of the retrieved data. Increasing the voltage of the electrons generated decreases the wavelength of the electron beam, which improves the resolution of the image. The voltage also determines how far through the sample the electron beam penetrates. The depth also depends on the material being imaged. The beam intensity, which is the current, improves the signal generated from the sample; as this increases the number of electrons in the beam, more are reflected off the sample. Increasing the electrons can, however, increase the charging of the sample and sample damage. Generally, lower beam intensities are used for imaging, to not damage the sample and minimise charging. Signal can also be increased by slowing down the scanning time. Focus is determined by the working distance; the distance from the tip of the pole piece to the sample. To improve resolution, the

working distance should be minimised to limit the distance travelled by the electron beam through the vacuum.

The sample is mounted onto a carbon disk for imaging, to ground the electrons fired at the sample. If a sample is insulating, then charging occurs which creates bright spots on the image. Sputter coating with gold or platinum reduces this, although if the layer is too thick surface features may be lost.

Detectors are used to record the image, and these are separated by the type of scattering the electron goes through after hitting the sample. Elastically scattered electrons are recorded by a backscatter electron detector. The intensity of this signal depends on the atomic number and beam voltage, giving contrast between different elements present in the sample.

A secondary electron detector is used for inelastic scattered electrons, which are considerably lower in energy. The penetration of this imaging is low and is used for looking into the surface topology and morphology of the sample. X-ray emission also occurs as electrons holes are formed during imaging. Electrons in higher energy shells drop down to fill the electron hole and release an X-ray. The energy of this X-ray is dependent on the energies of the electron shells. The X-ray emissions can therefore be used to identify the elements present in the sample. This is recorded by an energy dispersive X-ray detector (EDX).

A Tescan Maia2 field emission gun scanning electron microscope (FEG-SEM) with an Oxford Instruments XMAX^N 80 energy dispersive X-ray detector (EDX) was used to image the catalysts and identify the elements present in the sample. Samples were sputter coated with a 15 nm layer of gold and platinum before imaging to reduce

charging. Samples were mounted on a carbon disk. Images were generated using the backscattered electron detector.

2.7.7 *Microwave Plasma-Atomic Emission Spectroscopy (MP-AES)*

MP-AES uses the principle of atomic emission spectroscopy to identify and quantify elements in a liquid sample. When an atom is excited to a higher energy level, energy is released when the atom relaxes to a lower energy. The energy is released as photons, of which, the wavelengths are considered to be a "fingerprint" for different elements and can be used to identify unknown elements in a given sample. Intensity of the emission is dependent on the concentration, therefore, known concentrations of an element can be used for calibration purposes.

A magnetron is used to produce microwave energy around the torch, which forms the plasma that atomises the sample and excites the atoms present. This high energy input leads to high intensity emissions and therefore, low concentrations of elements can be detected.

For the analysis, herein an Agilent 4100 was used, which includes a cyclonic spray chamber and a concentric nebulizer. Samples were diluted with water to the desired concentration and calibration for the desired elements for analysis was completed before sample analysis.

2.7.8 *Inductively Coupled Plasma Mass Spectroscopy (ICP-MS)*

ICP-MS uses plasma to ionise the sample for identification *via* mass spectrometry. The plasma is generated by heating the inert gas with an electromagnetic coil, which ionises the gas and forms a plasma.[17] The liquid sample is then formed into an aerosol

by a nebuliser, so that when the sample aerosol reaches the plasma it is ionised.[18] After the sample is ionised the elemental ions are identified using mass spectroscopy.

Here, an Agilent 7900 ICP-MS equipped with an I-AS autosampler was used to detected metals in solution from the morin oxidation reaction. Reference materials from Perkin Elmer, with certified internal standard from Agilent, were used for a 5-point calibration to ensure accurate quantification of the metals in solution.[19]

2.7.9 *Thermogravimetric Analysis (TGA)*

TGA is used to assess the change in weight of a sample as it is heated, to characterise how the sample decomposes.[20] The sample is placed in a crucible on a highly sensitive balance is used to detect small changes in mass of the sample. The crucible is heated and the mass of the sample is recorded against the temperature of the sample.

Herein, samples were placed in the Setram Labsys TGA instrument under flowing air, 15 mL/min, and heated from 30 to 1000 °C with a heating rate of 10 °C/min.[15]

2.8 *References*

1 Y. Ma, Q. Sun, D. Wu, W.-H. Fan, Y.-L. Zhang and J.-F. Deng, *Appl. Catal. A Gen.*, 1998, **171**, 45–55.

2 S. Ishikawa, D. R. Jones, S. Iqbal, C. Reece, D. J. Morgan, D. J. Willock, P. J. Miedziak, J. K. Bartley, J. K. Edwards, T. Murayama, W. Ueda and G. J. Hutchings, *Green Chem.*, 2017, **19**, 225–236.

3 P. Ncube, T. Hlabathe and R. Meijboom, *Appl. Surf. Sci.*, 2015, **357**, 1141–1149.

4 IKW, *sofw Journal, Home Pers. Care Ingredients Formul.*, 2016, 37–38.

5 G. S. Cavallini, S. X. de Campos, J. B. de Souza and C. M. de S. Vidal, *Int. J. Environ. Anal. Chem.*, 2013, **93**, 906–918.

6 E. M. Rattenbury, in *Introductory titrimetric and gravimetric analysis*, Pergamon Press, Oxford, England, 1st edn., 1966, pp. 3–23.

7 K. Binnemans, in *Handbook on the Physics and Chemistry of Rare Earths*, eds. J.-C. Bünzli and V. K. Pecharsky, Elsiver, 2006, vol. 36, pp. 281–392.

8 E. C. Hurdis and H. Romeyn, *Anal. Chem.*, 1954, **26**, 320–325.

9 E. M. Rattenbury, in *Introductory titrimetric and gravimetric analysis*, Pergamon Press, Oxford, England, 1st edn., 1966, pp. 108–129.

10 W. J. (W. J. Lough and I. W. Wainer, *High performance liquid chromatography : fundamental principles and practice*, Blackie Academic & Professional, 1995.

11 Peter J.Larkin, in *Infrared and Raman Spectroscopy (Second Edition) Principles and Spectral Interpretation*, 2018, pp. 7–28.

12 P. J. Larkin, *Instrumentation and Sampling Methods*, 2018.

13 J. H. Carter, S. Althahban, E. Nowicka, S. J. Freakley, D. J. Morgan, P. M. Shah, S. Golunski, C. J. Kiely and G. J. Hutchings, *ACS Catal.*, 2016, **6**, 6623–6633.

14 P. J. Smith, PhD Thesis, Cardiff University, 2015.

15 M. Douthwaite, X. Huang, S. Iqbal, P. J. Miedziak, G. L. Brett, S. A. Kondrat, J. K. Edwards, M. Sankar, D. W. Knight, D. Bethell and G. J. Hutchings, *Catal. Sci. Technol.*, 2017, **7**, 5284–5293.

16 C. J. Powell, *J. Vac. Sci. Technol. A*, 2020, **38**, 1–14.

17 H. E. Taylor, in *Inductively Coupled Plasma-Mass Spectroscopy: Practices and Techniques*, 2000, pp. 15–27.

18 H. E. Taylor, in *Inductively Coupled Plasma-Mass Spectroscopy: Practices and Techniques*, 2000, pp. 53–90.

19 S. Wang, R. J. Lewis, D. E. Doronkin, D. J. Morgan, J.-D. Grunwaldt, G. J. Hutchings and S. Behrens, *Catal. Sci. Technol.*, 2020, **10**, 1925–1932.

20 W. M. Groenewoud, in *Characterisation of Polymers by Thermal Analysis*, 2001, pp. 61–76.

3 Chapter 3: Exploration of Optimal Bleaching Conditions in the presence of Homogeneous Manganese Catalysts

3.1 *Introduction*

New tablet formulations for cleaning dishes in automatic dishwashing are assessed using industry wide standard testing conditions. The bleaching of stains is a two-step process: the first involves the formation of peracetic acid (the active bleaching agent), and the second, the oxidation of the stains with peracetic acid. Elucidation of the step that limits bleaching activity under industrial standard conditions is required to improve optimal catalyst design. For example, if the formation of peracetic acid limits bleaching, a catalyst that enhances perhydrolysis would be required. Conversely, if the limiting step is the oxidation of the stain, optimisation of the oxidation catalyst is required to remove stains or bleach the chromophores.

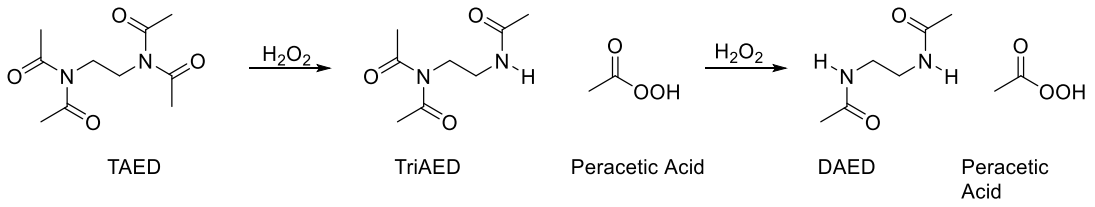

Scheme 6*: Perhydrolysis of TAED to form peracetic acid, the active bleaching species.*

With current dishwasher bleaching formulations, peracetic acid is formed *via* the perhydrolysis of tetraacetylethylenediamine (TAED) with H_2O_2 shown in Scheme 6.[1] Peracetic acid is present as the peracetate anion under alkaline conditions, which is

the active species that oxidises the chromophore, shown in Scheme 6. It is not clear how easily peracetic acid is formed under current wash conditions from the perhydrolysis of TAED. Industry standard wash conditions use sodium percarbonate (SPC, 5.3 mM), TAED (1.1 mM), (SPC : TAED molar ratio 4.8), pH = 9 – 10, 50 °C, with a main wash cycle of 8 min.

Industry standard testing (IST) uses 8 min wash cycles at 50 °C for comparison of performance of formulations from different brands.[2] These conditions have been replicated in a benchtop scale reaction for quick screening in the laboratory; the tea cup test (TC). In the TC, a teacup is placed in 1.8 L of H_2O. SPC, TAED, the builder and catalyst are all added simultaneously and stirred at 50 °C for 8 min. The bleaching performance is then evaluated by a qualitative visual score. As the structure of the tea stain is unknown, it would be preferable to investigate the activity of the system using a well-defined quantitative model, rather than a visual score. The structure of the tea stain is unknown, though it does contain tannins, which contain aromatic rings and alcohol groups.[3] Catechol and natural tannin dyes are therefore considered to be suitable model compounds and have been used by Sorokin *et al.*[4] and Topalovic *et al.*[5] for such investigations previously.

To assess how varying the reagent concentrations and reaction conditions affect the formation of peracetic acid, peracetic acid was quantified in solution using a titration method. TAED conversion was also monitored *via* HPLC. Understanding further the formation of peracetic acid, and how the conditions affect the formation, will lead to an understanding of how a catalyst might aid the bleaching process.

Finally, Mn catalysts are currently ubiquitous in dishwasher bleaching applications, in addition to cotton and pulp bleaching applications.[6] Unilever developed MnTACN[7], which is a highly effective bleach catalyst that has also been commercialised in various dishwasher formulations. MnTACN was chosen as the performance benchmark and tested in the TC and model reactions. The overall aim of this work is to develop heterogeneous catalysts that, at the very least, could match the activity exhibited by homogeneous catalysts currently employed in automatic dishwashing.

3.2 *Results*

3.2.1 *Screening Conditions for the Optimal in-situ Synthesis of Peracetic Acid*

Industrial standard test (IST) utilises an 8 min wash cycle at 50 °C as a standard set of conditions for the performance comparison of different formulations.[2] To assess whether the bleaching performance is limited by peracetic acid formation under these conditions, methods for the quantification of peracetic acid were developed. Furthermore, conditions in the reaction were varied to evaluate how the concentration of reagents, temperature and pH influences the bleaching performance.

3.2.1.1 *Formation of Peracetic Acid*

Quantification of peracetic acid in the presence of H_2O_2 is complex, due to the similar reactivity of both species. Many methods for the quantification of peracetic acid and H_2O_2 have been reliably demonstrated in the literature, including the use of nuclear magnetic resonance (NMR), HPLC, UV-Vis and titration.[8,9,10] After screening different methods, a titration method using cerium (IV) sulfate and iodometry was developed and employed to quantify peracetic acid and H_2O_2 during the wash. The details of this method are presented in Chapter 2, Section 5.

A standard reaction was designed to emulate the conditions found in a dishwasher with appropriate ratios of sodium percarbonate (SPC) to bleach activator – tetraacetylethylenediamine (TAED). H_2O_2 is typically used in excess, in most formulations, as additional H_2O_2 can improve bleaching performance by also participating in the oxidation of stains.[11] Therefore, it was important to establish how

the ratio of sodium percarbonate : TAED ,and TAED concentration, influenced peracetic acid formation. Under standard conditions, full conversion of TAED to peracetic acid resulted in H_2O_2 conversion of 26 %, which equates to 2.2 mM of peracetic acid being formed during the reaction. Theoretical maximum H_2O_2 conversion for the perhydrolysis reaction with TAED was calculated and included in the data for comparison.

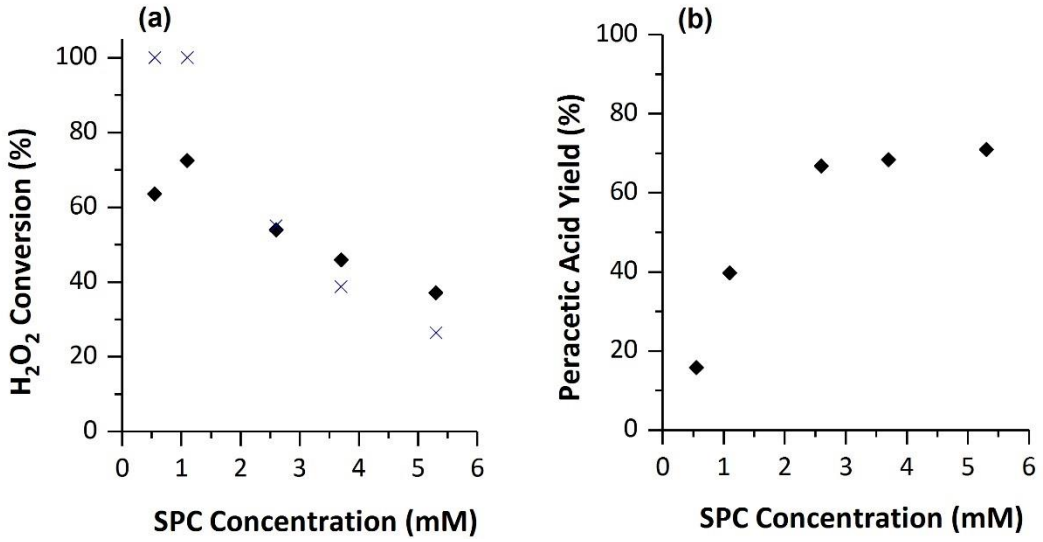

***Figure 24**: Effect of sodium percarbonate (SPC) on (a) H_2O_2 conversion and (b) peracetic acid yield. Water (90 mL), sodium percarbonate, TAED (1.1 mM), 50 °C, pH = 10, 30 s. ♦ = measured conversion from experiment, x = theoretical maximum H_2O_2 conversion from the perhydrolysis reaction of H_2O_2 and TAED. Average error = 7%.*

Figure 24 shows the relationship between the conversion of H_2O_2 and yield of peracetic acid with increasing SPC concentration. Increasing the concentration of SPC yields a lower H_2O_2 conversion, with the largest increase in conversion observed at lower concentrations. Above a concentration of 3.4 mM, increasing the concentration of SPC results in little improvement in conversion. The relationship

between H_2O_2 conversion and SPC concentration follows a similar trend to the theoretical maximum conversion, of the perhydrolysis reaction. The conversion of H_2O_2 is above the theoretical maximum conversion, as the theoretical conversion was calculated from the perhydrolysis reaction only, H_2O_2 can also undergo decomposition to form H_2O and O_2. Decomposition of H_2O_2 could explain the conversion of H_2O_2 being greater than the theoretical maximum. At lower H_2O_2 concentrations however, the measured and theoretical rates of H2O2 conversion diverge. At higher SPC concentrations the conversion plateaus, suggesting that another factor is limiting the reaction. Similarly, the yield of peracetic acid increases with increased SPC concentration until a concentration of 2.4 mM was achieved. The rate of peracetic acid formation is lower than the theoretical maximum, suggesting that the reaction does not go to completion within 30 s. At high SPC concentrations, further increasing the SPC concentration results in no improvement to the yield of peracetic acid. The difference between the measured and theoretical peracetic acid rates could be due to hydrolysis of TAED, shown in Scheme 7, to form acetic acid rather than peracetic acid.[12]

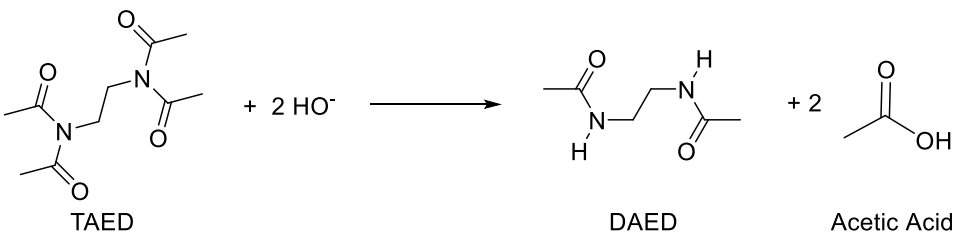

***Scheme 7**: Hydrolysis of TAED*

The results shown in Figure 24 suggest that a parameter other than SPC concentration is limiting the yield of peracetic acid and H_2O_2 conversion, as there is a large difference between the measured and theoretical conversion. At stoichiometric amounts (and below) of sodium percarbonate and TAED, H_2O_2 conversion and peracetic acid formation is observed; which indicates that sodium percarbonate does not need to be in excess of TAED to form peracetic acid. This suggests that excess sodium percarbonate is not needed to drive the perhydrolysis reaction to completion, and could be reduced in formulations without decreasing peracetic acid concentrations. An excess of sodium percarbonate does, however, increase the peracetic acid yield, indicating a benefit to bleaching as the active species is formed faster.

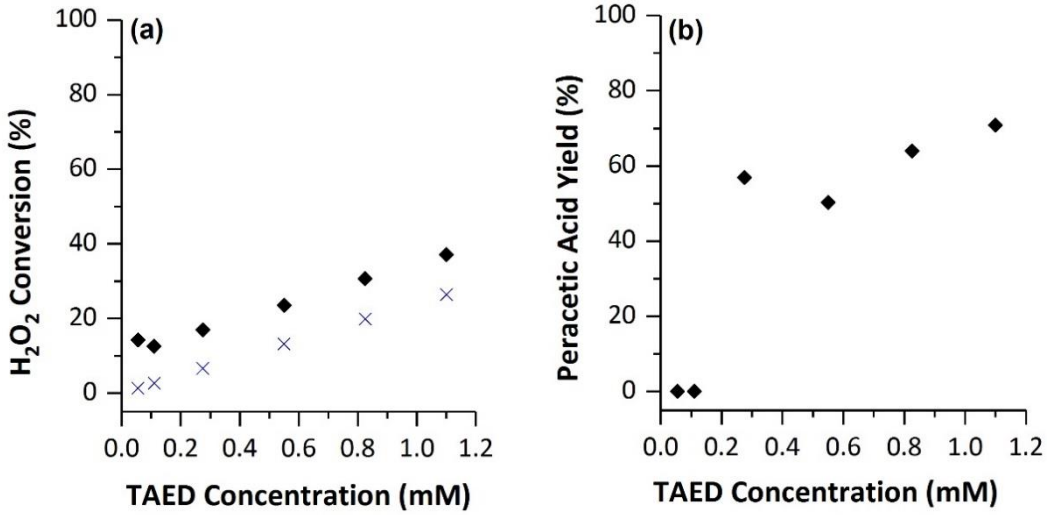

***Figure 25**: Effect of TAED concentration on (a) H_2O_2 conversion and (b) peracetic acid yield. Water (90 mL), sodium percarbonate (5.3 mM), TAED, 50 °C, pH = 10, 30 s. ♦ = measured conversion from experiment, x = theoretical maximum H_2O_2 conversion from the perhydrolysis reaction of H_2O_2 and TAED. Average error = 7%.*

The relationship between TAED concentration and both H_2O_2 conversion and peracetic acid yield are shown in

Figure **25**. In both, H_2O_2 conversion and peracetic acid yield increases linearly with TAED concentration. This suggests that the TAED concentration is the limiting factor for perhydrolysis. Interestingly, at low concentrations no peracetic acid formation is observed, but H_2O_2 conversion is observed. The lack of observed peracetic acid formation at TAED concentrations below 0.1 mM may be due to the peracetic acid concentration being below the detection limits of the titration method employed.

Bleaching at lower temperatures and pH generally leads to a lower bleaching performance in the dishwasher.[13] At lower temperatures, H_2O_2 is more stable, meaning less perhydroxyl anions are formed, which are an active species and required for perhydrolysis.[13] Hydroxyl groups found in tea stains, under alkaline pH, are anionic in nature, which increases the ease of stain removal by increasing nucleophilicity, compared to stain removal at neutral or acidic conditions. Operating at temperatures below 50 °C, and under more acidic pH, the rate of peracetic acid formation may become limited. Under such conditions, a catalyst could be used to increase the rate of peracetic acid formation and therefore enhance bleaching performance at these conditions. This would be beneficial as consumers push for lower temperature wash cycles while maintaining the bleaching performance of the formula. In order to understand how the reaction parameters influence the formation of peracetic acid, temperature was varied from 15 – 70 °C and the reaction pH from 6 – 11.

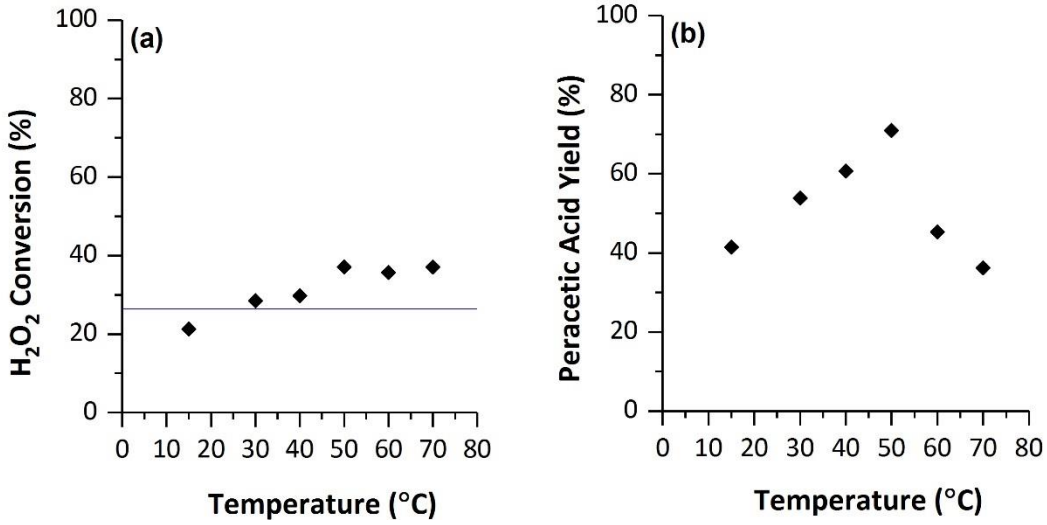

***Figure 26**: Effect of temperature on (a) H_2O_2 conversion and (b) peracetic acid yield. Water (90 mL), sodium percarbonate (5.3 mM), TAED (1.1 mM), pH = 10, 30 s. Line indicates the theoretical maximum H_2O_2 conversion from the perhydrolysis reaction of H_2O_2 and TAED. Average error = 7%.*

In Figure 26(a), the relationship between temperature and conversion of H_2O_2 was explored. H_2O_2 conversion increases with temperature, up until 50 °C. Further increasing the temperature from 50 to 70 °C results in similar rates of conversion. At temperatures of 30 °C and above, H_2O_2 conversion is higher than the theoretical maximum when all the TAED has reacted with H_2O_2, demonstrating H_2O_2 partakes in side reactions including decomposition at higher temperatures. This aligns with literature data that shows that, at higher temperatures, increasing H_2O_2 decomposition leads to an increase in bleach active perhydroxyl anions in solution.[13]

Figure 3(b) presents the effect of temperature on peracetic acid yield. The peracetic acid yield increases with temperature up to 50 °C. Above 50 °C, the yield of peracetic acid decreases, from 71 % at 50 °C to 36 % at 70 °C. This decrease in formation at

higher temperatures may be due to an increase in decomposition of peracetic acid, or hydrolysis of TAED being favoured at higher temperatures. Peracetic acid is known to decompose via a reaction with H_2O_2 or with another molecule of peracetic acid shown in Scheme 8.[12] Decomposition of peracetic acid is increased at higher temperatures, which is discussed in detail in Chapter 3, Section 3.2.1.3. H_2O_2 conversion and peracetic acid formation is still observed at temperatures as low as 15 °C, indicating that low temperatures do not halt the formation of peracetic acid. The formation of peracetic acid increases with temperature up to a maximum of 50 °C, then decreases above 50 °C, whereas H_2O_2 conversion increases with temperature and plateaus above 50 °C. Temperature does affect the yield of peracetic acid, which may be evidenced in bleaching performance, as less peracetic acid is available at the beginning of the wash cycle to remove stains. The addition of a catalyst could therefore be used to improve the yield of peracetic acid at lower temperatures, resulting in improved bleaching performance at conditions that are typically challenging for conventional dishwashing formulations.

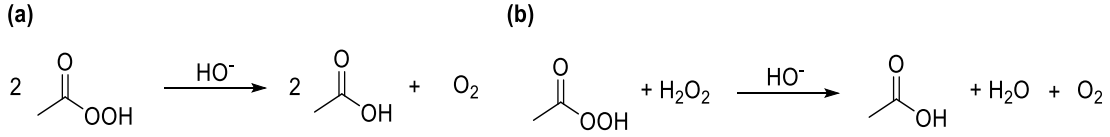

***Scheme 8**: Decomposition of peracetic acid, (a) = via reaction with another molecule of peracetic acid and (b) with H_2O_2.*

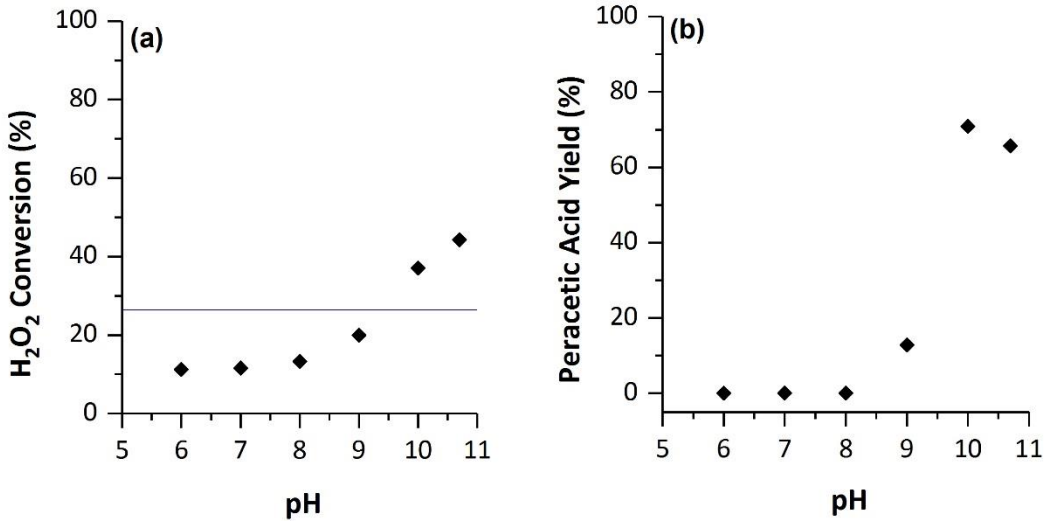

***Figure 27**: Effect of pH on (a) conversion of H_2O_2 and (b) peracetic acid yield. Water (90 mL), sodium percarbonate (5.3 mM), TAED (1.1 mM), 50 C, 30 s pH adjusted with H_2SO_4 (0.5 M) and sodium carbonate (1 M). A horizontal line indicates the theoretical maximum H_2O_2 conversion from the perhydrolysis reaction of H_2O_2 and TAED. Average error = 7%.*

Figure 27(a) shows how pH effects the rate of H_2O_2 conversion. H_2O_2 conversion increases substantially at pH 8 and above, indicating that pH has a large effect on the conversion of H_2O_2. The conversion of H_2O_2 is only above the theoretical maximum when all the TAED is reacted at pH 10, indicating that highly alkaline pH is most beneficial for perhydrolysis. More H_2O_2 is converted than required for the perhydrolysis of TAED at pH 10, demonstrating that, at alkaline pH, H_2O_2 is also consumed by side reactions and decomposition. In addition, this suggests that, at pH 10, H_2O_2 decomposition occurs simultaneously to perhydrolysis.

The effect of pH on the yield of peracetic acid is shown in Figure 27. Between pH 9 and 10, peracetic acid yield increases roughly 5-fold from 13 % to 71 %. At pH 6 to 8 there is no peracetic acid formation observed, again which may be due to the

concentration of peracetic acid being below that of the detection limit of the titration, or hydrolysis being favoured over perhydrolysis at acidic pH.

Overall, the perhydrolysis reaction is significantly reduced below pH 9, suggesting that high pH increases perhydrolysis and therefore improves bleaching activity. Davies and Deary investigated the rate of perhydrolysis and hydrolysis of TAED under various conditions.[14] It was also shown that rate of perhydrolysis of TAED increases with pH, which is in agreement with the trend observed in this work.

3.2.1.2 *Conversion of TAED and Formation of Acetic Acid*

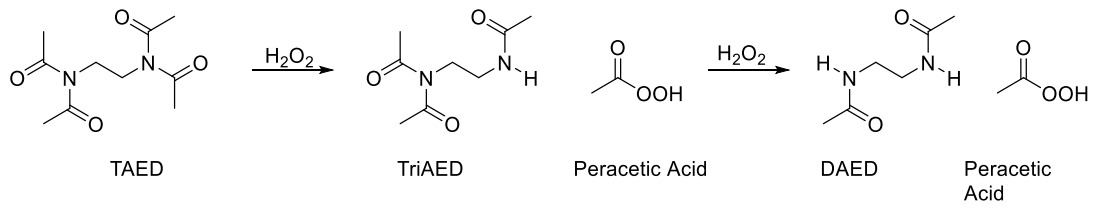

***Scheme 9**: Perhydrolysis of TAED to form peracetic acid.*

Further investigation into the perhydrolysis of TAED, Scheme 9, was also conducted by following the conversion of TAED *via* HPLC. To form peracetic acid, TAED undergoes perhydrolysis and forms triacetylethylenediamine (TriAED) as an intermediate and diacetylethylenediamine (DAED) as the final product. TAED can also form acetic acid *via* a hydrolysis reaction, which is in competition with the perhydrolysis pathway. Acetic acid is also formed during the decomposition of peracetic acid; due to chemical similarities between peracetic and acetic acid, quantification of both using HPLC can be difficult. HPLC separation and quantification of peracetic and acetic acids is further complicated by the decomposition of peracetic

acid on the HPLC C18 column to form acetic acid. This can be observed in Figure 28, where the peracetic acid peak shifts over time to a retention time consistent with acetic acid, 11.2 min. Therefore, acetic acid cannot be quantified accurately using HPLC to compare rates of perhydrolysis and hydrolysis.

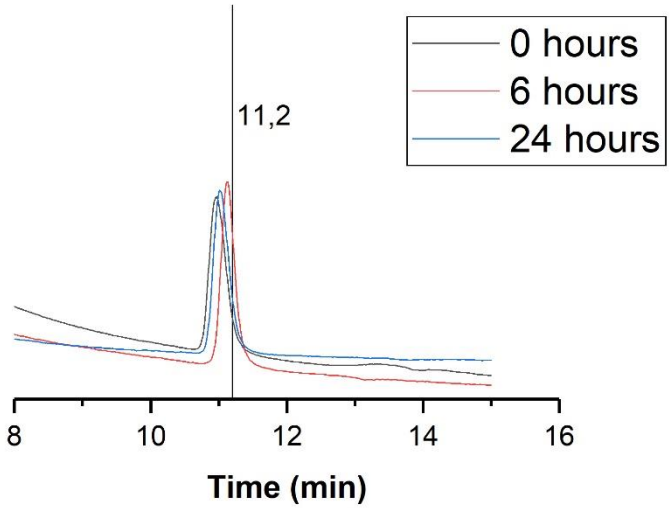

***Figure 28**: Peracetic acid stock solution (2.2 mM) injected over time on HPLC column. 11.2 min = observed retention time for acetic acid.*

Given that HPLC could reliably quantify the concentration of TAED, a study was undertaken to investigate the effect of reagent concentration and conditions on both TAED conversion and product formation. Due to the unavailability of the TriAED intermediate, only the final TAED decomposition product, DAED, was quantified in the HPLC. The chromatograms recorded for the reactions possessed unidentified peaks, which may have been the TriAED intermediate. The rate of TAED conversion and product formation has been calculated after both 30 s and 8 min, the standard wash time used in industry testing.

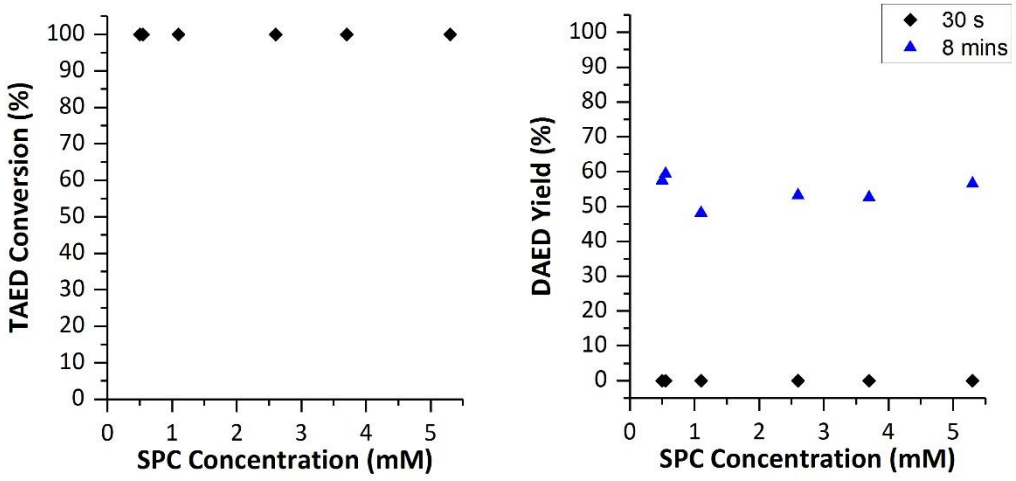

***Figure 29**: Effect of sodium percarbonate concentration, (a) TAED conversion and (b) DAED yield. Water (90 mL), sodium percarbonate, TAED (1.1 mM), 50 °C, pH = 10. Samples taken for HPLC analysis after 30 s and 8 min. Average error = 0.01%.*

The effect of sodium percarbonate concentration on TAED conversion and formation of DAED are shown in Figure 29(a) and (b), respectively. After 30 s, the TAED was fully converted at all sodium percarbonate concentrations. Figure 29(b) shows that DAED formation is not observed at 30 s but is observed at 8 min. As TAED conversion reaches 100 % within 30 s, but DAED formation does not, this indicates that the formation of TriAED is faster than DAED. TAED was observed to be more susceptible towards nucleophiles than TriAED by D.M Davies and co-workers, suggesting that perhydrolysis of the reactant (TAED) is faster than that of the intermediate (TriAED).[14] Over an 8 min wash, the slower reaction of TriAED with HOO^- to DAED, and the competing hydrolysis reaction, may explain why the yield of peracetic acid formed is lower than 100 % despite full TAED conversion,(Figure 24). Perhydrolysis does not account for the full conversion of TAED to DAED as fewer moles are formed of peracetic acid than expected. Overall, the data presented in Figure 29(a) and (b)

indicates that both TAED conversion and DAED formation are independent of the sodium percarbonate concentration.

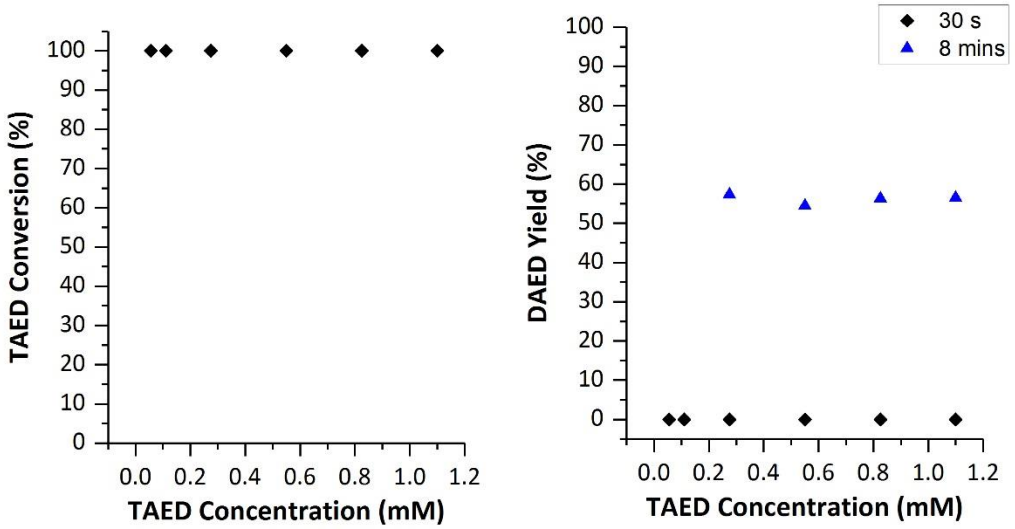

***Figure 30**: Effect of TAED concentration, (a) = TAED conversion, (b) = DAED yield. Water (90 mL), sodium percarbonate (5.3 mM), TAED, 50 °C, pH = 10. Samples taken for HPLC analysis after 30 s and 8 min. Average error = 0.01%.*

Figure 30 shows the effect of TAED concentration on TAED conversion and DAED formation. The TAED concentration does not affect the TAED conversion, with complete conversion being observed after 30 s at all TAED concentrations. The rate of TAED conversion does therefore increase as the concentration of TAED increases, but this is merely due to the fact there is more TAED available to react. This indicates that the reaction of TAED with sodium percarbonate is facile. DAED formation is similarly only observed after 8 min, which further evidences that the perhydrolysis of TriAED is slower than TAED.

The formation of the product, DAED, is evidently not affected by the initial TAED concentration. The yield of DAED formed is the same, irrespective of the initial TAED

concentration. This is true, even when there is a large excess of H_2O_2; no higher formation of the final product is exhibited.

Figure **25**, discussed previously, evidences that peracetic acid formation increases with increasing TAED concentration. It was also established that the theoretical maximum of peracetic acid that could be formed is dependent on the initial TAED concentration. The theoretical maximum of peracetic acid is not achieved even at higher TAED concentrations, which can be explained by the observed yields of DAED. The yield of DAED never reaches 100 %, which ultimately decreases the number of peracetic acid moles that are formed *via* perhydrolysis. One possible explanation for this is the competitive reaction of TAED with HO^-, which leads to the formation of acetic acid.

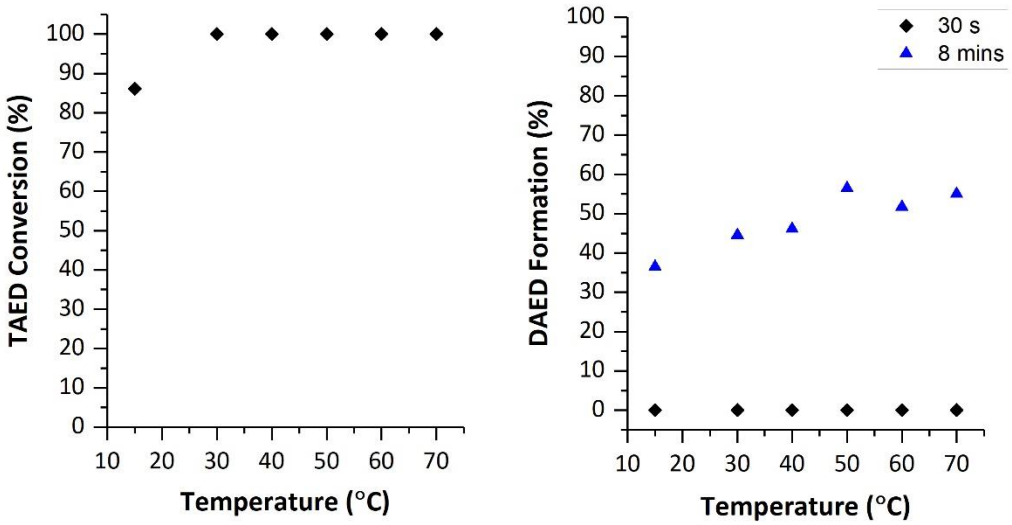

***Figure 31**: Effect of temperature on (a) = TAED conversion, (b) = DAED yield. Water (90 mL), sodium percarbonate (5.3 mM), TAED (1.1 mM), pH = 10. Samples taken for HPLC analysis after 30 s and 8 min. Average error = 0.01%.*

In order to further probe the effect of the reaction conditions, the reaction temperature was varied from 15 °C to 70 °C, as shown in Figure 31. TAED conversion remains constant at 100 % for temperatures between 30 to 70 °C for each of the 30 s reactions. At 15 °C, however, the conversion for a 30 s reaction decreases to 86 %, indicating that the reaction temperature does influence the rate of this reaction. Overall, it appears that temperature has a limited impact on the conversion of TAED with sodium percarbonate. As previously shown in Figure 26, peracetic acid formation increases with temperature up to 50 °C. The temperature dependence of the formation of peracetic acid could be explained by the increase in DAED formation with temperature from 30 to 50 °C, as shown in Figure 31. At 60 and 70 °C, peracetic acid yield decreases; however, DAED formation does not decrease, with the difference between the two evidencing higher rates of peracetic acid decomposition.

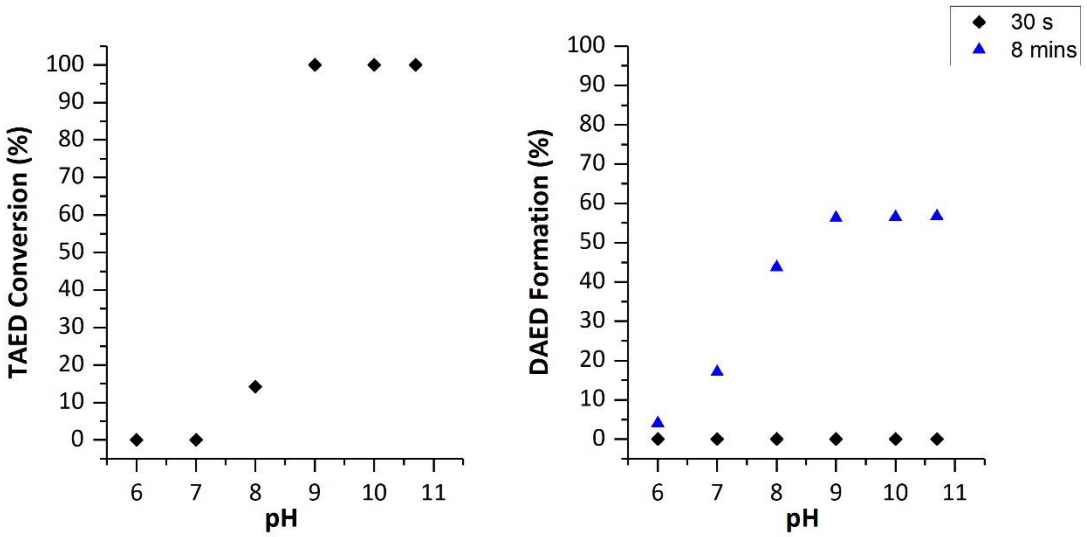

***Figure 32**: Effect of pH on (a) = TAED conversion, (b) = DAED yield. Water (90 mL), sodium percarbonate (5.3 mM), TAED (1.1 mM), 50 °C. Samples taken for HPLC analysis after 30 s and 8 min. Average error = 0.01%.*

Further work was undertaken to investigate the effect of pH on TAED conversion and DAED formation, as shown in Figure 32. No TAED conversion is observed at pH 6 and pH 7 after 30 s, indicating that neutral and acidic pH inhibits the perhydrolysis of TAED in the presence of sodium percarbonate. TAED conversion further increases as the pH is increased from pH 7 to pH 8. Interestingly at pH 9 and above, a dramatic increase in the rate of TAED conversion is observed (full TAED conversion is observed after 30 s). This pH dependence of TAED conversion indicates scope of a catalyst being used to aid bleaching at neutral pH by prolonging the active species. DAED formation is observed for all pH values after 8 min but not during the first 30 s of the reaction. At pH 6, the conversion reaches 4 % after 8 min compared to the 56 % conversion observed at pH 9 and pH 10. This suggests that TAED is still capable of being converted to DAED at lower pH either *via* perhydrolysis or hydrolysis. Hydrolysis has been previously shown to be acid catalysed, so at lower pH values this may be favoured and therefore decreasing the formation of peracetic acid.[14]

Figure 27 shows that the yield of peracetic acid formed at pH 9 and above correlates with the conversion of TAED at different pH, Figure 32. This suggests that, at a lower pH, the hydrolysis reaction is more dominant; TAED undergoes hydrolysis to acetic acid instead of peracetic acid, as DAED is still formed.

3.2.1.3 *Rate of Peracetic Acid Formation from Perhydrolysis*

The rates of peracetic acid formation and H_2O_2 conversion at varying pH and temperature were calculated, using the following equation,

$$R0 = \frac{(C_F - C_I)}{t}$$

Where R0 = initial rate of the reaction, C_F = final concentration in M, C_I = initial concentration in M and t = time in seconds. The rate constant, k, was calculated for peracetic acid formation using the following equation

$$k = -ln\left(\frac{(C_T - C_F)}{t}\right)$$

Where C_T = maximum theoretical concentration of peracetic acid in M, C_F = final concentration of peracetic acid in M and t = time in seconds. For all the calculations t was 30 secs as the reagents were only quantified at 0 secs and 30 secs. A pseudo first order reaction was assumed from the plot of $\ln(C_T - C_F)$ vs time which gave a straight line. The initial rate and rate constant are shown in Table 5.

***Table 5**: Initial rate of reaction of H_2O_2 and peracetic acid and k for peracetic acid formation.*

Temperature (°C)	pH	H_2O_2 R0 (M/s)	Peracetic Acid R0 (M/s)	k (peracetic acid, s^{-1})
50	10	9.7×10^{-6}	4.7×10^{-6}	13.1
50	9	4.0×10^{-6}	8.5×10^{-7}	12.1
15	10	3.2×10^{-6}	6.8×10^{-7}	12.4

The initial rate of hydrogen peroxide conversion decreases with pH and temperature, the rate of peracetic acid formation follows the same trend. The calculated rates and rate constant is not accurate due to the high conversion of TAED observed after 30s, and, a first-order reaction assumed from a plot of two point at 0s and 30s.

3.2.1.4 *Decomposition of Peracetic Acid*

Peracetic acid is the primary bleaching agent used in modern formulations and is consumed during oxidation of the stain, forming acetic acid as the by-product. In addition to consumption through stain bleaching, peracetic acid can also decompose through several other pathways. This includes its reaction with HO^- to form acetic acid and O_2, as well as reacting with H_2O_2 to form acetic acid, water and O_2. The possible decomposition pathways of peracetic acid are shown in Scheme 10. The reaction conditions, such as pH and temperature, also affect the decomposition of peracetic acid, which can ultimately impact the amount of peracetic acid available in solution for bleaching of stains. This in turn can influence the overall bleaching performance of the system; it is therefore important to understand how the conditions impact peracetic acid decomposition, as this ultimately affects bleaching performance.

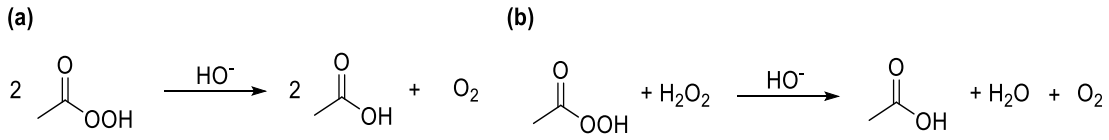

***Scheme 10**: Decomposition pathways of peracetic acid.*

To assess how the reaction conditions and various reagents used in bleaching influence the decomposition of peracetic acid, a series of reactions were conducted using a standard peracetic acid stock solution. The peracetic acid and H_2O_2 concentrations were monitored over time using a cerium (IV) sulfate and iodometric titration. As the peracetic acid solution was purchased, the solution also contained

H_2O_2, acetic acid and H_2SO_4, which maintains the equilibrium in solution. Therefore, the concentration of peracetic acid in this stock solution is known. Initially, the effect of temperature on peracetic acid decomposition was investigated.

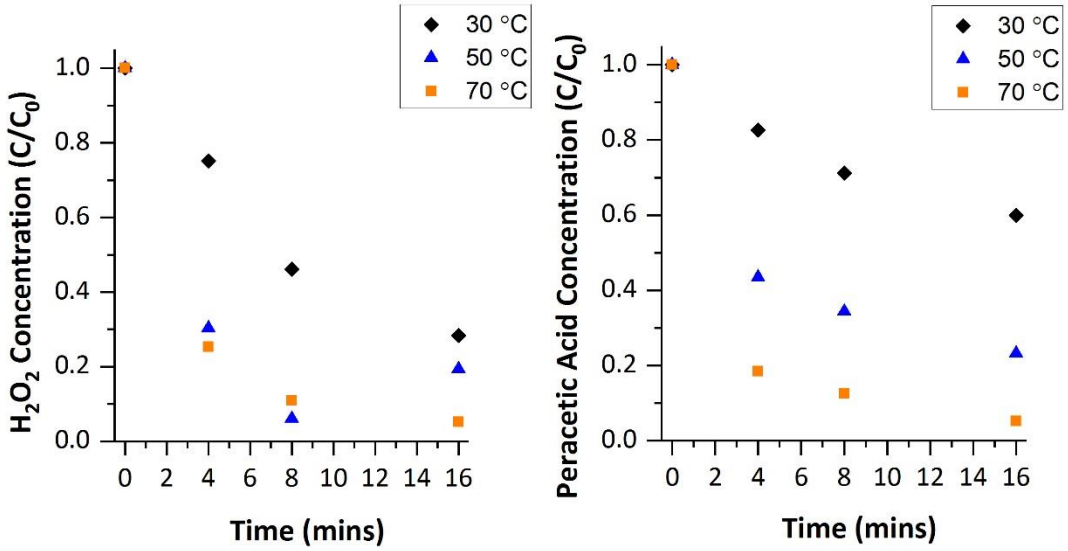

***Figure 33**: Effect of temperature on decomposition of active oxygen species, (a) = H_2O_2 concentration and (b) = peracetic acid concentration. Water (90 mL), peracetic acid (2.2 mM), H_2O_2 (1.5 mM), pH = 10, 16 min. Average error = 7%.*

The effect of temperature on peracetic acid decomposition is shown in Figure 33. For each experiment, 2.2 mM of peracetic acid was added at the start of the reaction as this is the theoretical maximum concentration that could be formed from TAED used in the standard TC. The concentration of both H_2O_2 and peracetic acid was quantified at 0, 4, 8 and 16 min. The results in Figure 33(a) demonstrate that the H_2O_2 decomposes gradually over 16 min, with the greatest difference in decomposition observed between reactions at 30 and 50 °C. No significant difference in the rate of H_2O_2 decomposition was observed in the experiments run at 50 and 70 °C. After 16

mins at 50 °C an increase in H_2O_2 was observed, when compared to 8 mins, which could be due to the low concentrations of H_2O_2 and peracetic acid present in the solution limiting the accuracy of the titration method.

Similar to H_2O_2, the rate of peracetic acid decomposition increases with temperature. After 4 min at 70 °C, 80 % of the peracetic acid is decomposed, which is in stark contrast to the 8 % conversion observed after 4 min of reaction at 30 °C. Such a trend is observed regardless of the reaction length; with higher temperatures, peracetic acid has a higher rate of decomposition. Previously, in Figure 26, it was shown that less peracetic acid is formed from the reaction of TAED with H_2O_2 at 70 °C, than at 50 °C. The data presented in Figure 31 indicates that the reduced peracetic acid formation rate at higher temperatures must therefore be attributed to the undesirable decomposition of peracetic acid in solution, once it is generated.

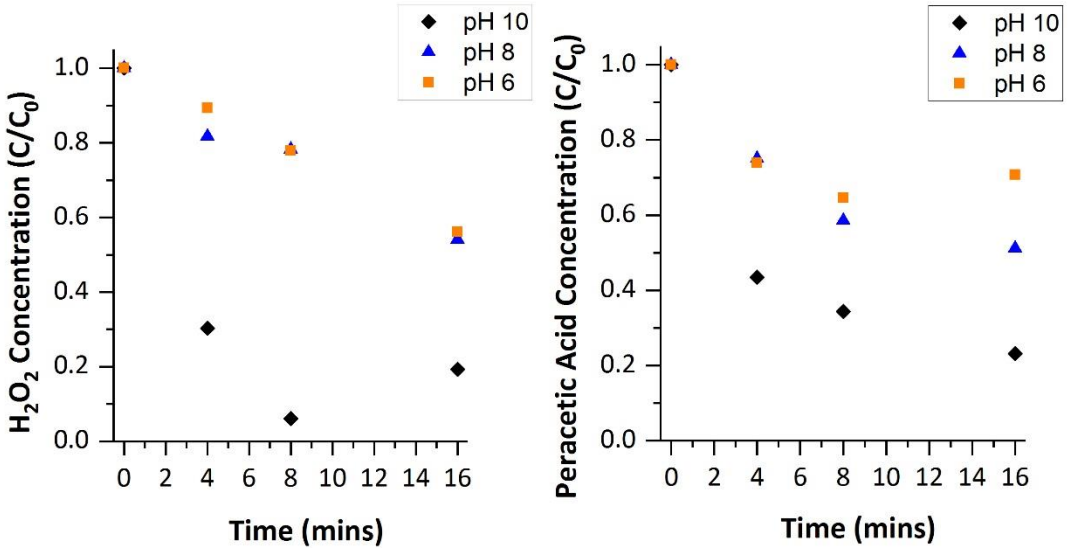

***Figure 34**: Effect of pH on the decomposition of active oxygen species, (a) = H_2O_2 concentration and (b) = peracetic acid concentration. Water (90 mL), peracetic acid (2.2 mM), H_2O_2 (1.5 mM), 50 °C, 16 min. Average error = 7%.*

The effect of pH on the decomposition of peracetic acid and H_2O_2 was also investigated, as shown in Figure 34. The decomposition of H_2O_2 remains stable between pH 6 and 8, but increases at pH 10, suggesting that H_2O_2 is less stable at more alkaline conditions. Peracetic acid decomposition follows a similar trend to H_2O_2. After 8 min of reaction at pH 6, 37 % of the H_2O_2 present has undergone decomposition. After 8 min of reaction at pH 10, however, this increases to 56 %. This shows that both peracetic acid and H_2O_2 are more stable at a lower pH. At 16 mins an increase of H_2O_2 and peracetic acid was observed, which is due to the limited accuracy of the titration method at low reagent concentration.

Figure 27 and Figure 32, discussed previously, indicated that there was minimal TAED conversion below pH 7; no peracetic acid was detected after 30 s of reaction. Peracetic acid formation could still be occurring, but the concentration formed could be below the detection levels of the titration method. Regardless of this, there was significantly less peracetic acid formed, and less TAED converted, than in reactions under more alkaline conditions. This indicates that an alkaline pH is highly beneficial to the rate of perhydrolysis of TAED.

At alkaline pH, above the pKa of both peracetic acid and H_2O_2, the corresponding anion is formed,[1] which is considered to be the active bleach species.[15] It is known that this anion is formed during the decomposition of peracetic acid under alkaline conditions, shown in Scheme 12[16]. Therefore, it is likely that the bleaching mechanism requires formation of the highly active anion species.

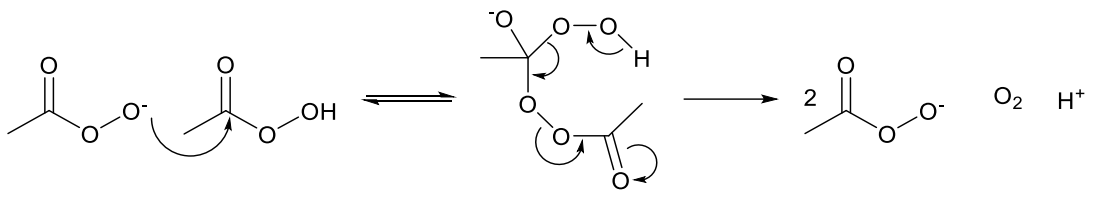

***Scheme 11**: Spontaneous decomposition of peracetic acid under alkaline conditions*

In a standard tablet formulation, additional compounds other than sodium percarbonate and TAED are included, as they are considered to aid the bleaching process.[17] Methylglycinediacetic acid (MGDA) is added as a chelating agent to sequester metal ions. Metal ions, which are present in tap water, such as Ca^{2+} and Mg^{2+}, can reduce bleaching performance through interaction with the active oxygen species. These cations are known to contribute to the decomposition of the active oxygen species.[18] To understand how MGDA influenced the decomposition of peracetic acid and H_2O_2 in this system, additional experiments were conducted in the presence of MGDA.

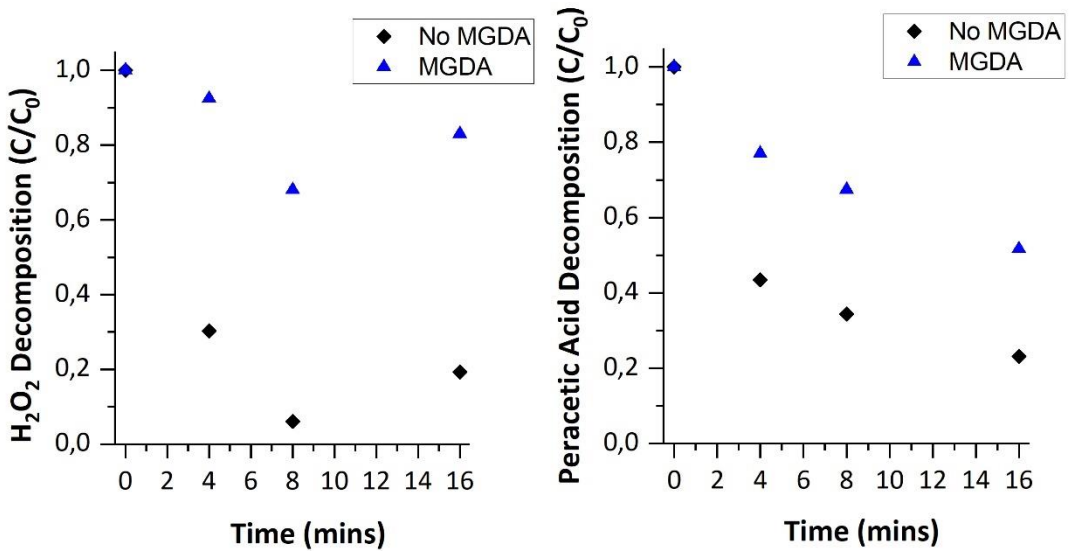

***Figure 35**: Effect of MGDA on the decomposition of peracetic acid, (a) = H_2O_2 concentration and (b) = peracetic acid concentration. Water (90 mL), peracetic acid (2.2 mM), H_2O_2 (1.5 mM), MGDA (0.4 mM), 50 °C, 16 min. Average error = 7%.*

Figure 35 shows the effect MGDA has on peracetic acid decomposition. The addition of MGDA at 50 °C reduces peracetic acid decomposition from 77 % to 46 % after 16 min of reaction. Similarly, MGDA also reduces the decomposition of H_2O_2 from 80 % to 17 % after 16 min. An increase in H_2O_2 was observed after 16 mins in the presence of MGDA, that can be explained by the decrease in accuracy of the titration at low reagent concentrations. As deionised water is used in the reaction, and not distilled, there will still be a small quantity of metal ions present in the solution that may promote the decomposition of peracetic acid above room temperature. Evidently, the addition of MGDA to the solution reduces the rate of decomposition for both H_2O_2 and peracetic acid; this in turn would likely increase the concentration of active species in solution, highlighting the important role of MGDA and other builder in commercial bleaching applications.

Quantification of peracetic acid, H_2O_2 and TAED during the reactions, with reagent concentrations and conditions varied, showed that the conversion of TAED and formation of peracetic acid is facile. Decreasing sodium percarbonate (Figure 24) and TAED concentration (

Figure **25**) does limit the amount of peracetic acid formed, due to the decrease in concentration of reactants available to form peracetic acid. Furthermore, the experiments confirmed that TAED is rapidly converted, regardless of the reaction conditions used and reagent concentrations employed. Temperature has been observed to have minimal effect on the rate of TAED conversion over the time scale observed (Figure 31), however, increasing temperature can influence the decomposition rate of peracetic acid, Figure 33.

Of the reaction conditions assessed, the pH of the reaction was determined to have the largest impact on the perhydrolysis of TAED to peracetic acid. Peracetic acid was only observed in reactions conducted at pH 9 and above (Figure 27). This is likely due to alkaline pH favouring the formation of the hydroxyl anion, which is required for the perhydrolysis of TAED to form peracetic acid.[14]

Overall, the investigation into the perhydrolysis of TAED and formation of peracetic acid shows that the reaction is facile under a range of conditions and reagent concentrations, which demonstrates that a catalyst is not required for the effective formation of peracetic acid.

3.2.1.5 *Effect of Varying Conditions on Tea Stain Bleaching*

As discussed in the introduction to this chapter, new formulations in the industry are tested in a dishwasher using set conditions, and bleaching performance is qualified

using tea stains prepared on teacups. The cups are scored from a scale of 1 – 10, which is dependent on how clean the cup appears after the wash. A quick teacup test using 1 cup was developed to screen potential catalysts for bleaching. In this test, the ratios of the reagents used are kept the same as that present in a typical dishwashing tablet, to ensure that the bleaching performance observed in the beaker test would be similar to the conditions used in a typical dishwasher test. In addition to this, tap water was used to replicate the industrial standard testing protocol; tap water in Cardiff is classified as soft, with 0 – 90 ppm of Ca present.

Given that peracetic acid formation has been quantified under a range of conditions, it was important to establish how this affected the bleaching of tea stains. Therefore, TCs were run using the same range of reagent concentrations and bleach conditions to assess how the perhydrolysis of TAED affects bleaching of tea stains.

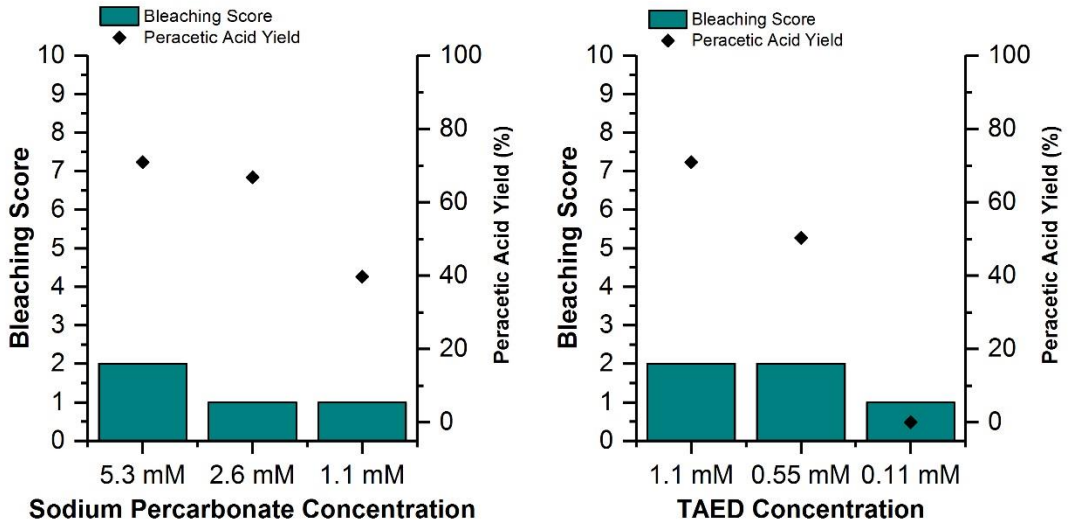

***Figure 36**: Effect of varying reagent concentrations on bleaching performance, (a) = varying sodium percarbonate concentration and (b) = varying TAED concentration. Water (1.8 L), sodium percarbonate (5.3 mM), TAED (1.1 mM), MGDA (0.4 mM), 50 °C, pH = 10, 8 min. Average error = ± 1 bleaching score.*

Figure 36 shows the effect of decreasing the sodium percarbonate and TAED concentration on stain bleaching score. At a sodium percarbonate concentration of 5.3 mM, the bleaching score was highest; typically 2 ± 1. Decreasing the sodium percarbonate concentration below 5.3 mM to 2.6 mM or 1.1 mM reduces bleaching performance by a score of 1, to 1 ± 1.

A similar trend is observed when the TAED concentration is decreased; 1.1 or 0.55 mM of TAED produces a score of 2 ± 1, dropping to 1 ± 1 at 0.11 mM. For comparative purposes, previous data acquired for peracetic acid yield has been overlaid onto the teacup data (Figure 13). As peracetic acid formation does increase with sodium percarbonate concentration, the teacup score increases with increasing SPC concentration, from 2.6 to 5.3 mM, suggests that increasing peracetic acid does aid bleaching; however, this observed trend may also be due to experimental error.

Decreasing TAED concentration does significantly decrease peracetic acid formation, which is also mirrored in the bleaching scores, and indicates that decreasing peracetic acid concentration decreases the bleaching performance of the formulation.

Given that bleaching performance decreased when both the TAED and sodium percarbonate concentrations decreased, this suggests that bleaching performance is promoted by the generation of peracetic acid. H_2O_2 also plays a role in bleaching performance, especially above stoichiometric ratios of sodium percarbonate to TAED. Spiro and co-workers have demonstrated that the activity of H_2O_2 in bleaching is attributed to the formation of a HOO^- species.[19] In bleaching formulations, H_2O_2 is often used in excess to the bleach activator, TAED, to promote bleaching performance.[12]

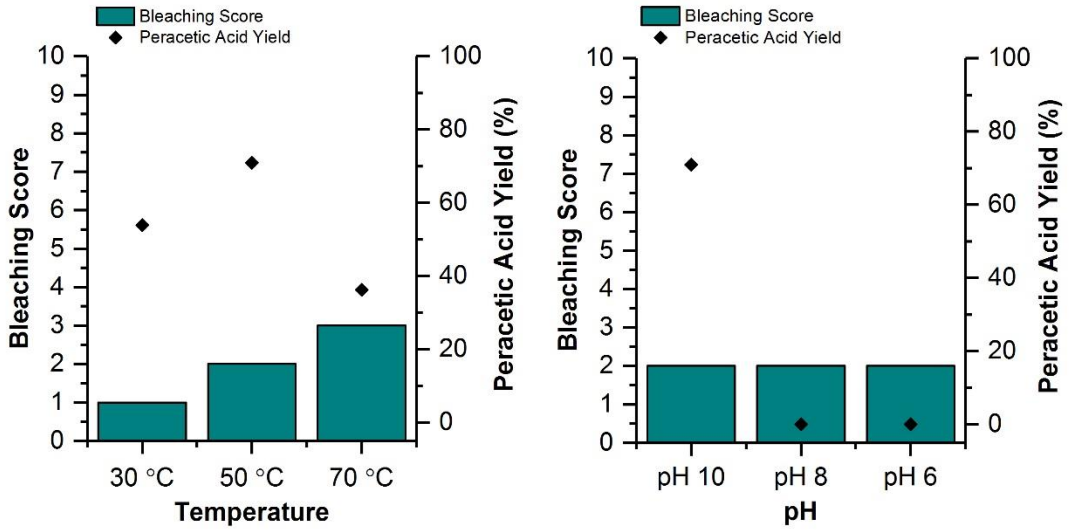

***Figure 37**: Effect of (a) = temperature and (b) = pH on bleaching performance. Water (1.8 L), sodium percarbonate (5.3 mM), TAED (1.1 mM), MGDA (0.4 mM), 50 °C, pH = 10, 8 min. Average error = ± 1 bleaching score.*

The effect of temperature and pH on bleaching performance is shown in Figure 37. The bleaching score increases from 1 to 3 as the temperature of the reaction is increased from 30 to 70 °C, indicating that higher temperatures improve bleaching of stains. Figure 26 previously showed that peracetic acid yield increases then decreases again between 30 and 70 °C. Similarly, Figure 33 shows that higher temperatures increase peracetic acid decomposition. Dithmar *et al.*[13] demonstrated that a higher rate of H_2O_2 decomposition was observed at 85 °C compared to 60 °C, and a higher bleaching activity for stains was observed at 85 °C. The authors suggested that the high decomposition rates lead to an increase in active species and, therefore, an improved bleaching performance. As peracetic acid and H_2O_2 decomposition is increased up to 70 °C, alongside bleaching performance, this

indicates that the concentration of the active species formed is increased at higher temperatures.

Figure 37 also shows the effect of pH on the bleaching score and peracetic acid formation. Bleaching score does not appear to be affected by pH, remaining constant at 2 ± 1 for pH between 6 and 8. Figure 27 previously suggested that, at lower pH, smaller quantities of peracetic acid are formed, which is consistent with the peracetic acid yield determined from these TCs. This may indicate that, even though peracetic acid is not formed at a pH below 7, bleaching can still occur at 50 °C with H_2O_2 predominantly present.

Overall, peracetic acid may be beneficial for bleaching under alkaline conditions but not under acidic conditions when peracetic acid is formed *in situ*. H_2O_2 bleaching occurs over a wider range of conditions in comparison to peracetic acid.

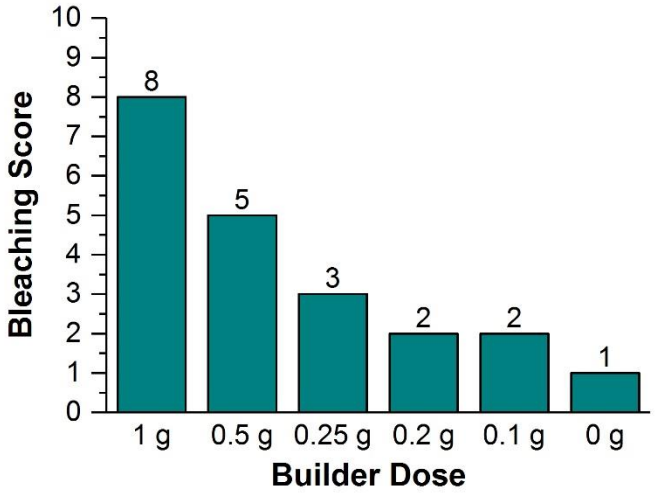

***Figure 38**: Effect of builder dose on bleaching performance. Water (1.8 L), sodium percarbonate (5.3 mM), TAED (1.1 mM), MGDA (0.2 – 2 mM), 50 °C, pH = 10, 8 min. Average error = ± 1.*

As tap water was used in the TCs, the effect of MGDA dose on bleaching performance was assessed in Figure 38. For hard water, higher doses of MGDA are needed to improve bleaching performance; however, if the same dose is used in softer water, this increases the bleaching score without increasing the concentration of active species in the wash. MGDA sequesters metal ions in solution and has a high affinity for Fe(III) and Cu(II) ions.[18] MGDA is highly stable over a wide range of temperatures and pH, which leads to highly stable metal complexes:

$$M^{2+} + H_nMGDA^{n-3} \leftrightharpoons [M(H_nMGDA)]^{n-2}$$

Where n = 0,1,2. As tap water hardness in the lab was recorded as 37 – 38 ppm over the course of 3 days, the MGDA dose was varied to assess what dose would be most suitable to use for the benchmark experiments. The standard bleaching score for the current formulation concentrations and conditions (sodium percarbonate (5.3 mM, SPC : TAED 4.8), TAED (1.1 mM), 50 °C, pH = 10) is 2, which is referred to as the negative reference. Figure 38 shows that a dose of 1 g of MGDA increases the score from 2 to 8. Stain bleaching has been indirectly improved by the addition of excess MGDA as metal ions are sequestered in solution, improving the stability of active species in the wash. This is evidenced in Figure 35, which shows that the addition of MGDA decreases peracetic acid and H_2O_2 decomposition during the reaction. MGDA only improves bleaching by the removal of metal ions that can decompose the active bleaching species; the benefit of MGDA is therefore only observed in tap water where these ions are present.

The dose was decreased from 1 g to 0.1 g and the bleaching score decreases with MGDA dose from 8 to 2. Therefore, to ensure the bleaching score in further tests is

not increased by the builder alone, a dose of 0.2 g was chosen for further experiments.

3.2.2 *Development of Quantitative Analysis for Bleaching Performance*

The applicative TC, as used previously, is a good indication of bleaching performance in the dishwasher. However, it can only be considered semi-quantitative and there is a large error of ± 1 score associated with it. As such, it is difficult to accurately investigate the influence of catalysts on bleaching. For this reason, attempts were made to develop a more accurate model reaction.

For a model reaction to be successful in measuring applicative bleaching performance, the following criteria must be met:

- The conversion of the substrate must occur through oxidative chemistry, as the bleaching process is an oxidation of the stain
- The activity of the blank and benchmarked catalysts must align with the TC
- The reaction must be reproducible and have a low error to be able to further investigate the differences between reaction conditions and catalysts added to the reaction

A suitable model should have a similar structure and/or consist of similar functional groups to compounds responsible for the stain colour, which are shown in Figure 39.[3]

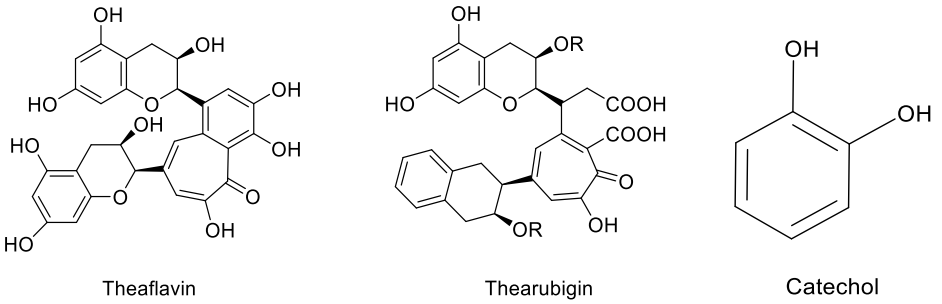

***Figure 39**: Structure of Theaflavin and Thearubigin found in tea alongside catechol.*

The composition of the stain is affected by a number of factors, which include: the tannin content of the tea, the age of the stain and the hardness of the water used to make the tea.[20] Given their inherent complexity, the structure of a tea stain is not fully known. It is however evident from the compounds in Figure 39 that both theaflavins and thearubigins consist of catechol moieties as displayed in Figure 39. Sorokin *et al.*[21] used catechols to investigate phthalocyanine metal complexes for bleaching. As the model reaction was successful for Sorokin, catechol was used as a model substrate here to further investigate the influence of different conditions and the addition of catalysts on bleaching performance

3.2.2.1 *Development of Catechol Model Reaction*

Previously, catechol has been used as a model compound for the removal of organics from waste, as well as a model compound for bleaching.[4,22,23] Sorokin *et al*.[4] investigated Fe and Mn metallophthalocyanines for the oxidation of catechols, using a ratio of 5 : 1 of oxidant to catechol.

With this in mind, a HPLC method was developed to quantify reactions where catechol was used as a substrate. For these reactions, the sodium

percarbonate/TAED concentrations were kept the same as the TCs shown in section 1.2.1. Initially, the ratio of oxidant to catechol was investigated with the aim of reducing the blank conversion of catechol without a catalyst present.

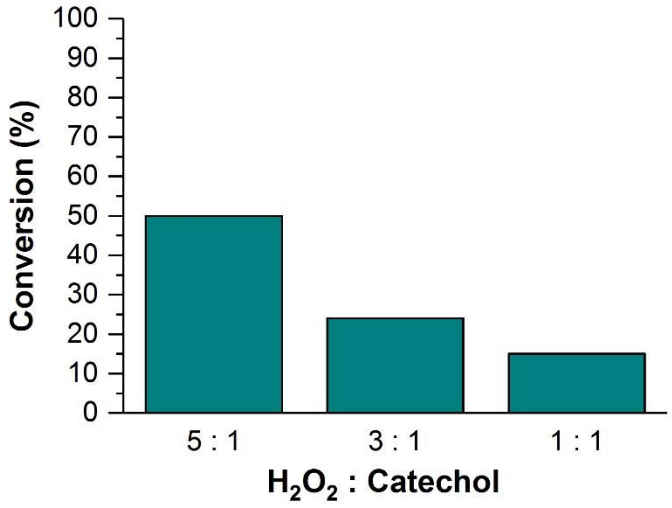

***Figure 40**: Screening of catechol : H_2O_2 molar ratios for catechol oxidation with no catalyst present. Water (90 mL), catechol (8 mM), sodium percarbonate (5.3 – 26.5 mM), TAED (1.1 mM), pH = 9, 50 °C, 8 min.*

Figure 40 shows how the ratio of H_2O_2 and catechol influences the conversion. Decreasing the H_2O_2 : Catechol ratio from 5:1 to 1:1 results in a decrease in conversion from 50 % to 15 %. When the oxidant is in excess, the conversion is above 20 % as evidenced in Figure 40 where the H_2O_2 : catechol ratio is 3 : 1 or higher. Therefore, to reduce the catechol converted from this blank reaction a ratio of 1 : 1 H_2O_2 : catechol was chosen. All reactions following were conducted with an oxidant to catechol ratio of 1 : 1.

At the end of the reaction, the oxidant remains present in the solution and may therefore contribute to further catechol conversion prior to analysis. For this reason,

it was important to develop a method to quench the reaction once it had finished, to ensure that the obtained data was accurate.

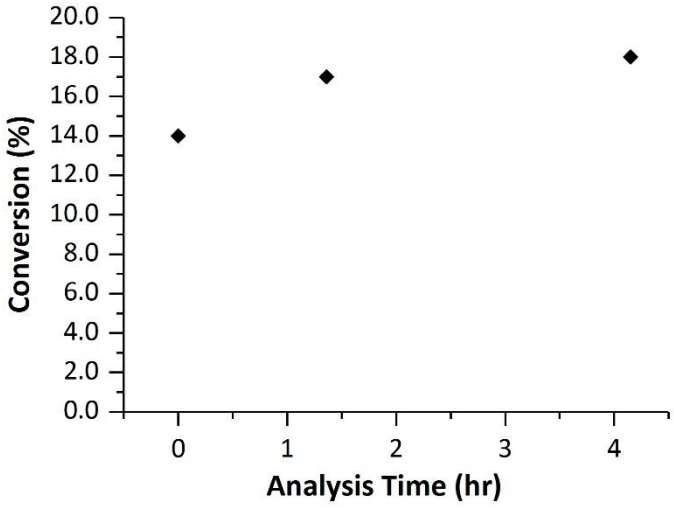

***Figure 41**: Continuation of catechol oxidation after analysis. Water (90 mL), catechol (8 mM), sodium percarbonate (5.3 mM), TAED (1.1 mM), pH = 9, 50 °C, 8 min.*

To establish the extent of the continued reaction, the same post reaction sample was analysed over time *via* HPLC, the results of which are shown in Figure 41. After 4 hours the conversion of catechol increases by 4 %, suggesting that the initial data acquired may not be accurate. Different methods of quenching the reaction were then trialled.

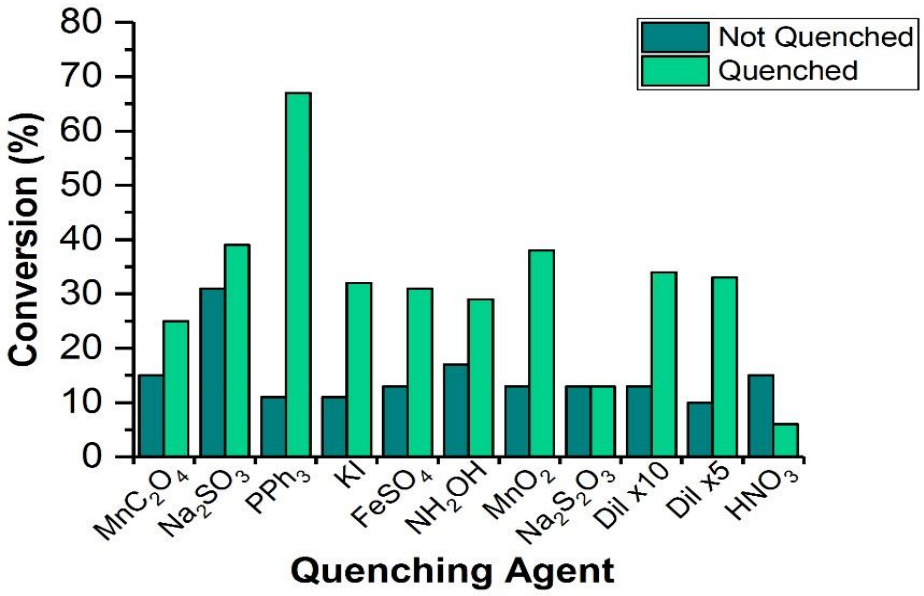

***Figure 42**: Screening of potential quenching agents and methods. Water (90 mL), catechol, (8 mM), sodium percarbonate (5.3 mM), TAED (1.1 mM), pH = 9, 50 °C, 8 min.*

Figure 42 shows the different reagents that were investigated for decomposing residual H_2O_2 to halt the reaction before analysis. For the unquenched reaction the conversion of catechol is not the same for each experiment as each reaction solution could not be analysed at the same time after the reaction was stopped. A series of compounds were added to decompose the excess H_2O_2 to halt the reaction before analysis. MnC_2CO_4, Na_2SO_3 [24], PPh_3 [8], KI [10], $FeSO_4$ [25], NH_2OH, MnO_2 [26], $Na_2S_2O_3$ [10] have been shown to decompose H_2O_2 to H_2O and O_2. Therefore, these compounds were added to the post reaction solution and filtered before analysis, as each is known in interact with H_2O_2 and potentially decompose. In all cases, the compounds added did not halt the reaction and appeared to catalyse the reaction and increase the conversion. As the reaction solution is alkaline, H_2O_2 will be in the form OOH^-, that maybe used by the added compounds to catalyse the reaction with catechol in

tandem with decomposition of H_2O_2. In addition, it has been shown that catechol can absorb onto the surface of metal oxides which would increase the apparent conversion in HPLC.[27] Addition of 0.5 M HNO_3 to neutralise the reaction successfully quenched the reaction, reducing the conversion of the blank reaction. In further reactions the post reaction solutions were cooled on ice and neutralised with 0.5 M HNO_3 before analysis *via* HPLC.

***Table 6**: Catechol oxidation blank reactions. Water (90 mL), catechol (8 mM), sodium percarbonate (5.3 mM), TAED (1.1 mM), sodium carbonate (0.1 g), pH = 9, 8 min.*

Reaction	Temperature (°C)	Conversion (%)
Catechol Only	24	2
Catechol Only	50	1
Catechol + TAED	50	1
Catechol at pH 9	50	11
Catechol + SPC	50	8
Catechol + SPC/TAED	50	11

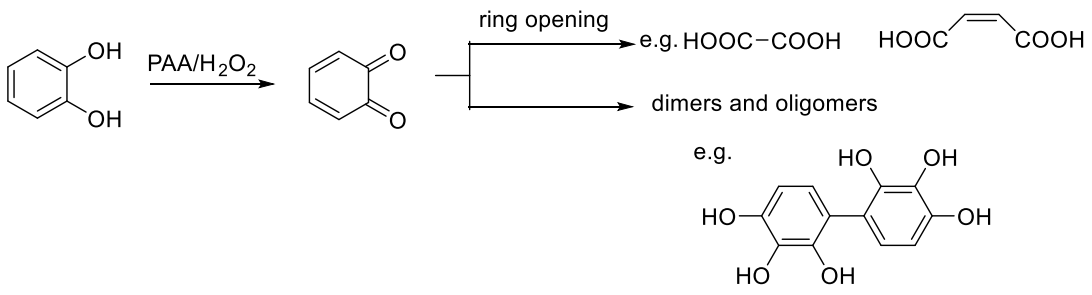

***Scheme 12**: Reaction pathways of catechol to form either ring opened oxidation products or condensation products.*

A series of blank reactions were run, the results of which are shown in Table 6. Sodium carbonate was added to the reaction to ensure that the pH remained at 10 during the reaction; carbonate was chosen as this is already formed by sodium percarbonate when added to water, releasing H_2O_2 and sodium carbonate. An experiment conducted in the absence of any bleaching reagents or catalysts at room temperature exhibited a conversion of 1%. The reaction was repeated at 50 °C, and again with the addition of TAED, and the conversion observed was close to 0 %; however, the conversion of catechol with sodium carbonate at pH 9, and the conversion of catechol in the presence of sodium percarbonate/TAED, was 11 %. This indicates, that under alkaline conditions, catechol may be partaking in a parallel condensation reaction. Sorokin *et al.*[4] observed the condensation of catechol in the presence of sodium percarbonate and TAED systems as the quinones formed from the first step of the reaction can polymerise. Guzman and co-workers[23] also observed polymerisation of catechol during oxidation reactions. Further oxidation of biphenyl products was observed to form heavier products.

To further investigate the effect of condensation side reactions, a series of additional experiments at different pH values were conducted with no oxidant present.

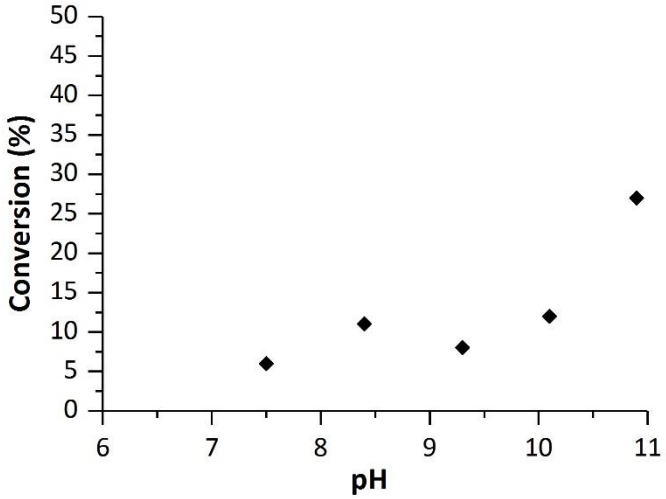

***Figure 43**: Effect of pH on catechol conversion. Water (90 mL), catechol (8 mM), sodium carbonate (1 M), 50 °C, 8 min.*

Figure 43 shows the effect of pH on catechol conversion, which was adjusted through the addition of sodium carbonate. At pH 7.5 – 9.3 conversion is around 10 % for each reaction, and this increases to 27 % at pH 11. The results show that catechol conversion increases with pH without oxidant present. Catechol is known to undergo ring opening and polymerisation, after the formation of quinones, in the first step of the reaction. Liquid chromatography mass spectrometry (LC-MS) and gas chromatography mass spectrometry (GC-MS) were used in an attempt to identify the products formed in these reactions; however, this was unsuccessful as the peaks were not clear enough to identify products, due to the amount of high molecular weight species present. A series of known oxidation products, such as maleic acid, were injected into the HPLC to record the retention times for comparison with the reaction samples. The post reaction mixture was then analysed, but no peaks that matched known oxidation products were observed. Demonstrating that known

oxidation products, shown in Scheme 12, were not present. This evidenced that no ring opening was occurring during these reactions. In conclusion, an inability to isolate the oxidation and condensation reactions of catechol meant that it was not a suitable model compound comparable to stain bleaching.

3.2.2.2 *Development of Morin Model Reaction*

Morin has also been used as a model compound for the bleaching of cotton and as a test dye for bleaching efficiency in laundry applications.[5] The oxidation of morin can be followed *via* UV-Vis, as morin exhibits a strong yellow colour in alkaline solution with a maximum absorbance at 400 – 425 nm.[28] R. Meijboom and co workers[29] investigated Co_3O_4 as potential catalysts to remove flavonoids from waste water. The authors used high morin to H_2O_2 ratios, with small catalyst doses (< 1 mg) added to each reaction. Morin concentrations greater than 0.1 mM can saturate UV-Vis detectors, and therefore a concentration of 0.1 mM was used to conduct the model reaction study presented in this work. Furthermore, dilution of reaction samples pre-analysis incurred a large error in reproducibility. For comparison between the TC and the morin oxidation reaction, reagent concentrations were kept the same as those used for the data presented in Figure 38, i.e. sodium percarbonate (5.3 mM) and TAED (1.1 mM) giving a morin : H_2O_2 of 1 : 80. These conditions align with the conditions used by R. Meijboom and co-workers[29], who also used a high morin to H_2O_2 ratio of 1 : 80.

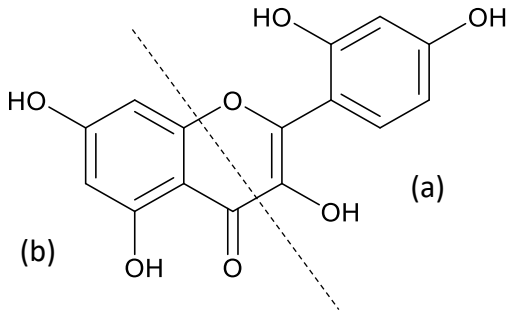

Morin

Figure 44*: Structure of Morin where (a) = cinnamyl moiety and (b) = benzoyl moiety.*

Figure 44 shows the structure of morin, which can undergo oxidation in such reactions. There are two bands observed for morin in UV-Vis spectroscopy.[30] The first band is associated with the cinnamyl system, Figure 44 (a), from 350 – 400 nm, and the second band is associated with the benzoyl moiety from 250 to 280 nm, Figure 44 (b). The absorbance of morin shifts to a higher wavelength under alkaline pH, where morin is present in an anionic form, and the longest wavelength observed is above 400 nm.[31] This absorption was observed for morin in $NaCO_3$, which had fully dissolved to give a bright yellow solution with the spectrum shown in Figure 45.

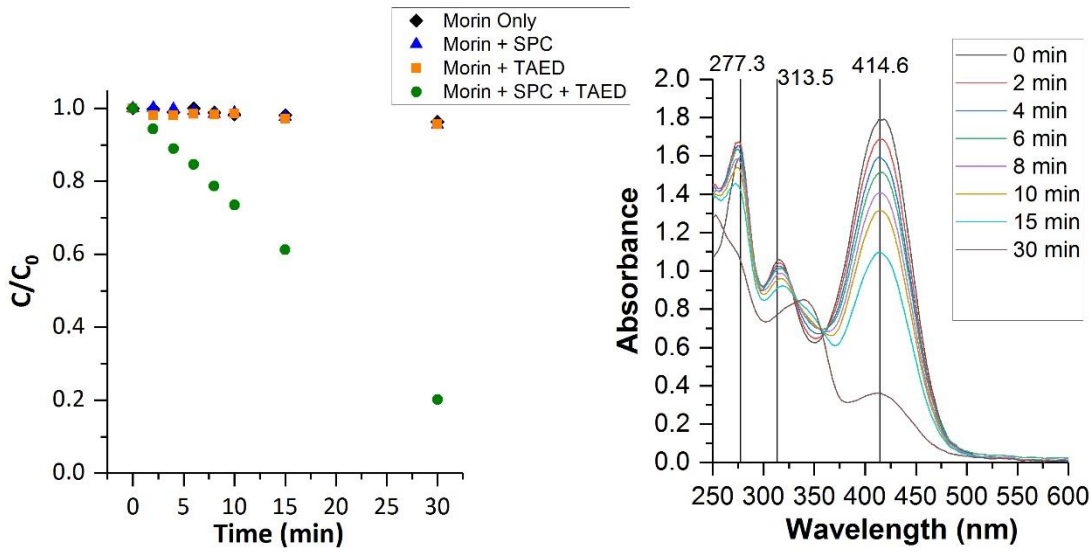

***Figure 45**: Morin blank reactions, (a) = comparison of reactions with different combinations of reagents and (b) = spectrum of morin only reaction over time. Water (90 mL), morin (0.1 mM), sodium percarbonate (SPC, 5.3 mM), TAED (1.1 mM), sodium carbonate (50 mM), 50 °C, pH = 10.5, 30 min. Average error = 7%.*

Figure 45 shows a series of blank reactions that were conducted to monitor the conversion of morin with and without the different reagents used in a typical bleaching experiment. From 0 min to 15 min, the absorbance decreases at 414 nm and increases at 350 nm. The two isosbestic points evidence that a single oxidation product has been formed.[32] From the literature, under similar conditions to those used here, benzofuranone was reported as a reaction product.[32,33,28] In the spectrum taken after 30 min of reaction, the spectrum and isosbestic points have shifted suggesting further oxidation of the benzofuranone products occurs. Colombini *et al.*[33] and Polzer *et al.*[28] postulated that the secondary oxidation products are aromatic, shown in Scheme 13.

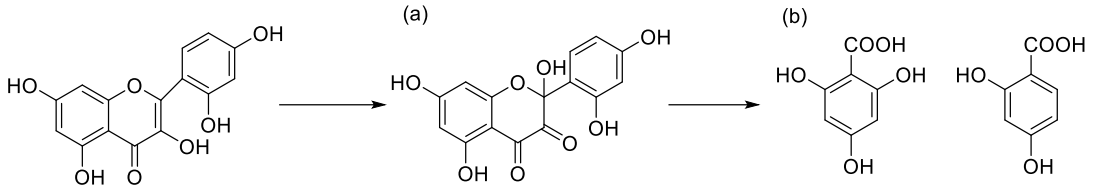

***Scheme 13**: Morin oxidation products, (a) = first oxidation product of substituted benzofuranone and (b) secondary oxidation products*

At 50 °C, with no oxidant or reagent present, no morin conversion is observed after 30 min. Addition of only TAED or sodium percarbonate, independently, was also observed to have no effect on the conversion of morin at 50 °C. Conversion of morin is only observed when both sodium percarbonate and TAED are present in solution. Oxidation of morin follows a linear trend over time and reaches a conversion of 80 % at 30 min. After 8 min of reaction, the conversion of morin is 21 %, which is acceptable for the reaction with no catalyst present for comparison of catalytic materials.

The oxidation of Morin is therefore a suitable model reaction as the observed activity is due to oxidation of the substrate. Furthermore, conversion of morin in the presence of H_2O_2 only and the associated blank reaction is minimal. The reaction with sodium percarbonate and TAED is low in the first ten minutes of the reaction.

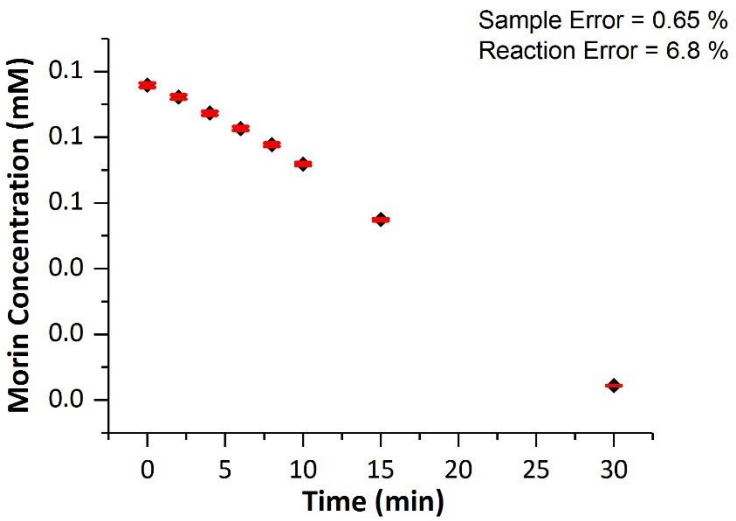

***Figure 46**: Morin oxidation error analysis for UV-Vis analysis of each sample and between reaction runs. Water (90 mL), morin (0.1 mM), sodium percarbonate (5.3 mM), TAED (1.1 mM), sodium carbonate (50 mM), 50 °C, pH = 10.5, 30 min.*

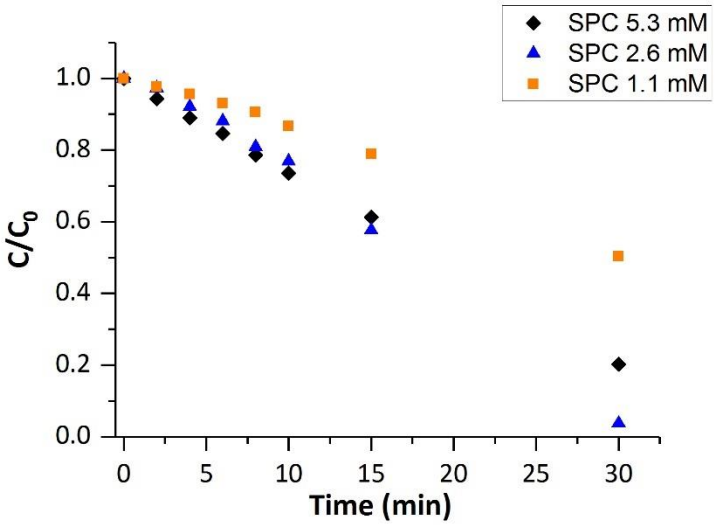

***Figure 47**: Effect of SPC concentration on morin oxidation. Water (90 mL), morin (0.1 mM), sodium percarbonate (5.3 mM), TAED (1.1 mM), sodium carbonate (50 mM), 50 °C, pH = 10.5, 30 min. Average error = 7%.*

To further investigate the relationship between the formation of peracetic acid in solution and bleaching of stains, reagent concentration and conditions were varied and the conversion of morin was quantified during the reaction. Figure 47 shows the effect of the SPC concentration on the oxidation of morin. Generally, decreasing the SPC concentration to 1.1 mM decreases the conversion of morin compared to reactions run in the presence of 5.3 or 2.6 mM SPC. At 10 min, the conversion observed with 1.1 mM of SPC was 13 %, whereas, at a concentration of 5.3 mM the conversion of morin at 10 min was 27 %. Peracetic acid formation decreases with decreasing SPC concentration as shown in Figure 24, suggesting that decreasing peracetic concentration decreases the bleaching performance. This further supports the role of peracetic acid as the active species both for morin oxidation as well as bleaching of tea stains.

As the reaction proceeds, after 15 min, there is no clear difference in the morin conversion when SPC concentration of 5.3 mM and 2.6 mM are used. After 30 min of reaction, however, the conversion is higher with 2.6 mM of sodium percarbonate. The similarities in conversion of both 5.3 mM and 2.6 mM of sodium percarbonate over time may be due to similarities in peracetic acid formation, as previously presented in Figure 24, than compared to a concentration of 1.1 mM sodium percarbonate.

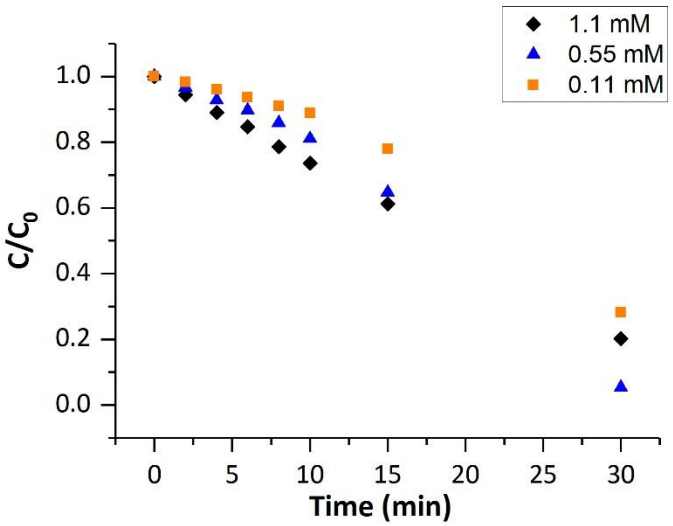

***Figure 48**: Effect of TAED concentration on morin oxidation. Water (90 mL), morin (0.1 mM), sodium percarbonate (5.3 mM), TAED (1.1 mM), sodium carbonate (50 mM), 50 °C, pH = 10.5, 30 min. Average error = 7%.*

Figure 48 shows the effect of TAED concentration on morin oxidation. Overall, decreasing the TAED concentration also decreases morin oxidation. After 10 min of reaction, the morin conversion was 27 % at 1.1 mM, 19 % at 0.55 mM and 11 % and 0.11 mM. According to the data presented in

Figure **25**, peracetic acid formation decreases linearly with TAED concentration, which was mirrored in morin oxidation reactions after 10 min. This similarly indicates that decreasing peracetic acid concentration in solution lowers the conversion of morin, which reduces the bleaching performance of a formulation.

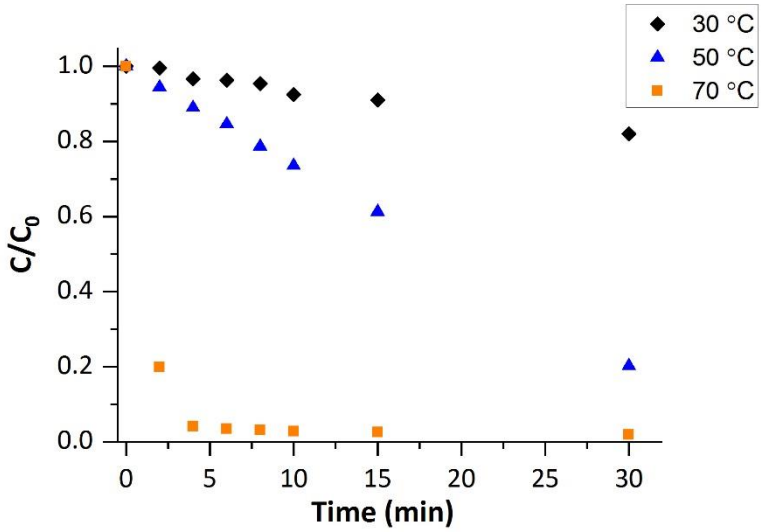

***Figure 49**: Effect of temperature on morin oxidation. Water (90 mL), morin (0.1 mM), sodium percarbonate (5.3 mM), TAED (1.1 mM), sodium carbonate (50 mM), pH = 10.5, 30 min. Average error = 7%.*

The effect of temperature on morin oxidation is shown in Figure 49. Increasing the temperature from 30 to 70 °C leads to an increase in the conversion of morin from 8 % to 97 % at 10 min. It was previously shown that both formation (Figure 26) and the rate of decomposition (Figure 33) of peracetic acid increases with temperature. Similar amounts of peracetic acid are formed at different temperatures and the decomposition has been shown to be faster at higher temperatures, as demonstrated in Figure 26 and Figure 33, which suggests the oxidation reaction is improved with temperature.

Finally, the effect of pH on morin oxidation was investigated. Changing pH may affect the absorption of morin and artificially increase the conversion of morin. J Groen and co-workers[31] showed how the maximum absorbance of morin changes with pH. Under acidic conditions, morin has no dissociated hydrogens and exhibits a maximum

absorption peak at 357 nm. When the pH is increased to 6, the peak is red shifted to 390 nm as morin is deprotonated and forms an anion. The maximum absorption then increases with pH as morin is deprotonated further as the pH is higher than the pKa values of morin, which are 5.06, 8.64 and 10.62. In the morin reaction, the pH is 10.5; therefore, it would be expected that the maximum absorption would be above 400 nm. To assess the effect of pH on morin absorption, the spectra were taken at varying pH of morin only, before addition of oxidant.

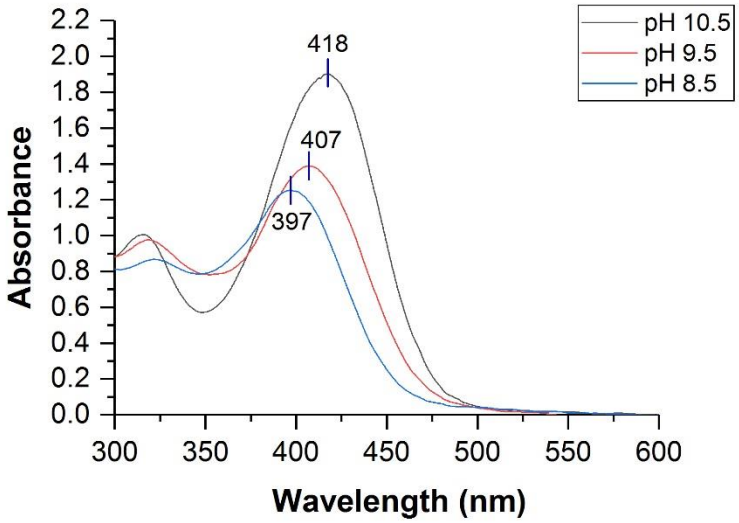

***Figure 50**: Effect of pH on morin absorption in UV-Vis, morin (0.1 mM in 50 mM sodium carbonate), pH adjusted with H_2SO_4 (0.5 M).*

Figure 50 shows how the absorption of morin changes at pH values from 8.5 to 10.5. All previous reactions were run at a pH of 10.5, which corresponds to a morin maximum absorption at 418 nm. As pH is decreased, the morin absorption is blue shifted to a lower wavelength, with a maximum absorbance of 397 nm observed at a pH of 8.5. Calibrations were completed at each pH and overall concentration of morin also appears to be lower at lower pH values. The calibration was adjusted to

account for the lower maximum absorption wavelengths at pH 8.5 and 9.5, and the morin reaction was repeated at different pH values with sodium percarbonate and TAED present.

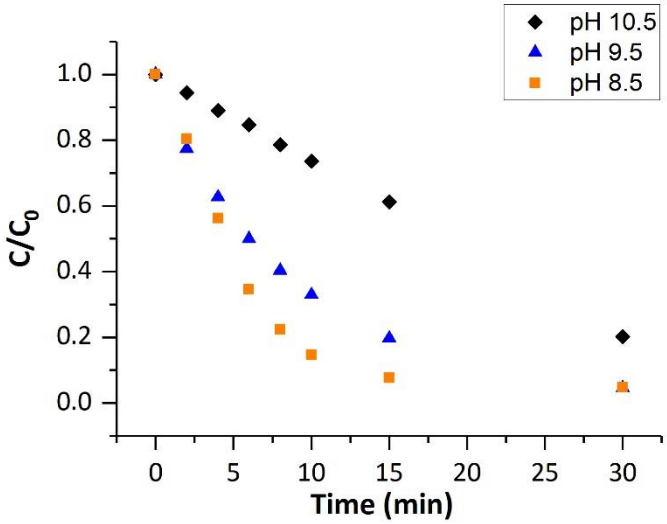

***Figure 51**: Effect of pH on morin oxidation. Water (90 mL), morin (0.1 mM), sodium percarbonate (5.3 mM), TAED (1.1 mM), sodium carbonate (50 mM), 50 °C, 30 min. Average error = 7%.*

The oxidation of morin in the presence of sodium percarbonate and TAED, at varying pH, is shown in Figure 51. As pH decreases, the oxidation of morin increases; conversion after 10 min at pH 10.5 is 27 % and 85 % at pH 8.5. As peracetic acid formation is decreased at lower pH, as it was previously shown in Figure 27, it is unexpected to observe an increase in morin oxidation at decreased pH,; however, the morin moiety will most likely have an extra protonated alcohol group compared to morin at pH 10.5 at a pH value of 8.5.[31] In addition, at pH 8.5, peracetic acid will still form the active anion species required for bleaching, as this is above the pKa of peracetic acid, which is 8.2. The perceived increase in substrate conversion as the

pH becomes more acidic may be due to the decrease in morin absorption observed at lower pH, which would artificially increase the conversion of morin observed over time. Therefore, it is not clear that morin is decomposed in the presence of sodium percarbonate and TAED, at a pH value lower than 10.5.

3.2.3 *Use of Manganese Homogeneous Catalysts for Bleaching*

The most common bleach catalysts used in modern dishwasher formulations are based on manganese. MnTACN has shown the highest bleaching performance in the literature[7,4,34,35] and is the benchmark for current catalyst bleaching performance. Mn is also used in formulations as Mn oxalate, which facilitates higher bleaching performance compared to bleaching without a catalyst but to a lesser extent than MnTACN.

As MnTACN is the benchmark for catalyst performance, the bleaching performance was assessed for both the TC and the morin oxidation reaction. Other Mn salts were also tested for comparison with MnTACN.

3.2.3.1 *Performance in Teacup Bleaching Tests*

Initially, MnTACN and a range of Mn salts were tested in the TC. 5 mg of catalyst is generally used in a formulation, with the main wash of the cycle using 3 – 5 L of water, dependant on the brand and age of the dishwasher. In 1.8 L, the volume of water present in the TC, 1.9 – 3 mg of catalyst would be present depending of the volume of water used in the main wash. The highest dose of catalyst (3 mg) was chosen to assess the bleaching performance of MnTACN in the TC.

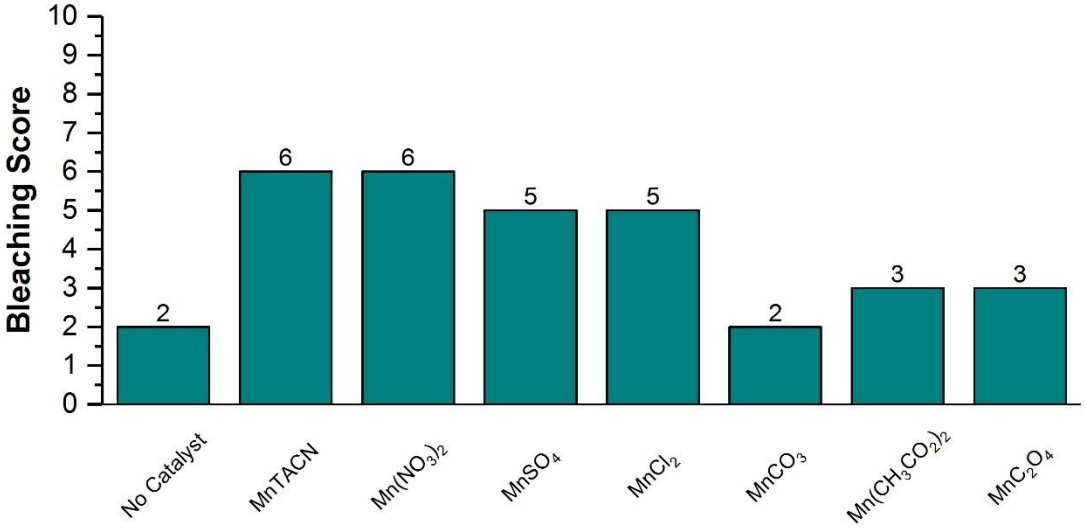

***Figure 52**: Range of manganese catalysts bleaching performance. Water (1.8 L), sodium percarbonate (5.3 mM), TAED (1.1 mM), MGDA (0.4 mM), catalyst (dose adjusted so Mn = 1 mg), 50 °C, pH = 10, 8 min. Average error = ± 1.*

Figure 52 shows the bleaching performance of MnTACN and a range of Mn salts in the TC. The dose was adjusted so that precisely 1 mg of Mn was present in each of the experiments. This was to ensure that the activity of the catalyst was not due to the counterion but rather the catalytic activity of the Mn. All the Mn catalysts that were tested showed an improvement in bleaching in comparison to the experiments with no catalyst present, apart from $MnCO_3$. MnTACN and $Mn(NO_3)_2$ exhibited the highest bleaching performance with a score of 6. Overall, Mn salts are active for bleaching but generally have a lower bleaching score than MnTACN. This may be due to the high thermodynamic and kinetic stability of MnTACN complexes[36], and the di-nuclear and high valent active species formed during the reaction.[35] In the wash solution, the ability of MnTACN to transfer oxygen to the stain, to remove the

chromophore from the cup surface, may explain the high bleaching performance exhibited.

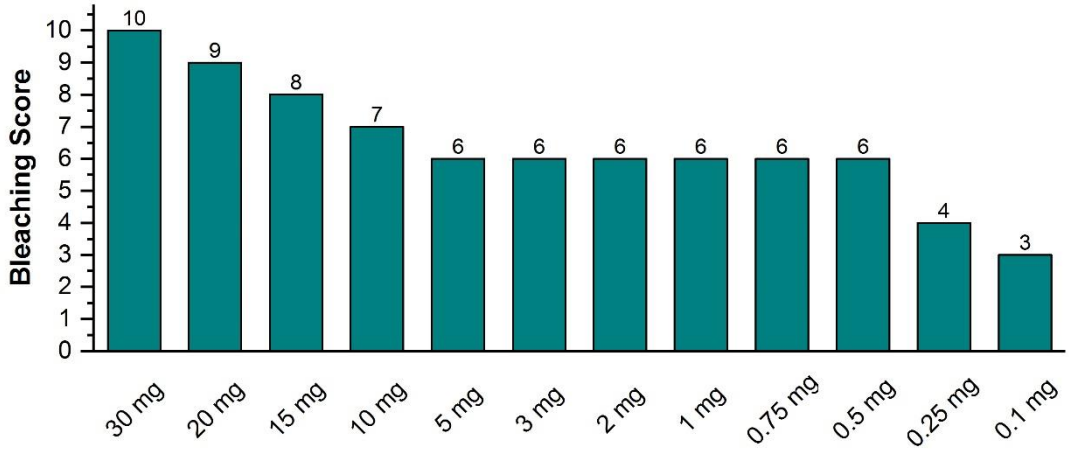

***Figure 53**: Effect of MnTACN dose on bleaching performance. Water (1.8 L), sodium percarbonate (5.3 mM), TAED (1.1 mM), MGDA (0.4 mM), MnTACN, 50 °C, pH = 10, 8 min. Average error = ± 1.*

For the data shown in Figure 52, 3 mg of MnTACN was used, the effect of varying the catalyst dose is shown in Figure 53. At the lowest dose, 0.1 mg, MnTACN still exhibits bleaching activity with a score of 3. This increases to a score of 10 with 30 mg of MnTACN present. This suggests that the reaction is catalytic and increasing the amount of catalyst present increases the oxygen transfer to the stain; however, between a catalyst dose of 0.5 mg to 5 mg, the bleaching performance remains the same, which may be because the teacup stain removal reaction not being a truly quantitative evaluation of catalytic performance, as it is a visual evaluation of the stain. Furthermore, the scores can be separated into three groups; from 1-4, 5-7 and 8-10. For a score to increase from one group into the next, there must be a significant step change in the bleaching performance. The observations indicates that, with

increasing dose there may not always be a large enough increase in stain oxidation for this to be evidenced in the visual evaluation of the final bleach score of the teacup. However, the trend observed may indicate that catalyst dose can be reduced to 0.5 mg and maintain an acceptable bleaching performance.

It must also be noted that tap water was used for these reactions, classified as soft water with a Ca concentration of 38 ppm. The soft tap water is known to increase observed bleaching scores, which was previously presented in this work in Figure 38, and can be evidenced by the fact that increasing the MGDA dose increases the bleaching score. As MGDA sequesters Ca and other metal ions in solution, the bleaching performance increases, which mirrors the effect of changing the effective water hardness on bleaching. Therefore, if water with a higher Ca content is used, the same bleach performance for lower MnTACN doses may not be observed.

3.2.3.2 *Performance for Morin Oxidation*

To further investigate the bleaching performance of MnTACN and other Mn salts, the morin model reaction was used. As MnTACN is known to be active for bleaching under aerobic conditions[32], the dose of the MnTACN used was first investigated for morin oxidation without any oxidant present.

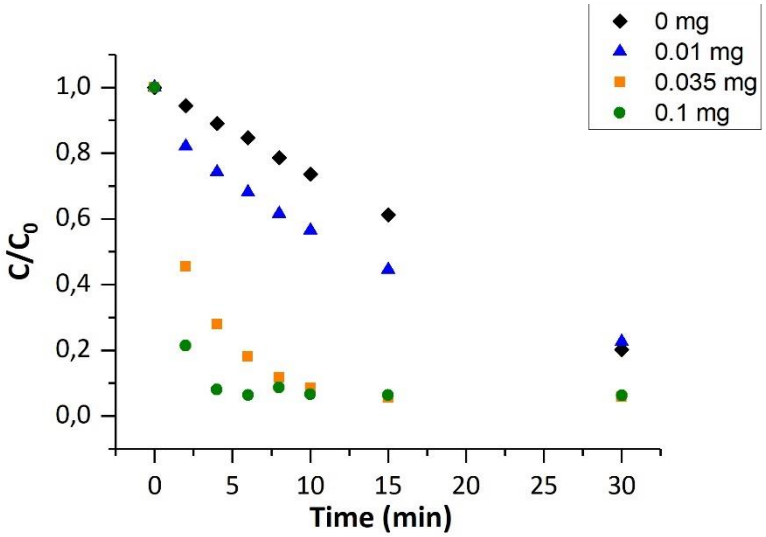

***Figure 54**: MnTACN dose effect on morin oxidation in the absence of oxidant. Water (90 mL), morin (0.1 mM), MnTACN (0.01 – 0.1 mg), sodium carbonate (50 mM), 50 °C, pH = 10.5, 30 min. Average error = 7%.*

Figure 54 shows the activity of varying MnTACN dose for the oxidation of morin with no sodium percarbonate or TAED present. Decreasing the dose of MnTACN decreases the conversion of morin. To be able to accurately distinguish between the catalytic oxidation reactions, a reaction without oxidant present must exhibit a low conversion. The conversion after 10 min of reaction over 0.1 mg MnTACN was 93 %, which decreased to 44 % when 0.01 mg of MnTACN was used. The dose could be decreased further; however, this would increase the error in the reaction from weighing out the catalyst. Therefore, a dose of 0.01 mg was chosen for Mn catalysts, and reactions with oxidant present were then carried out to investigate the bleaching performance of these catalysts.

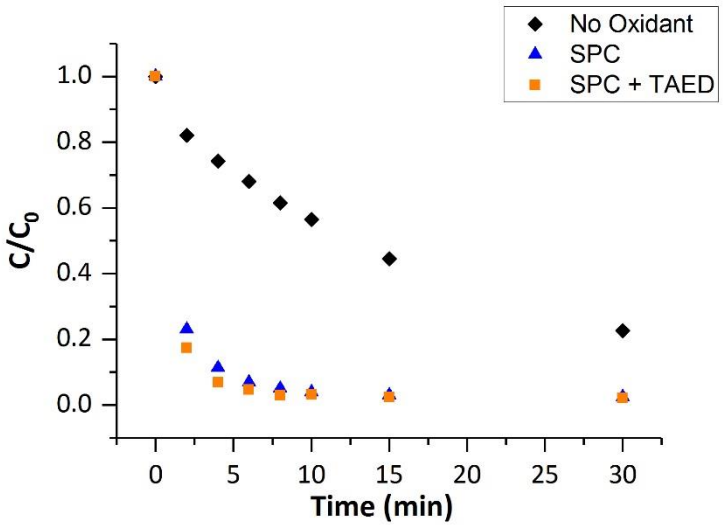

***Figure 55**: MnTACN in the presence of oxidant. Water (90 mL), morin (0.1 mM), sodium percarbonate (5.3 mM), TAED (1.1 mM), sodium carbonate (50 mM), MnTACN (0.01 mg), pH = 10.5, 50 °C, 30 min. Average error = 7%.*

The addition of sodium percarbonate and TAED to the morin oxidation reaction with 0.01 mg of MnTACN present is shown in Figure 55. Addition of sodium percarbonate only and addition of sodium percarbonate and TAED exhibit similar conversions, at 96 % and 97 %, respectively. The similarities in conversion between the reactions carried out using the various combinations of oxidants indicates that MnTACN can utilise both peracetic acid and peroxide derived active oxygen species. This is in agreement with the literature, where MnTACN can be used to oxidise a wide variety of substrates with different oxidants.[36,32] Therefore, in the applicative tea cup experiments, MnTACN can utilise the oxygen in the wash, which is present as H_2O_2 and peracetic acid, to oxidise the stains present on the surface of the tea cups.

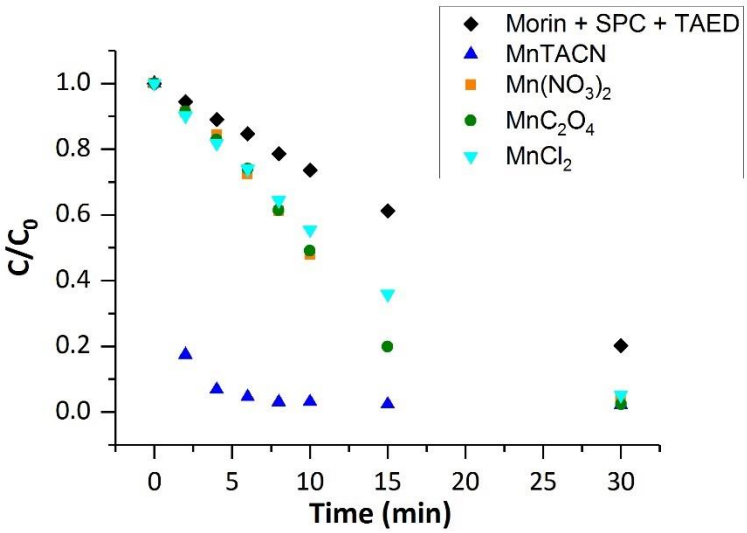

***Figure 56**: Range of Mn homogeneous catalysts for morin oxidation. Water (90 mL), morin (0.1 mM), sodium percarbonate (5.3 mM), TAED (1.1 mM), sodium carbonate (50 mM), Mn catalyst (0.01 mg), pH = 10.5, 50 °C, 30 min. Average error = 7%.*

For comparison $Mn(NO_3)_2$, MnC_2O_4 and $MnCl_2$ were also added to the morin reaction in the presence of sodium percarbonate and TAED (Figure 56). All three of the Mn salts exhibited similar activities for morin oxidation. $Mn(NO_3)_2$ and MnC_2O_2 exhibit slightly higher conversion after 10 min of 52 % and 51 % respectively, compared to 45 % for $MnCl_2$. The difference between morin oxidation activities of the Mn salts is not as substantial as the differences observed in the TC, previously shown in Figure 52. The difference observed may be due to morin being in solution and the tea stain being heterogeneous in the TC; this therefore suggests that the mechanism for bleaching may be different in the TC and the morin oxidation test, which could be due to a number of different factors. For example, in the morin oxidation reaction reactions, the substrate is homogeneous. Furthermore, in the morin oxidation reaction, there is a larger excess of H_2O_2 than in the teacup reaction, which may

suggest that the Mn salts are more effective catalysts in the presence of peracetic acid; the MnTACN is far more efficient at using H_2O_2 as an oxidant. The results shown in Figure 56 still show, however, that MnTACN is the catalyst with the highest bleaching performance, and the morin oxidation model can be considered a suitable method of identifying potential catalysts for applications in automatic dishwashing.

3.3 *Discussion*

Investigation into the formation of peracetic acid and the conversion of TAED, presented in Figure 24 to Figure 35, was carried out with the aim of identifying which step of the bleaching process would benefit from the addition of a catalyst. Formation of peracetic acid, the active bleaching species, is the first step followed by oxidation of the stain. Generally peracetic acid is synthesised commercially through reaction of H_2O_2 and acetic acid with H_2SO_4 as a catalyst.[37] In bleaching, peracetic acid is instead formed from the perhydrolysis of TAED, as shown in Scheme 14.[14]

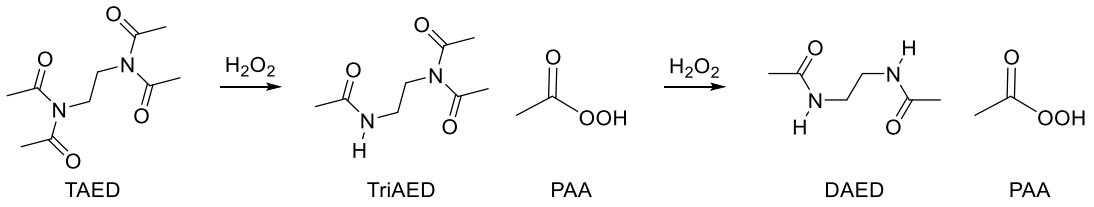

***Scheme 14**: Perhydrolysis of TAED with H_2O_2 to form PAA (peracetic acid).*

For every mole of TAED, a theoretical maximum of 2 moles of peracetic acid is formed. TAED can also undergo hydrolysis to form acetic acid; however, under alkaline conditions, H_2O_2 readily dissociates to form HOO^- (perhydroxyl anion).[38] As the perhydroxyl anion is a stronger nucleophile than HO^- (hydroxyl anion), the rate of TAED hydrolysis should be negligible under alkaline conditions.[39]

The effect of different reagent concentrations and the reaction conditions on the yield of peracetic acid was investigated in Figure 24 to Figure 27. In Figure 28 to Figure 32 DAED formation as well as the conversion of TAED was quantified. Initially the

sodium percarbonate concentration was lowered from 5.3 mM to 1.1 mM, which aligns with the concentrations used in standard wash conditions. Figure 24 shows the increase in formation of peracetic acid, which stabilises at 2.6 mM.

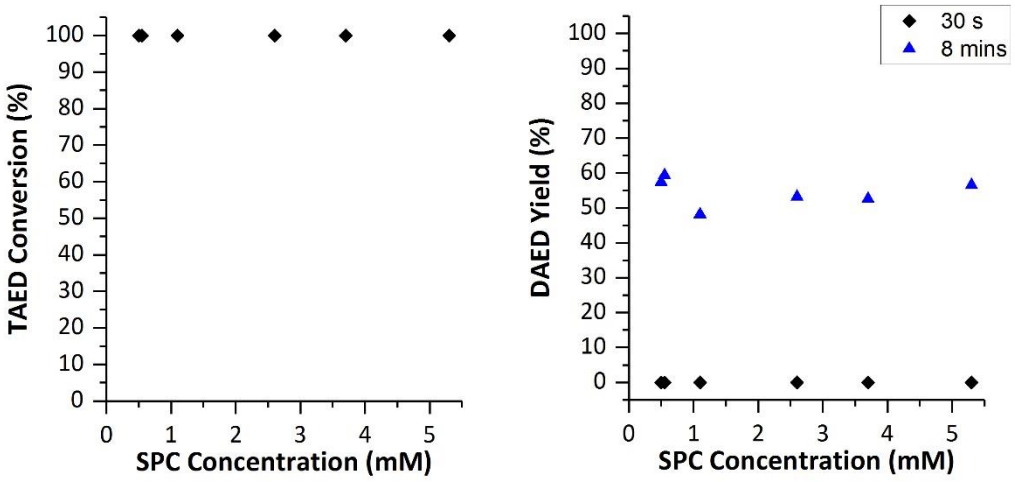

Figure 29 shows that the TAED conversion does not decrease with lower sodium percarbonate concentration, and neither does the yield of DAED. Figure 36 shows increasing the concentration of sodium percarbonate from 2.6 to 5.3 mM has only a minor effect on the overall bleaching performance in both the TC and the morin oxidation test, as exhibited in Figure 47.

Under the reaction conditions examined in this work, where a sodium percarbonate concentration of 5.3 mM is used, H_2O_2 is in a significant excess (7.3 times) to TAED. The excess H_2O_2 drives the perhydrolysis reaction to completion and the excess sodium percarbonate ensures an alkaline pH during the wash.[40] At a SPC to TAED ratio of 0.5, H_2O_2 is in stoichiometric amounts to TAED. Given that 2 moles of H_2O_2 are needed to form 2 moles of peracetic acid from 1 mole of TAED, stoichiometric amounts of H_2O_2 limits the amount of peracetic acid that can be formed. The results in Figure 36 show that the lower the quantity of peracetic acid formed, the lower

bleaching performance observed. This is demonstrated in both the tea cup and morin oxidation tests as found in Figure 47 and Figure 48. Even at lower sodium percarbonate concentrations, however, peracetic acid formation is facile and TAED readily converted.

As formation of peracetic acid is directly related to the concentration of TAED available in solution, the expected linear trend of formation of peracetic acid with increasing TAED concentration is observed in

Figure **25**. At a TAED concentration of 0.055 mM, no peracetic acid formation is observed. DAED formation was only recorded at the end of the reaction and not in the first 30 s of the reaction. TAED initially forms TriAED, which is less reactive due to the loss of one electron withdrawing acetyl group compared to the parent TAED.[14] The DAED concentration measured over time suggests that TAED is converted quickly in the first 30 s of the reaction forming TriAED, which then reacts at a slower rate to form further peracetic acid and DAED. DAED is unreactive to further perhydrolysis or hydrolysis reactions, due to resonance stabilisation of the amide bond. Overall, the formation of peracetic acid is facile, even at low TAED concentrations. Generally, lower concentrations of peracetic acid lead to lower bleaching performances in the tea cup and morin oxidation tests, as shown in Figure 36 and Figure 48.

Temperature and pH have large effects on the yield of peracetic acid. Temperature increases peracetic acid formation up to 50 °C, however, the yield decreases from 50 to 70 °C, as shown in Figure 26. At all temperatures below 50 °C the amount of peracetic acid formed after 30 s is reduced; however, the TAED conversion only decreases at the lowest temperature, 15 °C. This may be explained by the

competition between the hydrolysis reaction forming acetic acid, which still occurs at lower temperatures, and the perhydrolysis reaction that is slowed with decreasing temperature. In addition, the decrease observed at higher temperatures could be accounted for by the increase in decomposition of peracetic acid as per Figure 33.

Initial rates of the conversion of H_2O_2 and formation of peracetic acid were calculated and the results shown in Table 5. The rates decrease with both temperature and pH indicating that perhydrolysis reaction is favoured with temperatures of 30 °C and higher, and that an alkaline pH is required. Davies *et al.*[14] calculated the rate constant for the perhydrolysis and hydrolysis of TAED under similar conditions, it was found that the perhydroylsis of TAED, and the TriAED intermediate, was second order with the rate constant the same order of magnitude as calculated for peracetic acid in Table 5. The same trend was described with decreasing temperature and pH reducing the rates of TriAED perhydrolysis. Overall, the calculated rates and rate constants are not accurate as peracetic acid formation was only measure at two points, 0s and 30s, therefore, the order of reaction could not be accurately determined from a ln plot of change in concentration vs time. Furthermore, initial rates were calculated for the first 30s of the reaction when TAED conversion was above 85 %

As previously shown in Figure 37, the decrease in peracetic acid formation observed at temperatures above 50 °C does not lead to a decrease in bleach performance. Figure 33 shows that peracetic acid and H_2O_2 decomposition is increased at temperatures above 50 °C. As shown by K.Dithmar *et al.*[13], the increase in peracetic acid decomposition may lead to an increase in active species in the reaction that aid bleaching. Again, peracetic acid formation is facile at all temperatures, as shown by

Figure 26. Figures 13 and 22 show that even when similar amounts of peracetic acid are being formed in solution, bleaching performance increases with temperature. Which indicates that the oxidation step of the reaction is improved by an increase in temperature, as also reported in literature.[40] Long *et al.* found that 70 °C was the ideal temperature for improving the whiteness of cotton using a TAED/H_2O_2/$NaHCO_3$ system for bleaching, which also exhibits the importance of temperature for bleaching. The decrease in bleaching performance at lower temperatures adds scope for a catalyst to be added to improve bleaching and oxidation of surface stains.

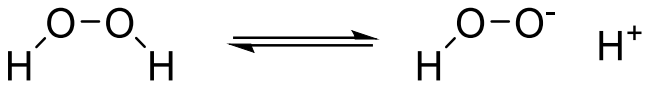

***Scheme 15**: Dissociation of H_2O_2 to perhydroxyl anion under alkaline pH*

As shown in Figure 27, under neutral and acidic conditions, no peracetic acid formation was observed. The trend is supported by the fact that TAED conversion is reduced at a lower pH, as shown in Figure 32. At pH 8 and below, H_2O_2 will not readily dissociate into the perhydroxyl anion that is required for perhydrolysis.[38] A reduction in the rate of perhydrolysis at near neutral and acidic pH was also observed by Xu *et al.*.[12] The perhydroxyl anion alone, however, cannot be responsible for all the activity observed, as some bleaching performance is still observed at pH 6 in the TC, as shown in Figure 37. Comparison of the bleaching performance observed under both acidic and alkaline conditions suggests that H_2O_2 is active for bleaching over a range of pH, with the perhydroxyl anion being the active species at a basic pH. Decomposition of

peracetic acid increases when the pH approaches the pKa of peracetic acid.[41] This indicates that peracetic acid formed at a neutral pH will be more stable than if formed at a more alkaline pH and the more stable peracetic acid increases bleaching,[12] however, from the large error associated with the visual evaluation scoring of the TCs, it is not possible to justify such conclusions.

The standard wash conditions and reagent concentrations currently used in industry wide testing are pH 9 – 10, 50 °C, sodium percarbonate : TAED ratio of *ca.* 5 and a wash time of 8 min. As shown in Figure 24 to Figure 32, under these conditions, the conversion of TAED and formation of peracetic acid is facile. Even at very mild conditions, where the temperature is reduced to 30 °C or low quantities of sodium percarbonate are used, full TAED conversion is still observed. Therefore, there is little need to develop a catalyst to improve the formation of peracetic acid. A catalyst is, however, needed to improve the oxidation step required to bleach the stain, which efficiently utilises the peracetic acid formed in the reaction.

Another key reagent deployed in dishwasher formulations is the builder. For this formulation, methylglycinediacetic acid (MGDA) is used. Builders are added to chelate any metal ions in solution, which can decompose peracetic acid and therefore decrease bleaching performance.[42] Figure 35 demonstrates that the addition of MGDA to peracetic acid in solution decreased the decomposition of peracetic acid over time in deionised water. Other builders have been shown to have a similar effect on limiting peracetic acid decomposition at a neutral pH;[42] however, it has also been reported that acetic acid in solution can hinder the chelating ability of a builder.[16] MGDA is a successful builder in these experiments as it improves

bleaching activity with increased dose, Figure 38. A low dose of MGDA was used in the TCs that followed this study, to ensure bleaching performance was due to the bleaching system being examined and not merely a function of excess builder in the reaction.

The TC has a high error associated with the visual evaluation of the bleached tea stain; therefore, a model reaction was developed. A key requirement of the model is that the conversion observed is due to the occurrence of an oxidation reaction. Catechol has been observed to polymerise under a variety of conditions and form a mixture of different linear products and oligermers.[23,4] A series of reactions were conducted with catechol in various combinations with sodium percarbonate and TAED only. As shown in Table 6, at pH 9 catechol was consumed despite their being no TAED or oxidant present. Figure 43 shows the further investigation into the effect of pH on catechol conversion with no oxidant present and showed that increasing pH lead to an increase in catechol decomposition. No products were readily identified from HPLC and GC – MS of post reaction solutions, which suggested that high molecular weight products with high boiling points were formed. The results indicate that, under the alkaline conditions, polymerisation occurred, and so catechol was not considered to be a suitable model substrate for this study.

Morin has been used as a model compound for bleaching and undergoes oxidation under alkaline conditions.[5,33] The conversion of morin with no catalyst present (Figure 45), shows that the decomposition of morin proceeds *via* an oxidation pathway, leading to the formation of benzofuranone, which itself can undergo subsequent oxidation.[43] This is evidenced by the two isosbestic points in the

absorption spectra that remained unchanged for the first 15 min of the reaction, before a shift of these points after 30 min suggests the further oxidation to single ringed products, as per Scheme 16.[32] The conversion of morin followed similar trends as the TCs under varying conditions and differing reagent concentrations, which are summarised in Figure 47 to Figure 51. These experiments showed that the morin reaction passed the three requirements needed to be a suitable bleach model reaction; firstly, the reaction proceeding *via* oxidative chemistry, secondly, the reactivity aligning with the TC, and finally, the data being reproducible with a low error.

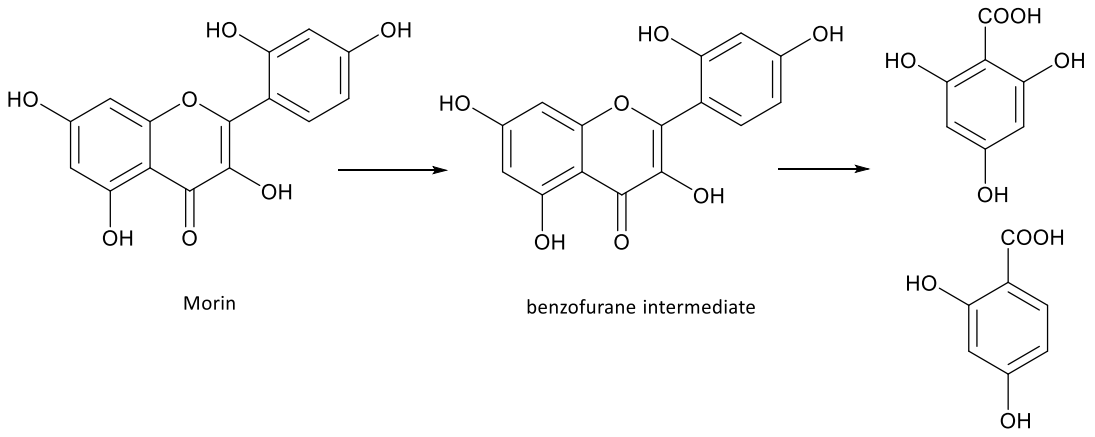

***Scheme 16**: Reaction pathway for morin oxidation.*

The reaction was then used to also quantify bleaching over a series of Mn catalysts, to see whether the performance aligned with the activity exhibited in corresponding the TCs (Figure 56). The activity of the Mn catalysts followed the same trend as the TCs, which further indicates that the morin oxidation reaction is a suitable bleach model system. Comparison of MnTACN with a range of Mn salts for both the tea cup and morin oxidation reactions, as per Figure 52 and Figure 56, show that MnTACN is

a more effective bleach catalysts than free Mn salts. The bleaching of morin solutions by MnTACN has previously been discussed in a thesis by Topalovic.[32] MnTACN forms highly stable complexes that allow the Mn centres to reversibly change oxidation states without precipitation of Mn into solution. Conversely, free Mn salts often precipitate out during oxidation reactions, forming inactive solid oxides. This difference in stability, and the redox potential of MnTACN, shows that MnTACN is a more effective bleaching catalyst compared to cheaper, more readily available Mn salts such as Mn oxalate.

Investigation of the use of MnTACN for morin oxidation indicates that MnTACN can utilize peracetic acid, H_2O_2 and O_2 as an oxidant, Figure 55. Topalovic[32] investigated the mechanism of bleaching of morin with MnTACN as a catalyst using O_2 and H_2O_2 as the oxidant, and found that MnTACN was highly active using either oxidant. Investigation into the mechanism with H_2O_2 had similar findings to previous studies by Gilbert *et al.*[35] where MnTACN forms high valent di-nuclear species that bind to the substrate. For the investigation into MnTACN using O_2 for the decomposition of morin, Topalovic[32] found that MnTACN utilises both superoxide (O_2^-) and H_2O_2 formed by O_2^- on reaction with the substrate, as is summarised in Scheme 17. This aerobic reaction is pH dependant and exhibits faster rates above a pH of 10.

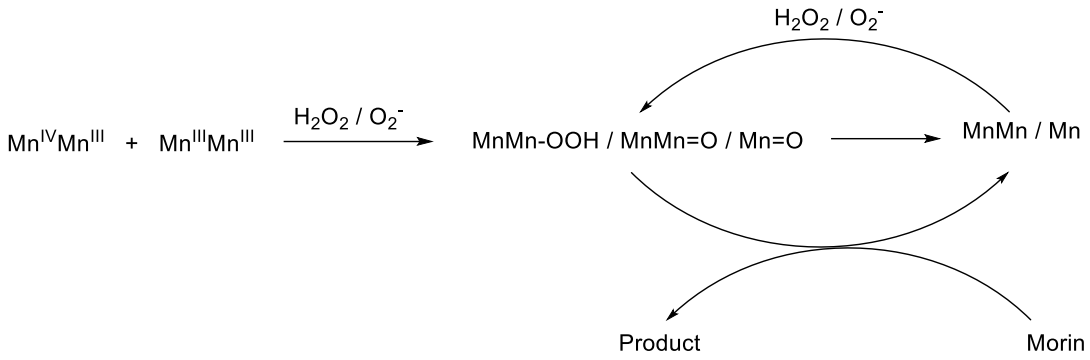

***Scheme 17**: Simplified MnTACN morin oxidation mechanism in the presence of H_2O_2 or O_2 as proposed by Topalovic.*[32]

Overall, from the literature it has been shown that MnTACN exhibits a high bleach performance, due to the ability of the complex to form stable di-nuclear complexes that can undergo reversible redox reactions without precipitation of Mn. For TC reaction and for morin oxidation, MnTACN has been shown to have a higher activity than Mn salts, which maybe explained by the stable di-nuclear species discussed by Topalovic.[32] As currently this has been the only commercialised bleach catalyst for consumer products, this is a suitable benchmark to assess the bleaching performance when developing heterogeneous catalysts.

3.4 *References*

1 G. O. Bianchetti, C. L. Devlin and K. R. Seddon, *RSC Adv.*, 2015, **5**, 65365–65384.

2 IKW, *sofw Journal, Home Pers. Care Ingredients Formul.*, 2016, 37–38.

3 Y. Tanizawa, T. Abe and K. Yamada, *Food Chem.*, 2007, **103**, 1–7.

4 A. Sorokin, L. Fraisse, A. Rabion and B. Meunier, *J. Mol. Catal. A Chem.*, 1997, **117**, 103–114.

5 T. Topalovic, V. A. Nierstrasz and M. M. C. G. Warmoeskerken, *Fibers Polym.*, 2010, **11**, 72–78.

6 R. Hage and A. Lienke, *Angew. Chemie - Int. Ed.*, 2005, **45**, 206–222.

7 European Patent Office, EP 0 458 397 B1, 1991.

8 U. Pinkernell, S. Effkemann and U. Karst, *Anal. Chem.*, 1997, **69**, 3623–3627.

9 N. A. Stephenson and A. T. Bell, *Anal. Bioanal. Chem.*, 2005, **381**, 1289–1293.

10 G. S. Cavallini, S. X. de Campos, J. B. de Souza and C. M. de S. Vidal, *Int. J. Environ. Anal. Chem.*, 2013, **93**, 906–918.

11 U. Zoller, *Handbook Of Detergents, Part E: Applications*, M. Dekker, 2008.

12 C. Xu, X. Long, J. Du and S. Fu, *Carbohydr. Polym.*, 2013, **92**, 249–253.

13 United States Patent Office, 2,898,181, 1959.

14 D. M. Davies and M. E. Deary, *J. Chem. Soc. Perkin Trans. 2*, 1991, 1549.

15 K. M. Thompson, W. P. Griffith and M. Spiro, *Faraday Trans*, 1993, **89**, 4035–4043.

16 X. Zhao, K. Cheng, J. Hao and D. Liu, *J. Mol. Catal. A Chem.*, 2008, **284**, 58–68.

17 United States Patent Office, US8048838B2, 2011.

18 D. Kołodyńska, *Expand. Issues Desalin.*, 2011, 342–343.

19 K. M. Thompson, W. P. Griffith and M. Spiro, *J. Chem. Soc. Chem. Commun.*, 1992, 1600–1601.

20 K. Yamada, T. Abe and Y. Tanizawa, *Food Chem.*, 2007, **103**, 8–14.

21 A. B. Sorokin and E. V. Kudrik, *Catal. Today*, 2011, **159**, 37–46.

22 L. F. Liotta, M. Gruttadauria, G. Di Carlo, G. Perrini and V. Librando, *J. Hazard. Mater.*, 2009, **162**, 588–606.

23 E. A. Pillar, R. Zhou and M. I. Guzman, *J. Phys. Chem. A*, 2015, **119**, 10349–10359.

24 P. M. Mader, *J. Am. Chem. Soc.*, 1958, **80**, 2634–2639.

25 F. Haber and J. Weiss, *The Catalytic Decom position o f Hydrogen Peroxide by Iron Salts*, 1932.

26 D. . Broughton, R. . Wentworth and E. Laing, *J. Am. Chem. Soc.*, 1947, **69**, 744–

747.

27 H. Gulley-Stahl, P. A. Hogan, W. L. Schmidt, S. J. Wall, A. Buhrlage and H. A. Bullen, *Environ. Sci. Technol.*, 2010, **44**, 4116–4121.

28 F. Polzer, S. Wunder, Y. Lu and M. Ballauff, *J. Catal.*, 2012, **289**, 80–87.

29 M. S. Xaba and R. Meijboom, *Appl. Surf. Sci.*, 2017, **423**, 53–62.

30 Q. Zhou, H. Zhang, Y. Wang and X. Zhou, *Spectrochim. Acta Part A Mol. Biomol. Spectrosc.*, 2009, **72**, 110–114.

31 S. Höfener, P. C. Kooijman, J. Groen, F. Ariese and L. Visscher, *Phys. Chem. Chem. Phys.*, 2013, **15**, 12572–12581.

32 T. Topalovic, PhD Thesis, University of Twente, the Netherlands, 2007.

33 M. P. Colombini, A. Andreotti, C. Baraldi, I. Degano and J. J. Łucejko, *Microchem. J.*, 2007, **85**, 174–182.

34 B. C. Gilbert, J. R. L. Smith, M. S. Newton, J. Oakes and R. P. Prats, *Org. Biomol. Chem.*, 2003, **1**, 1568–1577.

35 B. C. Gilbert, J. R. L. Smith, A. Mairata i Payeras and J. Oakes, *Org. Biomol. Chem.*, 2004, **2**, 1176–1180.

36 A. Murphy, A. Pace and T. D. P. Stack, *Org. Lett.*, 2004, **6**, 3119–3122.

37 X. Zhao, T. Zhang, Y. Zhou and D. Liu, *J. Mol. Catal. A Chem.*, 2007, **271**, 246–252.

38 S. H. Zeronian and M. K. Inglesby, *Cellulose*, 1995, **2**, 265–272.

39 J. E. McIsaac, L. R. Subbaraman, J. Subbaraman, H. A. Mulhausen and E. J. Behrman, *J. Org. Chem.*, 1972, **37**, 1037–1041.

40 X. Long, C. Xu, J. Du and S. Fu, *Carbohydr. Polym.*, 2013, **95**, 107–113.

41 R. E. Ball, J. O. Edwards, M. L. Haggett and P. Jones, *J. Am. Chem. Soc.*, 1967, **89**, 2331–2333.

42 Z. Yuan, Y. Ni and A. R. van Heiningen, *Can. J. Chem. Eng.*, 1997, **75**, 42.

43 M. P. Colombini, A. Andreotti, C. Baraldi, I. Degano and J. J. Łucejko, *Microchem. J.*, 2007, **85**, 174–182.

4 Chapter 4: Development of New Heterogeneous Catalysts for Bleaching in Automatic Dishwashing

4.1 *Introduction*

Current catalyst technology employed in automatic dishwashing relies on homogeneous "one-shot" catalysts, as previously discussed in Chapter 1, Section 1.3, which are added to the formula and lost at the end of each wash cycle. MnTACN is a highly effective catalyst and is the current highest performing catalyst used in dishwasher formulations;[1] however, the catalyst is expensive and significantly increases the overall cost of a tablet. Cheaper alternatives to homogeneous catalysts may be found in metal oxide heterogeneous catalysts. If active, further development in dishwashing technology could lead to these catalysts also being reusable and not lost at the end of each wash cycle, which would reduce the overall cost of the formulation. Active heterogeneous catalyst could be supported on a part of the dishwasher or added by the consumer as a separate product which is left in the dishwasher for a certain number of washes.

In the literature, heterogeneous catalysts have been trialled and compared to the known active homogeneous catalysts. The range of investigated heterogeneous catalysts, include; solid supported homogeneous catalysts[2], the addition of ligands to a heterogeneous catalyst[3], or generating POMs to create semi-heterogeneous catalysts with known active metals.[4] These approaches remain expensive, as the homogeneous catalyst is have a complex synthesis methods and are often difficult to scale up for production.

Metal oxide heterogeneous catalysts could therefore be a viable alternative. Previous work involving such materials has focused on the bleaching and removal of waste products from wastewater streams.[5] A wide range of catalysts have been tested with the most active typically comprising of precious metal nanoparticles, such as Au, Pd or Pt, supported on a metal oxide.[6] While methods to synthesise these catalysts can be facile, the expense and hazardous nature of these materials means that these catalysts would not be suitable for use in automatic dishwashing. Alternatively, first row transition metals are generally cheaper, more abundant, and less hazardous than precious metals. Developing materials from these metals may therefore be the solution to the production of cheap and easy to synthesise catalysts for addition in dishwasher formulations.

In Chapter 3, it was shown that the catalyst is not required to synthesise peracetic acid *in situ* but is required to aid bleaching, through utilisation of the active species in solution. One approach may be to induce radical generation, or disproportionation of peracetic acid and H_2O_2. Fe and Cu catalysts are both known to react with H_2O_2 to produce radical species,[7,8] known as the Fenton reaction; Cu(I) species in homogeneous catalysis have also been shown to be active for stain removal and bleaching. Copper oxide nanoparticles were found to be active for removal of organic pollutants[9] and that the nanoparticles formed hydroxy radicals which were active for the oxidation reaction. Therefore, these materials may be potential bleach catalysts. For a support material, ZrO_2 has been shown to stabilise super oxide and radical species, suggesting that it could be a suitable support material for a heterogeneous catalyst for dishwashing.[10]

In addition, Mn is already widely used in the bleaching industry, predominantly in a homogeneous form. MnTACN has also been tested in heterogeneous forms supported on heteropolyacids[2] and clay minerals[11] where the MnTACN was still active for bleach reactions after addition to the support, however, these materials have never been tested in a dishwasher. For the above reasons Fe, Cu, Mn and Zn oxides supported on ZrO_2 catalysts were chosen as potential bleach catalysts and trialled for tea stain bleaching.

A suitable synthesis method would be required that could easily be scaled up and produce the required catalysts. Sol-gel methods are often simple preparative methods to produce catalysts.[12] Only the precursors, precipitating agent and ethanol are required, and the process is a simple method to precipitate the desired metal oxalates, followed by .a heat treatment in flowing air which produces the metal oxides. This method is suitable for the requirements for catalyst preparation for dishwasher formulation.

The aim of this work is to develop a facile method to produce metal oxide catalysts consisting of cheap and abundant, first row transition metals, that is active for bleaching in automatic dishwashing. As discussed it is very important that the catalysts used are non-hazardous, which limits the range of metals that can be investigated for use in a dishwasher tablet The catalysts prepared herein were tested for tea stain bleaching according to industry standard testing methods.[13] The aim of the screening is to identify heterogeneous catalysts that are active for bleaching and have not been identified previously in the literature. The final aim is to use the morin

model reaction, developed in Chapter 3, to understand further the physical properties of the catalyst that lead to bleach activity.

4.2 *Results*

4.2.1 *Initial Screening of Possible Heterogeneous Catalysts*

The oxalate gel method was used to prepare the catalysts, as the method is simple and can easily be scaled up. The oxalate gel method has been shown to produce catalysts with high metal surface areas with well dispersed metal species and strong interactions between the metals in the catalyst.[14,15] Metal nitrates were dissolved in ethanol and an excess of oxalic acid was added to precipitate out the desired metal oxalates. Ethanol was chosen as a solvent following a study by Deng and co-workers on the effect of solvent on catalyst properties for the oxalate gel method.[16] The authors showed that copper catalysts prepared using ethanol exhibited the largest surface area and highest catalytic activity compared to using deionised water, DMF and diethylene glycol. In addition, the catalyst synthesised with ethanol produced uniform catalyst particle sizes. Following precipitation, the metal oxalates were then filtered and dried for 16 hours at 110 °C. The synthesised metal oxalates were then calcined at 550 °C for 2 hours with a ramp rate of 10 °C/min. This calcination temperature was chosen as the literature shows this leads to a catalyst structure with well dispersed metal particles on the catalyst surface and in the lattice.[17]

Guidelines were provided by Reckitt Benckiser on the choice of appropriate metals to test for a heterogeneous bleach catalyst. The metals must be relatively low cost and abundant; In addition, manufacturing and consumer safety had to be considered, with metals chosen exhibiting non-toxicity and minimal environmental impact. From these considerations copper, iron and manganese on a zirconia support material were deemed suitable and in line with the guidelines provided by the industrial

sponsor Reckitt Benckiser. Previous work carried out in the group by Orlowski *et al.*[18] using Cu/ZrO_2 catalysts prepared by the oxalate gel method showed molar amounts of 10 - 50 % Cu were active for hydrogenation of levulinic acid. Therefore, a similar molar ratio range was investigated for catalytic bleaching. Cu, CuO and Cu complexes all supported on SBA-15 were active for the oxidation of benzyl alcohol, with H_2O_2 as an oxidant, in the work by Cruz *et al*.[19] Their results indicate that Cu(II)-[(triethoxysilyl)propyl]imidazolium complex supported on SBA-15 was the most active for oxidation of benzyl alcohol with H_2O_2 which is required for bleaching. Manganese, is already utilised in bleaching formulations in a homogeneous form[1], whilst copper and iron are known oxidation catalysts in the presence of H_2O_2.[7,8] To ensure the stability of potential active species, zirconia was chosen as the support because Anpo *et al.*[10] demonstrated the generation and stabilisation of superoxide species on zirconia.

Following on from the preparation, a series of heterogeneous bleach catalysts were screened using the tea cup (TC) beaker method described in Chapter 2, Section 1.5.3. This quick screening method was used to identify potential active catalysts for bleaching heterogeneous stains by assessing the bleach performance on tea stains.

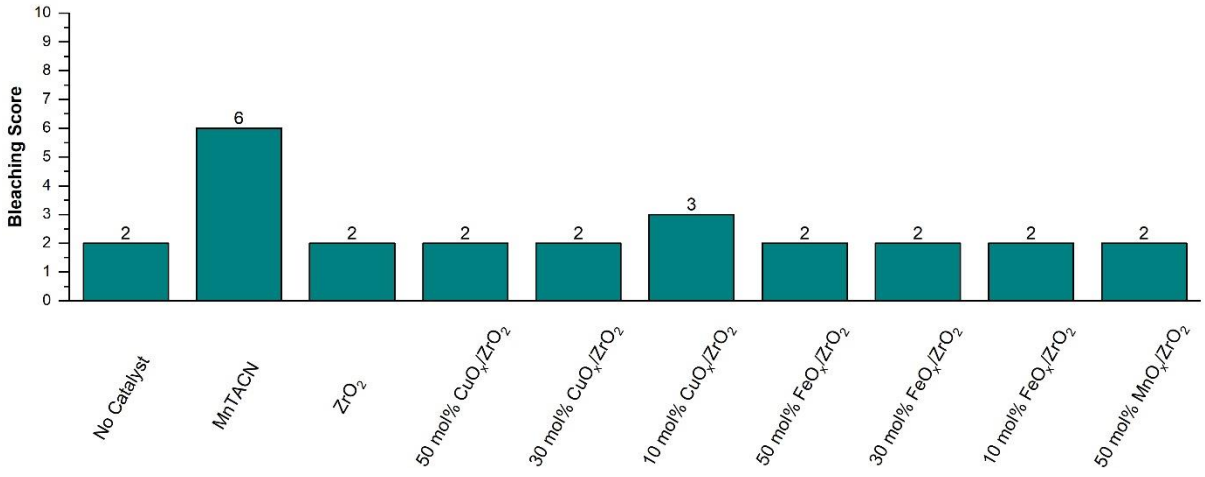

***Figure 57**: Initial screening of potential heterogeneous catalysts. Water (1.8L), sodium percarbonate (5.3 mM), TAED (1.1 mM), MGDA (0.4 mM), catalyst (3 mg), 50 °C, 8 mins, pH = 10, water hardness = 5 °dH. Average error = ± 1.*

Figure 57 shows that, without a catalyst, the sodium percarbonate and TAED system scores a 2, and the addition of MnTACN increases the score to a 6. ZrO_2 without added Cu, Fe or Mn oxide, does not improve bleaching performance, indicating that the support material is inactive for bleaching. From experiments employing Cu-based catalysts it is evident that Cu is active for bleaching, as the bleaching score is increased to 3 in the presence of a 10 mol% CuO_x/ZrO_2 catalyst. In this evaluation of bleach activity, no bleaching was exhibited by any of the iron and manganese containing catalysts. Given that the Cu containing material had exhibited some activity, it was selected as the focal point for further study.

A bleaching score of 3 is low in comparison to the MnTACN catalyst, which consistently exhibits a score of 6. The 50 mol% CuO_x/ZrO_2 exhibits a bleach score of 2, which increases to 3 when the copper concentration is decreased to 10 mol%. Therefore, further experiments were subsequently conducted, with varied loadings

of Cu to establish the optimum composition. The results of this are shown in Figure 58.

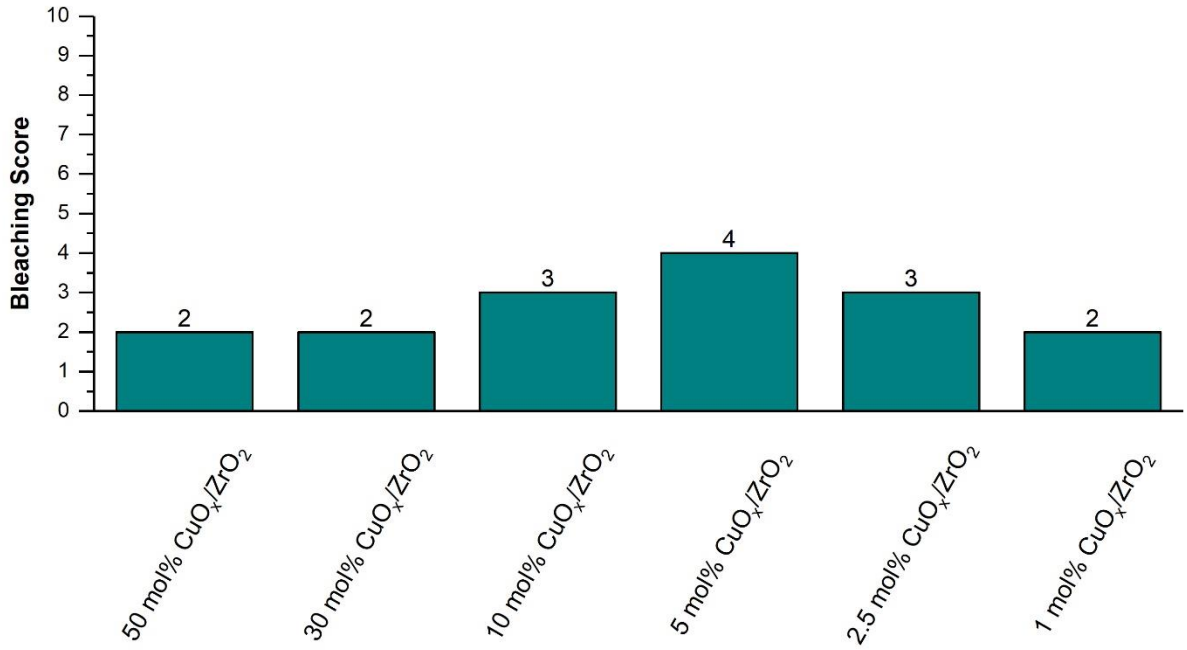

***Figure 58**: Investigation into the effect of copper concentration on bleach activity. Water (1.8 L), sodium percarbonate (5.3 mM), TAED (1.1 mM), MGDA (0.4 mM), catalyst (3 mg), 50 °C, 8 mins, pH = 10, water hardness = 5 °dH. Average error = ± 1.*

Decreasing copper concentration in the catalyst has a small effect on the bleaching activity. For the 5 mol% CuO_x/ZrO_2 material, the score increased to a maximum of 4, but then decreases back to a score of 2 as the concentration is decreased down to 1 mol%. The increase to a score of 4 in stain bleaching terms is minimal, as the consumer will see little difference ; A larger score increase to the next grouping (5,6,7) is required to see effective increase in the bleach activity of a catalyst. From these experiments, it is evident that the Cu concentration is a key factor in determining potential bleach activity.

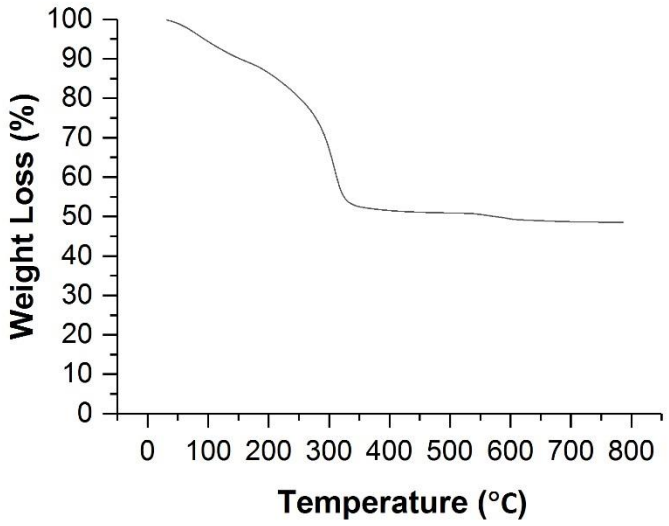

Figure 59*: TGA of 10 mol% copper/zirconia oxalate precursor under flowing air at 10 °C/min.*

Figure 59 shows the thermal decomposition of 10 mol% copper/zirconia oxalate, as both 10 and 5 mol% have similar bleaching scores according to the score groupings, 10 mol% was chosen as the copper concentration for further investigation A large decrease in mass is observed between 200 and 320 °C. The lower temperature mass loss, observed above 200 °C suggests, that calcination temperatures should be above 320 °C to fully decompose the oxalate precursor. Yu and co-workers[20] prepared a range of CuO-ZnO catalysts *via* oxalate co-precipitation; TGA analysis was conducted, which showed mass losses at 70 – 160 °C attributed to water both absorbed onto the surface and chemically bound in the catalyst. Similar loss in mass was observed in Figure 59 at 50 – 150 °C, suggesting the removal of water from the catalyst. Yu and co-workers also observed a large mass loss at 310 °C, which was attributed to the oxidation of Cu oxalate to CuO. A similar loss in mass is observed at 300 °C for the 10 mol% Cu/Zr oxalate material prepared in this work. The TGA data presented in Figure

59 indicates that the calcination temperature needs to be greater than 350 °C to thermally decompose Cu oxalate species into CuO. To assess the effect of calcination temperature on bleaching, 10 mol% CuO_x/ZrO_2 was prepared and calcined at varying temperatures.

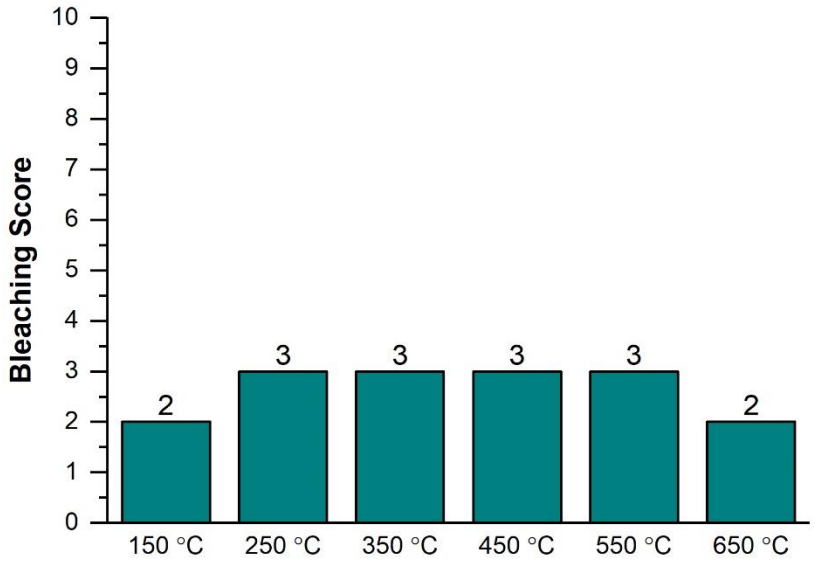

***Figure 60**: Effect of calcination temperature on bleach activity. Water (1.8 L), sodium percarbonate (5.3 mM), TAED (1.1 mM), MGDA (0.4 mM), 10 mol% CuOx/ZrO2 (3 mg), 50 °C, 8 mins, pH = 10, water hardness = 5 °dH. Average error = ± 1.*

Varying calcination temperatures were used to prepare the catalyst and the effect on bleach activity is shown in Figure 60. Through assessment of the TGA trace in Figure 59, it is expected that at the oxalate precursors are decomposed temperatures > 300 ˚C and the corresponding oxides formed; however, temperatures above 300 °C may lead to sintering of the copper oxide, which increases the copper oxide particle size. The reduction of copper oxide particle size would lead to a decrease in copper

surface area, which could reduce the activity of the catalyst. Decreasing the calcination temperature may lead to incomplete decomposition of the oxalate, as the bleaching activity of the copper catalyst decreases at 150 °C, suggesting that the oxalate is not active for bleaching and the oxide is needed Between 250 and 550 °C, the bleaching score is constant at 3. The score is lowered to 2 at the highest and lowest calcination temperatures trialled. From these results it is clear that a calcination temperature of 550 °C is acceptable for bleaching performance, as it is high enough to ensure complete oxalate decomposition and low enough to not decrease bleaching performance.

Wang *et al.* investigated the effect of temperature on the structure of Cu/ZrO_2 catalysts prepared by the oxalate gel method.[17] The study found that Cu surface area increased with calcination temperature, from 4 m^2/g_{cat} at 350 °C to 8.7 m^2/g_{cat} at 550 °C; Cu surface area then decreased to 2.4 m^2/g_{cat} at 750 °C. At a calcination of temperature of 550 °C, ZrO_2 changes phase from tetragonal to monoclinic at the surface of the catalyst, which affects the dispersion of Cu, due to enhanced metal-support interactions that stems from a geometric effect from the phase change. Wang *et al*. demonstrated that the change in ZrO_2 phase, which influences the Cu dispersion, is linked to higher activity of the catalyst.

Investigation into the species present on the 10 mol% CuO_x/ZrO_2 catalyst surface was conducted to assess whether the calcination step decomposes the copper oxalate to copper oxide. 10 mol% CuO_x/ZrO_2 catalysts were calcined at various temperatures, and the oxalate precursor were characterised by DRIFTS; the transmission of the sample in flowing carbon monoxide was recorded, Figure 61.

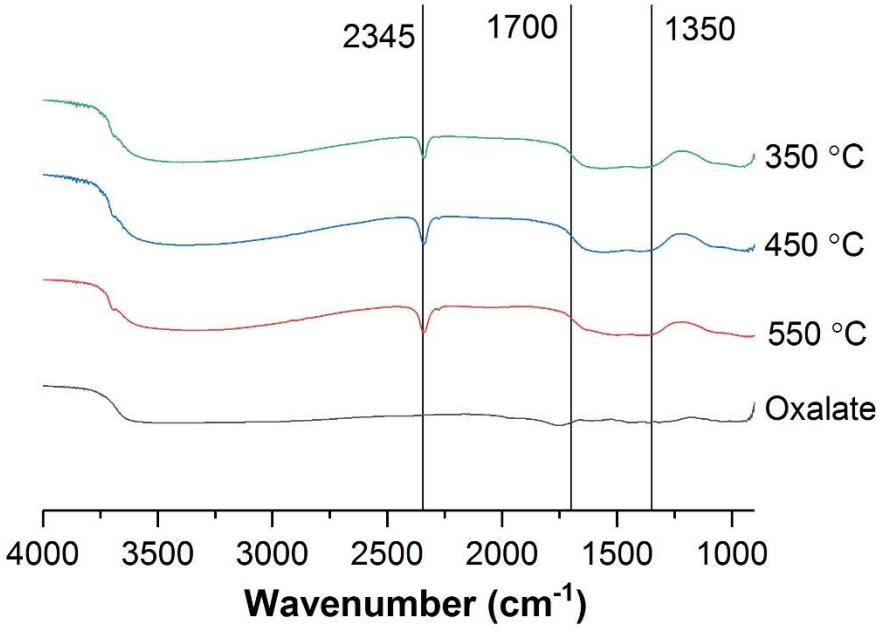

***Figure 61**: DRIFTS spectra of 10 mol% CuO_x/ZrO_2 before calcination and at various calcination temperatures where 1350 to 1700 cm^{-1} = carbonate/bicarbonate and 2345 cm^{-1} = carbon dioxide/monoxide.*

In Figure 61 the oxalate copper/zirconia precursor has no clearly defined peaks when compared to calcined 10 mol% CuO_x/ZrO_2. Each of the three CuO_x/ZrO_2 catalysts have the same vibrational bands present; a small sharp peak at 2345 cm^{-1}, and a broad peak from 1350 to 1700 cm^{-1}. The broad peak starts at a wavenumber of 1350 cm^{-1} aligning with literature values for carbonate and bicarbonate groups on a copper catalyst.[21] In addition, the peak at 2345 cm^{-1} also denotes the presence of CO_2 and CO groups on the surface.[22] A broad shallow peak also appears to present in the 3000 – 3500 cm^{-1} region of the spectrum, which could indicate the presence of surface hydroxyl groups.[21] It is unclear from the spectra whether the carbonyl or hydroxyl groups are associated with the Cu or Zr species on the surface. Overall, DRIFTS analysis has indicated the presence of carbonate and possible hydroxide groups on

the surface. Therefore, copper carbonate and copper hydroxide catalysts were prepared and tested, using the TC test, to assess if these groups are active for bleaching.

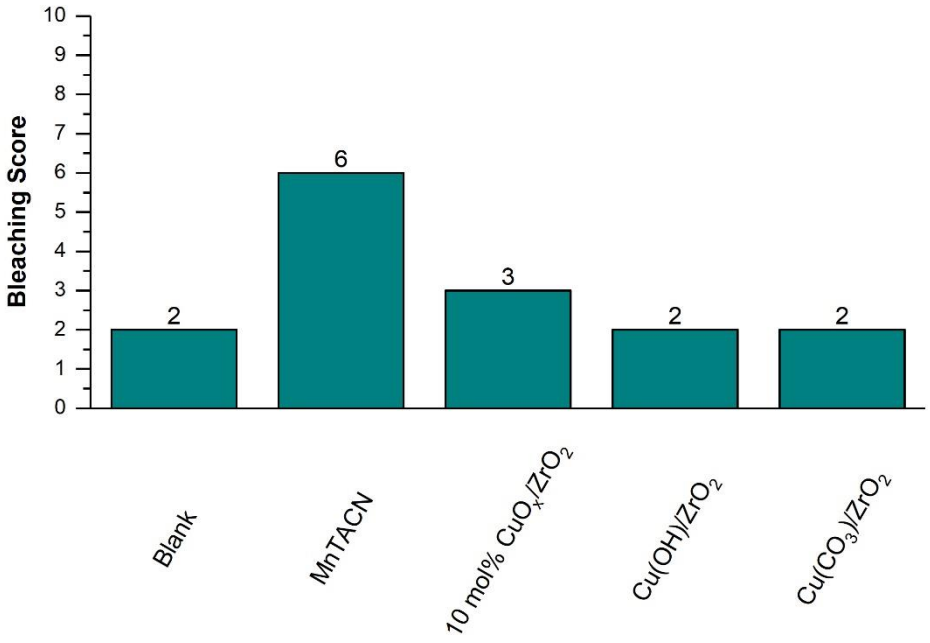

***Figure 62**: Bleaching activity of supported copper carbonate and copper hydroxide. Water (1.8 L), sodium percarbonate (5.3 mM), TAED (1.1 mM), MGDA (0.4 mM), catalyst (3 mg), 50 °C, pH = 10, 8 mins, water hardness = 5 °dH. Average error = ± 1.*

Figure 62 shows the bleaching activity of copper carbonate and copper hydroxide when supported on ZrO_2, with the support prepared by the oxalate gel method. The resulting catalysts, with Cu(OH) and $Cu(CO_3)$, were not heat treated, to avoid decomposition to CuO. An increase of activity was not observed for either the copper carbonate or the copper hydroxide catalysts, indicating that these groups are not responsible for the bleach activity observed for the 10 mol% CuO_x/ZrO_2 catalyst.

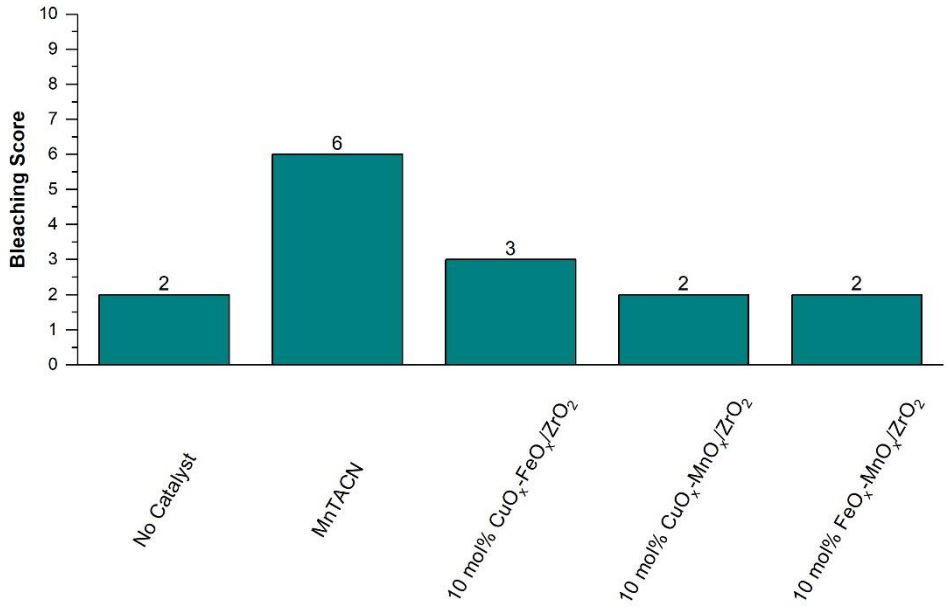

***Figure 63**: Bi-metallic catalyst bleach activity. Water (1.8 L), sodium percarbonate (5.3 mM), TAED (1.1 mM), MGDA (0.4 mM), catalyst (3 mg), 50 °C, 8 mins, pH = 10, water hardness = 5 °dH. Average error = ± 1.*

Figure 63 shows the effect of adding a second metal to the catalyst. Fortuny *et al.*[5] investigated Cu bimetallic catalysts with Fe, Mn, Zn and Co for the wet air oxidation of phenol. CuO-MnO and CuO-Fe_2O_3 exhibited phenol conversion of 99 % and 86 %, respectively, in the first 6 hours of the reaction. As iron and manganese catalysts are not bleach active, individually combining these metals with copper may improve bleaching performance. Therefore, bimetallic catalysts were tested in varying combinations with a total mol% of 10 for both the metals added in a 50:50 ratio to the zirconia. For CuO_x-MnO_x and FeO_x-MnO_x, there was no improvement in bleaching score in comparison to the reaction without catalyst, with a score of 2. CuO_x-FeO_x showed some bleaching activity, with a score of 3; however, this is no improvement

in comparison to CuO_x only, which scores 3. As there is no improvement with bleaching activity with bimetallic catalysts, Cu/Zr catalysts continued to be the focus.

4.2.1.1 *Heterogeneous vs Homogeneous Stain Bleaching*

In dishwasher detergents there is a known problem with detergents causing corrosion of the silver and copper metals that are used in the dishwasher or are part of the dishware being washed.[23,24] In addition, MGDA is added to the reaction as a chelating agent to bind to transition metal ions in solution, and this can react with H_2O_2, causing decomposition and a loss in bleach activity.[25] Due to potential interaction between the catalyst and the bleaching formulation, catalytic activity may arise from metal species in solution and not from heterogeneous oxide species. MGDA is a strong chelating agent for metal ions and forms complexes as shown in Figure 64[25]:

$$M^{2+} + H_n mgda^{n-3} \rightleftharpoons [M(H_n mgda)]^{n-2} \; where \; n = 0,1,2$$

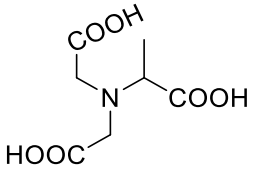

***Figure 64**: Structure of MGDA*

Therefore, metal species leaching from the catalyst surface, by binding to MGDA in solution, will be Cu^{2+}, Mn^{2+} and Zr^{2+}, and these solutes may be contributing to the bleach activity of the catalyst in solution. To assess if the leached metal from the catalyst is involved in the bleach reaction, metal nitrates were used as model salts, as the metal nitrates are the precursors to the catalysts and for Cu and Mn the

oxidation states are the same as the ions that bind to MGDA. Thus, metal nitrates were tested for bleaching in the TC test, as shown in Figure 65.

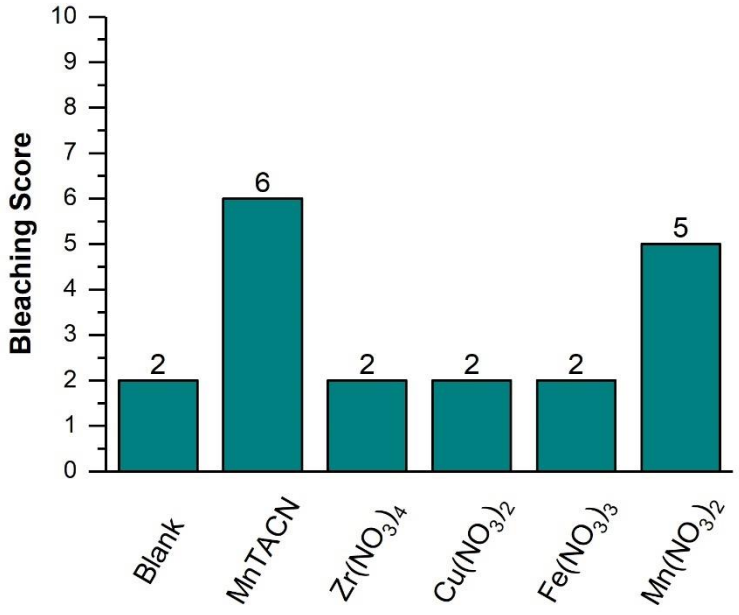

***Figure 65**: Bleaching activity of metal nitrate catalyst precursors. Water (1.8 L), sodium percarbonate (5.3 mM), TAED (1.1 mM), MGDA (0.4 mM), catalyst (3 mg), 50 °C, 8 mins, pH = 10, water hardness = 5 °dH. Average error = ± 1.*

Of the metal nitrate catalyst precursors tested, only manganese nitrate was more active for bleaching, than the test with no catalyst. Mn is in the oxidation state of 2+ in the nitrate salt, compared to Mn which is a dinuclear species in MnTACN, where the Mn is in 3+ and 4+ oxidation states.[26] MnTACN undergoes redox reactions as the dinuclear species is stabilised, whereas Mn salts cannot undergo redox, and often precipitate out of solution as inactive oxides. Therefore, whilst Mn nitrate is active for bleaching, the salt may be less stable in solution compared to MnTACN. Zirconia, copper and iron nitrates were inactive for bleaching, with a score of 2, indicating that copper in solution, in a Cu^{2+} oxidation state, is not active for bleaching.

To assess the level of leaching during a bleach reaction, solutions were analysed *via* MP-AES. The catalysts were stirred in solutions with reagent concentrations consistent with the TC bleaching test. The catalyst amount was increased to ensure that any metal leached was above the detection limit of the MP-AES. The percentage metal leaching without MGDA present is shown in Table 7.

***Table 7**: MP-AES measurement of catalysts without MGDA present. Water (18 mL), sodium percarbonate (5.3 mM), TAED (1.1 mM), catalyst (10 mg), 50 °C, 8 mins*

Catalyst	Calcination Temp (°C)	Metal Leaching (%)		
		Cu	Fe	Mn
50 mol% FeO_x/ZrO_2	550	0	0.3 ±0.02	0
50 mol% MnO_x/ZrO_2	550	0	0	0.4 ±0.02
10 mol% CuO_x/ZrO_2	150	5.2 ±0.26	0	0
10 mol% CuO_x/ZrO_2	550	0.2 ±0.01	0	0
10 mol% CuO_x/ZrO_2	650	0.2 ±0.01	0	0

Iron and manganese leaching from a 50 mol% catalyst calcined at 550 °C is minimal, both with metal leaching below 1%. For the 10 mol% CuO_x/ZrO_2 the leaching is affected by the calcination temperature of the catalyst; for the catalysts calcined at 550 °C and above, metal leaching is below 1%, butwhen the calcination temperature is decreased to 150 °C, metal leaching increased to 5.2%. The result suggests that the catalyst is less stable at lower calcination temperatures, and the partially oxidised

copper species is less strongly bound to the catalyst surface. As shown in Figure 60, the catalyst calcined at 150 °C exhibits no bleaching activity, suggesting that the leached copper species is inactive for bleaching.

Figure 59 previously showed the TGA of the oxalate precursor, with the temperature required to fully decompose oxalate to the oxide catalyst is above 300 °C, therefore, the catalysts calcined below 300 °C will have the oxalate still present on the catalyst surface It is likely that the leached species observed for 10 mol% CuO_x/ZrO_2 calcined at 150 °C is Cu oxalate, which is soluble in water and increases the leached copper in solution.[27]

The leached copper quantification was repeated in the presence of MGDA, to assess whether MGDA increases leaching through metal chelation. Table 8 shows that there is an increase in leaching for the copper catalysts in the presence of MGDA. An increase from 0.2 %, shown in Table 7 to 7.2 % was observed for the catalyst calcined at 550 °C, to 4.3 % for 650 °C, and to 18.3 % for 150 °C. The leaching may not be linear with calcination temperature due to the higher amount of more readily soluble oxalates on the surface of that catalyst at lower calcination temperatures. Conversely, the iron and manganese catalysts show minimal leaching, regardless of calcination temperature.

***Table 8**: MP-AES measurement of catalysts with MGDA present. Water (18 mL), sodium percarbonate (5.3 mM), TAED (1.1 mM), MGDA (0.4 mM), catalyst (10 mg), 50 °C, 8 mins*

Catalyst	Calcination Temp (°C)	Metal Leaching (%)		
		Cu	Fe	Mn
50 mol% FeO_x/ZrO_2	550	0	0.2 ±0.01	0
50 mol% MnO_x/ZrO_2	550	0	0	0.2 ±0.01
10 mol% CuO_x/ZrO_2	150	18.3 ±0.91	0	0
10 mol% CuO_x/ZrO_2	550	7.2 ±0.36	0	0
10 mol% CuO_x/ZrO_2	650	4.3 ±0.12	0	0

As MGDA is present in the TC test, it is clear that, for the 10 mol% CuO_x/ZrO_2 catalysts calcined at 550 and 650 °C, bleach activity may well be due to leached copper species in solution. To assess the bleaching performance of leached copper for tea stain removal, the 10 mol% CuO_x/ZrO_2 catalyst calcined at 150 °C was stirred under the same conditions with and without MGDA present. This solution, containing leached Cu species, was then filtered and added to the TC test.

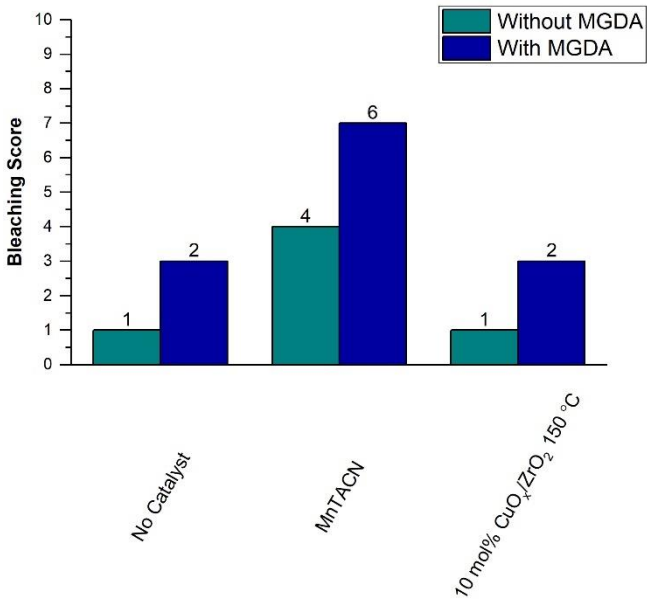

***Figure 66**: Effect of leached copper on bleaching performance. Water (1.8 L), sodium percarbonate (5.3 mM), TAED (1.1 mM), MGDA (0.4 mM), catalyst (3 mg), 50 °C, 8 mins, pH = 10, water hardness = 5 °dH. Average error = ± 1.*

Figure 66 shows the bleaching activity of the copper solution composed of leached copper species from 10 mol% CuO_x/ZrO_2 calcined at 150 °C. Without MGDA, the bleach score of the solution alone, which is comparable to the no catalyst test. MnTACN has the highest bleach activity, with a score of 4. With MGDA, the bleach score for the leached copper solution is 2 in the presence of MGDA. Again, MnTACN has the highest bleaching activity, with a score of 6 in the presence of MGDA. As the bleaching score of the leached copper solution is the same with no catalyst present, it can be concluded that copper in solution is not active for bleaching. The presence of MGDA does therefore contribute to the leaching of Cu from heterogeneous catalyst, but the leached Cu does not catalyse the bleaching reaction. Overall, heterogeneous copper is active for bleaching tea stains in solution.

4.2.2 *Morin Oxidation in the Presence of Heterogeneous Catalysts*

10 mol% CuO_x/ZrO_2 has been identified as an active bleach catalyst for removal of tea stains (Figure 58) in the presence of sodium percarbonate and TAED. To further investigate the catalysts activity, morin oxidation reactions were carried out. The full catalyst copper concentration range was tested.

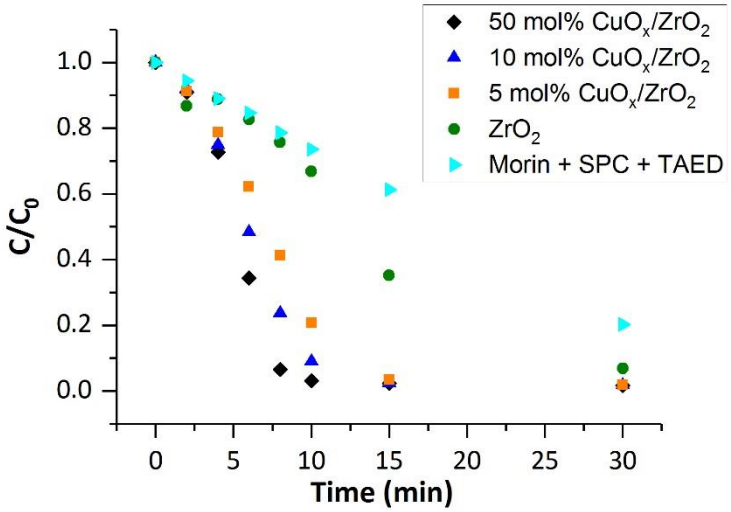

***Figure 67**: Morin oxidation activity for copper catalysts. Water (90 mL), morin (0.1 mM), sodium percarbonate (5.3 mM), TAED (1.1 mM), sodium carbonate (50 mM), CuO_x/ZrO_2 (0.1 mg), pH = 10.5, 50 °C, 30 min. Average error = 7%.*

Figure 67 shows the conversion of morin over time in the presence of copper catalysts, with a copper concentration of 5 - 50 mol%. A reverse trend in bleach activity is observed for morin oxidation, when compared to tea stain bleaching. 50 mol% CuO_x/ZrO_2 has the highest conversion of morin over 10 mins, with 1 mol%

having the lowest. The rate of morin conversion was calculated from 0 – 4 mins and 4 – 8 mins, and the results are shown in Table 9.

***Table 9**: Rate of morin conversion in the absence and presence of copper catalysts during the first 8 mins of the reaction. Water (90 mL), morin (0.1 mM), sodium percarbonate (5.3 mM), TAED (1.1 mM), sodium carbonate (50 mM), CuO_x/ZrO_2 (0.1 mg), pH = 10.5, 50 °C, 30 min.*

Catalyst	Rate of Morin Conversion 0 - 4 mins (mM s^{-1} x10^{-5})	Rate of Morin Conversion 4 - 8 mins (mM s^{-1} x10^{-5})
No Catalyst (morin + SPC + TAED)	4.2	4.0
ZrO_2	4.3	5.1
50 mol% CuO_x/ZrO_2	10.9	26.4
10 mol% CuO_x/ZrO_2	9.3	18.8
5 mol% CuO_x/ZrO_2	7.9	13.9

Without a catalyst present, the rate of morin oxidation is comparable in the first and second 4 mins of the reaction; with the addition of a copper catalyst at 50 mol%, 10 mol% and 5 mol% CuO_x/ZrO_2, the rate of morin conversion is higher in the first 4 minutes of the reaction. 50 mol% CuO_x/ZrO_2 increases the rate from 4.2 mM s^{-1} without a catalyst to 10.9 mM s^{-1}, with a further rate increase to 26.4 mM s^{-1} at 4 – 8 mins of the reaction. 10 and 5 mol% copper catalyst show an increase in rate during 4 – 8 mins by 9.3 mM s^{-1} and 7.9 mM s^{-1}, respectively. ZrO_2 also exhibits an increase in rate after 4 mins for morin oxidation, however, no bleach activity was observed for ZrO_2 in Figure 57, suggesting that ZrO_2 is active for morin oxidation but not bleaching of tea stains.

Overall, the addition of ZrO_2 or a CuO_x/ZrO_2 catalyst increases the rate of morin oxidation. 50 mol% CuO_x/ZrO_2 has the highest rate of reaction over 8 mins compared to the other catalysts. All the copper catalysts are active for morin oxidation, and the addition of copper to ZrO_2 improves the activity of the catalyst.

The activity ranking of the catalysts is different for the TC test and the morin oxidation reaction. As it is already known copper leaches in the TC reaction, ICP-MS analysis was performed on post reaction solutions for morin oxidation to assess the level of copper leached during a reaction. ICP was used instead of MP-AES as it is a more sensitive technique, due to the lower levels of catalysts used in these tests, 0.1 mg in the morin oxidation test, compared to 3 mg the TC test.

***Table 10**: ICP-MS results for 50 mol% CuO_x/ZrO_2.*

Catalyst	Cu Leaching (%)	Zr Leaching (%)
50 mol% CuO_x/ZrO_2	3.2	0.8
ZrO2	-	0.2
50 mol% CuO_x/ZrO_2 after stirring	0.1	0

ICP analysis, Table 10, was run after the morin reaction for 50 mol% CuO_x/ZrO_2, ZrO_2 and 50 mol% CuO_x/ZrO_2 stirred in water before adding into the reaction. 0.1 mg of catalyst was used in the morin oxidation reaction, to accurately add this amount, a suspension of the catalyst was made in water by stirring for 1 hour, this solution was then quantified v*ia* ICP-MS for copper leaching. Leaching of metal is minimal for the support material (ZrO_2) and the catalyst during suspension before dosing the reaction. During the 30 min reaction, the ICP shows that 3 % copper is leached from

the catalyst. Therefore, copper salts may be present in the reaction solution, as also found for the beaker test.

Leached copper is not responsible for tea stain bleaching in the TC test, but may contribute to morin conversion. Over time, the rate of morin oxidation increases, as demonstrated in Table 9, which could be due to the release of copper species from the surface during the reaction. To further investigate the effect of solution phase copper species on morin conversion, copper salts were added to the reaction. The results of which are shown in Figure 68.

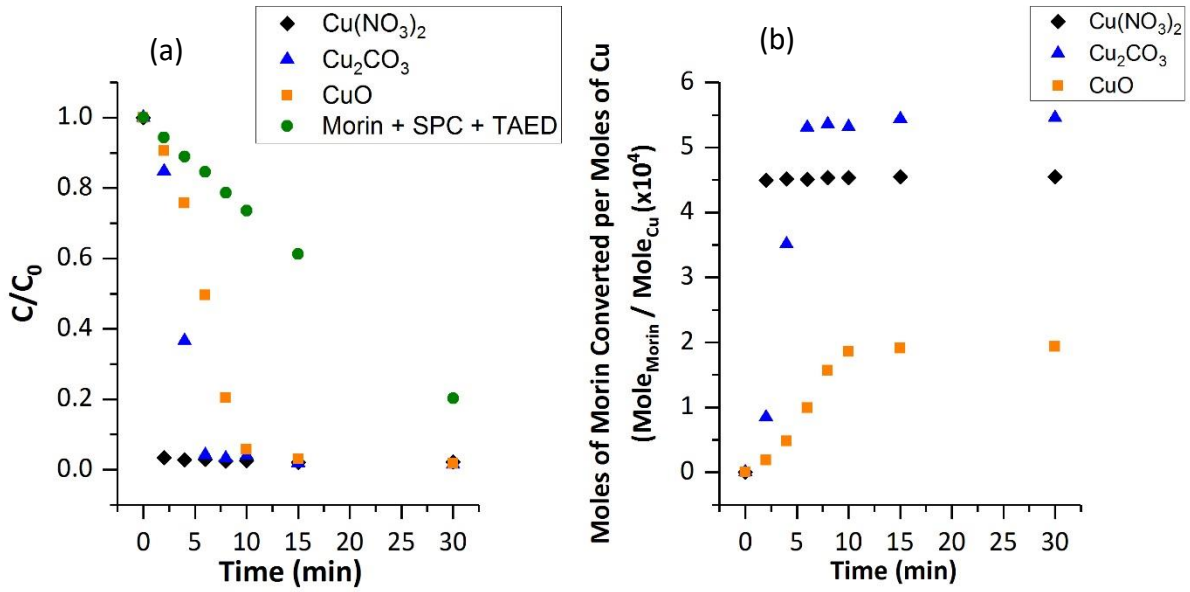

***Figure 68**: Copper salt morin conversion activity, (a) = conversion of morin over 30 mins, (b) = normalising moles of morin converted to the moles of copper present. Water (90 mL), morin (0.1 mM), sodium percarbonate (5.3 mM), TAED (1.1 mM), sodium carbonate (50 mM), copper salt (0.1 mg), pH = 10.5, 50 °C, 30 mins, Average error = 7%.*

The copper reagents used for these experiments were copper nitrate, copper carbonate and copper oxide, which are present in the catalyst. Copper carbonate was

also identified as present in the catalyst using DRIFTS analysis, as shown in Figure 61. All three copper salts were active for morin oxidation, with copper nitrate being the most active and copper oxide the least. Copper nitrate reaches 97% conversion after 2 mins, compared to 15% for copper carbonate and 8% for copper oxide. After 10 mins all three copper salts reach over 90% morin conversion.

The moles of morin converted was normalised against the moles of copper in the reaction. For the normalised data, the carbonate salt exhibited the highest conversion with respect to copper; however, Cu nitrate reaches the maximum activity the quickest (2 mins). In comparison, Cu oxide has less than half the activity of both Cu carbonate and nitrate, which may be due to Cu oxide being sparingly soluble[27] in water and therefore is less intimately mixed with morin than Cu nitrate and Cu carbonate.

Leached copper species are therefore concluded as active for morin oxidation but were not observably active in the TC test. Cu nitrate was not observably active for the TC test, with a score of 2; however, for morin oxidation a conversion of 98 % is observed after 8 mins. The results indicate that there are two different reaction mechanisms for the TC test and the morin oxidation test.

4.2.3 *Characterisation of Active Bleach Catalysts*

To further understand the copper catalysts that were active for bleaching of the stained TCs, the catalyst properties were probed in an attempt to identify the active components. To do this, a range of techniques were used, namely SEM, XRD and XPS. The surface area of the catalysts and copper metal on the catalysts were also

quantified to assess if surface area played a role in the activity of the catalyst; this was conducted using N_2 physisorption and N_2O titration methods, respectively.

4.2.3.1 *Surface Species*

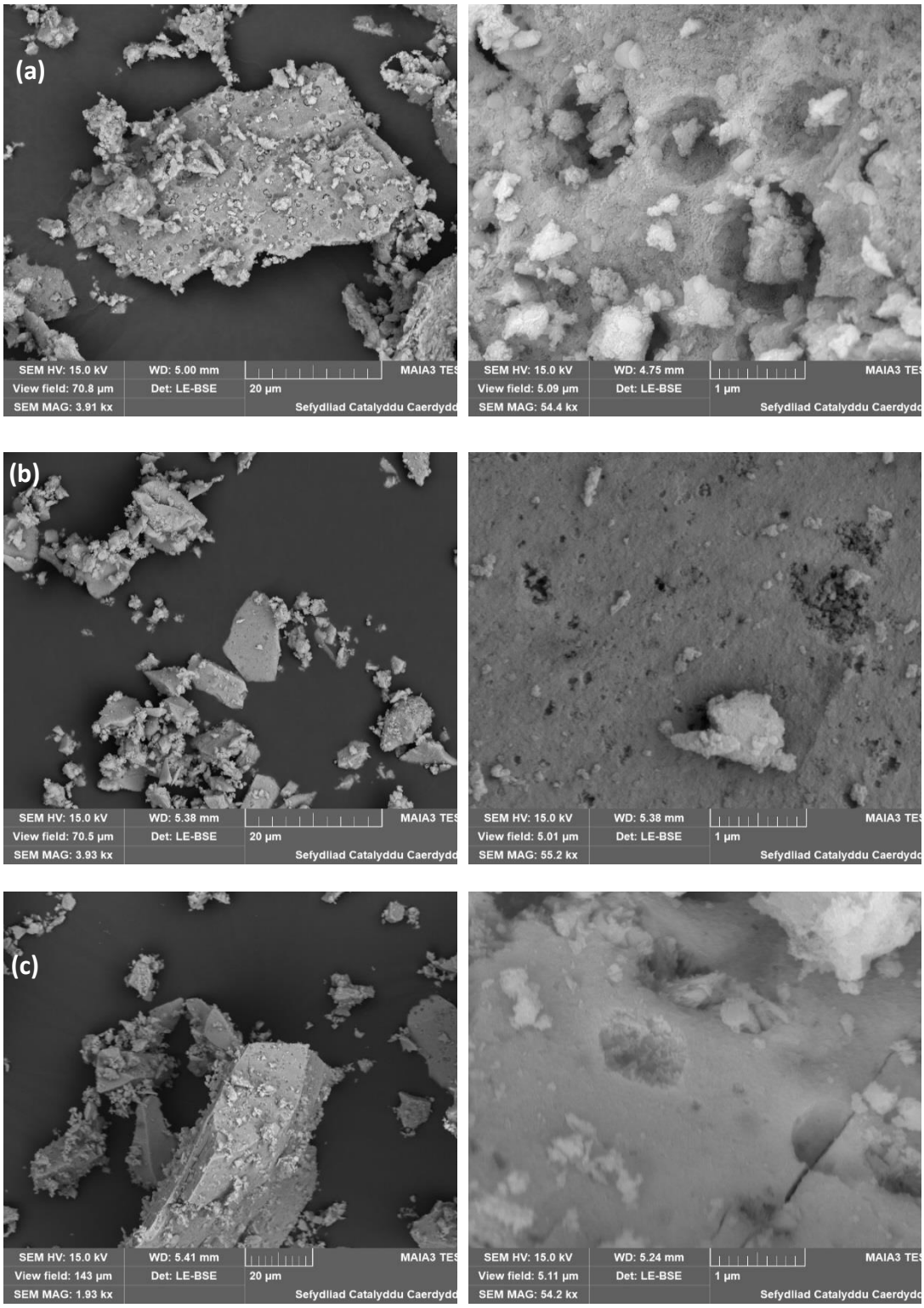

***Figure 69**: Scanning electron images of a) 50 mol%, b) 10 mol% and c) 5 mol% CuO_x/ZrO_2*

Figure 69 shows the scanning electron images of 50, 10 and 5 mol% CuO_x/ZrO_2 at two different magnifications. For all three copper concentrations, there is a mixture of particle sizes ranging from 1 μm to > 50 μm. Also, on the surface of larger particles, (>20 μm), there are non-ordered pores on the surface, which are most apparent in the 50 and 5 mol% CuO_x/ZrO_2 catalysts, and appear smaller for the 10 mol% CuO_x/ZrO_2. The observation is qualitative, however, and this may be due to low number of particles observed that are not representative of the whole sample and not that the difference in non-ordered pore size between catalysts is related to the different copper concentrations. In these non-ordered pores, there are also smaller particles present, which may indicate the larger particles form around smaller ones, or that these particles were deposited into the non-ordered pores during preparation.

To assess the catalyst compositions over the surface of the catalyst particles, EDX was used to identify the composition at various points along the catalyst, for 50 mol% CuO_x/ZrO_2. The results are shown in Figure 70 and Table 11.

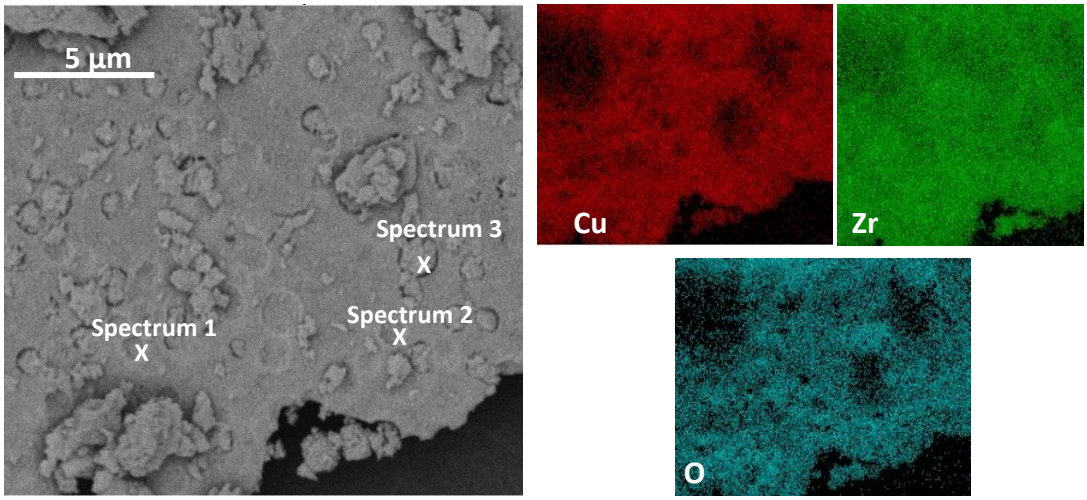

***Figure 70**: EDX compositional analysis of 50 mol% CuO_x/ZrO_2. Spectrum 1 – 3 were analysed via EDX to ascertain the composition, Table 11.*

Figure 70 shows the distribution of Cu, O and Zr over the sample surface by elemental mapping over the sample surface, the coloured areas show where is element is present. Zr is well distributed over the surface of the particle, which is expected as it is the support material; however, there are "dark" areas on the elemental map for Cu and O indicating areas that have lower Cu and O concentrations. These dark areas are in areas where particles that are on the surface. Point spectra were taken at different points of interest on the surface, and the elemental composition of these points, in mol%, are shown in Table 11.

***Table 11**: Composition analysis of different point in 50 mol% CuO_x/ZrO_2*

Spectrum	Mole (%)		
	Cu	Zr	O
1	22	25	53
2	23	20	58
3	12	18	69

Spectrum 1 was taken in a non-ordered pore in the surface; spectrum 2 on the flat surface; and spectrum 3 of a particle situated in another non-ordered pore. The mole ratio between Cu and Zr is close to 1 : 1 for spectrum 1 and 2, consistent with the ratio in the catalyst preparation. On the surface, there is a higher copper content than in the non-ordered pore, where there is a higher zirconium content. The differences suggest that the distribution of copper is not homogeneous across the catalyst. In addition, the particle in a non-ordered pore, spectrum 3, is oxygen rich, with a lower copper content compared to the bulk catalyst.

Figure 71, shows the EDX maps of a 10 mol% CuO_x/ZrO_2 particle. The distribution of Cu, Zr and O is even over the surface of the catalyst, indicating little difference between the composition of smaller particles on the surface or dark areas imaged.

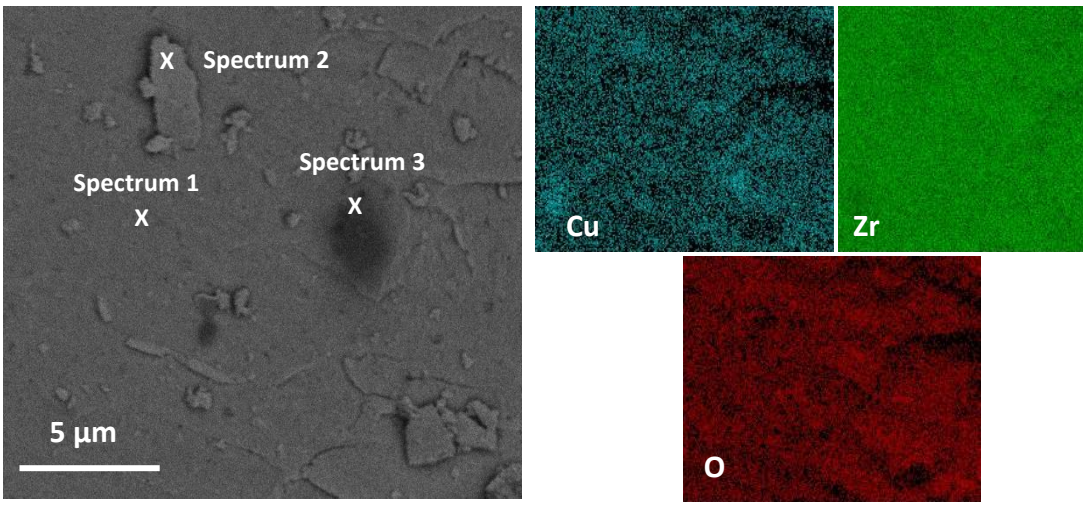

***Figure 71**: EDX compositional analysis of 10 mol% CuO_x/ZrO_2. Spectrum 1 – 3 were analysed via EDX to ascertain the composition, Table 12.*

The composition of the 10 mol% CuO_x/ZrO_2 catalyst was further investigated by measuring the mol% composition at different points of interest across the catalyst

surface. Spectrum 1 was taken on the flat catalyst surface, spectrum 2 on a smaller particle on the surface and spectrum 3 on a dark area imaged. The results are shown in Table 12.

***Table 12**: Composition analysis of different points in 10 mol% CuO_x/ZrO_2*

Spectrum	Mole (%)		
	Cu	Zr	O
1	5	33	62
2	5	28	66
3	5	33	62

The difference in Cu content to 50 mol% is due to the lower concentration of copper used in the preparation, however, EDX has a high error associated with quantification of elements so the difference in surface Cu may be less than appears. For all three points on the catalyst surface measured, the copper content is lower than the 10 mol% originally used in the catalyst preparation. Overall, the three investigated regions all have similar compositions, indicating that the copper is well dispersed across the catalyst sample. For the small surface particle, spectrum 2, there is an increase in relative copper amount, as there is less zirconium present, which suggests the presence of copper rich surface particles in the 10 mol% CuO_x/ZrO_2 catalyst. The presence of copper rich particles may be due to sintering during the calcination of the oxalate precursor.

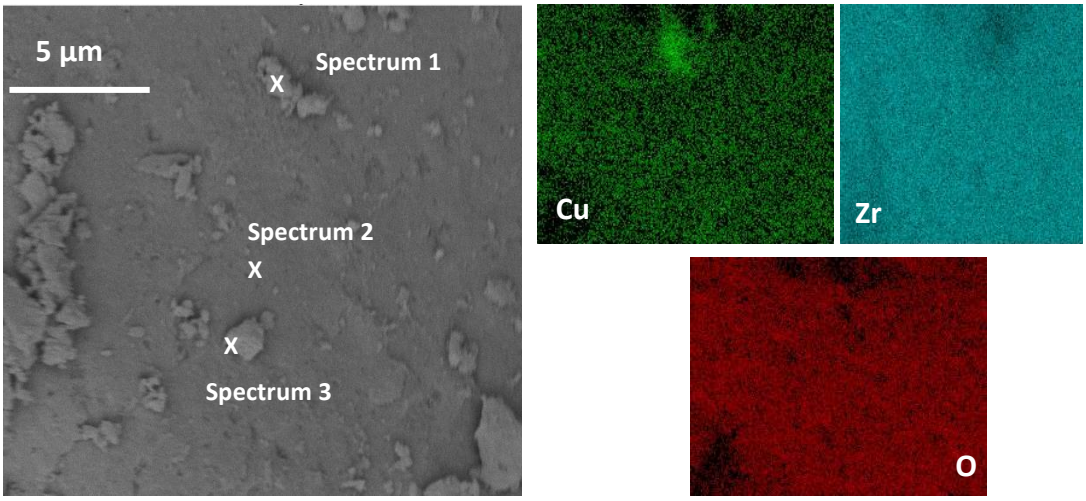

***Figure 72**: Composition analysis of 5 mol% CuO_x/ZrO_2. Spectrum 1 – 3 were analysed via EDX to ascertain the composition, Table 13.*

EDX compositional analysis was also completed for 5 mol% CuO_x/ZrO_2, Figure 72. For Zr and O, the compositional map shows an even distribution of over the surface; however, for Cu there is a brighter spot over an area with a smaller particle on the surface, and, there appears to be a decrease in O and Zr in the same area. In combination, these observations indicate a copper rich smaller particle on the surface. Composition of points of interest was quantified for the catalyst surface and the results are shown in Table 13.

***Table 13**: Composition at different points on 5 mol% CuO_x/ZrO_2*

Spectrum	Mole (%)		
	Cu	Zr	O
1	18	24	58
2	3	26	72
3	3	25	72

Spectrum 1 was collected for a small particle on the surface; spectrum 2 on the flat catalyst surface; and spectrum 3 of another smaller particle on the surface. For spectrum 2 and 3, points the copper content is lower than the 5 mol% used in the catalyst preparation, suggesting that the copper is mainly present on the surface of the catalyst. Spectrum 1 shows the highest mol% of copper at 18 %, indicating that there are copper rich particles on the surface of the catalyst; however, another surface particle, spectrum 3, does not show the same composition and has a similar composition to the catalyst surface. The presence of copper rich particles for both 10 and 5 mol% copper catalysts, whichhave higher bleach activity than the 50 mol% CuO_x/ZrO_2 catalyst, may indicate the importance of these copper rich particles for bleaching activity.

To further understand the CuO_x and ZrO_2 present in the samples, XRD was acquired for copper catalysts with varying copper concentrations from 1 to 50 mol%.

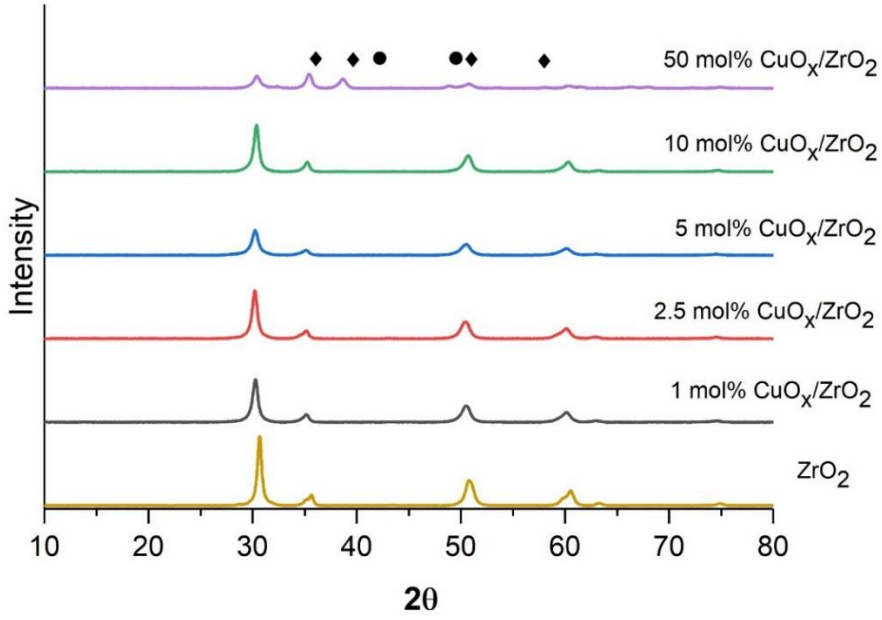

***Figure 73**: X-ray diffraction patterns of 1 - 50 mol% CuO_x/ZrO_2 with ZrO_2 for reference. ♦ = ZrO_2 peaks and ● = CuO peaks.*

Figure 73 shows the XRD spectrum for copper catalysts and ZrO_2 prepared using the oxalate gel method. The majority of the peaks in the copper catalysts are for ZrO_2, denoted by the black diamonds. These peaks occur at 30.7 °, 35.6 °, 50.9 ° and 60.3 ° for ZrO_2 which matches with cubic zirconia (ICCD 00-027-0997), indicating the cubic phase of ZrO_2 is present in the catalysts..

Addition of copper to ZrO_2 reduces the intensity of the peaks, and they appear broader than with ZrO_2 only, suggesting that the copper catalysts are more amorphous in structure than the ZrO_2 support material. No copper peaks are observed in the catalysts with a copper concentration lower than 50 mol%. 50 mol% CuOx/ZrO2 has two CuO_x peaks, denoted by the black circles, at 38.7 ° and 48.8 °. These peaks match CuO monoclinic (ICCD 01-089-5895), suggesting that the large copper particles present in 50 mol% CuO_x/ZrO_2 have monoclinic lattice structure. The absence of these peaks in lower copper concentration catalysts implies that the copper is more dispersed across the catalyst, leading to a smaller CuO particles size that would not be detected in the XRD analysis.

XRD shows the bulk lattice structure and composition of the catalyst. To investigate the species present on the surface that may be responsible for bleach activity, XPS spectra of the selected catalysts were recorded.

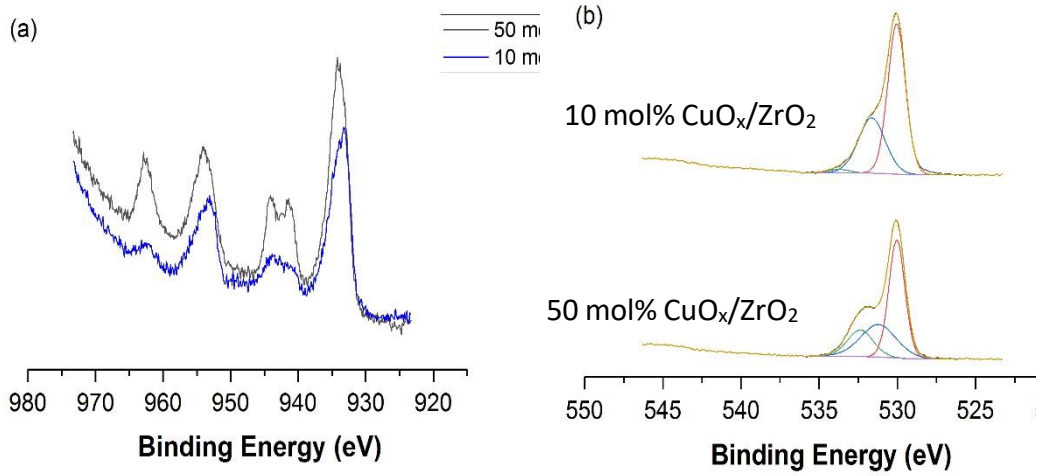

***Figure 74**: XPS analysis of (a) = copper 2p region and (b) = oxygen 1s region, in 50 mol% and 10 mol% CuO_x/ZrO_2*

Figure 74 (a) shows the XPS analysis of copper 2p region 50 and 10 mol% CuO_x/ZrO_2. 50 mol% CuO_x/ZrO_2 has five peaks at 934, 941, 944, 954 and 962 eV; 10 mol% CuO_x/ZrO_2 has similar peaks but there is a reduction in intensity of the satellite peaks and the satellite peaks have merged. The position and shape of the peaks for 50 mol% agree with characterisation of CuO by Biesinger *et al.*[28]. Poulston *et al.*[29] also investigated the oxidation of Cu_2O to CuO, which generates satellite peaks at 941, 944 and 962 eV. Therefore, it is likely that the copper species present on the surface of 50 mol% CuO_x/ZrO_2 is CuO.

Comparison of 50 to 10 mol% CuO_x/ZrO_2 shows a reduction and a merging of the satellite peaks, as well as a shift to lower binding energies. This merging of satellite peaks is characteristic of Cu(II)OH species and the reduction in peak intensity indicates a reduction in particle size.[28] Overall, the XPS data shows that, when the

copper concentration is decreased, the copper is present more as Cu(II)OH than CuO, but both species could be present on the surface of both samples.

Figure 74 (b) shows the oxygen 1s region of both 50 and 10 mol% CuO_x/ZrO_2. Both catalysts have peaks at 530 eV and shoulders at 531 eV. The peak at 530 eV is expected for copper oxide catalysts[30], and the shoulder peak is indicative of hydroxide species.[29] Overall, the XPS of 10 and 50 mol% CuO_x/ZrO_2 suggest that copper is present as CuO and Cu(II)O and, as the copper concentration is decreased, the amount of Cu(II)OH present increases, as well as a decrease in copper particle size.

4.2.3.2 *Surface Area*

***Table 14**: BET surface area of copper catalysts at varying copper concentrations, measurements were determined from a 5-point BET experiment.*

Catalyst	Surface Area (m^2/g)
ZrO_2	23
1 mol% CuO_x/ZrO_2	62
2.5 mol% CuO_x/ZrO_2	60
5 mol% CuO_x/ZrO_2	66
10 mol% CuO_x/ZrO_2	68
30 mol% CuO_x/ZrO_2	69
50 mol% CuO_x/ZrO_2	24

Table 14 shows the BET surface areas obtained for a range of the copper catalysts, with copper concentrations from 1 to 50 mol%. The 50 mol% CuO_x/ZrO_2 has the lowest surface area, of 24 m^2/g, which increases to 69 m^2/g when copper

concentration is decreased to 30 mol%. Copper concentrations of 1 – 30 mol% have similar surface area, from 60 – 69 m^2/g, suggesting that decreasing the copper concentration does not improve surface area below 30 mol%. This is in-line with the XRD findings (Figure 73), in that there are large copper particles present on the 50 mol% CuO_x/ZrO_2 which are no longer present as the copper content is reduced, these larger copper particles will reduce the surface area as evidenced in Table 14. Surface area remains constant between 1 – 30 mol% but there are no large copper particles present, indicating that the copper is more dispersed on the catalyst surface; however, there is no notable increase in activity. In conclusion, the increase in copper dispersion on the surface of the catalyst is not responsible for the increase in bleaching activity.

As copper concentration decreases, this should affect the copper surface area on the surface of the catalyst. Titration with N_2O was used to quantify the copper surface area in 50, 10 and 5 mol% CuO_x/ZrO_2 catalysts, Table 15.

***Table 15**: Copper surface area measured by titration with N_2O for varying copper concentrations*

Catalyst	Copper surface area (m^2/g)	Copper Surface Content from XPS (At %)
50 mol% CuO_x/ZrO_2	6.4	6
10 mol% CuO_x/ZrO_2	4.6	9
5 mol% CuO_x/ZrO_2	2.2	-

Copper surface area decreases from 6.4 m^2/g at 50 mol% Cu to 2.2 m^2/g at 5 mol% Cu. Decrease in copper surface area with copper concentration is expected; however, a linear decrease is not observed from 50 mol% to 5 mol%. Comparing the copper

surface area to the copper At. % at the surface, 50 mol% has 6 At. % whereas 10 mol% has 9 At.%, demonstrating that more of the copper is present in the lattice for 50 mol%, whereas, a larger proportion of Cu is present and more dispersed on the surface for 10 mol% Cu-ZrO_2 catalyst. The difference in copper surface area and At. % accounts for the non-linear trend expected in copper surface area from 5 – 50 mol%, as the copper is not on the surface but mainly in the lattice. The results also suggest that at, lower copper concentrations, copper particles are more dispersed and therefore exhibit a higher copper surface area.

4.2.4 *Bleach Activity of Developed Heterogeneous Catalysts*

From the characterisation of the copper catalysts, it was deduced that large copper rich particles may be present on the surface of the catalyst. Copper oxide has been known to decompose H_2O_2 to H_2O and O_2, which would reduce the active bleaching agents in the wash solution.[31] Removal of these particles from the surface may increase the bleach activity for tea stains of these catalysts.

One way to achieve this is with an acid treatment. Stirring the catalyst in a strong acid could remove large surface copper oxide particles from the surface and improve the bleaching activity of the catalyst. Orlowski *et al.*[18] observed large inactive copper species on the surface of Cu/Zr catalysts, which were then removed *via* acid treatment. The catalysts retained activity for hydrogenation of levulinic acid and showed that these copper species were spectator species in the reaction. Initially 10 mol% CuO_x/ZrO_2 was stirred in HNO_3 for 2 hours and the catalyst washed until the washings were pH 7, and the hydrogen peroxide decomposition was compared before and after acid treatment.

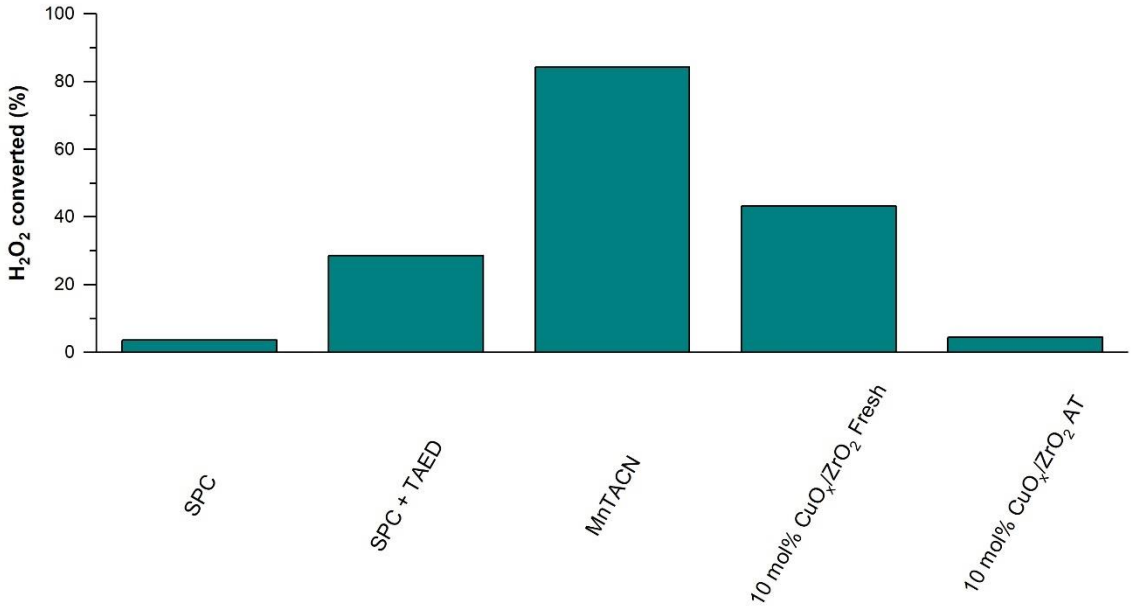

***Figure 75**: H_2O_2 decomposition from sodium percarbonate, all catalysts were run in the presence of sodium percarbonate and TAED. AT = acid treated catalyst. Water (90 mL), sodium percarbonate (5.3 mM), TAED (1.1 mM), catalyst (3 mg), pH = 10, 50 °C, 8 mins.*

Figure 75 shows the H_2O_2 decomposition over 8 mins without a catalyst present in the presence of MnTACN, and in the presence of 10 mol% CuO_x/ZrO_2 before and after acid treatment (AT). Under bleach conditions for 8 mins, H_2O_2 released from sodium percarbonate is stable and only 3.6% is lost over the duration of the experiment. The addition of TAED increased the decomposition of H_2O_2, as it reacts to form peracetic acid, and 28.6% is lost over 8 mins. As sodium percarbonate is in excess in comparison to TAED, the amount lost is equivalent to 100% TAED conversion. MnTACN decomposes the highest amount of H_2O_2 with 84.2% lost over 8 mins. This is due to MnTACN utilising H_2O_2 during bleaching to oxidise the stain.

MnTACN is active for both the decomposition of H_2O_2 to H_2O and O_2, and the activation of H_2O_2 generating HOO^- for oxidation; the pathway of H_2O_2 cannot be distinguished between using this reaction.

Comparison of 10 mol% CuO_x/ZrO_2 fresh (before acid treatment) and 10 mol% CuO_x/ZrO_2 AT (after acid treatment) shows a difference in the amount of H_2O_2 lost over 8 mins. For the fresh copper catalyst, 43.1% of H_2O_2 is lost over 8 mins, whereas only 4.5% H_2O_2 is lost for the acid treated catalyst. The result indicates that the acid treatment has indeed modified the surface of the catalyst, as less H_2O_2 decomposition is observed after the acid treatment. To assess if the reduced H_2O_2 decomposition is beneficial for tea stain bleaching, acid treated catalysts were tested in the TC reaction, shown in Figure 76.

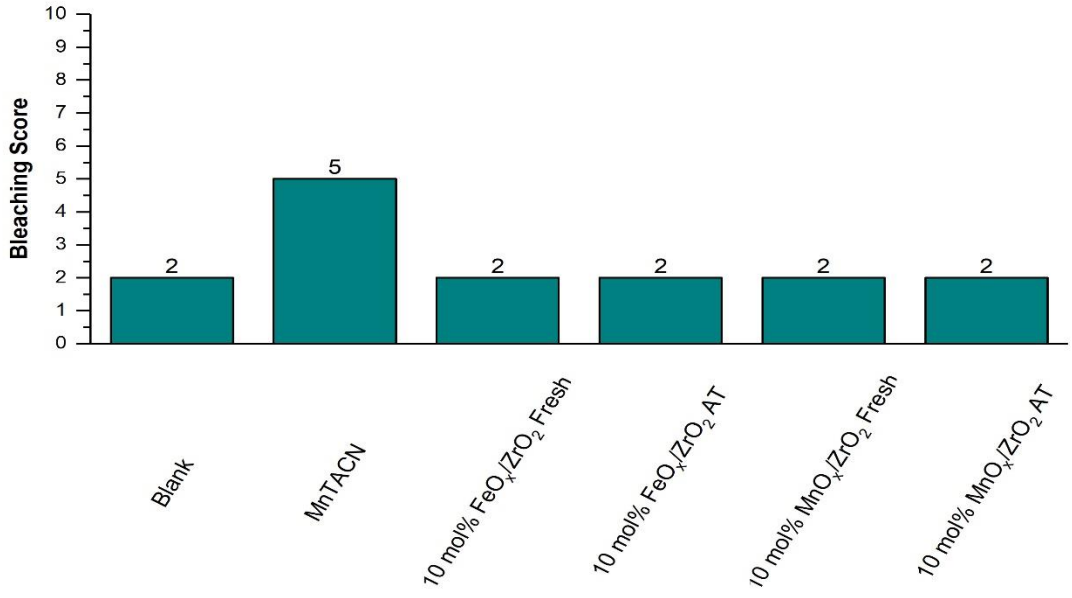

***Figure 76**: Bleaching activity of acid treated catalysts. Water (1.8 L), sodium percarbonate (5.3 mM), TAED (1.1 mM), MGDA (0.4 mM), catalyst (3 mg), 50 °C, 8 mins, pH = 10, water hardness = 5 °dH. Average error = ± 1.*

For 50 and 10 mol% CuO_x/ZrO_2, an increase in bleaching score after acid treatment is observed. Freshly prepared 50 mol% CuO_x/ZrO_2 has a score of 2, which increases to 4 after acid treatment. Therefore, after acid treatment the 50 mol% copper now shows activity for bleaching in comparison to having no catalyst present. The same 2-score increase is observed for 10 mol% CuO_x/ZrO_2 after acid treatment; it now has a score of 5, which is comparable to that observed by MnTACN, with a score of 6. As the bleach scores are grouped, 1-4, 5-7 and 8-10, with large increases in stain removal between each score group, a score of 5 for the acid treated catalyst is a large step change in the bleaching performance. Acid treatment of the 10 mol% CuO_x/ZrO_2 has led to a heterogeneous catalyst that is comparable to MnTACN for stain removal under these conditions.

4.2.5 *Comparison of Physical Properties of Developed Catalysts*

As shown in the previous section, acid treatment increases the bleach activity of copper catalysts. The acid treatment is expected to reduce the surface copper content and could change the surface composition and structure of the catalyst. Characterisation experiments were conducted for the acid treated catalyst for comparison with the catalyst pre acid treatment.

4.2.5.1 *Surface Species*

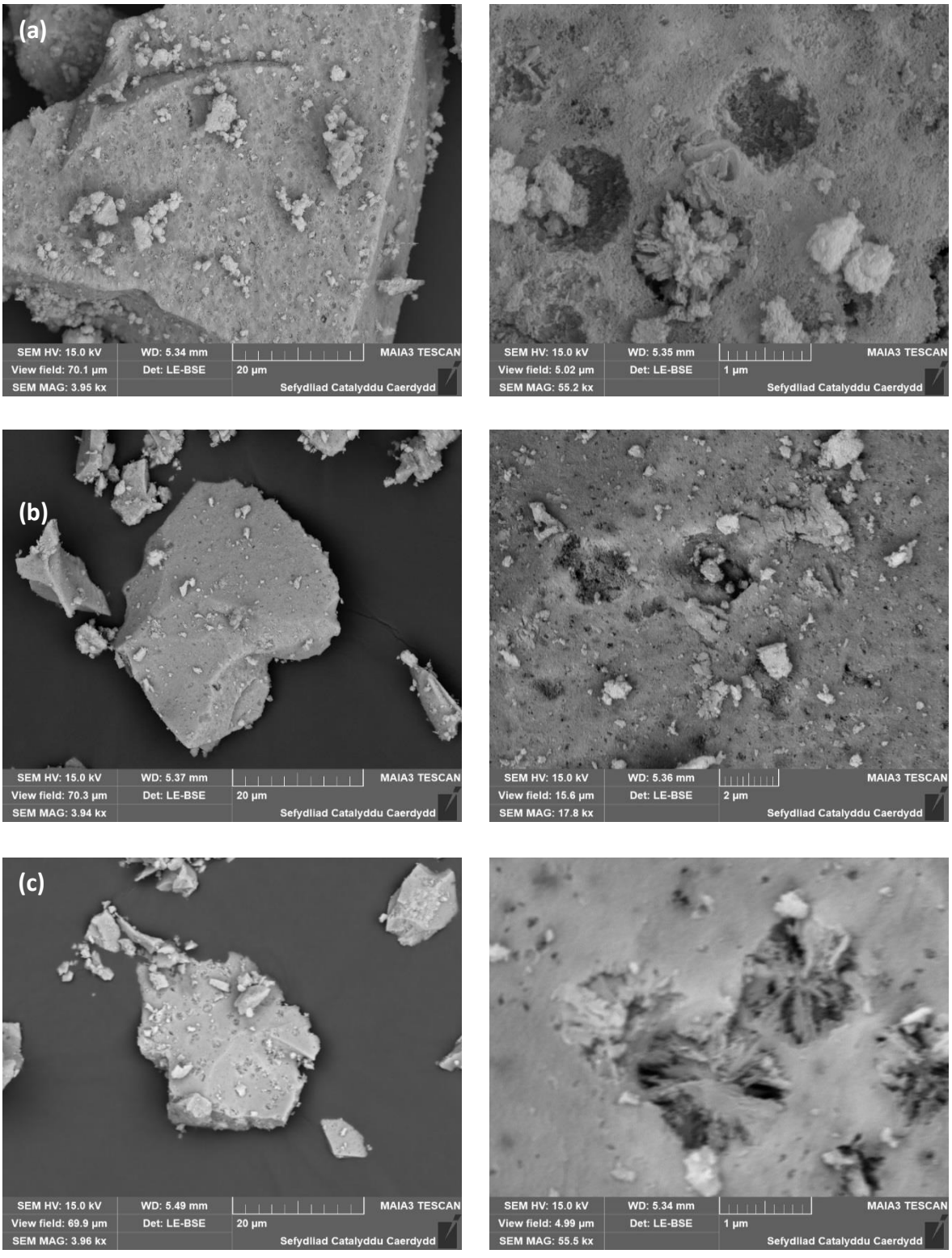

***Figure 77**: SEM images of copper catalysts post acid treatment, a) 50 mol%, b) 10 mol%, c) 5 mol%*

Figure 77shows the SEM images of copper catalysts post acid treatment at two different magnifications. Overall, particle size and distribution of particles has not visibly changed after the acid treatment. There is still a range of particles sizes, from 1 μm to > 50 μm. The catalyst surface is also comparable to pre acid treated catalysts of the same copper concentration (Figure 69), non-ordered pores are again present on the surface, with particles present inside. These non-ordered pores and particles are present for 50, 10 and 5 mol% CuO_x/ZrO_2 catalysts post acid treatment. 5 mol% CuO_x/ZrO_2 has needle like structures present in the non-ordered pores that have not been observed in other catalysts. The needle-like morphology suggests that either the larger particle formed around smaller structures, or that these needles grew out of the pores during the preparation of the catalyst.

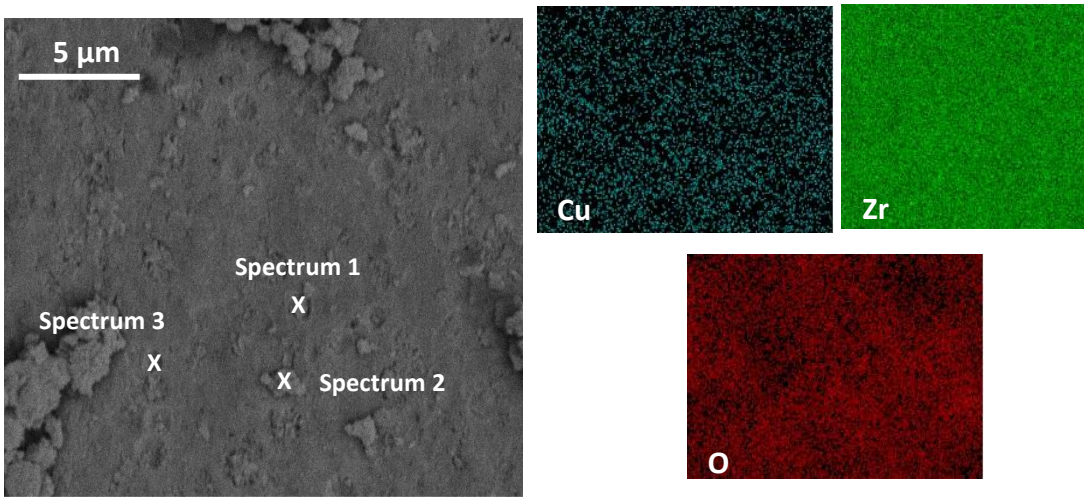

***Figure 78**: EDX analysis of the composition of 50 mol% CuO_x/ZrO_2 after acid treatment. Spectrum 1 – 3 were analysed via EDX to ascertain the composition.*

Figure 78 shows the EDX elemental map analysis of 50 mol% CuO_x/ZrO_2 after acid treatment. There is an even distribution of Cu, Zr and O across the catalyst surface,

in comparison to Figure 70 however, there appears to be less Cu present in the sample. The reduced copper surface concentration shows that the acid treatment has removed copper from the catalyst. To further investigate the composition of the catalyst, spectra were taken at specific points along the catalyst surface; spectrum 1 is on the flat catalyst surface; spectrum 2 of a small particle on the surface; and spectrum 3 of a non-ordered pore on the catalyst surface. The results are shown in **Table 16**.

***Table 16**: Compositional analysis of 50 mol% CuO_x/ZrO_2 after acid treatment*

Spectrum	Mole (%)		
	Cu	Zr	O
1	1	30	69
2	1	25	74
3	1	31	68

Comparison of the mol% of the elements from the three spectrums show that the amount of Cu is constant over the three points analysed and very low, which may be due to the high error associated with EDX, therefore, copper is present in the catalyst still but the amount may not be accurate. The small particle on the surface, spectrum 2, has a 5 mol% increase in O compared to the flat catalyst surface, spectrum 1. The high oxygen content observed in spectrum 2 suggests that small particles on the surface of the catalyst are oxygen rich. Cu mol% on the catalyst surface has decreased from 23 mol%, Table 11, to 1 mol% to after acid treatment, which indicates that the

overall copper amount is decreased and that the acid treatment was successful in removing copper from the surface.

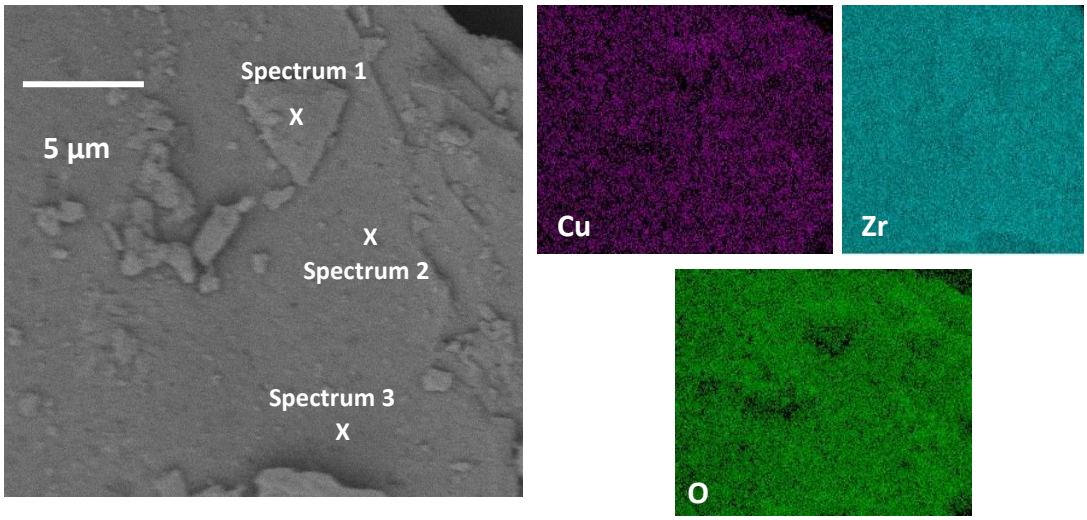

***Figure 79**: Compositional analysis of 10 mol% CuO_x/ZrO_2 after acid treatment. Spectrum 1 – 3 were analysed via EDX to ascertain the composition.*

Figure 79 shows the elemental composition of 10 mol% CuO_x/ZrO_2 acid treated. Over the surface of the catalyst there appears to be an even distribution of Cu, Zr and O. Around the edges of the surface particles, there appears to be less Cu and O present; however, this is most likely due to the detector not being directly over the sample and features may block the signal reaching the detector, creating dark areas on the map.

Specific points on the catalyst surface were chosen and the elemental composition analysed, **Table 17**; spectrum 1 was collected from a particle on the surface of the catalyst; spectrum 2 of a non-ordered pore; and spectrum 3 of the flat catalyst surface.

***Table 17**: Compositional analysis of 10 mol% CuO_x/ZrO_2 after acid treatment.*

Spectrum	Mole (%)		
	Cu	Zr	O
1	4	27	70
2	2	32	66
3	2	26	72

Spectrum 2 exhibits the lowest O mol% of 66, suggesting that the non-ordered pores on the catalyst surface are O deficient. The particles on the surface, as shown in spectrum 1, exhibit the lowest highest Cu mol% of 4, indicating the particles are copper rich in comparison to the flat catalyst surface and the non-ordered pores. The Cu mol% is higher than that observed for the 50 mol% CuO_x/ZrO_2 catalyst, which may suggest that less Cu is removed from the catalyst when the initial Cu content is reduced. Spectrum 3, representative of the general surface of the catalyst, shows that the acid treatment has successfully reduced the Cu content in the catalyst.

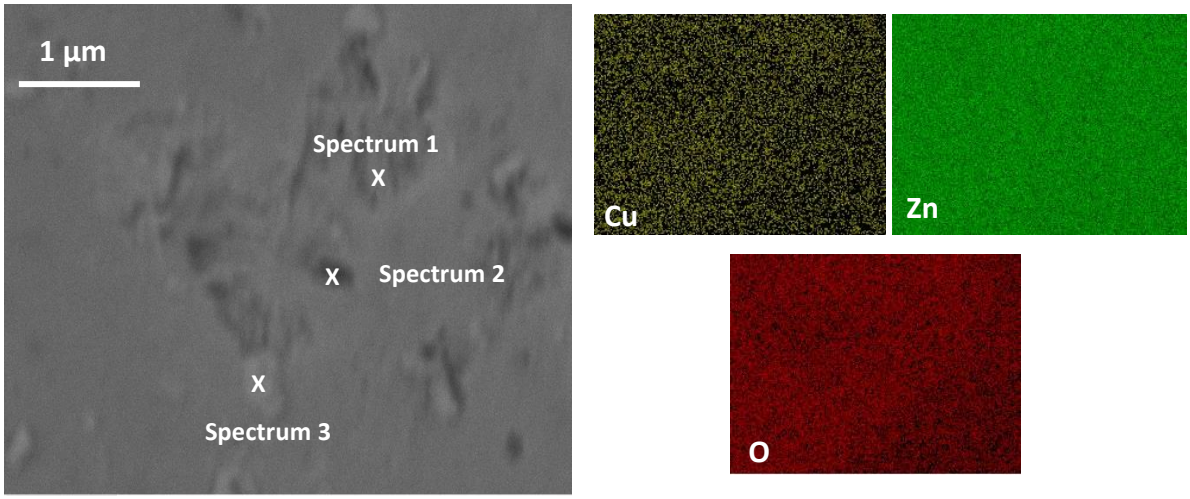

***Figure 80**: EDX analysis of 5 mol% CuO_x/ZrO_2 after acid treatment. Spectrum 1 – 3 were analysed via EDX to ascertain the composition.*

The elemental composition of 5 mol% CuO_x/ZrO_2 after acid treatment is shown in **Figure 80**. Over the surface of the catalyst there is a general distribution of Cu, Zr and O. The elemental maps of the surface of the catalyst show that Zr is evenly dispersed over the surface.

***Table 18**: EDX analysis of 5 mol% CuO_x/ZrO_2 acid treatment*

Spectrum	Mole (%)		
	Cu	Zr	O
1	1	44	55
2	1	55	44
3	1	31	68

Table 18 shows the mol% composition of point spectra on the surface of 5 mol% CuO_x/ZrO_2 post acid treatment, the Cu is less than 10 mol% but the same as 50 mol% due to the error associated with EDX which reduces accuracy of the amount of Cu

and is harder to distinguish between the low levels of Cu in the catalysts after acid treatment Spectrum 1 was taken of a particle situated in one of the non-ordered pores, spectrum 2 of a non-ordered pore on the surface, and spectrum 3 of a particle on the surface. Spectrum 3 has the highest O mol% of 68 %, with the lowest Zr mol% of 31, suggesting that particles on the surface are O rich in comparison to the rest of the catalyst surface. Spectrum 2 has the lowest amount of O, suggesting that the non-ordered pores on the catalyst surface are O deficient.

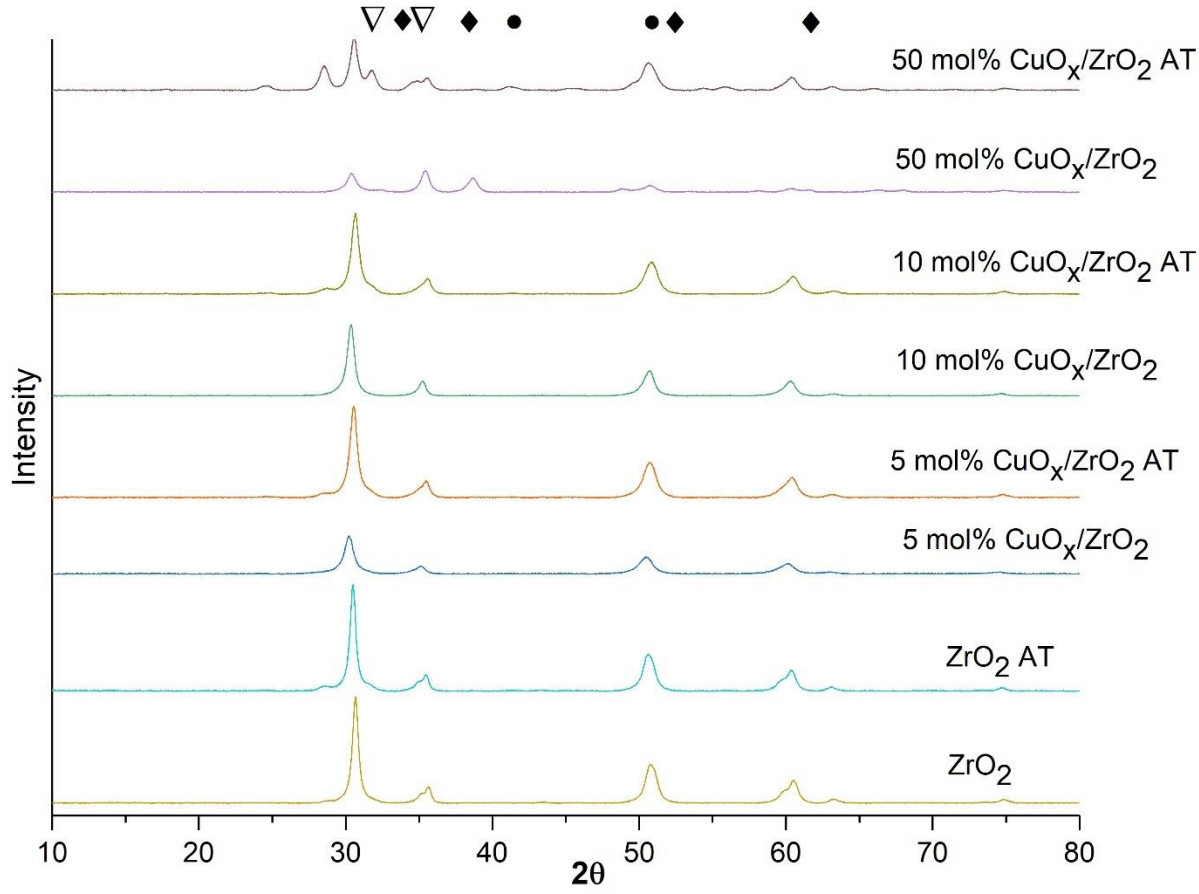

Figure 81*: XRD spectrum of catalysts pre and post acid treatment. AT = acid treated catalyst. ♦ = ZrO_2 peaks, ● = CuO peaks and ∇ = $CuZrO_3$.*

Figure 81 compares the XRD spectrum of the ZrO_2 support and copper catalyst pre and post acid treatment. The black diamonds denote the Zr peaks which were previously identified in Figure 73. The black circles denote the Cu, peaks which were previously identified as monoclinic CuO (ICCD 01-089-5895). For CuO_x/ZrO_2 with 5 and 10 mol%, before and after acid treatment, the same peaks are present.

In comparison to the 5 and 10 mol% CuO_x/ZrO_2 catalysts, the 50 mol% CuO_x/ZrO_2 material shows differences in the XRD peaks pre and post acid treatment. Both the monoclinic CuO peaks, 38.7 and 48.8 °, are no longer present after the acid treatment, which indicates that the acid treatment has removed larger CuO particles from the catalyst. Two new peaks are observed after acid treatment, denoted by black upside down triangles, at 28.5 and 31.8 °. These peaks correspond to orthorhombic $CuZrO_3$ (ICCD 00-043-0953). The presence of $CuZrO_3$ after acid treatment suggests that the acid treatment has induced a phase change of the bulk material and does not only affect the surface of the catalyst.

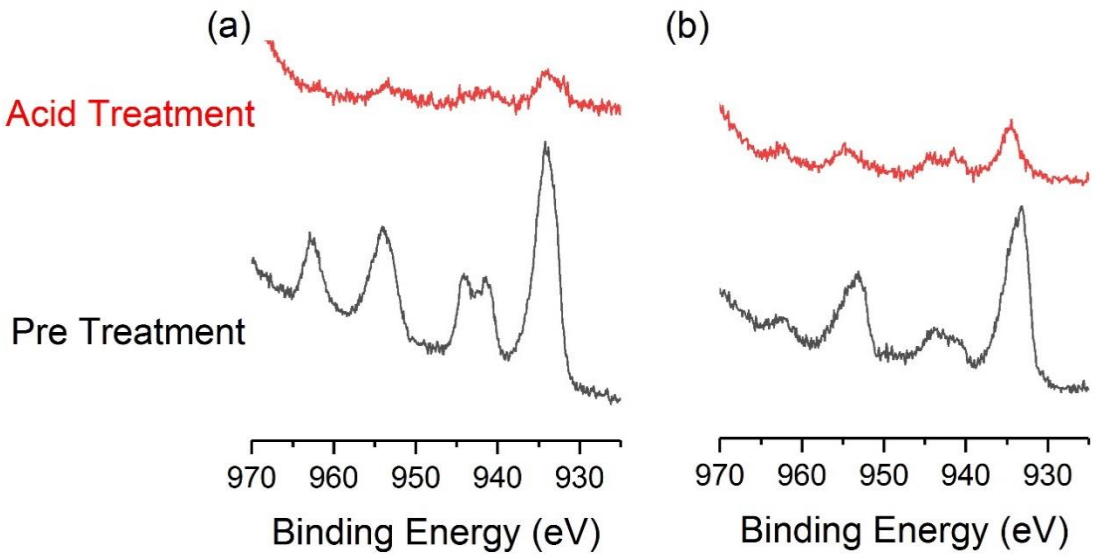

***Figure 82**: XPS analysis of copper 2p/2 peak pre and post acid treatment for (a) 50 mol% CuO_x/ZrO_2 and (b) 10 mol% CuO_x/ZrO_2*

Figure 82 shows the XPS analysis of copper 2p/2 peaks for copper catalysts before and after acid treatment. For the 50 mol% CuO_x/ZrO_2 catalyst, Figure 82 (a), there is a large decrease in the intensity of the peaks indicating the removal of copper from the surface of the catalyst. The peaks have not shifted after acid treatment, but, the satellite peak (941 eV) is more diffuse, indicating the presence of Cu(II)OH species alongside Cu(II)O.[28] A similar trend is observed for 10 mol% CuO_x/ZrO_2, Figure 82 (b), indicating the presence of Cu(II)OH. As there is a high noise to signal ratio in the spectrum of acid treated catalysts, it is difficult to draw robust conclusions from the data. The O 1s/4 peak was also analysed, displayed in Figure 83.

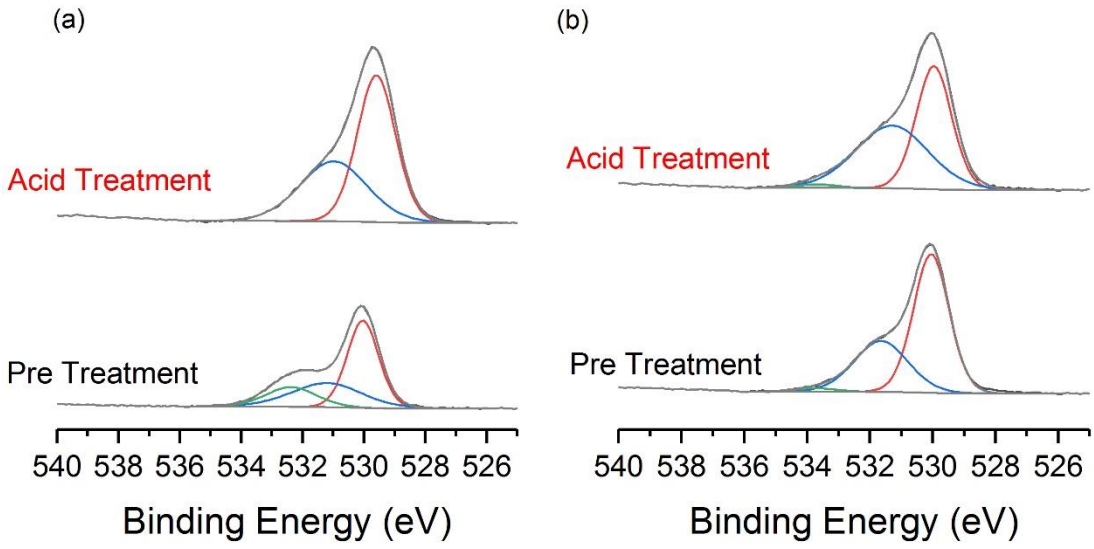

***Figure 83**: XPS analysis of O peak 1s/4 pre and post acid treatment for (a) = 50 mol% CuO_x/ZrO_2 and (b) = 10 mol% CuO_x/ZrO_2*

For both 50 and 10 mol% CuO_x/ZrO_2 catalysts pre and post acid treatment, the O 1s/4 peak is similar in shape and intensity. The broadening of the peak suggests the presence of hydroxide groups on the surface.[29] Overall, for both copper contents, pre and post acid treatment, this suggests the presence of hydroxide on the surface that is not removed by the acid treatment.

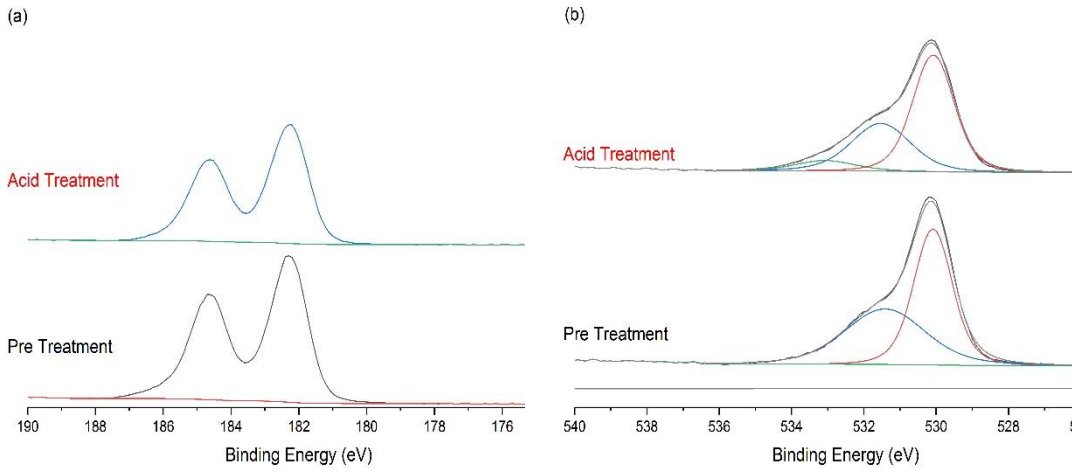

***Figure 84**: XPS analysis of ZrO_2 support material prepared by sol gel method, pre and post acid treatment. (a) = Zr 3d/7 peaks and (b) = O 1s/4 peaks*

Figure 84 shows the XPS analysis of (a) Zr 3d/7 peaks and (b) O 1s/4 peaks of ZrO_2 prepared by the oxalate gel method. Comparing the Zr peaks before and after acid treatment, there is little change in the shape and intensity of the peaks found at 182 and 184 eV. These align with the literature vales for cubic zirconia.[32] The peaks are, however, broader than expected and asymmetrical, which could indicate the presence of $Zr(OH)_2$ with a binding energy of 184 eV.[33] The O 1s/4 peaks, shown in Figure 84 (b), also show broadening, which indicates the presence of hydroxide groups.[28] The ratio of Cu and O to Zr was identified for copper catalysts pre and post acid treatment, to assess how the acid treatment affects the surface composition of the catalyst, and is presented in Table 19.

***Table 19**: Concentration ratio of elements present in catalysts analysed via XPS, in relation to Zr.*

Catalyst	Ratio to Zr	
	Cu	**O**
10 mol% CuO_x/ZrO_2 Pre-Acid Treatment	0.19	2.49
10 mol% CuO_x/ZrO_2 Post Acid Treatment	0.06	2.54
50 mol% CuO_x/ZrO_2 Pre-Acid Treatment	0.43	3.25
50 mol% CuO_x/ZrO_2 Post Acid Treatment	0.04	3.25
ZrO_2 Pre-Acid Treatment	-	2.39
ZrO_2 Post Acid Treatment	-	2.55

Comparing the copper content ratio pre and post acid treatment for 10 mol% CuO_x/ZrO_2, there is a reduction from 0.19 to 0.06, showing that the acid treatment has effectively removed surface copper from the catalyst. A larger reduction is observed for 50 mol%, from 0.43 to 0.04, again showing that the acid treatment has removed large amounts of copper from the surface. Overall, the decrease in surface copper content post acid treatment shows that the acid treatment was successful in removing copper from the surface.

4.2.5.2 *Surface Area*

Given the significant changes in the Cu surface concentration observed through EDX and XPS when comparing pre and post acid treated catalysts, BET and N_2O titration were used to investigate the surface area. Effect of acid treatment on the catalyst

surface area and the copper surface area was investigated with the results shown in Table 20 which compares the BET surface area of 50, 10 and 5 mol% CuO_x/ZrO_2 pre and post acid treatment.

***Table 20**: BET surface area before and after acid treatment for copper catalysts.*

Catalyst	Surface Area Pre-Acid Treatment (m^2/g)	Surface Area Post Acid Treatment (m^2/g)
50 mol% CuO_x/ZrO_2	24	62
10 mol% CuO_x/ZrO_2	68	110
5 mol% CuO_x/ZrO_2	66	50

For the 50 mol% CuO_x/ZrO_2 catalyst, the surface area increases from 24 to 62 m^2/g after the acid treatment, indicating that the acid treatment reduces the copper concentration on the surface of the catalyst as the acid treatment has removed large Cu particles that decrease the surface area. Lowering the copper concentration to either 10 or 5 mol% increases the surface area to 60 – 69 m^2/g, as shown in Table 13. A larger increase in surface area is observed for 10 mol% CuO_x/ZrO_2 from 68 to 110 m^2/g, indicating a reduction in surface copper, or the acid treatment may be increasing the number of surface non-ordered pores that have been observed and increase the total surface area. The 5 mol% CuO_x/ZrO_2 post acid treatment sample exhibits a decrease in surface area to 50 m^2/g.

Orlowski et al.[18] used a similar acid treatment for copper zirconia catalysts prepared by the oxalate gel method, with the amount of copper lost during the acid treatment, and the BET surface area after acid treatment, was measured.The percentage of copper lost was greater with increasing initial copper concentration, as well as the

BET surface area was lower at larger copper crystallite sizes. Therefore, for a higher copper concentration, a greater percentage of copper is lost, reducing the copper crystallite size and increasing the BET surface area; the effect is reduced as the initial copper concentration is decreased.

To assess the effect of the acid treatment on the copper surface area, N_2O titration was used to measure the surface area post acid treatment for comparison to the catalyst pre acid treatment.

***Table 21**: Copper surface area of copper catalysts before and after acid treatment*

Catalyst	Copper Surface Area Pre-Acid Treatment (m^2/g)	Copper Surface Area Post Acid Treatment (m^2/g)
50 mol% CuO_x/ZrO_2	6.4	0.4
10 mol% CuO_x/ZrO_2	4.6	0.2
5 mol% CuO_x/ZrO_2	2.2	0.2

Table 21 shows the 50, 10 and 5 mol% copper surface area pre and post acid treatment. Overall, acid treatment decreases copper surface area to 0.4 – 0.2 m^2/g, so no significant difference between different initial copper concentrations. Therefore, acid treatment does remove copper from the surface of the catalysts but a small amount does remain on the surface.

4.2.6 *Morin Oxidation of Developed Heterogeneous Catalysts*

Copper catalysts have been identified as bleach active for removal of tea stains from a cup surface. To further investigate the bleach activity of the acid treated catalyst, the acid treated catalysts were investigated for morin oxidation activity. The aim is

to assess the morin conversion in comparison to the fresh catalyst and how temperature and acid concentration may affect activity.

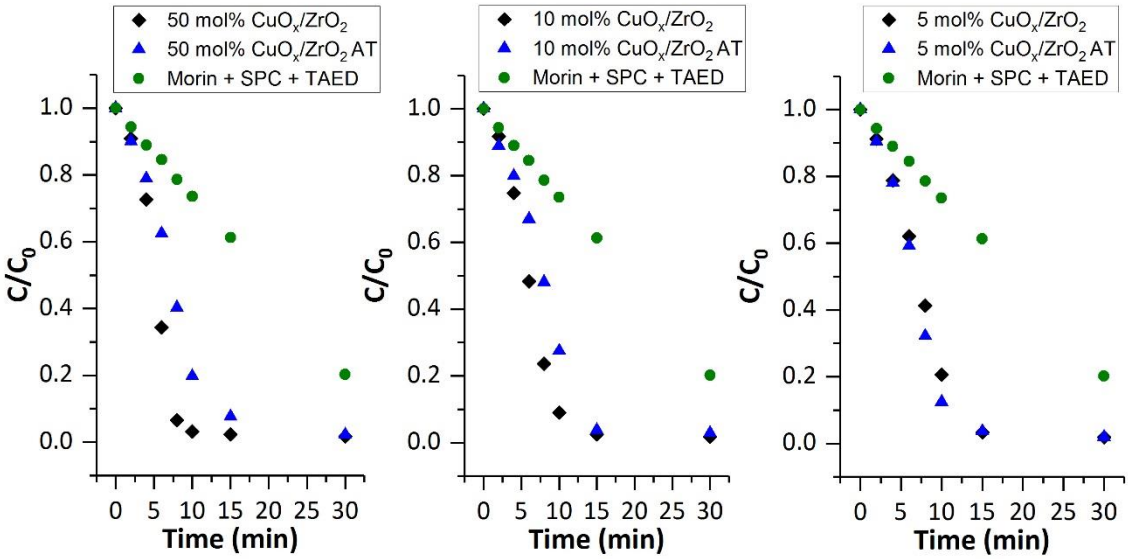

***Figure 85**: Copper catalyst post acid treatment morin conversion. Water (90 mL), morin (0.1 mM), sodium percarbonate (5.3 mM), TAED (1.1 mM), sodium carbonate (50 mM), catalyst (0.1 mg), pH = 10, 30 mins. Average error = 7%.*

Figure 85 shows the morin conversion of copper acid treated catalysts at 50, 10 and 5 mol% copper concentration. Overall, the acid treated catalysts are less active for morin oxidation than the fresh catalyst. Comparing the catalyst post acid treatment after 8 min, 5 mol% CuO_x/ZrO_2 has the highest conversion of 67.8%, with 10 mol% and 50 mol% displaying a conversion of 51.9% and 59.7% respectively. Although the 5 mol% CuO_x/ZrO_2 acid treated catalyst was the most active acid treated material, both the 50 mol% and 10 mol% Cu catalysts before acid treatment have a higher morin oxidation activity. Overall, the non-acid treated catalysts exhibit a higher morin oxidation activity than the acid treated catalysts, which is the opposite trend observed for the TC test.

***Table 22**: Rate of morin conversion comparison of pre and post acid treated catalysts.*

Catalyst	Rate of Morin Conversion 0 - 4 mins (mM s^{-1} x10^{-5})	Rate of Morin Conversion 4 - 8 mins (mM s^{-1} x10^{-5})
No Catalyst (morin + SPC + TAED)	4.2	4.0
50 mol% CuO_x/ZrO_2 pre acid treatment	10.9	26.4
50 mol% CuO_x/ZrO_2 post acid treatment	7.9	14.5
10 mol% CuO_x/ZrO_2 pre acid treatment	9.3	18.8
10 mol% CuO_x/ZrO_2 post acid treatment	8.0	12.6
5 mol% CuO_x/ZrO_2 pre acid treatment	7.9	13.9
5 mol% CuO_x/ZrO_2 post acid treatment	8.4	17.5

The rate during the first and second 4 mins of the reaction have been calculated for pre and post acid treated catalysts, as shown in **Table 22**. The rates of morin oxidation with the acid treated catalyst are lower than for the pre acid treated catalyst; however, the difference between the rate at 4 mins and the rate at 8 mins decreases with copper content. For 50 mol%, the difference is 3.0 mM s^{-1}, compared to at 10 mol% where the difference is 1.3 mM s^{-1}. The increase of rate for 8 mins indicates that the catalysts both pre and post acid treatment have an induction period, which may be due to the formation of radicals on the surface of the catalyst after the initial step of absorption of reagents.

For the 5 mol% CuO_x/ZrO_2 catalyst, acid treatment improves the morin oxidation activity of the catalyst. The positive improvement in catalyst activity with acid treatment is only observed with the 5 mol% catalysts, and the opposite is observed for 50 mol% and 10 mol%. In comparison to the TC test, as shown in Figure 58, morin

is in the homogeneous phase of the reaction, whereas a tea stain is heterogeneous. Similar to the previous data shown in section 1.2.1.1, metal leaching from the catalyst may play a role in the conversion of morin. To investigate the effect of metal leaching, reaction solutions were analysed by ICP-AES to determine copper concentration. Table 23 shows the metal leaching during morin oxidation reactions comparing 50 mol% CuO_x/ZrO_2 pre and post acid treatment.

***Table 23**: Copper leaching pre and post acid treatment measured via ICP*

Catalyst	Cu Metal Leaching (%)	
	Pre-Acid Treatment	**Post Acid Treatment**
50 mol%	3.2	0.0

Acid treatment decreases the metal leached during the solution from 3.2% to 0%, which could contribute to the lower morin conversion after acid treatment. As copper salts were previously shown to be active for the reaction in Figure 68, the high conversion observed could be due to homogeneous oxidation of morin alongside heterogeneous oxidation. The leaching would increase with copper content, and therefore 50 mol% CuO_x/ZrO_2 is more active for morin oxidation than 5 mol% CuO_x/ZrO_2. Having the oxidation of morin occur with both heterogeneous and homogeneous catalysts, unlike the TC test, shows how the catalyst activity is different when comparing morin oxidation and tea stain bleaching.

4.2.6.1 *Effect of Acid Concentration*

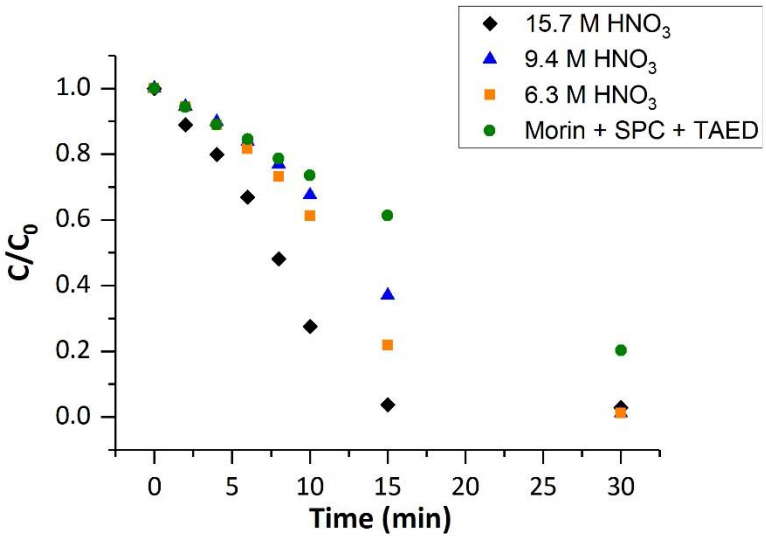

***Figure 86**: Effect of acid concentration on morin oxidation activity. Water (90 mL), morin (0.1 mM), sodium percarbonate (5.3 mM), TAED (1.1 mM), sodium carbonate (50 mM), catalyst (0.1 mg), pH = 10, 30 mins. Average error = 7%.*

As previously shown in Figure 60, the effect of changes in catalyst preparation on bleach activity can be difficult to detect using tea stains. Therefore, the effect of acid concentration used to pre-treat the catalyst on bleach activity was studied using the oxidation of morin as shown in Figure 86. The concentration of HNO_3 used in the acid treatment of 10 mol% CuO_x/ZrO_2 was decreased from 15.7 to 9.4 and 6.3 M. The catalysts were then tested for morin oxidation in the presence of sodium percarbonate and TAED over 30 mins. In the first 8 mins of the reaction, the concentration of 15.7 M HNO_3 used for acid treatment has a higher conversion than the reaction without a catalyst; however, 9.4 and 6.3 M, exhibit similar conversions to the reaction without a catalyst. At 15 mins, 15.7 M has the highest conversion, with 6.3 M then 9.4 M with the lowest conversion. During the reaction both the 9.4 and 6.3 M catalysts have similar conversions. The result suggests that stirring the

catalyst in 15.7 M HNO_3 produces the most active catalyst and, at lower acid concentrations, there is little difference in bleach activity between catalysts produced.

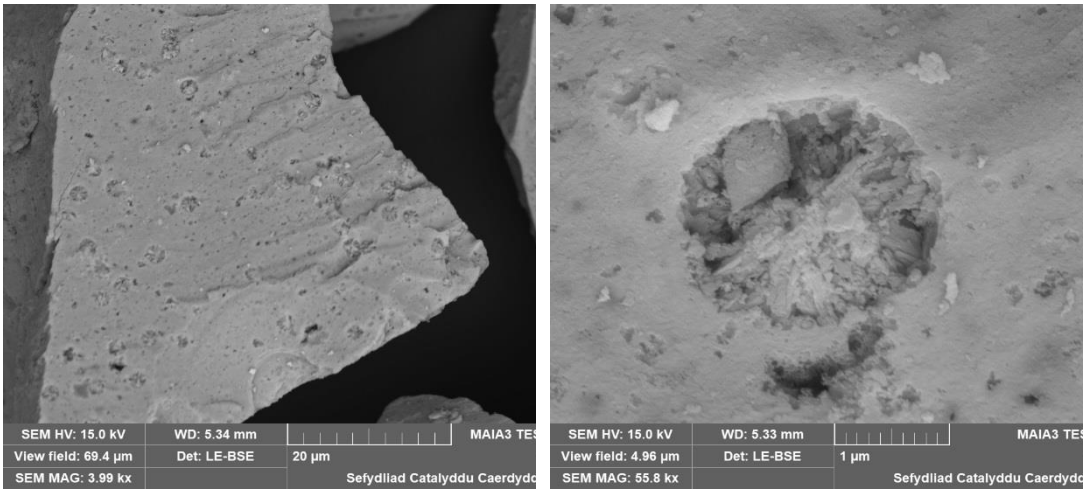

***Figure 87**: SEM images of 10 mol% CuO_x/ZrO_2 acid treated with 6.3 M HNO_3*

Overall, the particle sizes and surface of the catalyst treated with 6.3 M HNO_3, displayed in Figure 87, is similar to the catalyst acid treated with 15.7 M HNO_3, Figure 77, indicate that decreasing the acid concentration does not affect the catalyst surface and particles size. The surface composition was analysed *via* EDX as shown in Figure 88.

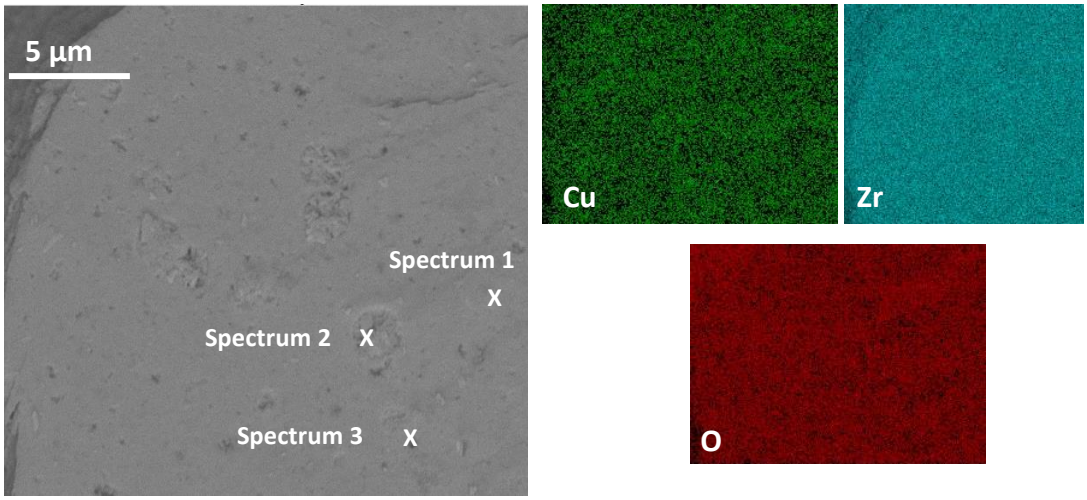

***Figure 88**: EDX elemental analysis of the surface of 10 mol% CuO_x/ZrO_2 acid treated with 6.3 M HNO_3. Spectrum 1 – 3 analysed via EDX to ascertain the composition.*

A map analysis of the surface shows that Cu, Zr and O are present across the surface with no clear areas of abundancy or deficiency. Point spectra were analysed presented in Table 24. Spectrum 1 is of the catalyst surface; spectrum 2 of a particle in a non-ordered pore; and spectrum 3 of a surface non ordered pore.

***Table 24**: EDX elemental analysis of 10 mol% CuO_x/ZrO_2 acid treated with 6.3 M HNO_3*

Spectrum	Mole (%)		
	Cu	Zr	O
1	3	32	65
2	3	24	73
3	3	57	40

The amount of Cu present on the surface is comparable to 10 mol% CuO_x/ZrO_2 after acid treatment with 15.7 M HNO_3, as displayed in **Table 17**. Spectrum 3 has the lowest O mol% of 40, suggesting that non ordered pores on the surface are oxygen

deficient. The particle in a non-ordered pore on the surface presented in spectrum 2 has the lowest Zr mole% of 24, indicating that the particles present in the non-ordered pores are Cu rich and O deficient in comparison to the catalyst surface. Overall, it appears that decreasing the concentration of acid used to treat the catalyst does not decrease the amount of copper removed from the surface.

4.2.6.2 *Effect of Radical Scavenger (RS) on Morin Oxidation in the Presence of Copper Heterogeneous Catalysts*

The bleaching system with sodium percarbonate and TAED is generally accepted to go *via* hydroxyl anion.[34] The addition of MnTACN to the bleach system improves the bleach activity of the system and the stain is oxidised using Mn-Mn-OOH species and does not go *via* a radical mechanism.[26] Therefore, to investigate if heterogeneous catalysts for bleaching goes *via* a radical mechanism, a radical scavenger was added to the morin oxidation reaction to assess if this affected the activity of the catalyst.

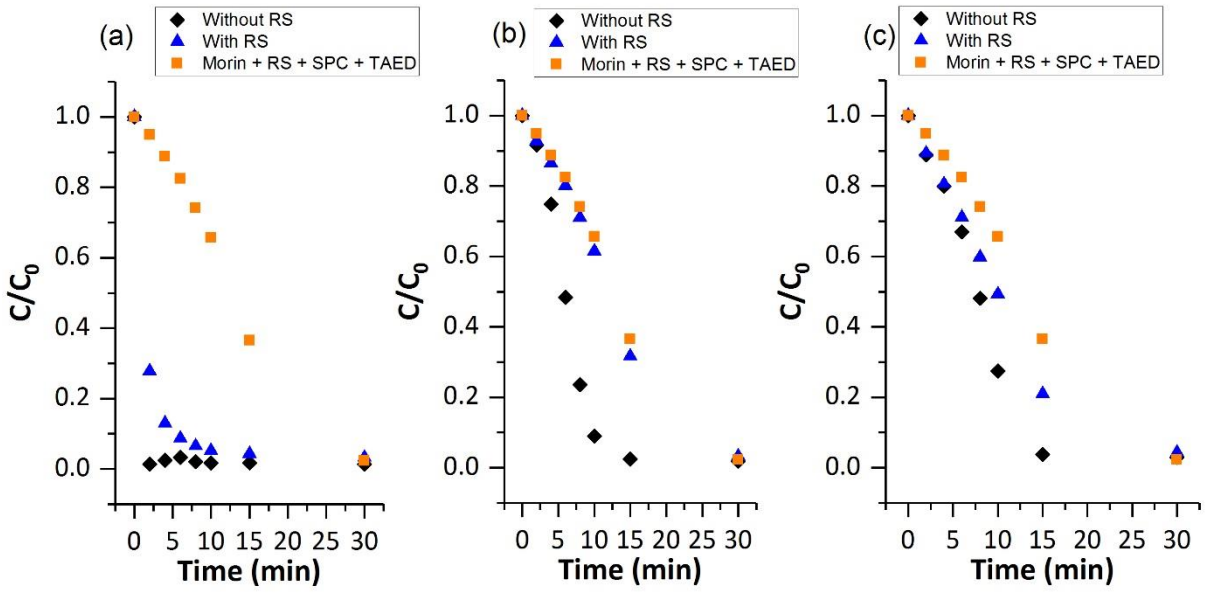

***Figure 89**: Morin oxidation in the presence of a radical scavenger, (a) = MnTACN catalyst, (b) = 10 mol% CuO_x/ZrO_2 pre acid treatment, (c) = 10 mol% CuO_x/ZrO_2 post acid treatment. Water (90 mL), morin (0.1 mM), sodium percarbonate (5.3 mM), TAED (1.1 mM), Mannitol (5.3 mM), sodium percarbonate (50 mM), catalyst (0.1 mg), pH = 10.5, 50 °C, 8 mins, Average error = 7%.*

Mannitol is a known radical scavenger and can react with radicals in solution. Therefore, if a reaction proceeds *via* a radical route, an excess of Mannitol would reduce the conversion or halt the reaction. An excess of mannitol was added to the morin oxidation reaction in the presence of MnTACN and 10 mol% CuO_x/ZrO_2 pre and post acid treatment displayed in Figure 89.

***Table 25**: Rate of morin oxidation with and without a radical scavenger (RS) present.*

Catalyst	Rate of Morin Conversion 0 - 4 mins (mM s^{-1} x10^{-5})	Rate of Morin Conversion 4 - 8 mins (mM s^{-1} x10^{-5})
Morin + RS + SPC + TAED	4.5	5.8
MnTACN	37.8	0.16
MnTACN + RS	34.8	2.6
10 mol% CuO_x/ZrO_2 pre acid treatment	9.3	18.8
10 mol% CuO_x/ZrO_2 pre acid treatment + RS	5.7	6.5
10 mol% CuO_x/ZrO_2 post acid treatment	8.0	12.6
10 mol% CuO_x/ZrO_2 post acid treatment + RS	7.4	7.9

The rate of morin conversion calculated for the 0-4 and 4-8 minute intervals of the reaction, are shown in **Table 25**. Addition of mannitol (RS) to the reaction, in the presence of MnTACN, reduces the rate of morin conversion from 37.8 to 34.8 mM s^{-1}, which is a small reduction. An increase in rate appears from 4 – 8 mins, as the MnTACN converts the remaining morin, which suggests that some MnTACN activity could be attributed to the presence of radicals.

For both pre and post acid treated 10 mol% CuO_x/ZrO_2, the rate of morin oxidation is reduced in the presence of mannitol, with a higher reduction of rate observed for 4 – 8 mins. The pre acid treated catalyst had a reduction of 12.3 mM s^{-1}, and the post acid treated catalyst a reduction of 4.7 mM s^{-1} during 4 – 8 mins of the reaction. The

reduction in rate during the second time interval suggests that the induction period of the catalyst is due to the formation of radicals, as the induction period is not observed in the presence of mannitol.

Overall, the heterogeneous oxidation of morin indicates that radicals are generated on the catalyst surface or in solution and are used to oxidise morin. Without mannitol present, the rate of conversion increases at 4 – 8 mins compared to 0 – 4 mins, suggesting that there is an induction phase that could be the propagation of the active radical species on the catalyst surface. The addition of a radical scavenger does not completely remove the activity of the copper catalysts, and the activity of the catalysts is comparable to the reaction with no catalyst present. The comparable activity of the reaction with no catalyst and a copper catalyst in the presence of a radical scavenger indicates that the catalyst does not use all the reagents present to produce radicals and the oxidation can still proceed *via* hydroxyl anions.

4.2.7 *Other Metal Catalysts*

Mn, Fe and Zn were also investigated for bleach activity. These metals have been investigated for similar reactions with H_2O_2 and in bleaching in the literature. As it was found that acid treatment improved the bleach activity of copper catalysts, the same acid treatment was also used for Fe and Mn catalysts. These catalysts had previously not shown any bleach activity for tea stain removal shown in Figure 57.

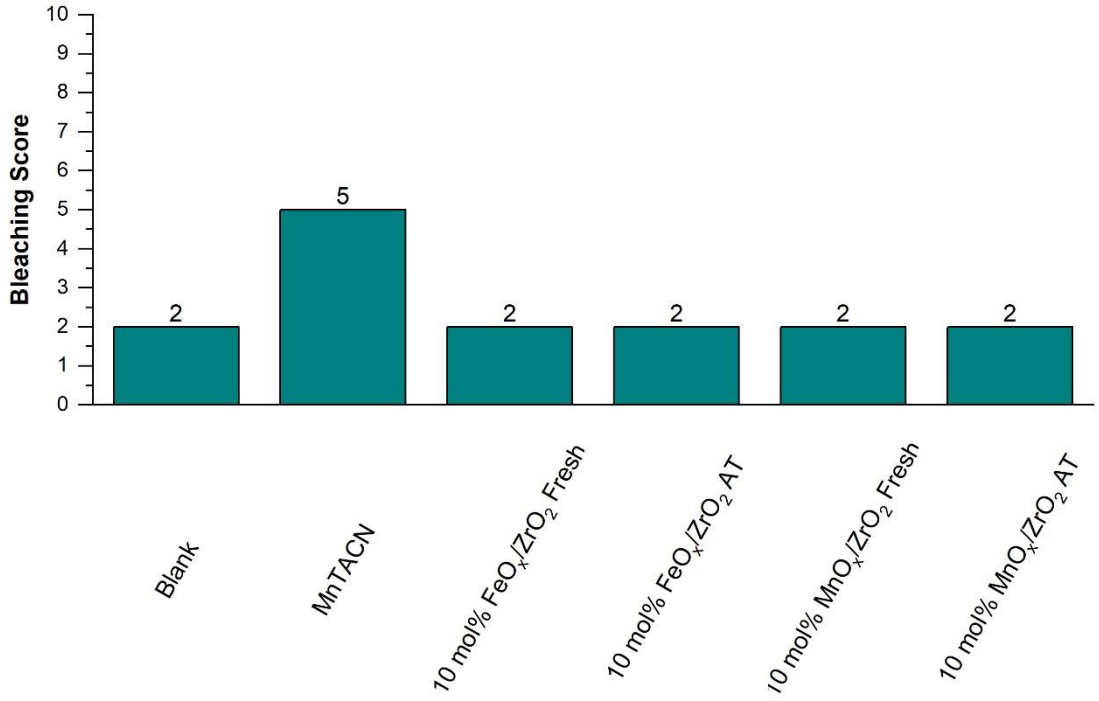

***Figure 90**: Water (1.8 L), sodium percarbonate (5.3 mM), TAED (1.1 mM), MGDA (0.4 mM), catalyst (3 mg), 50 °C, 8 mins, pH = 10, water hardness = 5 °dH. Bleach activity of Mn and Fe catalysts before and after acid treatment. Average error = ± 1.*

10 mol% Fe and 10 mol% Mn pre and post acid treatment were tested for tea stain removal presented in Figure 90. All heterogeneous catalysts scored a 2 for tea stain removal, indicating that the catalysts even after acid treatment are not active for bleaching.

A series of Zn derived ZnO/ZrO_2 catalysts were prepared and tested for bleach activity displayed in **Figure 91**. In addition to this, $ZnCO_3$ and ZnO was also tested, to assess if carbonate groups on the surface or ZnO particles were responsible for bleach activity. Carbonate groups were on the surface of the copper catalysts when characterised *via* DRIFTS, presented in Figure 61, which could then be active species on the catalyst surface.

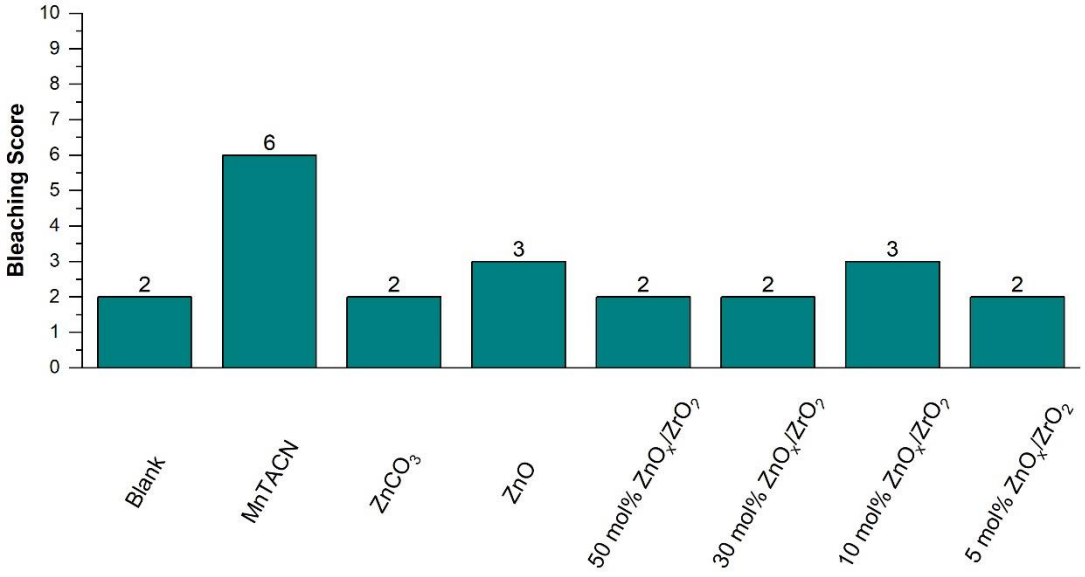

***Figure 91**: Initial investigation into bleach activity of Zn catalysts. Water (1.8 L), sodium percarbonate (5.3 mM), TAED (1.1 mM), MGDA (0.4 mM), catalyst (3 mg), 50 °C, 8 mins, pH = 10, water hardness = 5 °dH. Average error = ± 1.*

Overall, ZnO and 10 mol% ZnO_x/ZrO_2 were shown to be bleach active with a bleaching score of 3. In comparison, higher Zn concentration catalysts were not active for bleaching and exhibited the same score as the reaction with no catalyst (2). As Zn is active for bleaching, a series of bimetallic catalysts were prepared to increase the bleaching performance of copper heterogeneous catalysts. A ratio of Cu:Zn of 1:1, at varying overall concentration of Cu/Zr mixture, was used, the bleach activity of these catalysts are shown in **Figure 92**.

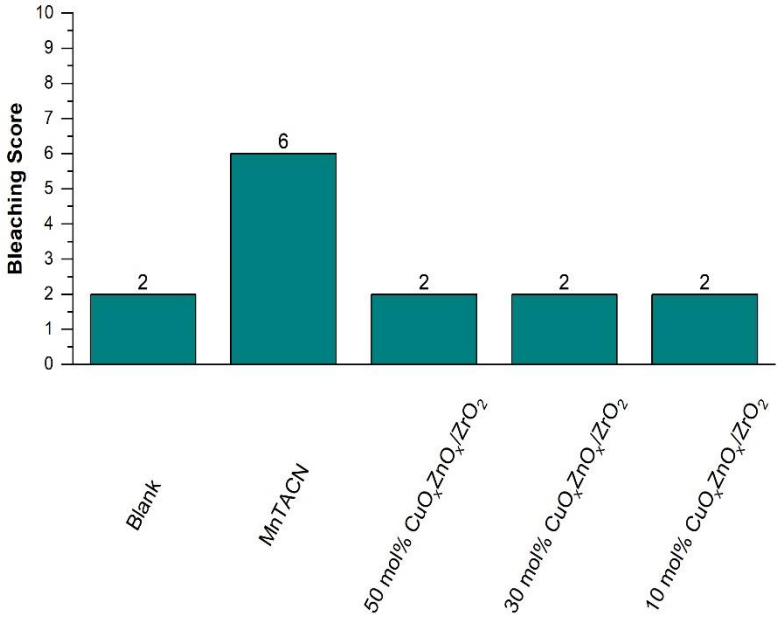

***Figure 92**: Bimetallic catalyst bleach activity. Water (1.8 L), sodium percarbonate (5.3 mM), TAED (1.1 mM), MGDA (0.4 mM), catalyst (3 mg), 50 °C, 8 mins, pH = 10, water hardness = 5 °dH. Average error = ± 1.*

Addition of Zn to the Cu catalysts, from concentration of 50 to 10 mol%, does not improve the bleaching without a catalyst.

To further investigate bleach activity of different metal oxide besides Cu catalysts, a range of Mn and Zn catalysts, with and without acid treatment, were assessed for oxidation of morin in solution. Mn was used as Mn based homogeneous catalysts are already used in current bleach formulations. Initially, 10 mol% MnO_x/ZrO_2 pre and post acid treatment was tested for morin oxidation activity shown in **Figure 93**.

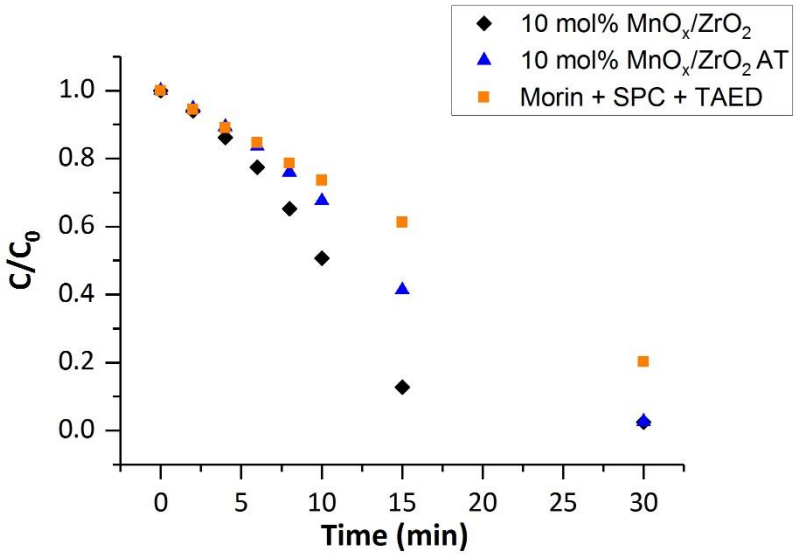

***Figure 93**: Activity of Mn catalyst pre and post acid treatment. Water (90 mL), morin (0.1 mM), sodium percarbonate (5.3 mM), TAED (1.1 mM), sodium carbonate (50 mM), catalyst (0.1 mg), pH = 10, 30 mins. Average error = 7 %.*

During the first 4 mins of the reaction there is no significant difference in the reaction with the addition of a Mn based heterogeneous catalyst. Morin oxidation increases in the presence of 10 mol% MnO_x/ZrO_2 pre acid treatment after 6 mins, and overall morin conversion is higher after 15 mins for the 10 mol% MnO_x/ZrO_2 without acid treatment when compared with the catalyst with acid treatment. At 15 mins, conversion with the pre acid treatment catalyst is 87%, and with the post acid treated catalyst is 59%.

The same reaction was then carried out with Zn catalysts. 50 and 10 mol% pre and post acid treatment were tested for morin oxidation displayed in Figure 94.

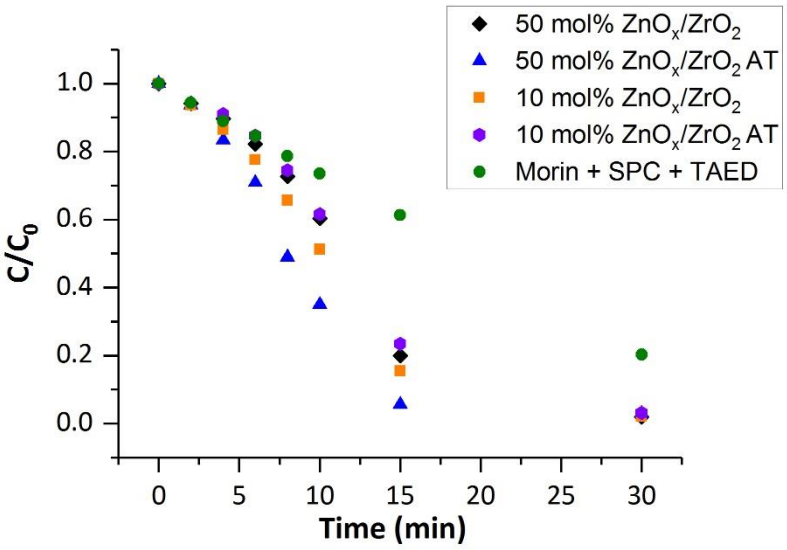

***Figure 94**: Activity of Zn catalysts pre and post acid treatment. Water (90 mL), morin (0.1 mM), sodium percarbonate (5.3 mM), TAED (1.1 mM), sodium carbonate (50 mM), catalyst (0.1 mg), pH = 10, 30 mins. Average error = 7 %.*

***Table 26**: Rate of morin oxidation with ZnO/ZrO_2 catalysts pre and post acid treatment.*

Catalyst	Rate of Morin Conversion 0 - 4 mins (mM s^{-1} x10^{-5})	Rate of Morin Conversion 4 - 8 mins (mM s^{-1} x10^{-5})
No Catalyst (morin + SPC + TAED)	4.2	4.0
50 mol% ZnO_x/ZrO_2 pre acid treatment	4.2	6.8
50 mol% ZnO_x/ZrO_2 post acid treatment	6.4	13.1
10 mol% ZnO_x/ZrO_2 pre acid treatment	5.2	8.1
10 mol% ZnO_x/ZrO_2 post acid treatment	3.5	6.4

As with the Mn catalysts, there is no significant difference in conversion with and without a catalyst present in the first 4 mins of the reaction. After 15 mins, each Zn catalyst resulted in a conversion of morin above 75%. The activity order of the catalyst from lowest to highest conversion after 15 mins is: 10 mol% post acid treatment < 50 mol% pre acid treatment < 10 mol% pre acid treatment < 50 mol% post acid treatment.

Comparing catalysts pre acid treatment, 10 mol% is more active for morin oxidation than 50 mol% with a conversion difference of 5%. Acid treatment decreases the activity of the 10 mol% catalyst but increases the activity of the 50 mol% catalyst, which could be due to a difference in Zn leaching during the reaction, as shown in **Table 27** As morin oxidation is catalysed by homogeneous catalysts, an increase in metal leaching may lead to active metal salts, improving the morin oxidation activity. This trend is however only observed for the 10 mol% catalyst and the trend is reversed for 50 mol%.

To assess the leaching during the morin reaction, samples were taken post reaction and analysed *via* ICP. Results are shown in **Table 27**.

***Table 27**: ICP analysis of Zn and Mn catalysts after morin oxidation reaction.*

Catalyst	Metal Leaching (%)	
	Zn	Mn
50 mol% ZnO_x/ZrO_2 Pre-Acid Treatment	14.8	-
50 mol% ZnO_x/ZrO_2 Post Acid Treatment	12.1	-
10 mol% MnO_x/ZrO_2 Pre-Acid Treatment	-	5.2

For the 50 mol% Zn catalyst, acid treatment decreases metal leaching by 2.7%, from 14.8 to 12.1 %. This is a small change in metal concentration in solution during the reaction, with both catalysts leaching significant amounts of Zn into solution. The result suggests that metal salts leaching into solution are responsible for morin oxidation activity observed, because the acid treated catalysts is more active than the catalyst without and similar levels of Zn leaching is observed.

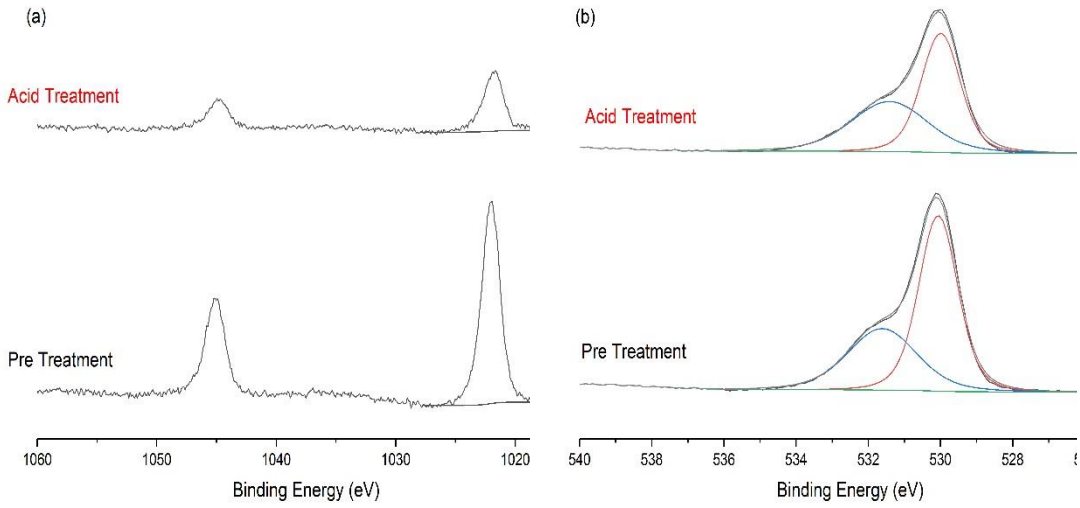

***Figure 95**: XPS analysis of 10 mol% ZnO_x/ZrO_2 pre and post acid treatment, (a) = Zn region and (b) = O 1s/4 region*

To further understand the surface of the Zn catalysts, XPS was used to characterise the ZnO_x/ZrO_2 catalysts. **Figure 95** shows the XPS of the Zn and O regions of 10 mol% ZnO_x/ZrO_2 pre and post acid treatment. For the Zn region, two peaks are observed at 1022.0 and 1045.1 eV, which correspond to 2p3/2 and 2p1/2.[35] The peaks do not shift after acid treatment, but there is a reduction in the intensity, suggesting that there is a removal of Zn from the surface after the acid treatment. As with the Cu catalysts, there is broadening observed in the Zn and O XPS, suggesting the presence of OH groups on the surface.[28] **Table 28** shows the composition of the catalyst surface, which also indicates the reduction of Zn concentration on the surface of the catalyst after acid treatment.

Table 28*: Compositional analysis via XPS of 10 mol% ZnO_x/ZrO_2 pre and post acid treatment, concentration ratios in relation to Zr*

Catalyst	Ratio to Zr	
	Zn	O
10 mol% ZnO_x/ZrO_2 pre acid treatment	0.13	2.64
10 mol% ZnO_x/ZrO_2 post acid treatment	0.05	2.45

4.3 *Discussion*

A range of mixed metal oxide catalysts were tested for bleaching activity using morin oxidation as a bleach model and on tea stains prepared on TCs. Mn, Fe, Cu, and Zn derived catalysts were prepared using the oxalate gel method, with ZrO_2 serving as a support material. Initial investigation into the bleach activity with Mn, Fe, and Cu showed that Cu was active for bleaching tea stains, compared to bleaching with no catalyst present, (Figure 57). 10 mol% CuO_x/ZrO_2 was found to be an active catalyst, and decreasing the copper concentration to 5 mol% improved bleach activity for tea stains.

Leaching was investigated to assess if the activity of the catalyst was due to surface bound species or copper salts that had been leached from the catalyst surface. Using the TC test displayed in Figure 65, it was shown that only Mn nitrate was active for bleaching, and Cu, Fe, and Zr nitrate were not effective bleach catalysts.

TGA of 10 mol% CuO_x/ZrO_2 indicated that calcination temperatures above 300 °C are required to achieve full decomposition of the catalyst precursor. This is linked to bleaching activity; the 10 mol% CuO_x/ZrO_2 calcined at temperatures of 250 °C and above exhibit bleaching activity in the TC experiment. This suggests that the oxide formed from the thermal decomposition of the oxalate was required for bleaching.

Finally, hot filtration experiments were performed with the leached copper species from the catalyst calcined at 150 °C, shown in Figure 66. The copper leached from the catalyst was not active for bleaching; the inactivity indicates that the active catalyst is heterogeneous.

The surface species present on the catalyst were investigated using a wide range of techniques. BET, N_2O titration and XRD were used to investigate the effect of lowering the copper concentration, which increases bleach activity. Decreasing copper concentration from 50 mol% to 30 mol% increases surface area 3-fold; however, further decreasing copper concentration does not increase surface area. The results may be due to the quantity, dispersion, and distribution of copper in the sample; for low copper concentration catalysts, the amount of copper on the surface compared to in the lattice did not change by lowering the copper concentration. Therefore, at low Cu concentrations, the surface area of the catalyst did not increase when the Cu concentration was lowered further. Titration with N_2O shows that copper surface area decreased when the copper concentration in the materials decreased from 50 to 5 mol%. The Cu surface area did not, however, decrease linearly with Cu concentration, suggesting that smaller, well dispersed particles are present in the 10 mol% and 5 mol% copper catalysts. XRD also shows a similar trend, where monoclinic Cu(II)O phases are observed for 50 mol% CuO_x/ZrO_2 but not for the catalysts with lower copper concentration. Therefore, decreasing the copper concentration in the catalyst decreased the size and dispersion of Cu(II)O particles present in the catalyst, and increased the overall surface area of the catalyst.

The surface properties of the copper catalysts were further probed with SEM-EDX and XPS. EDX analysis of showed that, in comparison to the rest of the large particle surface, the smaller particles were Cu and O rich, and the non-ordered pores were oxygen deficient. Similar to the XRD data, this indicated the presence of large CuO particles. XPS indicates that Cu(II) species were present; in the 50 mol% CuO_x/ZrO_2

catalyst, the satellite peaks were indicative of Cu(II)O species and, for 10 mol% CuO_x/ZrO_2, the satellite peaks changed shape indicating the presence of $Cu(II)(OH)_2$. The broadening of the Zr peaks in both copper catalysts, in comparison to ZrO_2, indicated the presence of Zr(OH) species. The O regions of both 50 and 10 mol% CuO_x/ZrO_2 and ZrO_2 show similar peaks with broadening, indicating OH groups, with smaller peak present indicating carbonate groups.

Hydroxide and carbonate groups were also observed through probing the samples with DRIFTS; analysis of the 10 mol% CuO_x/ZrO_2 catalyst after calcination at different temperatures (Figure 61) confirmed the presence of these two species. To establish whether these two species were active, two additional catalysts were synthesised; the aim was to produce Cu(OH) and $Cu(CO_3)$ species supported on ZrO_2 and test them for bleach activity (Figure 62). Neither catalyst was active, however, suggesting that bulk phases of hydroxide and carbonate are not active for bleaching. Unfortunately, characterisation of these materials was not conducted and therefore it is not known if these materials were Cu(OH) and $Cu(CO_3)$.

CuO nanoparticles are active for the removal of textile dyes, namely reactive Black 5 and Basic Blue 3, from waste water streams, as well as the removal of organics, such as phenanthrene, using H_2O_2 *via* the generation of hydroxy radicals. [36,9] Ben-Mosche *et al.*[9] synthesised active CuO particles that were all below 50 nm, which may not be present in the copper catalysts prepared using the oxalate gel method.

Cu(II) complexes are active with H_2O_2 for the oxidation of alkanes, benzylic oxidation, phenol oxidation and alcohol oxidation.[37] Cyclohexane can be oxidised with Cu(II) amine species anchored onto MCM-41;[38] when deposited on a support, copper oxide

is formed that is active for the oxidation of cyclohexane. Copper hydroxyphosphate $Cu_2(OH)PO_4$ is active for the oxidation of 2,3,6-trimethylphenol with a conversion of 40%.[39] Copper hydroxide, carbonate and oxide groups have been identified on the copper catalyst surface both pre and post acid treatment in this work. As these species are active for oxidation reactions, they could be active for bleaching tea stains using copper catalysts.

Heterogeneous copper catalysts with similar species to active homogeneous catalyst are active for various oxidation reactions. For benzyl alcohol oxidation, supported Cu(II) complexes on SBA-15, along with copper and copper oxide nanoparticles, were found to be active by Cruz *et al.*[19], Ben-Mosche *et al*. [9] and Saravanan *et al*. [36] the copper oxide nanoparticles were active for the removal of organic pollutants from phenanthrene and textile dyes, respectively. The activity was attributed to the formation of hydroxy radicals and nanoparticle sizes lower than 50 nm. Nanoparticle size dependency for H_2O_2 decomposition in the oxidation of cinnamyl alcohol was investigated for gold nanoparticles on TiO_2.[6] The study showed that decomposition was strongly affected by the nanoparticle size, and particles possessing mean diameters of 4.6 nm gave the highest conversion of cinnamyl alcohol.

Literature stated that copper oxide and hydroxide could be used for bleaching. For Cu(II) oxide, nanoparticle size plays a role in the activity of the catalyst and the interaction with H_2O_2.[40] For 50 mol% CuO_x/ZrO_2, in this work large CuO particles were detected by XRD. It is unlikely that these large particles are active for bleaching and may hinder the formation of peracetic acid by increasing the decomposition of H_2O_2 to H_2O and O_2.

50, 10 and 5 mol% CuO_x/ZrO_2 were tested for morin decomposition in the presence of sodium percarbonate and TAED. All three copper concentrations were active for morin oxidation; however, the activity order was reversed in comparison to the tea stain bleach test. 50 mol% CuO_x/ZrO_2 had the highest conversion, and 5 mol% CuO_x/ZrO_2 had the lowest conversion. Copper leaching was observed during the reaction and copper salts were shown to be highly active for morin oxidation. The result indicates that for morin oxidation, copper leached from the catalyst into solution is likely to be responsible for some of the conversion observed. The leaching activity was not observed the tea stain reaction.

Xaba *et al.*[40] studied Co_3O_4 particles for morin oxidation and found a link between the surface area of the Co_3O_4 particles and conversion of morin; the higher the surface area, the higher the conversion of morin, and surface area could be influenced by the calcination temperature. In this work, 50 mol% CuO_x/ZrO_2 has the highest Cu surface area, of 6.4 m^2g^{-1}, compared to 5 mol% CuO_x/ZrO_2 with 2.2 m^2g^{-1}, which suggests that Cu surface area impacts catalyst activity for morin oxidation. In addition, high copper content leads to higher metal leaching, and copper salts are active for morin oxidation (Figure 68). The leaching may explain the higher activity for 50 mol% CuO_x/ZrO_2 compared to catalysts with lower copper concentrations.

Calculation of rates of morin oxidation during 0 – 4 mins and 4 – 8 mins indicate an induction period for the Cu catalysts, as the rate increases in the second 4 mins of the reaction. Formation of another active species, such as a surface bound O or radical species, could account for the induction period observed in the reaction. Ncube *et al.*[41] postulated that, for the oxidation of morin in the presence of platinum

and palladium nanoparticles, both H_2O_2 and morin needed to be absorbed onto the surface; O^- species are then formed, which oxidises morin. A similar reaction could be taking place on the copper catalyst surface, with the formation of an intermediate species being the rate limiting step at the beginning of the reaction; for example CH_3OOH^-, OOH^-, O^-, a proposed mechanism is shown in Figure 96

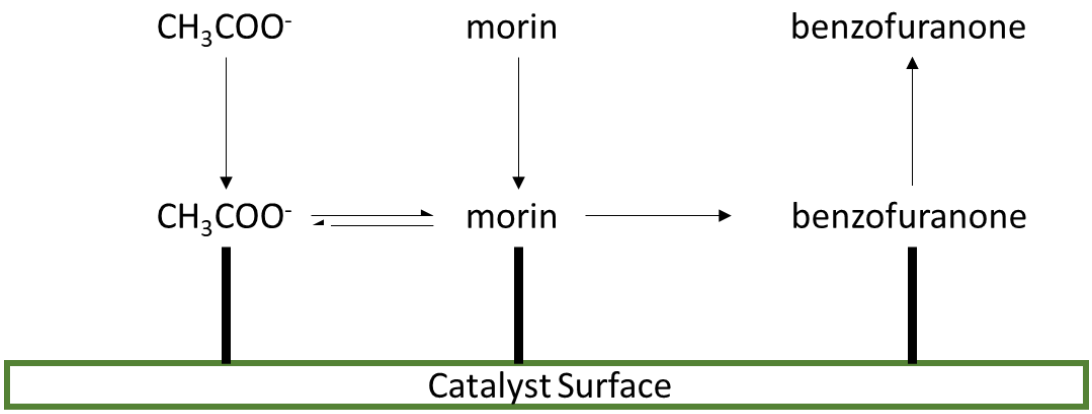

***Figure 96**: Suggested possible mechanism for morin oxidation on catalyst surface.*

Due to the differences in observed activity between the TC bleach reaction and morin oxidation reaction for the heterogeneous catalysts, it is clear that morin oxidation may not accurately predict the bleach activity. The key differences between the reactions are that morin is in a homogeneous phase and intimately mixed with the catalysts, whereas the stain is heterogeneous in the TC test. Tea stains have a complex and ill-defined chemical structure, and the reaction pathway for morin oxidation may not apply to tea stains or aid in the full bleaching of the stain. Never-the-less, morin oxidation is a good indicator as to which catalysts may be active for bleaching tea stains. The model reaction could be further improved by the immobilisation of morin onto a surface, which may then show the same activity orders as observed for tea stains.

There are key differences between the TC bleaching test and the morin oxidation reaction that would lead to the differences in activity observed. Therefore, from a catalyst design perspective, it is difficult to understand what is required from an active bleach catalyst. If a catalyst is active for morin oxidation, it can successfully oxidise chromophores in morin that are equivalent tobleaching a tea stain to remove the colour. In the results, however, this is not always the case and it could be that active catalysts for bleaching immobilised tea stains also need to be active for cleaving the bond between the stain and the cup surface. The bond between the tea stain and the cup is different in nature as it contains Ca, which strengthens the bond, and bonds between the alcohol groups in the tea stain and silicates in the cup.[42] Therefore, the active species required to remove the stain from the cup surface may be different that the species required to remove chromophores from the stain.

As particle size of copper oxide or other copper species may hinder the bleach reaction, an acid treatment with HNO_3 was used to remove large particles from the surface. Decomposition of H_2O_2 was decreased by 30% after the acid treatment displayed in Figure 75. Acid treatment did improve the bleaching performance, and increased the score of 10 mol% CuO_x/ZrO_2 catalyst from 3 to 5, making the bleaching performance comparable to the MnTACN catalyst. Investigation into the copper content of the catalysts after acid treatment, *via* N_2O titration, XPS and EDX analysis, shows a decrease in copper content and copper surface area after the acid treatment. In addition, XRD of 50 mol% CuO_x/ZrO_2 after acid treatment no longer shows diffraction peaks for larger CuO regions in the catalyst. Overall, the acid successfully removes copper from the surface, and there is an indication that larger

CuO particles or Cu rich regions in the catalyst are also removed. The Cu removed correlates with the decrease in the H_2O_2 decomposition, which suggests that large CuO particles are responsible for decomposition of H_2O_2 and removing this competing reaction therefore increases bleach activity.

SEM/EDX still shows the presence of Cu and O rich smaller particles on the surface after acid treatment, and O deficient holes. There is no clear difference of the copper catalysts pre and post acid treatment apart from the overall copper content. XRD for 50 mol% CuO_x/ZrO_2 shows a Cu/Zr phase present in the catalyst, indicates that the acid treatment may etch away larger copper oxide particles and lead to more mixed, dispersed copper throughout the catalyst. XPS of the copper region for 50 mol% CuO_x/ZrO_2 shows a change in the satellite peaks, which is consistent with a change from Cu(II)O and Cu(II)(OH). The Zr region also shows broadening, suggesting the presence of Zr(OH) species on the surface of the catalyst. The same effect is not seen in the Zr region for the blank ZrO_2 catalyst. Overall, it appears that a second metal is needed to form the hydroxide species on the catalyst; the ZrO_2 only catalyst is not active for bleaching, and the copper catalysts are active for bleaching, pointing to hydroxide species on the surface being active for bleaching.

Morin oxidation activity of the acid treated catalyst is less than the catalyst pre acid treatment, for 50 and 10 mol% copper. For 5 mol% CuO_x/ZrO_2, however, the post acid treated catalyst is more active than the pre acid treated catalyst. After the acid treatment, there is no leaching of copper during the reaction, which would explain the decrease in morin oxidation activity for the acid treated catalysts. The

productivity in terms of copper surface area displays the same trend for pre and post acid treated catalysts, as well as an increase in rate over time.

A radical scavenger was added to the morin reaction in the presence of 10 mol% CuO_x/ZrO_2 post acid treatment. There was a decrease in conversion with the addition of the scavenger but the substantial conversion of morin was still observed. The rate of morin oxidation in the presence of post acid treated copper catalysts increases over time, which could indicate radical propagation that increases morin oxidation as the reaction proceeds. Cu(II) and Cu (I) species can form hydroxy radicals in the presence of H_2O_2 to oxidise organics in solution.[43,44] Zhou *et al* [43] demonstrated that the redox reaction of Cu(II) to Cu(I) generates oxygen and hydroxide radicals that boosts the activity for ascorbic acid oxidation. The observed induction phase for CuO_x/ZrO_2 catalysts could be explained by the generation of oxygen and hydroxide radicals that are active for oxidation reactions. The radicals may also explain why a heterogeneous copper catalyst is active for bleaching a heterogeneous tea stain, as the radicals generated bridge the gap and oxidise the stain.

4.4 *References*

1 R. Hage and A. Lienke, *Angew. Chemie - Int. Ed.*, 2005, **45**, 206–222.

2 D. Veghini, M. Bosch, F. Fischer and C. Falco, *Catal. Commun.*, 2008, **10**, 347–350.

3 N. Zhang and X. F. Zhou, *J. Mol. Catal. A Chem.*, 2012, **365**, 66–72.

4 I. A. Weinstock, R. H. Atalla, R. S. Reiner, M. A. Moen, K. E. Hammel, C. J. Houtman, C. L. Hill and M. K. Harrup, *J. Mol. Catal. A Chem.*, 1997, **116**, 59–84.

5 A. Fortuny, C. Bengoa, J. Font and A. Fabregat, *J. Hazard. Mater.*, 1999, **64**, 181–193.

6 T. Kiyonaga, Q. Jin, H. Kobayashi and H. Tada, *ChemPhysChem*, 2009, **10**, 2935–2938.

7 J. R. J. Zazo, J.A. Casas, A. F. Mohedano, M.A Gilarranz and Ä. Guez, *Environ. Sci. Technol*, 2005, **39**, 9295–9302.

8 J. F. Perez-Benito, *J. Inorg. Biochem.*, 2004, **98**, 430–438.

9 T. Ben-Moshe, I. Dror and B. Berkowitz, *Appl. Catal. B Environ.*, 2009, **85**, 207–211.

10 M. Anpo, M. Che, B. Fubini and E. Garrone, *Top. Catal.*, 1999, **8**, 189–198.

11 A. Nuzzo and A. Piccolo, *J. Mol. Catal. A Chem.*, 2013, **371**, 8–14.

12 L. C. Wang, Q. Liu, M. Chen, Y. M. Liu, Y. Cao, H. Y. He and K. N. Fan, *J. Phys. Chem. C*, 2007, **111**, 16549–16557.

13 IKW, *sofw Journal, Home Pers. Care Ingredients Formul.*, 2016, 37–38.

14 X. R. Zhang, L. C. Wang, C. Z. Yao, Y. Cao, W. L. Dai, H. Y. He and K. N. Fan, *Catal. Letters*, 2005, **102**, 183–190.

15 C. Z. Yao, L. C. Wang, Y. M. Liu, G. S. Wu, Y. Cao, W. L. Dai, H. Y. He and K. N. Fan, *Appl. Catal. A Gen.*, 2006, **297**, 151–158.

16 Y. Ma, Q. Sun, D. Wu, W.-H. Fan, Y.-L. Zhang and J.-F. Deng, *Appl. Catal. A Gen.*, 1998, **171**, 45–55.

17 L. C. Wang, Q. Liu, M. Chen, Y. M. Liu, Y. Cao, H. Y. He and K. N. Fan, *J. Phys. Chem. C*, 2007, **111**, 16549–16557.

18 I. Orlowski, M. Douthwaite, S. Iqbal, J. S. Hayward, T. E. Davies, J. K. Bartley, P. J. Miedziak, J. Hirayama, D. J. Morgan, D. J. Willock and G. J. Hutchings, *J. Energy Chem.*, 2019, **36**, 15–24.

19 P. Cruz, Y. Pérez, I. Del Hierro and M. Fajardo, *Microporous Mesoporous Mater.*, 2016, **220**, 136–147.

20 J. Xiao, D. Mao, X. Guo and J. Yu, *Appl. Surf. Sci.*, 2015, **338**, 146–153.

21 A. Davó-Quiñonero, M. Navlani-García, D. Lozano-Castelló, A. Bueno-López and J. A. Anderson, *ACS Catal.*, 2016, **6**, 1723–1731.

22 F. Adler, P. Masłowski, A. Foltynowicz, K. C. Cossel, T. C. Briles, I. Hartl and J. Ye, *Opt. Express*, 2010, **18**, 21861.

23 United States Patent Office, 6194368 B1, 2001.

24 United States Patent Office, 3707502, 1972.

25 D. Kołodyńska, *Expand. Issues Desalin.*, 2011, 342–343.

26 T. Topalovic, University of Twente, the Netherlands, 2007.

27 D. L. Perry and S. L. Phillips, *Handbook of inorganic compounds*, CRC Press, 1995.

28 M. C. Biesinger, L. W. M. Lau, A. R. Gerson and R. S. C. Smart, *Appl. Surf. Sci.*, 2010, **257**, 887–898.

29 S. Poulston, P. M. Parlett and P. Stone, *Surf. Interface Anal.*, 1996, **24**, 811–820.

30 P. O. Larsson, A. Andersson, L. R. Wallenberg and B. Svensson, *J. Catal.*, 1996, **163**, 279–293.

31 C. W. Jones, *Applications of hydrogen peroxide and derivatives*, Royal Society of Chemistry, 1999.

32 S. Tsunekawa, K. Asami, S. Ito, M. Yashima and T. Sugimoto, *Appl. Surf. Sci.*, 2005, **252**, 1651–1656.

33 C. Huang, Z. Tang and Z. Zhang, *J. Am. Ceram. Soc.*, 2001, **84**, 1637–1638.

34 N. J. Milne, *J. Surfactants Deterg.*, 1998, **1**, 253–261.

35 R. Al-Gaashani, S. Radiman, A. R. Daud, N. Tabet and Y. Al-Douri, *Ceram. Int.*, 2013, **39**, 2283–2292.

36 S. Saravanan and T. Sivasankar, *Environ. Process Sustain. Energy*, 2016, **35**, 669.

37 T. Punniyamurthy and L. Rout, *Coord. Chem. Rev.*, 2008, **252**, 134–154.

38 W. A. Carvalho, M. Wallau and U. Schuchardt, *J. Mol. Catal. A Chem.*, 1999, **144**, 91–99.

39 X. Meng, Z. Sun, S. Lin, M. Yang, X. Yang, J. Sun, D. Jiang, F. S. Xiao and S. Chen, *Appl. Catal. A Gen.*, 2002, **236**, 17–22.

40 M. S. Xaba and R. Meijboom, *Appl. Surf. Sci.*, 2017, **423**, 53–62.

41 P. Ncube, T. Hlabathe and R. Meijboom, *Appl. Surf. Sci.*, 2015, **357**, 1141–1149.

42 K. Yamada, T. Abe and Y. Tanizawa, *Food Chem.*, 2007, **103**, 8–14.

43 P. Zhou, J. Zhang, Y. Zhang, Y. Liu, J. Liang, B. Liu and W. Zhang, *RSC Adv.*, 2016, **6**, 38541–38547.

44 M. R. Gunther, P. M. Hanna, R. P. Mason and M. S. Cohen, *Arch. Biochem. Biophys.*, 1995, **316**, 515–522.

5 Chapter 5: Conclusions and Future Work

5.1 *Current Bleaching System*

The current bleaching system in most formulations uses sodium percarbonate and TAED as a bleach activator to form the active bleaching species peracetic acid; see Scheme 18.[1]

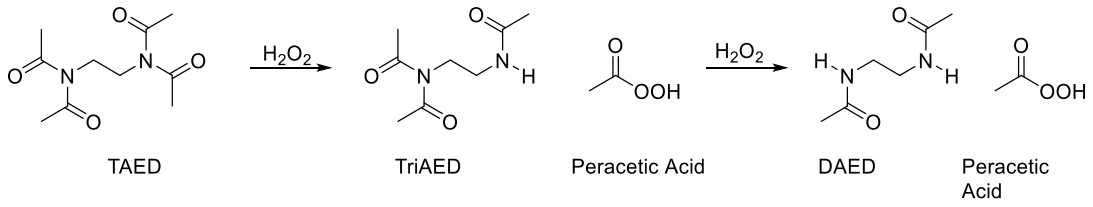

***Scheme 18**: Perhydrolysis of tetraacetylethylenediamine (TAED) to form peracetic acid, the active bleaching species*

Hydrogen peroxide and peracetic acid are both bleaching agents, with peracetic acid being the stronger of the two; therefore, it was necessary to understand if perhydrolysis of TAED to form peracetic acid is the limiting factor for bleaching.[2] Consumers are pushing for lower wash temperatures and shorter cycle times without losing cleaning performance, and the addition of a catalyst could aid in this goal. Currently premium products utilise MnTACN as a bleach catalyst; however, this is lost at the end of each cycle and is expensive.[3] Use of a heterogeneous catalyst could decrease the cost of a tablet by direct placement in the dishwasher and utilised for multiple wash cycles. A heterogeneous catalyst could either increase the formation of peracetic acid or increase the oxidation of the stain to improve bleaching performance, depending on whether peracetic acid formation limits the bleaching performance. To assess which pathway needed a catalyst to improve activity, the

formation of peracetic acid was quantified and aligned with tea stain bleaching and morin oxidation as well as establishing how each of the reagents used influences bleaching performance.

5.1.1 *Formation of peracetic acid*

Peracetic acid formation linearly increased with sodium percarbonate concentration, up to a sodium percarbonate concentration of 3.4 mM (pH = 10.5). This result ultimately showed that total number of peracetic acid moles formed is dependent on the amount of H_2O_2 available at a pH of 10.5. At low TAED concentrations, no peracetic acid formation was observed; however, TAED conversion was at 100 %, indicating that the amount of peracetic acid formed was below detection limits of the titration method used for quantification. Temperature also had an impact on the formation of peracetic acid; total number of peracetic acid moles formed decreased at both high and low temperatures. At low temperatures the rate of perhydrolysis is decreased, reducing peracetic acid formation, and at high temperatures peracetic acid decomposition increases, reducing the amount of peracetic acid in solution. Comparing the formation of peracetic acid to the conversion of TAED, conversion is 100 % apart from at 15 °C, suggesting that the rate of this reaction slows at low temperatures. Peracetic acid decomposition also increases with temperature, which was attributed to the decrease in peracetic acid formation at temperatures above 50 °C. pH had the highest impact on TAED conversion and peracetic acid formation, with no formation or conversion observed below a pH of 9, indicating that alkaline pH is required for the perhydrolysis of TAED to form peracetic acid. Alkaline pH is necessary for perhydrolysis as hydrogen peroxide is then in the form OOH^-, which is

a strong nucleophile and can attack TAED to form peracetic acid.[4] Formulations on the market are all used at an alkaline pH to enhance bleaching, minimise glass erosion, and aid in enzyme activity; therefore only alkaline conditions are relevant to bleaching chemistry in consumer products. Overall, the formation of peracetic acid was determined to be facile under a range of reagent concentrations and temperature.

Comparison of peracetic acid formation and the bleaching activity of these varying formulations shows that peracetic acid formation is linked to tea stain removal from a cup surface. Decreasing sodium percarbonate and TAED leads to a decrease in the observed bleach score, which mirrors the decrease in peracetic formation under such conditions. Increasing the temperature also improves bleaching performance, indicating that, at higher temperatures, the formation of peracetic acid may be higher than quantified. Stain bleaching is also promoted by higher temperatures with only hydrogen peroxide present; therefore, a combination of peracetic acid moles generated and temperature leads to improved bleaching at higher temperatures.[5] Bleaching activity, however, did not decrease by lowering to an acidic pH when no peracetic acid formation was observed. The basic scoring system used to quantify bleaching in the tea cup test highlights the issue with the qualitative method for assessing the performance of potential formulations, therefore a quantitative model reaction needed to be developed.

Catechol is not a suitable model reaction, as polymerisation of catechol occurred under alkaline pH conditions; therefore, it would not be clear if conversion observed during reaction was due to polymerisation or oxidation. Morin is a suitable model

compound for tea stains, as the bleaching could be easily monitored by UV-Vis, and there was no conversion of morin without the presence of bleaching reagents. The conversion of morin also aligned with the amount of peracetic acid formed when varying the concentration of sodium percarbonate and TAED, as well as the temperature of the reaction.

The maximum absorption of morin was determined to be influenced by pH; decreasing the pH of the morin solution in the absence of the bleaching agents, the maximum absorption decreased and shifted to a lower wavelength, which has been observed previously.[6] The observed morin conversion at pH values below 10.5 was not only due to oxidation but also the shift and decrease in intensity of the peak. Therefore, as low pH reactions are not relevant for dishwashing conditions, morin oxidation was not performed at a pH below 10.5 and morin was still found to be a suitable model compound for stain bleaching.

Peracetic acid formation is facile under the reagent concentrations and conditions, which are within scope of relevant concentrations and conditions for the automatic dishwashing application.

5.1.2 *Use of MnTACN*

Mn salts and MnTACN have been used in bleaching formulations for dishwashing as a homogeneous oxidation catalyst in premium products in selected countries, due to the expense of the catalyst. A range of Mn salts and MnTACN are active for bleaching in the tea cup test and for morin oxidation, with MnTACN being more active than the Mn salts. Mn salts may be less active as they are less stable in the reaction than MnTACN and precipitate out as inactive metal oxides during the reaction as

described by Hage *et al*.[3] MnTACN was also active for bleaching without sodium percarbonate or TAED present, showing that MnTACN can utilise O_2 to oxidise chromophores. The high performance of MnTACN therefore may be attributed to a combination of different processes taking place, for example the formation of Mn di-nuclear species that can undergo redox reactions and transfer oxygen to the stain exhibited in Scheme 19.[7]

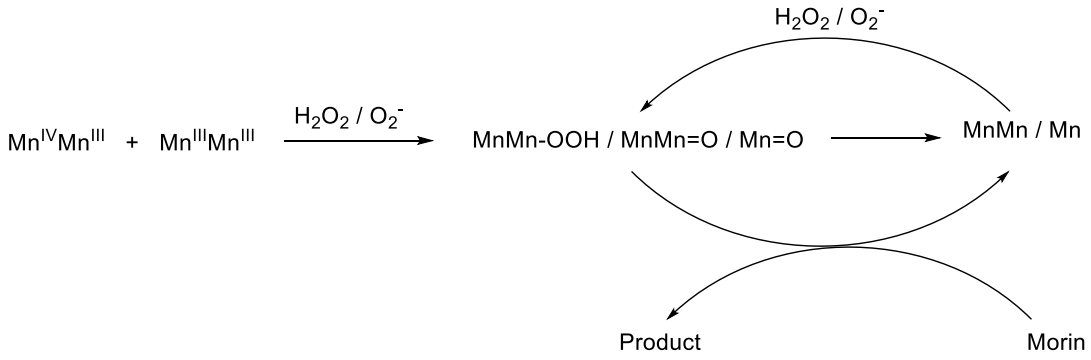

***Scheme 19**: Simplified MnTACN morin oxidation mechanism in the presence of H_2O_2 or O_2 as proposed by Topalovic.*

It was important to test MnTACN in the tea cup and morin oxidation tests, as it is currently the only industrially used catalyst for bleaching in automatic dishwashing; therefore, it is the benchmark of performance for a new heterogeneous catalyst.[3] MnTACN is active for tea stain bleaching as well as morin oxidation in the presence of peracetic acid, hydrogen peroxide or O_2. The highly active bleach nature of MnTACN, using a wide range of oxidants, has been explained in the literature by oxygen transfer and the proximity of the catalyst to the stain. Understanding the activity of MnTACN, and the possible reasons for the high bleach activity it exhibits,

would aid in the design of a heterogeneous catalyst. Furthermore, it was hoped that understanding the bleaching mechanism would assist with the design of a heterogeneous catalyst for such an application.

5.2 *Developed Heterogeneous Bleaching Catalysts*

A series of metal oxides supported on ZrO_2 were prepared using the oxalate gel method. Copper and iron were chosen in addition to manganese, as both are known to react with hydrogen peroxide to form radical species.[8,9] Furthermore, ZrO_2 is known to stabilise superoxide and radical species that may be generated by the added metal oxides. Copper and zinc catalysts were active for bleaching tea stains and morin in solution,[10] and a range of characterisation techniques were employed to investigate what physicochemical properties promote performance for this bleaching application.

5.2.1 *Copper*

A series of CuO_x/ZrO_2 catalysts (50 – 5 mol% Cu) were tested for bleaching tea stains on a tea cup surface, with lowering the copper concentration in the catalyst lead to an improved bleaching performance. The first heterogeneous catalyst that was determined to be active was 10 mol% CuO_x/ZrO_2. After characterisation by DRIFTS, the catalyst was determined to possess CO_3 and OH surface species. Further investigation through targeted synthesis of catalysts containing these surface species was subsequently conducted; these catalysts were, however, poor at bleaching, suggesting that CO_3 and OH surface species may not be important. Further characterisation of these catalysts is required to accurately assess whether the surface did indeed possess the desired surface species.

The same series of copper catalysts were subsequently tested for morin oxidation and increasing copper concentration led to a higher activity. Leaching during the reaction was investigated, and the leached copper in solution was determined to

increase with increasing copper content in the catalyst. Copper salts were tested for morin oxidation activity and found to be highly active, suggesting that the leached copper contributed to morin bleaching, which evidently functioned in parallel to a heterogeneous pathway taking place on the catalyst surface.

There are key differences between the tea cup reaction and the morin oxidation reaction that may explain why the efficiency of the catalysts differ in these reactions. For the tea cup reaction, the stain is supported on a cup surface and is therefore heterogeneous, whereas morin is in solution; this means the catalyst can get into closer contact with the morin compared to the tea stain. In addition, morin is a well-defined molecule and the tea stain is not, which could mean that different mechanisms are taking place to oxidise and bleach the different compounds.

Characterisation of the copper catalysts demonstrated that copper and oxygen rich areas were dependent on the copper concentrations of the catalyst. XPS analysis provided evidence that Cu hydroxide surface species were present and, in fact, were more prevalent in the material than for CuO when the copper concentration was decreased. At higher copper concentrations, the surface area of the catalyst decreased and CuO phase was observed by XRD in the 50 mol% Cu-ZrO_2 catalyst; the CuO phase was not observed for lower copper concentrations. It was proposed that these larger CuO particles may be responsible for the decomposition of H_2O_2, thus reducing the amount of peracetic acid that could form and, ultimately, explain why reduced bleach activity is observed over catalysts with higher concentrations of copper. This led to the use of an acid treatment; the aim of which was to remove these large CuO particles to prevent undesirable H_2O_2 decomposition.

Acid treatment of the copper catalysts with HNO_3 was determined to be successful for removing surface copper, decreasing the decomposition of H_2O_2 and increasing the bleach performance of the catalyst. The removal of large CuO surface particles has been demonstrated previously,[11] and here leads to the formation of a $CuZrO_3$ phase, which was identified in the XRD analysis of 50 mol% CuO_x/ZrO_2. The result suggested that the acid treatment removes larger copper particles and induces a morphological change from ZrO_2 species to more intimately mixed Cu/Zr species. After acid treatment, the XPS showed that the surface of the catalyst still had Cu hydroxide species present.

Bleaching activity of the copper catalysts was improved by acid treatment, but this did not improve the activity of the catalysts for morin oxidation, except for the 5 mol% CuO_x/ZrO_2 catalyst. Quantification of copper leaching during the reaction showed that, after acid treatment, the amount of copper leaching into solution from the catalyst surface was negligible; as copper in solution is active for morin oxidation, this would account for the drop-in catalyst activity after acid treatment.

Using a radical scavenger, mannitol, the activity of the non-acid- and acid-treated copper catalysts could also be decreased, indicating the possibility of a radical mechanism that is not observed for the homogeneous MnTACN catalyst. The rate of morin oxidation in the presence of copper catalysts increases over time, which could be due to radical propagation. The initial morin oxidation rate would be low as the catalyst starts generating radicals on the surface, and then, as the reaction proceeds, more radicals are generated on the surface and these radicals propagate and oxidise the morin, increasing the rate of morin oxidation. The formation of radicals would

also explain how a heterogeneous catalyst can bleach a heterogeneous stain without needing to be in close contact to the stain. Radicals produced on the catalyst surface would propagate through the solution and reach the stain to oxidise and bleach the stain on the cup surface. This discovery may well provide a good foundation for further study into the use of heterogeneous catalysts for applications in automatic dishwashing.

5.2.2 *Other Metals*

Mn, Fe, and Zn supported on ZrO_2 were also tested for tea stain bleaching, with only Zn active. For morin oxidation, both Mn and Zn, pre and post acid treatment, were active for morin oxidation. Zn post acid treated catalysts were more active for morin oxidation than the non-acid treated catalyst, unlike copper, where the opposite was found. The Zn catalyst still leaches into solution during the reaction; however, the acid treatment does not reduce the amount of leaching significantly, as with the copper catalysts. Overall the acid treated catalyst was determined to be more active for morin oxidation than the non-acid treated catalyst, and the leaching remained constant for both catalysts. The result suggests that Zn salts in solution are not active for morin oxidation, but further work using Zn salts may be required to confirm.

XPS characterisation of the Zn catalysts showed a decrease in the Zn with acid treatment, suggesting that Zn is removed from the surface of the catalyst after acid treatment. Zn hydroxide species were found on the surface of the catalyst, similar to the copper catalysts, but the same hydroxide species were not found for ZrO_2 pre or post acid treatment. The presence of hydroxide species when another metal is

supported on ZrO_2 indicates that a second metal is needed to make the catalyst active and can change the surface composition of the catalyst significantly.

5.3 *Key Findings*

Firstly, the role of different reagents and bleach conditions affects the bleach performance observed for both tea stains and morin oxidation, within the scope of current dishwasher formulations and wash conditions. It had already been shown that the perhydrolysis of TAED is facile under different temperatures and near neutral pH; however, the conditions and reagent concentrations were not relevant to the automatic dishwashing application.[12,13] After investigation into the formation of peracetic acid for relevant formulations and conditions, the formation of peracetic acid was determined to be facile and therefore a catalyst is required for oxidation of the stain and not the formation of the active bleaching agent, peracetic acid. As the push for washing at lower temperatures continues, it would then be beneficial to use a catalyst for improving the amount of peracetic acid formed at room temperature washing. Furthermore, the ZnO_x/ZrO_2 catalysts that were identified in this work for stain bleaching should be added to a solution of sodium percarbonate and TAED to assess if this catalyst is also active for the perhydrolysis of TAED to form peracetic acid.

Secondly, highly active heterogeneous catalysts were found for tea stain bleaching and morin oxidation. Previously Cu/ZrO_2 catalysts have been used for hydrogenations or methanol synthesis and now have been shown to be active for bleach reactions and oxidation of model stain compounds.[11,14] Currently the active species on the

surface of the catalyst has not been identified, which would aid in further catalyst design.

Thirdly, the mechanism of bleaching with copper heterogeneous catalyst is based on radicals that bridge the gap between the heterogeneous catalyst and the heterogeneous stain. Copper is known to produce and propagate oxygen and hydroxide radicals *via* redox reaction of Cu(II) to Cu(I), and these radicals could be the active bleach species when a heterogeneous catalyst is used to remove stains.[15] Due to the short lived nature of radical species in solution, the use of a heterogeneous catalyst that initiate radicals to bleach heterogeneous stains might not be suitable for use in automatic dishwashing.[16]

5.4 *Future Work*

The aim of the project was to produce a heterogeneous bleach catalyst for use in automatic dishwashing. A 10 mol% CuO_x/ZrO_2 acid treated was active for both morin oxidation and bleaching of tea stains on a cup surface. The catalyst was tested in a dishwasher with the full tablet formulation for Finish Quantum Max present, and the results are shown in Figure 97.

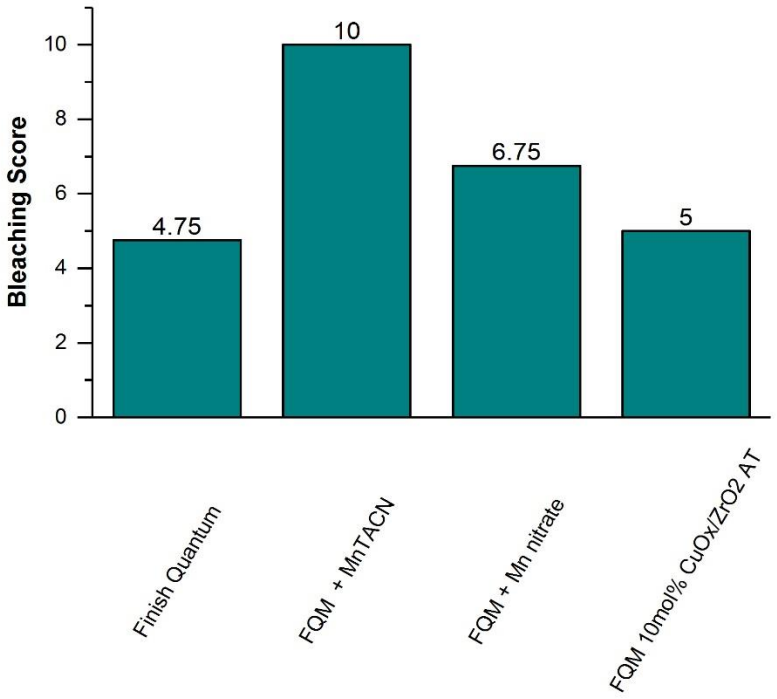

***Figure 97**: Dishwasher bleaching scores. Finish Quantum Max (1 tablet), catalyst (10 mg), IKW soil (50 g), 50 °C and 8 min main wash cycle.*

The addition of the copper catalyst to the full formulation in the dishwasher does not have an added benefit to the bleaching of tea stains compared to the full formulation without a catalyst present. This lack of activity displayed by the heterogeneous catalyst, compared to the bleaching activity in the tea cup test can be explained by

the distance of the catalyst from the stain, as the radical species are too short lived to reach the stain to bleach. A similar effect is observed when comparing the tea cup test to the morin oxidation test, as the heterogeneous catalyst must be in close proximity to the stain is required for bleach performance. To improve the morin model reaction to investigate and quantify bleach activity of heterogenous catalysts, the morin would be immobilised on an inactive support.[17] Using a method to immobilise the morin on a surface would more closely imitate the conditions observed in the tea cup and dishwasher tests. Almeida and co-workers[17] adsorbed anionic dyes using chitosan beads, showing that different coloured dyes were successfully adsorbed between 25 and 50 °C. A similar method could be used with morin to give coloured beads, which are then bleached in the solution, and the bleaching quantified *via* spectrophotometry.

Morin oxidation in the presence of copper catalysts was reduced when Mannitol, a radical scavenger was added to the solution, suggesting the role of radicals in bleaching with heterogeneous catalysts. Smith *et al.* investigated the bleaching of melanin with hydrogen peroxide and metal ions with radical species using electron paramagnetic resonance (EPR).[18] The use of (2,2,6,6-tetramethylpiperidin-1-yl)oxyl (TEMPO) as a radical trap was used to assess the possible mechanism of hydroxide radicals for bleaching, and then EDTA added to switch off the radical pathway and analyse the effect of the perhydroxyl anion. Both species play a role in the bleaching of melanin, and having both present boosts the bleaching as the perhydroxyl anion is a strong nucleophile which breaks down the melanin and the hydroxide radical is a strong oxidant which bleaches the melanin. EPR could be used in the morin

oxidation and tea stain reaction to quantify the radical generation of different catalysts and further understand the bleaching mechanism. This combined, with further radical trap experiments, would elucidate the importance of radicals to bleaching with a heterogeneous catalyst as well as if perhydroxyl anion is still required for bleaching.

In addition, if radical species and the amount of radicals generated is key to bleaching with a heterogeneous catalyst, a radical carrier could be used to improve the lifetime of these species in automatic dishwashing. Zhang and co-workers showed that peracetic acid in combination with Co_3O_4 generated radical species that in turn lead to the degradation of orange G, an azo dye, which formed radicals.[19] These radical species are longer lived than hydroxide or oxygen radicals and could therefore be added to the bleaching formula, to be activated by peracetic acid and the copper catalyst. EPR would be used to ensure that the organic species chosen was forming radicals, and experiments with morin would be conducted to ensure that the longer-lived radicals were contributing to oxidation.

Another solution to closing the gap between the heterogeneous catalyst and the heterogeneous stain is to use colloids instead of a supported metal oxide-based catalyst. Rothbart *et al*. investigated Mn (II) salts for the degradation of Orange II with peracetic acid as the oxidant.[20] Investigation of the mechanism with Mn(II) salts found that MnO_x colloidal like species are formed, which are active for the oxidation of Orange II. Therefore, a range of Mn, Cu, Fe, and Zn colloids could be tested for stain bleaching, which would bring the catalyst into closer contact with the stain and improve bleaching.

Overall, the project has developed a new heterogeneous catalyst that can be used to bleach substrates in solution; however, further development is required for a heterogeneous catalyst to be used in automatic dishwashing. Tea stain bleaching tests shows that the developed catalysts have potential for use in bleaching. Morin oxidation tests in the presence of mannitol, a radical scavenger, showed that radical species are involved in the oxidation of morin. The use of radicals in bleaching is different than the current bleaching systems without a catalyst or with MnTACN, providing new understanding of different possible mechanisms that can be utilised for bleaching in automatic dishwashing. Further understanding of the active species of the catalyst, and the mechanism, is required to develop the catalyst for use in automatic dishwashing.

5.5 *References*

1 D. M. Davies and M. E. Deary, *J. Chem. Soc. Perkin Trans. 2*, 1991, 1549.

2 J. J. Dannacher, *J. Mol. Catal. A Chem.*, 2006, **251**, 159–176.

3 R. Hage and A. Lienke, *Angew. Chemie - Int. Ed.*, 2005, **45**, 206–222.

4 N. J. Milne, *J. Surfactants Deterg.*, 1998, **1**, 253–261.

5 United States Patent Office, 2,898,181, 1959.

6 S. Höfener, P. C. Kooijman, J. Groen, F. Ariese and L. Visscher, *Phys. Chem. Chem. Phys.*, 2013, **15**, 12572–12581.

7 T. Topalovic, *Catalytic bleaching of cotton: molecular and macroscopic aspects*, 2007.

8 J. A. Zazo, J. A. Casas, A. F. Mohedano, M. A. Gilarranz and J. J. Rodríguez, *Environ. Sci. Technol.*, 2005, **39**, 9295–9302.

9 J. F. Perez-Benito, *J. Inorg. Biochem.*, 2004, **98**, 430–438.

10 M. Anpo, M. Che, B. Fubini and E. Garrone, *Top. Catal.*, 1999, **8**, 189–198.

11 I. Orlowski, M. Douthwaite, S. Iqbal, J. S. Hayward, T. E. Davies, J. K. Bartley, P. J. Miedziak, J. Hirayama, D. J. Morgan, D. J. Willock and G. J. Hutchings, *J. Energy Chem.*, 2019, **36**, 15–24.

12 C. Xu, X. Long, J. Du and S. Fu, *Carbohydr. Polym.*, 2013, **92**, 249–253.

13 X. Long, C. Xu, J. Du and S. Fu, *Carbohydr. Polym.*, 2013, **95**, 107–113.

14 E. Frei, A. Schaadt, T. Ludwig, H. Hillebrecht and I. Krossing, *ChemCatChem*, 2014, **6**, 1721–1730.

15 P. Zhou, J. Zhang, Y. Zhang, Y. Liu, J. Liang, B. Liu and W. Zhang, *RSC Adv.*, 2016, **6**, 38541–38547.

16 E. V. Rokhina, K. Makarova, E. A. Golovina, H. Van As and J. Virkutyte, *Environ. Sci. Technol.*, 2010, **44**, 6815–6821.

17 A. R. Cestari, E. F. S. Vieira, A. G. P. Dos Santos, J. A. Mota and V. P. De Almeida, *J. Colloid Interface Sci.*, 2004, **280**, 380–386.

18 R. A. W. Smith, B. Garrett, K. R. Naqvi, A. Fülöp, S. P. Godfrey, J. M. Marsh and V. Chechik, *Free Radic. Biol. Med.*, 2017, **108**, 110–117.

19 W. Wu, D. Tian, T. Liu, J. Chen, T. Huang, X. Zhou and Y. Zhang, *Chem. Eng. J.*, 2020, **394**, 124938.

20 S. Rothbart, E. E. Ember and R. Van Eldik, *New J. Chem.*, 2012, **36**, 732–748.